AN INVESTIGATION INTO THE PI3-K/AKT SIGNALLING PATHWAY IN TNF-A-INDUCED MUSCLE PROTEOLYSIS IN L6 MYOTUBES

Balindiwe JN Sishi

Thesis is presented in partial fulfilment of the requirements for the degree of Master of Science (Physiological Sciences) at Stellenbosch University

Supervisor: Dr A.-M. Engelbrecht

December 2008

DECLARATION

By submitting this thesis electronically, I declare that the entirety of the work contained therein is my own, original work, that I am the owner of the copyright thereof (unless to the extent explicitly otherwise stated) and that I have not previously in its entirety or in part submitted it for obtaining any qualification.

Date: December 2008

SUMMARY

Introduction: Skeletal muscle atrophy is a mitigating complication that is characterized by a reduction in muscle fibre cross-sectional area as well as protein content, reduced force, elevated fatigability and insulin resistance. It seems to be a highly ordered and regulated process and signs of this condition are often seen in inflammatory conditions such as cancer, AIDS, diabetes and chronic heart failure (CHF). It has long been understood that an imbalance between protein degradation (increase) and protein synthesis (decrease) both contribute to the overall loss of muscle protein. Although the triggers that cause atrophy are different, the loss of muscle mass in each case involves a common phenomenon that induces muscle proteolysis. It is becoming evident that interactions among known proteolytic systems (ubiquitin-proteosome) are actively involved in muscle proteolysis during atrophy. Factors such as TNF-α and ROS are elevated in a wide variety of chronic inflammatory diseases in which skeletal muscle proteolysis presents a lethal threat. There is an increasing body of evidence that implies TNF-α may play a critical role in skeletal muscle atrophy in a number of clinical settings but the mechanisms mediating its effects are not completely understood. It is also now apparent that the transcription factor NF-κB is a key intracellular signal transducer in muscle catabolic conditions. This study investigated the various proposed signalling pathways that are modulated by increasing levels of TNF-α in a skeletal muscle cell line, in order to synthesize our current understanding of the molecular regulation of muscle atrophy.

Materials and Methods: L6 (rat skeletal muscle) cells were cultured under standard conditions where after reaching ± 60-65% confluency levels, differentiation was induced for a maximum of 8 days. During the last 2 days, myotubes were incubated with increasing concentrations of recombinant TNF-α (1, 3, 6 and 10 ng/ml) for a period of 40 minutes, 24 and 48 hours. The effects of TNF-α on proliferation and cell viability were measured by MTT assay and Trypan Blue exclusion technique. Morphological assessment of cell death was conducted using the Hoechst 33342 and Propidium Iodide staining method. Detection of apoptosis was assessed by DNA isolation and fragmentation assay. The HE stain was used for the measurement of cell size. In order to determine the source and amount of ROS production, MitoTracker Red CM-H_2 X ROS was utilised. Ubiquitin expression was assessed by immunohistochemistry. PI3-K activity was calculated by using an ELISA assay and the expression of signalling proteins was analysed by Western Blotting using phospho-specific

and total antibodies. Additionally, the antioxidant Oxiprovin was used to investigate the quantity of ROS production in TNF-α-induced muscle atrophy.

Results and Discussion: Incubation of L6 myotubes with increasing concentrations of recombinant TNF-α revealed that the lower concentrations of TNF-α used were not toxic to the cells but data analysis of cell death showed that 10 ng/ml TNF-α induced apoptosis and necrosis. Long-term treatment with TNF-α resulted in an increase in the upregulation of TNF-α receptors, specifically TNF-R1. The transcription factors NF-κB and FKHR were rapidly activated thus resulting in the induction of the ubiquitin-proteosome pathway. Activation of this pathway produced significant increases in the expression of E_3 ubiquitin ligases MuRF-1 and MAFbx. Muscle fibre diameter appeared to have decreased with increasing TNF-α concentrations in part due to the suppressed activity of the PI3-K/Akt pathway as well as significant reductions in differentiation markers. Western blot analysis also showed that certain MAPKs are activated in response to TNF-α. No profound changes were observed with ROS production. Finally, the use Oxiprovin significantly lowered cell viability and ROS production. These findings suggest that TNF-α may elicit strong catabolic effects on L6 myotubes in a dose and time dependent manner.

Conclusion: These observations suggest that TNF-α might have beneficial effects in skeletal muscle in certain circumstances. This beneficial effect however is limited by several aspects which include the concentration of TNF-α, cell type, time of exposure, culture conditions, state of the cell (disturbed or normal) and the cells stage of differentiation. The effect of TNF-α can be positive or negative depending on the concentration and time points analysed. This action is mediated by various signal transduction pathways that are thought to cooperate with each other. More understanding of these pathways as well as their subsequent upstream and downstream constituents is obligatory to clarify the central mechanism/s that control physiological and pathophysiological effects of TNF-α in skeletal muscle.

OPSOMMING

Inleiding: Skeletspieratrofie is ‘n versagtende komplikasie wat deur ‘n verlaging in spierveseldeursnee area en proteïeninhoud gekenmerk word, verlaagde krag, verhoogde uitputtingskapasiteit en insulienweerstand. Dit wil voorkom asof dit ‘n hoogs geordende en gereguleerde proses is waarin simptome van hierdie toestand soms gesien kan word in inflammatoriese toestande soos byvoorbeeld kanker, VIGS, diabetes en chroniese hartversaking (CHV). Dit is lank reeds bekend dat ‘n wanbalans tussen beide proteïenafbraak (toename) en proteïensintese (afname) bydra tot die gesamentlike verlies aan spierproteïen. Alhoewel die sneller wat atrofie veroorsaak verskillend is, is die verlies aan spiermassa in elke geval deel van ‘n algemene verskynsel wat spierproteolise induseer. Dit is alom bekend dat interaksies tussen bekende proteolitiese sisteme (ubikwitien-proteosoom) aktief betrokke is in spierproteolise tydens atrofie. Faktore soos byvoorbeeld TNF-α en ROS is verhoog in ‘n wye verskeiedenheid chroniese inflammatoriese siektes waarin skeletspierproteolise ‘n lewensgevaarlike toestand is. Daar is reeds toenemende bewyse in ‘n aantal kliniese omgewings wat die kritiese rol van TNF-α in skeletspieratrofie beskryf, maar die meganismes wat die effekte medieer is nog onduidelik. Verder is dit duidelik dat die transkripsie faktor NF-κB ‘n belangrike rolspeler in intrasellulêre seintransduksie in spierkataboliese toestande is. Hierdie studie poog om die verskeie, voorgestelde seinweeë wat deur die toenemende TNF-α vlakke in ‘n skeletspiersellyn te ondersoek om sodoende die huidige begrip van molekulêre regulering van spieratrofie te verbreed.

Materiaal en Metodes: L6 (rotskeletspier) selle is onder standaard toestande gekweek waarna ± 60-65% eenvormigheid bereik is, differsiasie gevolg vir ‘n maksimum van agt dae. Gedurende die laaste twee dae, is miobuise (myotubes) geïnkubeer met toenemende konsentrasies van rekombinante TNF-α (1, 3, 6 en 10 ng/ml) vir ‘n tydperk van 40 minute, 24 en 48 uur. Die effekte van TNF-α op proliferasie en selvatbaarheid is deur ‘n MTT assay en Trypan Blue uitsluitingstegniek gedoen. Morfologies is seldood bepaal deur van Hoechst 33342 en Propidium Iodide kleuringsmetodes gebruik te maak. Apoptose is deur DNA isolasie en fragmeteringsassay gedoen. Die HE kleuringstegniek is aangewend om selgrootte en bepaal. Die bron en kwantiteit ROS is bepaal deur MitoTracker Red CM-H_2 X ROS. Ubikwitienuitdrukking is deur middel van immunohistochemie gedoen. PI3-K aktiwiteit is bereken deur van ELISA assay sowel as die uitdrukking van seinproteïene met behulp van Western Blotting en fosfo-spesifieke en totale anti-liggaam gebruik te maak. Bykomend is die

antioksidant Oxiprovin gebruik om die kwantiteit ROS produksie in TNF-α geïnduseerde spierselatrofie te ondersoek.

Resultate en Bespreking: Inkubasie van L6 myotubes met toenemende rekombinante TNF-α konsentrasies het getoon dat geen van die konsentrasies toksies vir die selle is nie. Data analise het wel getoon dat seldood by 10 ng/ml TNF-α apoptose en nekrose induseer. Langtermyn behandeling met TNF-α veroorsaak 'n toename in opregulering van TNF-α reseptore, spesifiek TNF-R1. Die transkripsie faktore NF-κB en FKHR is vinnig geaktiveer en het die ubikwitien-proteosoomweg geïnduseer. Aktivering van hierdie weg het betekenisvolle toename in die uitdrukking van E_3 ubikwitienligase, MuRF-1 en MAFbx, tot gevolg gehad. Spierveseldeursnee is gevolglik verlaag met toenemende TNF-α konsentrasies wat deels as gevolg van onderdrukte aktiviteit van die PI3-K/Akt weë sowel betekenisvolle verlaging in differenesiasie merkers verklaar kan word. Western blot analiese het verder getoon dat sekere MAPKs geaktiveer is in reaksie op TNF-α. Geen uitgesproke veranderinge is waargeneem ten opsigte van ROS vorming nie. Ten slotte, die insluiting van Oxiprovin het sellewensvatbaarheid en ROS vorming betekenisvol verlaag. Hierdie bevindinge beweer dat TNF-α moontlik sterk kataboliese effekte op L6 myotubes in 'n dosis en tyd afhanglike wyse meebring.

Gevolgtrekking: hierdie waarnemings bring mee/beweer dat onder sekere omstandighede TNF-α moontlik voordelige effekte in skeletspiere toon. Hierdie voordelige effekte is beperk in sekere gevalle wat onder andere die konsentrasie TNF-α, seltipe, blootstelligns periode, kultuurtoestande, die toestand van die sel (versteur of normal) en of die sel in differensiasie is, insluit. Fundamenteel beweer hierdie resultate dat sekere konsentrasie en tydspunte van TNF-α, beide positiewe en negatiewe effekte toon in spierproteolise in L6 myotubes. Hierdie aksie word gemediëer deur verskeie seintransduksie weë wat moontlik saam funksioneer. Om heirdie weë beter te verstaan asook hulle gevolglike upstream and downstream constituents is dit noodsaaklik om die sentrale fisiologiese en patofisiologiese beheermeganisme/s van TNF-α in skeletspier te ondersoek.

I dedicate this thesis to my all my siblings

“Only those who risk going far can possibly know how far one can go” TS Elliot

ACKNOWLEDGEMENTS

My sincerest appreciation to the following people, for without their assistance this study would not have been completed:

Thank you **Heavenly Father** for giving me the strength, ability and endurance to persevere in challenging times

Dr Anna-Mart Engelbrecht (supervisor): who patiently guided and supported me every step of the way. Thank you for entrusting me with this project and the opportunity to learn something new. Thank you for having so much faith in me even though at times I didn't have any

Mrs Beverly Ellis: for her patience, assistance and friendship which she extended to me in spite of her own busy schedule

My parents: for their years of financial support and faith. They never once failed to come to my aid when I was lacking in both. Thank you mom for the emotional support as well as your steadfast prayers for I would never have come this far in life

Thando Makomazi (Nana): for his deep understanding, enthusiasm, humour, tolerance and encouragement when it was most needed

Dr Theo Nell: for help in translating my abstract from English to Afrikaans

Academic Staff: for their GREAT leadership

My friends and colleagues: for their help, encouragement and support. Their spirit, enthusiasm, sense of humour and laughter helped insure an uplifting environment everyday

NRF: for their financial support which allowed me to continue with my studies

ABBREVIATIONS

AIDS	Acquired Immunodeficiency Syndrome
ALS	Amyotrophic lateral sclerosis
AMP	Adenosine monophosphate
ANOVA	Analysis of variance
AP-1	Activator protein-1
Apaf-1	Apoptosis protease activation factor-1
ATM	Ataxia-telangectasia mutated
ATP	Adenosine triphosphate
Bax	Bcl-associated partner containing six exons
Caspase	Cysteine aspartate-specific protease
CHF	Chronic Heart Failure
CO_2	Carbon dioxide
$COOH^-$	Carboxyl terminal
COPD	Chronic Obstructive Pulmonary Disease
Cu	Copper
DAPI	4',6-Diamidino-2-phenylindole
dATP	Deoxyadenosine triphosphate
DED	Death effector domain
DMEM	Dulbecco's modified Eagle's medium
DMSO	Dimethyl sulfoxide
DNA	Deoxyribonucleic acid
EDTA	Ethylenediaminetetraacetic acid
ELISA	Enzyme-Linked ImmunoSorbent Assay
ERK	Extracellular signal-regulated kinases
FADD	Fas-associated death domain
Fbps	F-box containing proteins
FCS	Fetal calf serum
FITC	Fluorescein isothiocyanate
FOXO	Forkhead box
GSK3β	Glycogen synthase kinase 3β
H&E	Hematoxylin and Eosin
H_2O_2	Hydrogen peroxide

HCL	Hydrogen chloride
HS	Horse serum
HSF1	Heat shock transcription factor 1
IFN-γ	Interferon gamma
IGF-1	Insulin growth factor-1
IKK	IκB kinase
IL-6	Interleukin-6
IRS-1	Insulin receptor substrate-1
JAK	Janus protein kinase
JNK	c-Jun-N-terminal kinase
MAFbx	Muscle atrophy F-box
MAPK	Mitogen activated protein kinase
Mn	Manganese
MRFs	Myogenic regulatory factors
mRNA	Messenger Ribonucleic acid
mTOR	Mammalian target of rapamycin
MTT	3-(4,5-dimethylthiazol-2-yl)-2,5-diphenyltetrazolium bromide
MuRF-1	Muscle RING finger-1
NaCl	Sodium chloride
NADH	Nicotinamide adenine dinucleotide reduced
NADPH	Nicotinamide adenine dinucleotide phosphate
NaF	Sodium fluoride
NF-κB	Nuclear factor- κB
O_2^-	Superoxide anion
OD	Optical density
OH	Hydroxyl radical
OPCs	Oligometric proanthocyanidins
p70S6-K	p70S6-kinase
PBS	Phosphate buffered saline
PCI	Phenol chloroform isoamyl
PDK-1	Phosphoinositide-dependent kinase-1
Peg3	Paternally expressed gene 3
Penstrep	Penicillin/Streptomycin
PGC-1α	Peroxisome-proliferator-activated receptor γ-1α
PHAS-1	Phosphorylated heat- and stable protein-1

PI	Prodium Iodide
PI3-K	Phosphotidylinositol 3-kinase
PIP_2	Phosphotidylinositol-4,5-biphosphate
PIP_3	Phosphotidylinositol-3,4,5-triphosphate
PKB	Protein kinase B
PKC	Protein kinase C
PLC-γ1	Phospholipase C- γ1
PMSF	Phenylmethyl sulphonyl fluoride
PTEN	Phosphatase and tensin homologue
RIPA	Radio immunoprecipitation assay
ROS	Reactive oxygen species
SBTI	Soybean trpsin inhibitor
SCF	Skp, Cullin, F-box containing complex
SDS-PAGE	Sodium dodecyl sulphate polyacrylamide gel electrophoresis
SEM	Standard error of the mean
Ser/Thr	Serine/Threonine
SHIP	SH2-domain-containing inositol 5' phosphate
SOD	Superoxide dismutase
STAT	Signal transducers and activators of transcription
TBS-T	TRIS-buffered saline-Tween
TNF-R1	TNF-receptor 1
TNF-R2	TNF-receptor 2
TNF-α	Tumor necrosis factor-α
TRADD	TNFR1-associated death domain
TRIS-HCL	Tri-(hydroxyl-methyl)-aminomethane-HCl
TSC	Tuberous sclerosis complex
Zn	Zinc

LIST OF TABLES

LIST OF FIGURES

Crystal structure of TNF-α

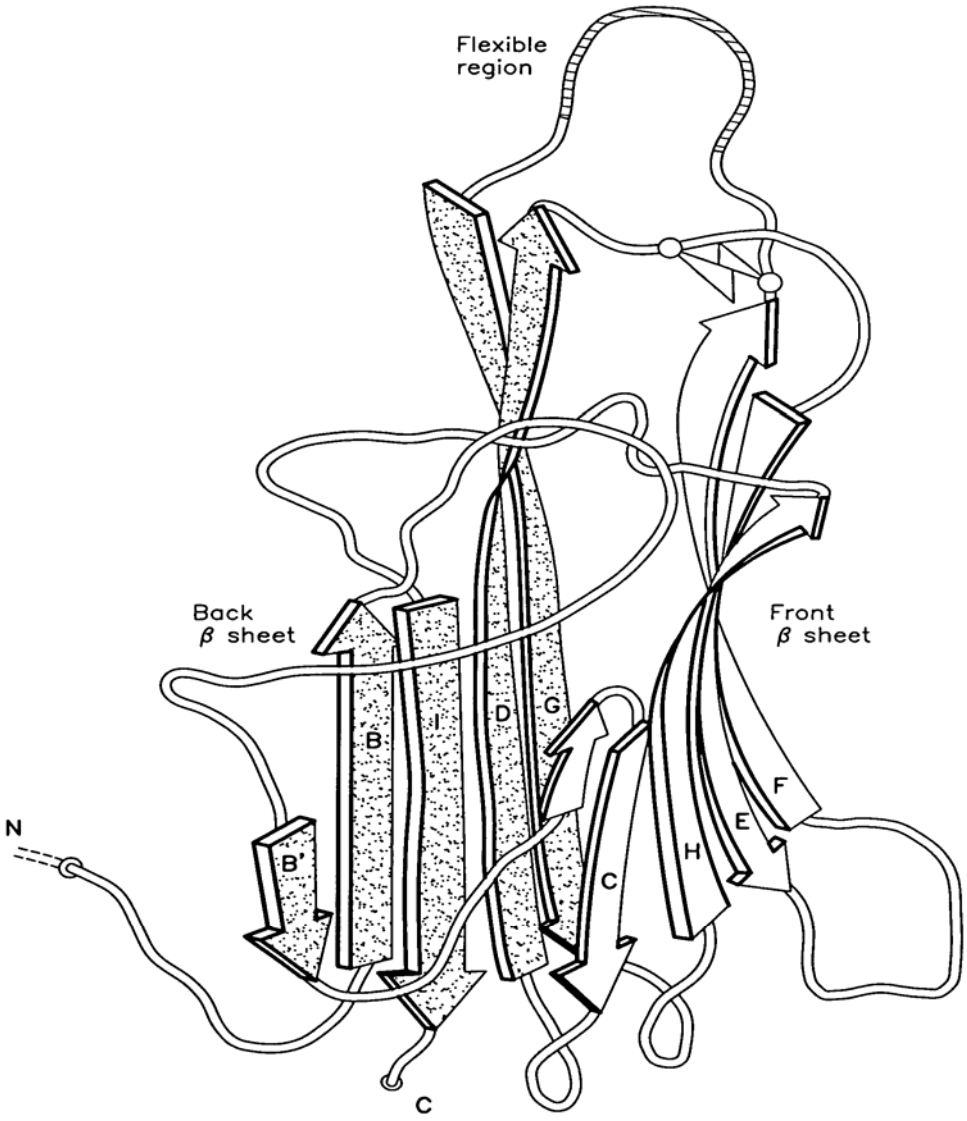

Figure 1.1: Crystal structure of TNF-α

TABLE OF CONTENTS

CHAPTER 1

CHAPTER 2

CHAPTER 3

Results I

CHAPTER 4

Results II

CHAPTER 5

Results III

CHAPTER 6

CHAPTER 7

CHAPTER 1

1.1. *Introduction*

The ability to use chemical energy to produce force and movement is present to a limited extent in most cells. It is, however, in muscle cells that this process has become the dominant cell function. The primary function of these specialised cells is to generate the forces and movements used by multicellular organisms in the regulation of their internal environments and to produce the movements of the entire organism in the external environment. In humans, the ability to communicate, whether by speech, writing, or artistic expression, also depends on muscle contractions. Indeed, it is only by controlling the activity of muscles that the human mind ultimately expresses itself. Three types of muscle tissue can be identified on the basis of structure, contractile properties, and control mechanisms: (i) skeletal muscle, (ii) smooth muscle, and (iii) cardiac muscle. For the purpose of this thesis, only skeletal muscle will be discussed.

Most skeletal muscle, as the name implies, is attached to bone, and its contraction is responsible for supporting and moving the skeleton. The contraction of skeletal muscle is initiated by impulses in the neurons to the muscle and is usually under voluntary control. A single skeletal muscle cell is known as a muscle fiber, formed during development by the fusion of numerous undifferentiated, mononucleated cells, known as myoblasts, into a single cylindrical, multinucleated cell (Figure 1.2). Skeletal muscle differentiation is completed at birth, and these differentiated fibers continue to increase in size during growth from infancy to adulthood, but no new fibers are formed from myoblasts. If, however, skeletal muscle is damaged or destroyed after birth as a result of injury, they cannot be replaced by the replication of other existing muscle fibers. New fibers can be formed from undifferentiated cells known as satellite cells which undergo differentiation similar to that observed in embryonic myoblasts.

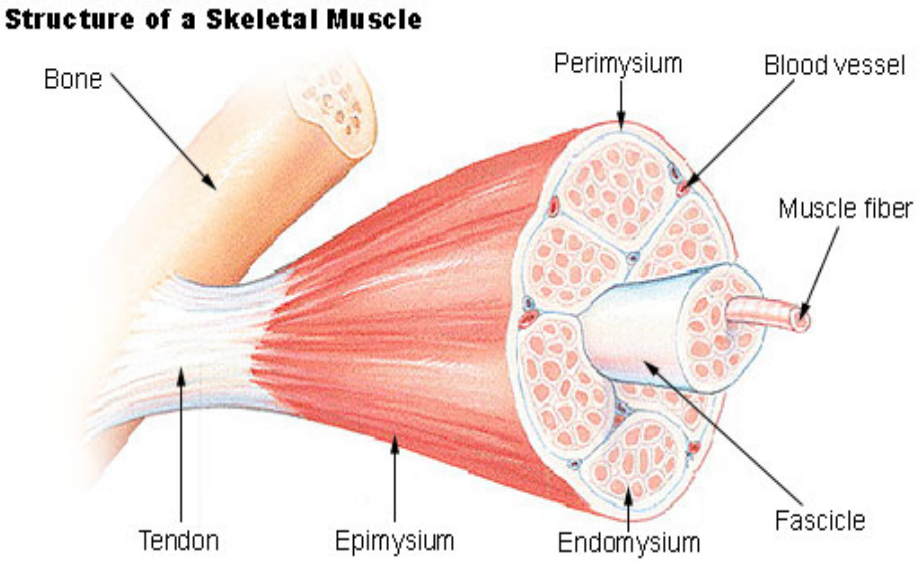

Figure 1.2: Structure and organization of skeletal muscle fibers that are attached to bone by tendons (adopted from http//www.musclehelp.com/initiatives/education/musclesedu)

The most striking feature of a muscle fiber is a series of light and dark bands situated perpendicular to the long axis of the fiber. The fiber of skeletal (and cardiac) muscle have this characteristic banding due to the arrangement of the thick and thin filaments within the myofibrils and are therefore known as striated muscle. The thick and thin filaments in each myofibril are arranged in a repeating pattern along the length of the myofibril. One unit of this repeating pattern is known as a sarcomere. The thick filaments are composed almost entirely of the contractile protein myosin, whereas the thin filaments contain the contractile protein actin, as well as two other regulatory proteins – troponin and tropomyosin (Figure 1.3). Both the thick and thin filaments are situated in the center of each sarcomere, where their parallel arrangement produces a wide, dark band known as the A band. Each sarcomere contains two sets of thin filaments, one at each end. One end of each thin filament is anchored to a network of interconnecting proteins known as the Z line, whereas the other end overlaps a part of the thick filament. The light band, known as the I band, lies between the ends of the A bands of two adjacent sarcomeres and contains those portions of the thin filaments that do not overlap the thick filaments. Two additional bands are present in the A band area of each sarcomere. The H zone is a moderately light band in the center of the A band which corresponds to the space between the ends of the two sets of thin filaments in each sarcomere. The narrow, dark band in the middle of the H zone is known as the M line and corresponds to the proteins that link the central region of the thick filaments.

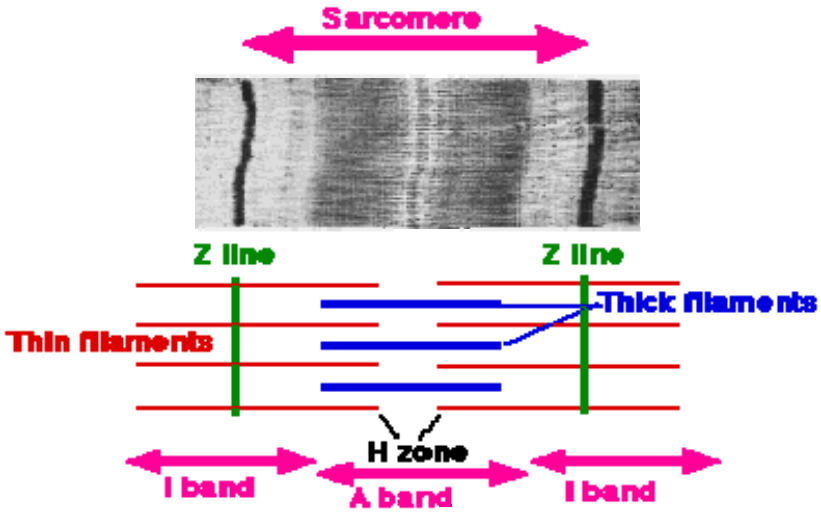

Figure 1.3: The composition of filaments in skeletal muscle that produces the striated pattern (adopted from http//www.nicksnowden.net/Module_4_pages/cardiovascular_system_Introduction.htm)

Skeletal muscle is the largest single organ in the human body, comprising about 40% of the body weight (Phillips *et al*, 2005). As described above, it is highly compartmentalized, and yet we often think of each compartment as a separate entity. The mass and composition of skeletal muscle are vital for its function and may be regulated in response to changes in workload, activity or pathological conditions. Poor nourishment, poor circulation, loss of hormonal support, denervation to the target organ, immobilization, disuse or lack of exercise or disease intrinsic to the tissue itself, are all examples which can result in significant muscle atrophy (Zhang *et al*, 2007; Jackman *et al*, 2004). Skeletal muscle atrophy is a mitigating complication that is characterized by a reduction in muscle fibre cross-sectional area as well as protein content, reduced force, elevated fatigability and insulin resistance. It seems to be a highly ordered and regulated process and signs of this condition are often seen in a variety of inflammatory conditions such as cancer, sepsis, diabetes, tuberculosis, cystic fibrosis, acquired immunodeficiency syndrome (AIDS), chronic obstructive pulmonary disease (COPD) and chronic heart failure (CHF) (Azzawi *et al*, 1999), as well as severe burns and trauma (Li *et al*, 2000 and 2005; Tisdale, 2005; Peterson *et al*, 2006). This condition has also been observed during extended periods of weightlessness, such as prolonged space flight. These diseases often produce a body wasting syndrome known as cachexia, which is notable for the severe muscle atrophy seen. Cachexia manifests as a secondary complication that contributes to the morbidity and mortality in individuals with such diseases causing chaotic abnormalities in fat

and carbohydrate metabolism, despite adequate nutritional intake (Li *et al*, 2000; Peterson *et al*, 2006; Di Marco *et al*, 2005). Windsor *et al* (1988) revealed that death occurs when the total body weight loss reaches 30% and is thought to be caused by respiratory failure through erosion of the diaphragm ultimately leading to hypostatic pneumonia (Tisdale, 2005). In all cases of skeletal muscle atrophy, the loss of fat-free mass involves only skeletal muscle and not visceral protein, where protein synthesis takes place. Therefore, it is different from plain starvation, where it is the visceral protein that is lost in proportion to skeletal muscle mass. Unfortunately, there are no effective treatments to combat muscle atrophy and it is for this reason that loss of skeletal muscle is associated with a very poor prognosis.

It has been stated that approximately one half of the total muscle protein is made up of myofibrillar protein, which is lost at a much faster rate than the other proteins during atrophy (Munoz *et al*, 1993). In a study by Acharyya and colleagues (2004), a considerable decrease in the expression of the myosin heavy chain, the core myofibrillar protein responsible for muscle contraction was demonstrated in response to cachectic cytokines such as interferon gamma (IFN-γ) and tumor necrosis factor-alpha (TNF-α). The other core proteins present in muscle tissue which include troponin, tropomyosin and actin seemed to be unaffected. This denotes a high degree of selectivity between muscle proteins. The loss of muscle protein seems to transpire through a RNA-dependent process *in vitro*, whereas *in vivo* studies on mice have indicated a discriminating degradation process involving a two- to fourfold increase in messenger RNA (mRNA) for polyubiquitin (multiple ubiquitin molecules) and proteosome (protease that cleaves proteins into smaller fragments) subunits (Tisdale, 2005; Du *et al*, 2000; Lecker *et al*, 2004). Muscle atrophy is thus highly selective as to which proteins are targeted for degradation and is not a consequence of a general downregulation of muscle proteins. It has long been understood that an imbalance between protein degradation and protein synthesis both contribute to the overall loss of muscle protein but the key molecular mediators of hypertrophy and atrophy have only just begun to be elucidated. Protein synthesis requires an accurately balanced mixture of 20 amino acids, together with a source of energy to form a peptide bond. Although the triggers that cause atrophy are different, the loss of muscle mass in each case involves a common phenomenon that induces muscle proteolysis (Jackman *et al*, 2004). Protein degradation systems have been studied at length, however the specific molecular mediators of atrophy-related degradation still remain to be identified, nor has it been revealed that whether blocking these specific mediators can hinder muscle atrophy. It is not known whether muscle atrophy induced by contrasting perturbations is managed by a univer-

sal signalling pathway or whether a more general mechanism is employed. Major advances have been made in the elucidation of signalling pathways involved in skeletal muscle atrophy, but we have only recently begun understanding the behaviour of upstream molecules involved in the proteolytic degradation of muscle mass. The loss of muscle mass contributes to the morbidity and mortality of individuals suffering from inflammatory disorders where TNF-α is widely implicated as a mediator of muscle catabolism.

1.2. *Tumor necrosis factor-alpha (TNF-α)*

Most of the body's organs seem to be affected by TNF-α since it is produced by a variety of different cell types. *In vivo*, the main sources of TNF-α production after stimulation are fibroblasts, endothelial cells, macrophages, monocytes, lymphocytes, B- and T-cells, granulocytes, chondrocytes, eosinophils, mast cells, smooth muscle cells, osteoblasts, keratinocytes and glial cells. TNF-α can also be detected in human milk and cerebrospinal fluid. This cytokine possesses a wide variety of functions, serving both inhibitory and stimulatory properties as well as having self-regulatory properties even though many of these functions are not fully understood. For example, during inflammation TNF-α stimulates neutrophil proliferation, but upon binding to its receptor, TNF-R1 (tumor necrosis factor-α-receptor 1), can also induce neutrophil apoptosis (Murray *et al*, 1997) (Figure 1.4).

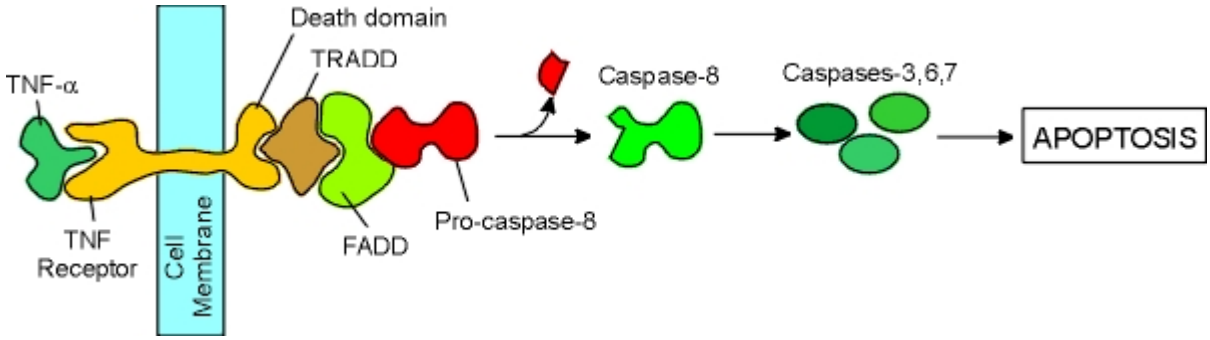

Figure 1.4: The induction of apoptosis by TNF-α binding to its receptor. *Abbreviations*: TNF-α, tumor necrosis factor-α; TRADD, TNFR1-associated death domain; FADD, Fas-associated death domain

A study by Tracey and Cerami (1990) revealed that TNF-α may have two beneficial functions. Firstly, low levels of TNF-α regulates the body's circadian rhythm thus aiding in the maintenance of homeostasis. Secondly, low levels of TNF-α stimulates fibroblast growth which promotes the replacement of senescent and injured tissue (Davidson College; Collins *et al*, 2001). Other advantageous functions of TNF-α comprise its role in immune responses to baterial, parasitic, viral and particular fungal (microorganisms) infections. TNF-α is a finely tuned protein that induces the elevation of vascular permeability and the manufacture of certain chemokines, in that way attracting macrophages as well as neutrophils to the location of infection. Additionally, TNF-α which is secreted by macrophages, prevents the onset of infection by clotting blood. Rink and Kirchner (1996) have implicated that high levels of TNF-α positively correlate with increased risk of mortality. As noted, TNF-α contributes to both "inflammatory disorders of inflammation" and disorders of non-inflammatory origin (Strieter et al, 1993). In the beginning, sepsis was highly considered to be caused by infesting bacteria, but it was soon comprehended that the hosts' proteins including TNF-α are responsible for stimulating sepsis in response to invading bacteria. Sepsis however arises when the synthesis of cytokines is augmented and begins to leak from the restricted infection area or when the infection escapes and enters the bloodstream. Although exogenous and endogenous aspects from these microorganisms are known to induce TNF-α production, it is the complex structural lipopolysaccharide of the bacterial wall that is a powerful stimulator of TNF-α production. In addition to these effects, TNF-α displays chronic effects as well as ensuing in acute pathologies (Table 1). From these observations it is clear that TNF-α is a mediator of certain pathologies, but the underlying mechanisms remain a mystery.

ACUTE, HIGH DOSE	**CHRONIC, LOW DOSE**
Shock and tissue injury	Weight loss
Catabolic hormone release	Anorexia
Vascular leakage syndrome	Protein catabolism
Adult respiratory distress disorder	Lipid depletion
Gastrointestinal necrosis	Hepatosplenomegaly
Acute renal tube necrosis	Subendocardial inflammation
Adrenal hemorrhage	Insulin resistance
Decreased muscle membrane potentials	Enhanced rate of tumor metastis

Disseminated intravascular coagulation	Acute phase protein release
Fever	Endothelial activation

Table 1: Systemic effects in acute and chronic exposure to TNF-α

1.3. *TNF-α, the ubiquitin-proteosome pathway and muscle-specific ubiquitin ligases*

In order to get a greater understanding of the multiple cellular pathways that can cause muscle protein degradation, one needs to understand the basic mechanism/s as to how this process is activated. This is not only in the interest of scientists, but may aid us in the direction towards therapeutic intervention and prevention (Tisdale, 2005). In order to achieve this goal, a great number of studies have implicated the fact that many degradation enzymes are upregulated and activated during muscle degradation.

Virtually all chronic conditions that lead up to the massive effect of muscle protein loss as in all other tissue types appears to be strongly associated with the activation of the ubiquitin proteosome-dependent pathway to degrade proteins (Hu *et al*, 2007; Di Marco *et al*, 2005; Li *et al*, 2005; Zhang *et al*, 2007). Insulin or insulin-like growth factor-1 (IGF-1) inhibits the ubiquitin-proteosome pathway (Zhang *et al*, 2007; Latres *et al*, 2004). Conversely, cytokines such as TNF-α, IFN-γ, interleukin-6 (IL-6), hormones including glucocorticoids, and myostatin upregulate the ubiquitin-proteosome pathway (Latres *et al*, 2004; Zhang *et al*, 2007; Peterson *et al*, 2006; Di Marco *et al*, 2005; Li *et al*, 2000; 2005 and Jackman *et al*, 2004). The current concept is that the nuclear factor-κB (NF-κB) transcription family mediates the activation of the ubiquitin-proteosome pathway in most if not all muscle catabolic states via upstream signalling molecules that include cytokines or reactive oxygen species (ROS) (Peterson *et al*, 2006; Di Marco *et al*, 2005; Li *et al*, 2000; 2005 and Jackman *et al*, 2004). Ubiquitin is a 8600 kD peptide that is involved in the targeting of proteins undergoing cytosolic proteolysis. During this process, proteins to be degraded are first bound by the covalent attachment of multiple ubiquitin molecules which marks them as targets for degradation (Lecker *et al*, 1999; Saini *et al*, 2006). Muscle protein breakdown depends on two critical events: (i) the cleavage of actinomyosin/myofibrils (process by which actomyosin complexes or myofibrils are broken down to 14 kD monomeric actin or myosin) by caspase-3, resulting in substrates required

by the ubiquitin-proteosome pathway and (ii) the increased expression of muscle specific ubiquitin ligases (Hu *et al*, 2007; Li *et al*, 2005). Proteins degraded via this mechanism usually involve the action of three distinct components: E_1- ubiquitin activating enzyme, E_2- ubiquitin conjugating enzyme and E_3- ubiquitin protein ligase (Li *et al*, 2005; Zhang *et al*, 2007; Glass, 2005; Kandarian *et al*, 2006; Granado *et al*, 2006).

Ubiquitin modification is an ATP (adenosine triphosphate)-dependent process beginning with the activation of ubiquitin itself via bond formation with E_1. ATP hydrolysis causes the formation of an acyl-adenylate intermediate, binding to the liberated AMP (adenosine monophosphate) with the carboxyl-terminal carboxyl group of glycine in ubiquitin. This renders ubiquitin to be highly reactive (Glickman *et al*, 2002). The adenylate carboxyl group then forms a thioester link with a cysteine residue in E_1 (Lecker *et al*, 1999; Tisdale, 2005). Activated ubiquitin is then transferred to the active cysteine site of the second enzyme, the ubiquitin carrier (E_2). The E_2 ubiquitin ligases are found in skeletal muscle but it is only the 14 kD E_2 that is activated during muscle proteolysis (Tisdale, 2005). The E_2s have a very limited capacity to transfer the activated ubiquitin to some proteins but *in vivo* they serve as ubiquitin carriers, a process catalyzed by the E_3 ligases. Studies by Lecker *et al* (1999) and Hesselgren *et al* (1997) have shown that conjugation has been regarded as the rate limiting step in the regulation of this pathway (Saini *et al*, 2006). The E_3 ubiquitin ligases, a family of enzymes that catalyze this transfer of activated ubiquitin to a lysine residue on the substrate, are a specific class of proteins that play a critical role in determining which proteins are to be degraded by the 26S proteosome (Zhang *et al*, 2007; Li *et al*, 2005; Lecker *et al*, 1999). These E_3 ligases are viewed as the primary determinants of substrate specificity and are able to recognise various structural motifs and specific domains such as amino terminal residues of the substrates, phosphorylation and the “destruction box” respectively. The E_3 proteins also contain binding sites for the substrate E_2, and at least one binding site for the ubiquitin molecule.

Two novel muscle-specific E_3 ligases have been identified and seem to be significantly upregulated more than the other components of this pathway. These include the muscle atrophy F-box (MAFbx) and the muscle RING finger-1 (MuRF-1) and their expression is increased in catabolic conditions that ultimately result in muscle loss (Glass, 2007; Bodine *et al*, 2001; Zhang *et al*, 2007; Jackman *et al*, 2004; Li *et al*, 2000 and 2005; Di Marco *et al*, 2005). This suggests that these E_3 ligases may prove to be potential targets for therapeutic intervention. MAFbx, also known as Atrogin-1, contains an F-box domain, uniquely characteristic of

proteins that belong to a family of E_3 ubiquitin ligases called the SCF (Skp, Cullin, F-box containing complex) ubiquitin-ligase complex. The SCF complex is so named because it involves stable interactions with Skp1, Cullin1 and one of the many F-box containing proteins (Fbps) (Bodine *et al*, 2001; Zhang *et al*, 2007). The mRNA for MAFbx rises eight to forty fold in all types of atrophy studied thus far and this increase is said to precede the onset of weight loss. MuRF-1 on the other hand encodes a structural protein which contains the following three canonical domains: a RING-finger domain required for ubiquitin-ligase activity, a "B-box", and a coiled-coil domain required for the activation of heterodimers between MuRF-1 and a related protein, MuRF-2 (Bodine *et al*, 2001; Zhang *et al*, 2007). This outcome implies that these muscle specific ligases play an important role in muscle atrophy even though their substrates are unknown. Therefore, further studies are required to better understand their roles in muscle atrophy. Studies conducted on knockout animals lacking either MAFbx or MuRF-1 revealed a decrease in the rate of muscle degradation after denervation (Bodine *et al*, 2001). Although the bulk of myofibrillar protein degradation exhibited during muscle atrophy occurs via the ATP-dependent ubiquitin-proteosome pathway, it is however not the only proteolytic system implicated in muscle atrophy due to disuse or disease. The cytosolic calcium-dependent calpain system and the lysosomal proteases (cathepsins) are the other two known proteolytic systems (Figure 1.5). The relative contribution of each of the three major proteolytic systems to skeletal muscle atrophy is yet to be determined. But it appears that these systems work in pairs during muscle protein degradation rather than one specific system being utilised (Jackman *et al*, 2004).

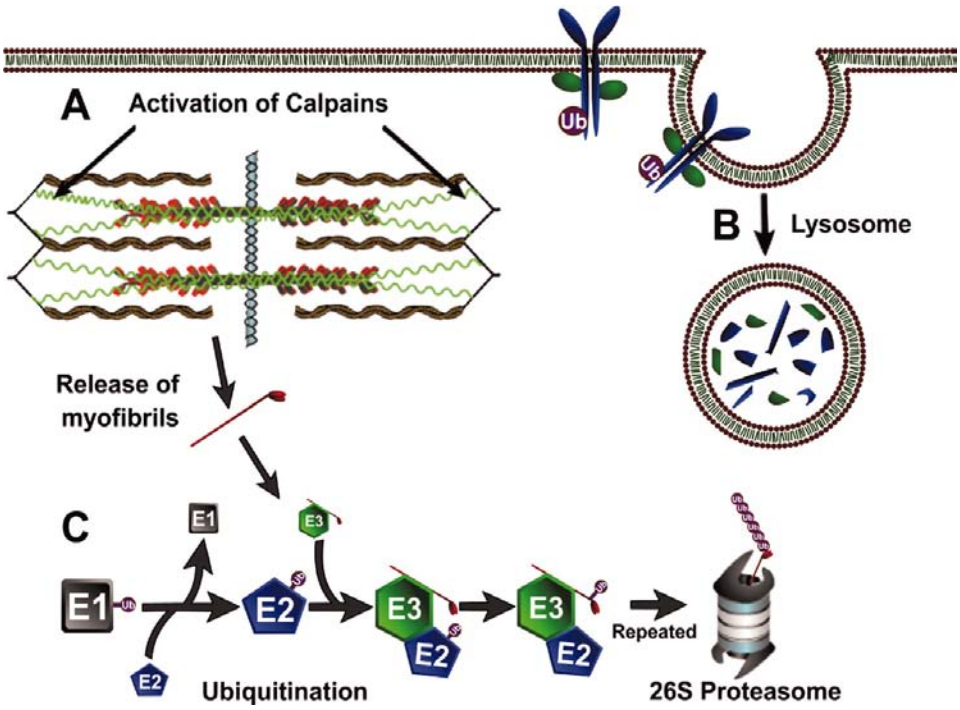

Figure 1.5: The three known proteolytic systems implicated in skeletal muscle atrophy. (A): the calcium-dependent calpain system, (B): the lysosomal protease system (cathepsins) and (C): the ubiquitin-proteosome system (Jackman *et al*, 2004)

1.4 *TNF-α and the NF-κB pathway*

Circulating TNF-α levels are elevated in a wide variety of conditions including rheumatoid arthritis, diabetes, obesity, cancer and chronic inflammatory diseases in which skeletal muscle proteolysis presents a lethal threat to patients (Li *et al*, 2000 and 2005; Peterson *et al*, 2006). This has attracted much attention to TNF-α which induces necrosis in some tumor types while it stimulates the growth of others. This cytokine has also shown increased expression in lipid overloaded tissues. Since its discovery in the mid-1970s by Carswell *et al* (1975) in an attempt to identify factors responsible for necrosis of sarcoma Meth A as well as an endotoxin-induced serum factor, the number of studies related to its precise function has increased exponentially (Atish *et al*, 2006; Peterson *et al*, 2006). In addition TNF-α is an important stimulator of the so called ’second wave’ cytokines such as IL-6 and other chemokines. There is increasing evidence that TNF-α may play a critical role in skeletal muscle atrophy in a number of clinical settings (Dirks *et al*, 2006; Dehoux *et al*, 2007; Vescovo *et al*, 2006). Direct evidence that elevated serum and/or muscle TNF-α concentrations promote muscle catabolism was first obtained from studies of animals treated with exogenous TNF-α, transgenic animals

that over expressed TNF-α, and animals with experimental diseases (Li *et al*, 2005). In an attempt to elucidate the signalling mechanisms by which TNF-α may promote muscle catabolism, the majority of previous investigations have studied how TNF-α influences cultured skeletal muscle cells (Peterson *et al*, 2006; Li *et al*, 2000 and 2005; Di Marco *et al*, 2005).

TNF-α is a popular known stimulator of a multifaceted assortment of post-receptor signalling events that induce pleiotropic, cell-type-specific responses. Three major pathways have been indicated to mediate these cellular responses. The first pathway appears to evoke apoptosis through interaction with the TNF-α receptor complex and the Fas-associated protein with their death domain. The second pathway seems to induce and activate the c-Jun-N-terminal-kinases (JNK) as well as the transcription factor, AP (activator protein)-1. The third pathway triggers NF-κB stimulation, the principal moderator of transcription and one of the chief candidates for catabolism (Reid *et al*, 2001). TNF-α is a potent stimulator of the NF-κB pathway and can induce catabolic actions in different ways (Kandarian *et al*, 2006). Possible mechanisms include the direct action of TNF-α on skeletal muscle to induce catabolism or by indirectly modifying the hormones that regulate protein turnover such as IGF-1 or simply by just inducing anorexia (Granado *et al*, 2006). The catabolic effect induced by TNF-α on skeletal muscle is evident. A study conducted in our laboratory demonstrated that increased TNF-α levels in the blood of obese rats is associated with the activation of the NF-κB pathway ultimately leading to muscle atrophy (unpublished data). Animals infused with increasingly high TNF-α concentrations also exhibited significant muscle wasting. TNF-α signalling is mediated through its two sarcolemmal receptors, TNF-R1 (or p55 in rodents, p60 in humans) and TNF-R2 (or p75 in rodents, p80 in humans) (Qi *et al*, 2000) which then cause the activation of NFκB. Genetically altered mice lacking TNF-R1 and further implanted with cachexia-inducing tumors which produce TNF-α, demonstrate significantly lower muscle atrophy compared to their control counterparts. These data insinuate that TNF-α undeniably stimulates substantial muscle wasting *in vivo*, and signalling events initiated by TNF-R1 may be responsible for these effects. In response to TNF-α, activation of the apoptotic pathway and/or elevated myofibrillar protein degradation appears to be the probable causes of muscle degradation.

The NF-κB family of transcription factors mediate a series of processes depending on the cell type and upstream triggers. This transcription factor has appealed to extensitive attention in many areas of research based on the following facts:

1. its atypical and rapid regulation,
2. its broad variety of genes that it manipulates,
3. its essential role in immunological processes (Celec, 2004),
4. the intricacy of its subunits and
5. its noticeable contribution in many diseases (Baldwin Jr., 1996)

The family consists of 5 members namely: c-Rel, Rel B, p65 (Rel A), p50 and p52. p50 and p52 are derived from the processing of p105 and p100 respectively and can form homodimers that undergo nuclear translocation. Upon TNF-α exposure, the classical NF-κB pathway is activated. Activation of this pathway is tightly regulated by the inhibitory protein IκB kinase (IKK). The IKK complex phosphorylates IκBα on Ser^{32} and Ser^{36}, leading to their polyubiquitination and subjection to proteosomal degradation. This results in the translocation of NF-κB dimers to the nucleus, binding to specific DNA (deoxyribonucleic acid) sites and regulating the expression of many target genes. In this case the many target genes that are transcriptionally upregulated include the E_3 ligases, MAFbx and MuRF-1 (Li *et al*, 2005; Zhang *et al*, 2007; Jackman *et al*, 2004). p50 and p52 are derived from the processing of p105 and p100 respectively. These NF-κB family members are able to form homodimers that undergo nuclear translocation. During disease however, this classical NF-κB pathway forms heterodimers (p65/p50) that translocate to the nucleus. An alternate NF-κB pathway speculated to be triggered in disuse atrophy involves the homodimers (p50/p50) rather than heterodimers, which bind to a nuclear IκB family member, Bcl-3, before translocation to the nucleus can take place (Figure 1.6) (Zhang *et al*, 2007; Jackman *et al*, 2004; Hunter *et al*, 2002). Activation and nuclear translocation of NF-κB in skeletal muscle cells is a prompt, dose-dependent response which peaks within 30 minutes of TNF-α exposure and then rapidly perishes. This momentary stimulus leads to modified gene expression thus causing extended changes of protein levels (Reid *et al*, 2001).

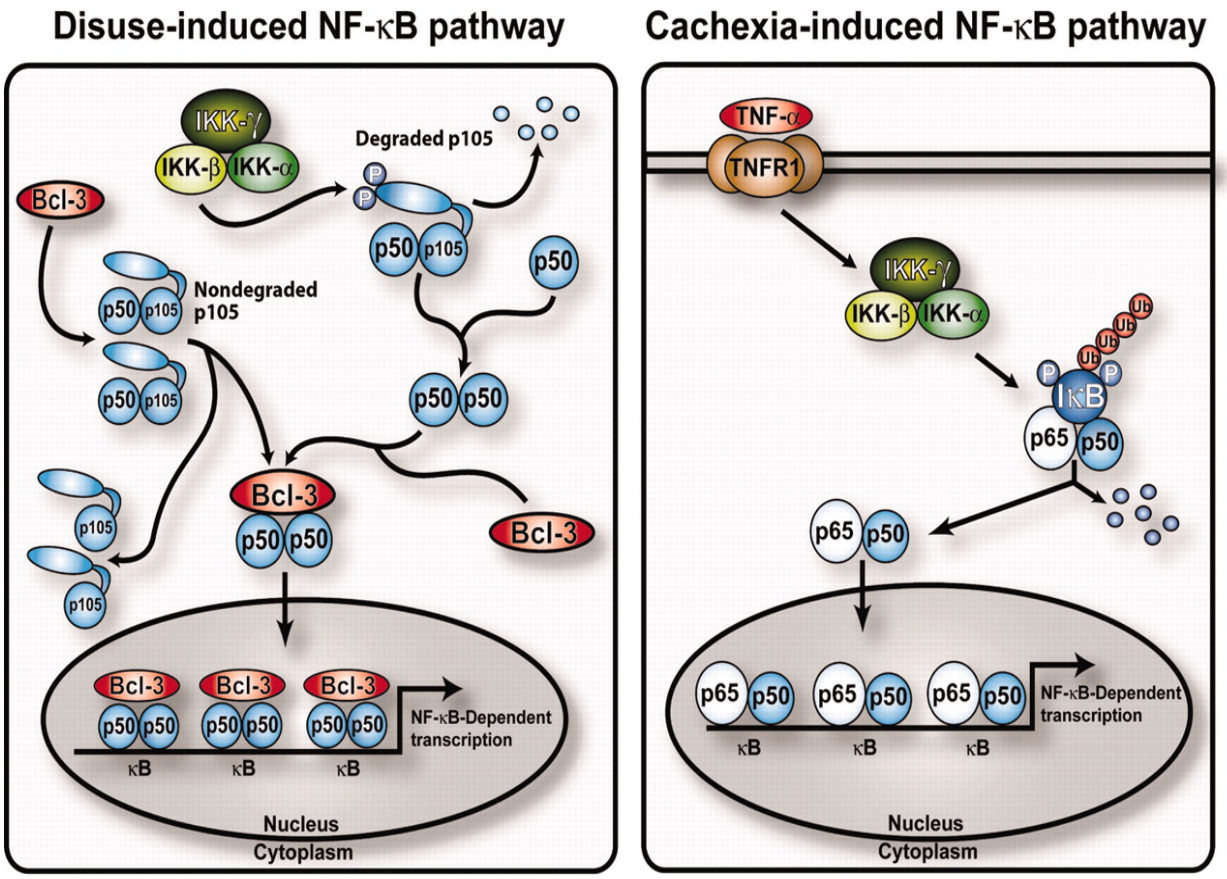

Figure 1.6: The proposed pathways that may be activated during disuse- and cachexia-induced skeletal muscle atrophy. The NF-κB pathway being central to these two types of atrophy, requires p50 (derived from the processing of p105) and Bcl-3 for disuse-induced atrophy and p65 (Rel A) for cachexia-induced atrophy. There are many target genes including members of the ubiquitin proteosome pathway. TNF-R1, TNF receptor 1 (Jackman *et al*, 2004)

Although NF-κB may be activated by either receptor, data suggests that TNF-R1 rather than TNF-R2 is the receptor subtype which is responsible for the stimulation of muscle protein loss (Llovera *et al*, 1998). There is no direct evidence linking the involvement of TNF-α or inflammatory molecules with disuse atrophy, but the NF-κB/IκB transcription factors appear to be the favourable candidates. The specific NF-κB transcription factor complexes involved in the two types of atrophy are distinct and this is important because it implies that there are definite differences in the molecular signalling of these two types of atrophy and thus there may be more specific molecular targets for the possible development of therapies.

1.5. *The relationship between oxidative stress (ROS) and TNF-α*

Dioxygen (O_2; molecular oxygen) is vital for the survival of all aerobic organisms. The metabolism of aerobic energy is solely dependent on the process of oxidative phosphorylation (Thannickal *et al*, 2000). This complex process serves as the third, and quantitatively the most essential mechanism by which energy derived from fuel molecules can be transferred to ATP. There is a basic and simple principal behind this pathway: Energy that is transferred to ATP is derived from the energy released when hydrogen atoms combine with molecular oxygen to form water. The source of hydrogen occurs via a multicomponent NADH (nicotinamide adenine dinucleotide reduced) dehydrogenase enzymatic complex which includes coenzymes generated by the Krebs cycle and glycolysis (Vander *et al*, 1998). Highly reactive and momentary molecular oxygen derivatives can be formed during this and other electron transfer reactions. These derivatives include hydrogen peroxide (H_2O_2) and the free radicals superoxide anion (0_2^-) as well as the hydroxyl radical (OH), formed in the presence of transition metal ions. "Reactive oxygen species" (ROS) as they are often referred to as, have higher reactivities than molecular oxygen and present a persistent risk to cells living in an aerobic environment, as they can result in severe damage to lipids, proteins and DNA thus resulting in cellular injury, and in extreme conditions to cell death (Thannickal, *et al*, 2000; Martindale *et al*, 2002; Powers *et al*, 2007). Cells possess several defence systems to protect against and combat the potentially destructive effects of ROS. These defence systems include the enzymatic scavengers of ROS such as catalase, superoxide dismutase (SOD) (which reduces O_2^- to H_2O_2), glutathione peroxide (which reduces H_2O_2 to O_2) as well as various non-enzymatic molecules including Vitamin A, C and E, flavenoids and glutathione (Thannickal *et al*, 2000; Martindale *et al*, 2002; Andreyev *et al*, 2005; Ferreira *et al*, 2008). Unfortunately, these defence systems are not always sufficient to neutralize the production and accumulation of ROS. When ROS production in the cells exceeds the antioxidant capacity to eliminate these oxidants, a state of oxidative stress occurs (Powers *et al*, 2007; Thannickal *et al*, 2000).

Investigations of the cell signalling pathways that regulate muscle atrophy have increased our knowledge and the understanding of this complex process. Emerging evidence indicates oxidative stress is a key regulator of the cell signalling pathways (Figure 1.7) leading to increased muscle catabolism due to prolonged periods of disuse (Saini *et al*, 2006; Martindale *et*

al, 2002). This observation has been confirmed by various other studies which implicate mitochondrial dysfunction in hindlimb unloading (Powers *et al*, 2005; Kondo *et al*, 1992; Appell *et al*, 1997) and atrophying mouse muscle from Amyotrophic lateral Sclerosis (ALS) transgenic mice (Muller *et al*, 2007; Mahoney *et al*, 2006). Muscle atrophy caused by unloading or immobilization results in the upregulation of Cu (Copper), Zn (Zinc), superoxide dismutase, glutathione peroxide and Mn (Manganese) superoxide dismutase, all of which represent systems that would normally act to metabolise increases in ROS production as stated in the previous paragraph. Previously, it was believed that ROS production was strictly confined to non-contracting skeletal muscle and that oxidative injury does not occur in inactive muscles but the revolutionary work of Kondo *et al* (1991) proved otherwise. This work also showed that disuse muscle atrophy can and may be delayed by exogenous antioxidants (Kondo *et al*, 1991).

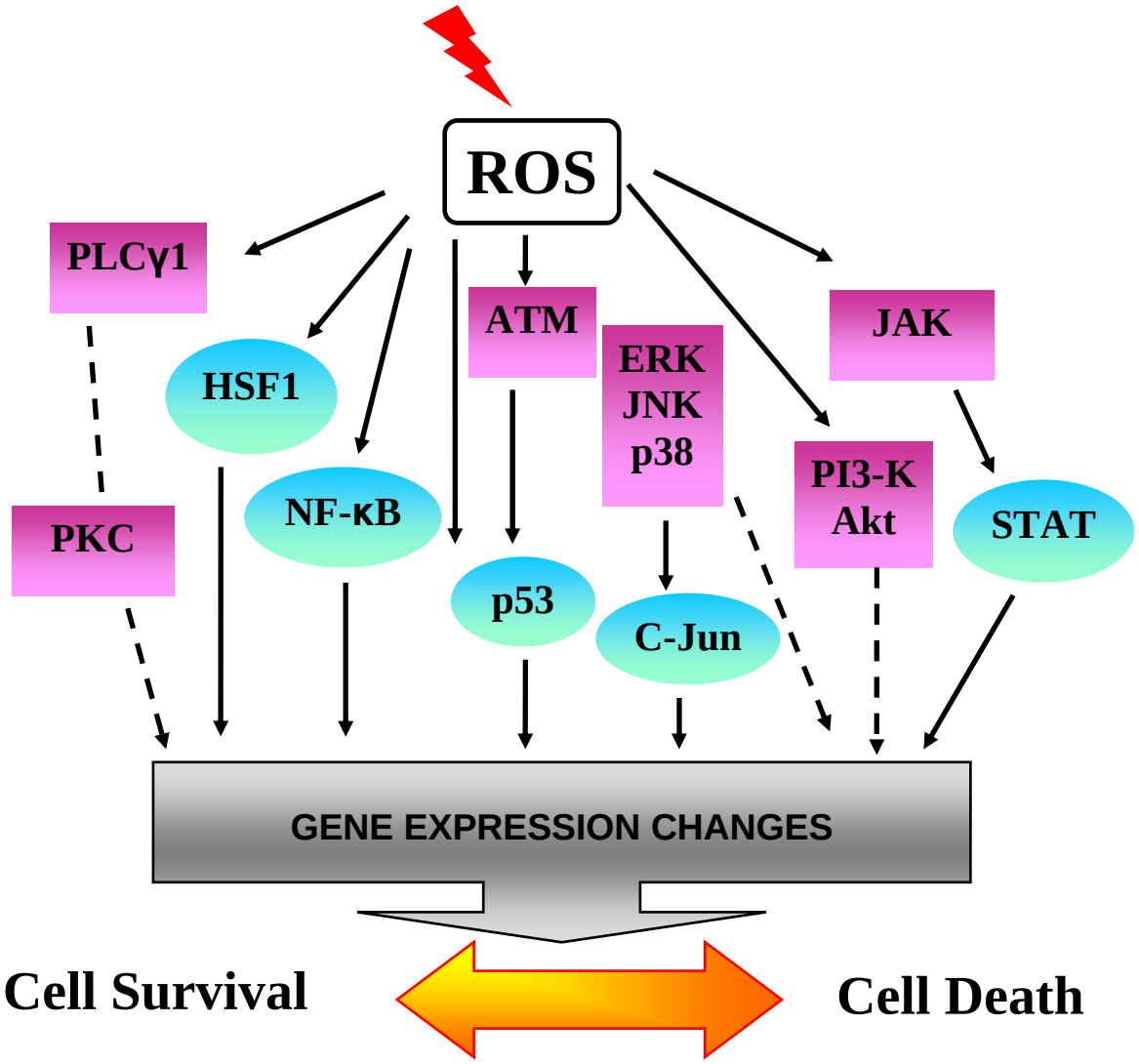

Figure 1.7: Oxidative stress induces a wide variety of cellular reactions and activates a number of key signalling pathways. These responses depend on the severity of the damage, which is further influenced by the type of cell, the magnitude of the dose as well as the duration of the exposure. Highly reactive ROS can directly or indirectly modify the functions of many enzymes (in boxes) and transcription factors (in ovals) through a multitude of signalling cascades. Eventually this will result in changes in gene transcription which manipulates the ability of the cell to survive or die. ATM, ataxia-telangectasia mutated; ERK, extracellular signal-regulated kinases; HSF1, heat shock transcription factor 1; JAK, Janus protein kinase; JNK, c-Jun N-terminal kinases; NF-κB, nuclear factor-κB; PI3-K, phosphotidylinositol 3-kinase; PKC, protein kinase C; PLC-γ1, phospholipase C-γ1; STAT, signal transducers and activators of transcription. (Adopted from Martindale *et al*, 2002)

Currently it is unknown which pathways responsible for ROS production are the governing contributors of inactivity-induced oxidative injury in skeletal muscle though it may be plausible that oxidative stress in inactive skeletal muscle is caused by the interaction of several dominant oxidant production processes. These would include xanthine oxidase (being the most comprehensively studied), aldehyde oxidase, nitric oxide synthase, dihydroorthotate dehydrogenase, NADPH (nicotinamide dinucleotide phosphate) oxidase and flavoprotein dehydrogenase (Thannickal *et al*, 2000; Powers *et al*, 2005). What intracellular signalling pathways link oxidative stress to muscle atrophy? A complete and thorough answer to this question is not available at this point in time but it emerges that oxidative stress plays a role in disuse muscle atrophy by manipulating one or more of the following pathways: (i) the adaptation of cytosolic calcium levels and consequently activation of calpain, (ii) the regulation of MAPK (mitogen activated kinase) signalling and (iii) activation of the NF-κB pathway (Cuschieri *et al*, 2005; Kabe *et al*, 2005; Pantano *et al*, 2006; Pearson *et al*, 2001; Qi *et al*, 2005). Activation of the NF-κB pathway by TNF-α binding to sarcolemmal surface receptors appears to be dependent on TNF-α-induced ROS production, evidently released from the mitochondrial electron transport (Zhang *et al*, 2007; Li *et al*, 2000 and 2005; Jackman *et al*, 2004). TNF-stimulation then increases redox-sensitive transcription factors and protein kinases. This causes rapid conjugation of ubiquitin to muscle proteins following IκB-α proteosomal degradation and translocation of activated NF-κB to the nucleus. Studies by Li *et al* (1998) and Gomes-Marcondes *et al* (2002) suggest that components of the ubiquitin-proteosome pathway are transcriptional targets of ROS (Li *et al*, 1998; Jackman *et al*, 2004). Furthermore, ROS production is not induced by TNF-α alone. Treatment of skeletal muscle myotubes with H_2O_2 resulted in ROS production (Li *et al*, 2005) as well as the activation of the forkhead box (FOXO) family of transcription factors. The forkhead family contains three members, namely: FOXO-01 (FKHR), FOXO-03 (FKHRL-1) and FOXO-04 (AFX), which are suspected to play a role in the regulation of target genes involved in cell cycle progression, metabolism and apoptosis (Zhang *et al*, 2007). Dephosphorylation of FOXO factors causes nuclear translocation resulting in growth attenuation and apoptosis. In severe pathological conditions such as diabetes, FOXO-01 is significantly upregulated in skeletal muscle and enhanced expression of MAFbx/Atrogin-1 and MuRF-1 genes is observed. This suggested that the increased protein loss contributed to loss of muscle mass (Kamei *et al*, 2003 and 2004).

Given that most of the treatments used to activate NF-κB also stimulate ROS production, and antioxidants are able to hinder NF-κB activation in response to such stimuli, ROS were formerly linked as the principal mediators of NF-κB activation. Present studies have however been unsuccessful in defending this theory. On the whole, the most significant conclusions to these studies are that (i) activation of NF-κB by H_2O_2 appears to be cell type specific, (ii) in many occurrences, increases in ROS is not necessary for NF-κB stimulation and (iii) antioxidants are able to inhibit the activity of NF-κB through mechanisms that are apparent from redox regulation (Martindale *et al*, 2002). Even so, in specific cell types, oxidative stress is a powerful inducer of NF-κB and this consequence is vital for cell survival. These experiments and others imply that NF-κB activation is a novel mechanism by which ROS may trigger cytokine induced muscle wasting.

1.6. *IGF-1/PI-3K/Akt/mTOR pathway*

Virtually all conditions accelerating skeletal muscle atrophy are usually associated with a defective PI3-K/Akt signalling pathway and decreased PI-3K-generated phosphatidylinositol-3,4,5-triphosphate (PIP_3) (Hu *et al*, 2007). Over the past 5 years, a prominent growth pathway, IGF-1/PI-3K/Akt, has been shown to play a dominant role in muscle hypertrophy (Saini *et al*, 2006; Glass, 2003; Kandarian *et al*, 2006; Hu *et al*, 2007; Latres *et al*, 2004). The binding of IGF-1 induces a conformational change in the receptor tyrosine kinase, resulting in its transphosphorylation and subsequent phosphorylation of the insulin receptor substrate-1 (IRS-1). This in turn results in the activation of a key anabolic signalling molecule-PI3-K (phosphatidylinositol 3-kinase). Activation of this lipid kinase, PI3-K results in the phosphorylation of the membrane phospholipid phosphatidylinositol-4, 5-biphosphate (PIP_2) to PIP_3 (Latres *et al*, 2004; Zhang *et al*, 2007), thus creating a lipid membrane-binding site for a serine/threonine kinase-Akt (also called PKB for protein kinase B) (Glass, 2003; Saini *et al*, 2006; Latres *et al*, 2004). Akt is then phosphorylated after translocation to the membrane by the kinase, phosphoinositide-dependent $kinase_1$ (PDK_1). Once activated, Akt phosphorylates an ever increasing array of substrates, including proteins that block apoptosis or mediate protein synthesis, gene transcription and cell survival (Saini *et al*, 2006; Glass, 2003; Stitt *et al*, 2004). Of the proteins operating downstream of Akt, is mammalian target of rapamycin (mTOR), an intermediate between PI3-K and p70S6 kinase (p70S6K). Activated Akt would then phosphorylate and activate mTOR resulting in an increase in protein translation via two

pathways: first mTOR stimulates p70S6K, a positive regulator of protein translation; second, mTOR inhibits the activity of PHAS-1 (phosphorylated heat- and-stable protein, also known as 4E-BP1), a negative regulator of the protein initiator factor eIF-4E (Saini *et al*, 2006; Glass, 2003; Stitt *et al*, 2004) (Figure 1.8).

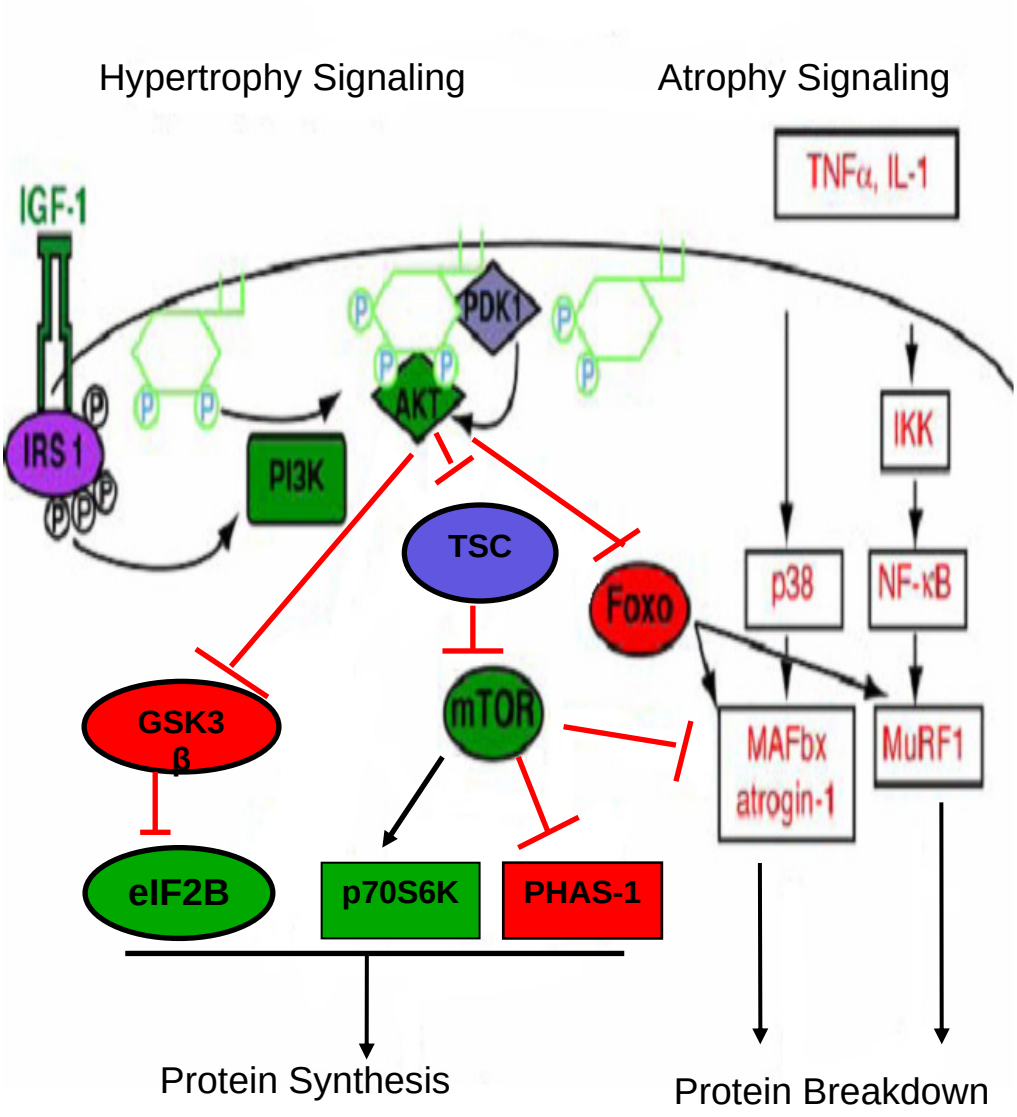

Figure 1.8: The IGF-1/PI3-K/Akt signalling pathway induces protein synthesis and blocks atrophy pathways. On the left, signalling molecules that have been shown to negatively affect hypertrophy are coloured in red and the proteins known to induce to hypertrophy when activated are coloured in green. On the right, various different stimuli can induce skeletal muscle atrophy. Pictured here is TNF-α, a known inducer of the NF-κB pathway. This transcription factor (NF-κB) is required for utmost atrophy resulting in the upregulation of two E_3 ubiquitin ligases MuRF-1 and MAFbx. Activation of Akt however, inhibits the upregulation of MuRF-1 and MAFbx via the inhibition of FOXO, a family of transcription factors as well as by a sec-

ond mechanism further downstream of mTOR. GSK, glycogen synthase kinase 3 beta; TSC, tuberous sclerosis complex; mTOR, mammalian target of rapamycin; PI3-K, phosphotidylinositol 3-kinase (Glass, 2003)

Various lines of evidence have made a critical connection between the deactivation of the IGF-1/PI3-K/Akt pathway and proteolytic activity and the expression of proteolytic genes (Ozes *et al*, 2001; Zhang *et al*, 2007; Hu *et al*, 2007; Lee *et al*, 2004). Muscle atrophy induced via serum deprivation in L6 myotubes showed suppressed PI3-K activity, consequently decreased Akt phosphorylation and increased actin cleavage. Both effects were reversed in the presence of insulin (Kandarian *et al*, 2006). Another mechanism by which PI-3K activity is suppressed in catabolic conditions is demonstrated in insulin resistance due to the phosphorylation of the serine residue instead of the tyrosine residue. This phosphorylation impairs the docking of IRS-1 with PI3-K to debilitate PI3-K/Akt activity (Lee *et al*, 2004). These changes have been attributed to TNF-α and could apply to many catabolic states associated with elevated TNF-α levels (Li *et al*, 2007; Li *et al*, 2005). Pharmacological blockade of PI3-K activity with the PI3-K inhibitor LY294002 (LY) further decreases Akt phosphorylation and thus IGF-1 induced hypertrophy (Latres *et al*, 2004). mTOR, so-named because of its inhibition by rapamycin, has been pharmacologically demonstrated to be required for mTOR-mediated signalling in hypertrophy and is thought to play a role when chronically deactivated, in the progression of muscle atrophy. Similarly, deactivation of p70S6K by rapamycin but not Akt, leads to the inhibition of hypertrophy *in vivo* (Glass, 2003; Kandarian *et al*, 2006; Latres *et al*, 2004). In addition, the absence of growth or survival factors in various cell types causes deactivation of Akt and resulting in FOXO dephosphorylation. As mentioned previously, FOXO localizes to the nucleus to activate genes involved in cell cycle inhibition, cell death and metabolism. But when Akt is activated, FOXO is phosphorylated and bound by 14-3-3 proteins in the cytoplasm that prohibit entry to the nucleus (Kandarian *et al*, 2006). These data demonstrate the direct effects of a depressed PI3-K/Akt/ mTOR and FOXO pathway on atrophy-induced augmentation in proteolytic gene expression and protein catabolism, required for normal skeletal muscle atrophy. This is a vital point as it shows that decreased PI3-K/Akt signalling in muscle proteolysis not only cripples protein synthesis, but leads to an intensified protein degradation rate, actinomyosin cleavage and expression of proteolytic genes *in vivo* and *in vitro*.

1.7. *Inhibition of Akt signalling by lipid phosphatases*

Previous experimental studies on the role of inactivated PI3-K/Akt on proteolytic genes and proteolytic processes during atrophy have provided pivotal insight in PI-3K/Akt involvement in the atrophy process. In the case of Akt however, its activation can be controlled by regulating the levels of lipid-binding site PIP_3 (Beguinot, 2007; Saini *et al*, 2006; Yoo *et al*, 2006; Hu *et al*, 2007). PIP_3 is dephosphorylated by two lipid phosphatases, PTEN (phosphatase and tensin homologue on chromosome 10) and SHIP (SH2-domain-containing inositol 5' phosphatase, which has two forms, SHIP1 and SHIP2) (Glass, 2003; Saini *et al*, 2006). PTEN, also known as MMAC1 or TEP1, is a tumor suppressor gene that is inactivated in many common malignancies (Mayo *et al*, 2002; Beguinot, 2007; Yoo *et al*, 2006; Hu *et al*, 2007). It (PTEN) encodes for both lipid and protein phosphatases that represent an important 3-phosphatase in the PI3-K/Akt signalling pathway (Beguinot, 2007). PTEN dephosphorylates PIP_3 at the D3 position of the inositol ring to produce an inactive PIP_2, thus serving as a major regulator of the PI3-K/Akt pathway (Mayo *et al*, 2002; Yoo *et al*, 2006; Ozes *et al*, 2001). PTEN ablation results in the inactivation of Akt and subsequently a decrease in cell size (Glass, 2003). Other studies have reported that tissue specific ablation of PTEN plays a critical role in insulin sensitivity as well as metabolic regulation (Beguinot, 2007; Wijesekara *et al*, 2005). A possibility that an endogenous mechanism that changes the activity of PTEN to regulate changes in protein turn-over has been raised because PTEN varies in many catabolic conditions. This is supported by the fact that high fat diet-induced insulin resistance increases insulin resistance via p38-MAPK stimulation. In addition, muscle-specific PTEN can be down-regulated via posttranslational modification. Torres *et al* (2003) suggested that attenuation of PTEN is feasible because caspase-3 is able to cleave the carboxyl (COOH-) terminus of PTEN thus decreasing PTEN expression. Another mechanism proposed by Birle *et al* (2002) that could decrease PTEN, is the stabilization by PIP_3-induced PKC (protein kinase C) phosphorylation, indicating the ability of insulin deficiency to reduce PTEN stability, resulting in PTEN degradation. Interestingly, partial deletion of PTEN counteracts insulin deficiency-induced atrophy. Suppression of actinomyosin cleavage and increasing phosphorylated FOXO, which decreases the expression of ubiquitin ligases and reduces protein catabolism via the ubiquitin proteosome pathway, appears to be the mechanism involved to augment muscle proteolysis (Hu *et al*, 2007).

1.8. *Muscle proteolysis and apoptosis*

A closely related area of investigation on muscle protein breakdown during atrophy is the interaction of the ubiquitin-proteosome pathway and caspases. Apoptosis is an active and physiological mode of cell death in which the cell designs and executes the program of its own demise and subsequent disposal. Caspases accomplish cell death in response to various stimuli including cytokines such as TNF-α, by the well organised annihilation of the cell's own repair mechanisms. The majority of muscle proteins exists in actinomyosin complexes and myofibrils, and in many catabolic conditions, some of the contractile proteins from these complexes are degraded by the ubiquitin-proteosome pathway (Du *et al*, 2004). Although the sequence of events leading up to muscle atrophy remain obscure, an impaired PI3-K activity appears to be the major influence controlling both apoptosis and muscle proteolysis (Lee *et al,* 2004; Du *et al*, 2004; Kandarian *et al*, 2006). The notion that caspase-3 activation is involved in the initial steps of myofibrillar protein degradation was suggested because recombinant caspase-3 could increase actin fragmentation of purified actinomyosin in L6 cell lysates and of whole muscle (Du *et al,* 2004). This was further confirmed by the fact that Solomon and Goldberg (1996), who had constructed a reconstituted system containing components of the ubiquitin-proteosome system, showed that the ubiquitin-proteosome system only degrades monomeric actin or myosin but not actinomyosin complexes (Du *et al*, 2004; Kandarian *et al*, 2006). Lee *et al* (2004) showed that the upregulation of apoptotic signals related to suppressed PI3-K activity results in the activation of a pro-apoptotic protein Bax (Bcl-associated partner containing six exons), leading to cytochrome c release from the mitochondria and eventually activation of caspase-3 (Lee *et al,* 2004). The connection between these two processes (proteolysis and apoptosis) in support of this relationship is insulin resistance due to TNF-α responses. Therefore, this mechanism may apply to many catabolic conditions linked with elevated TNF-α levels. The binding of TNF-α to its receptor, TNFR1, which possesses an analogous cytoplasmic death domain known as the TNFR1 associated death domain (TRADD), is responsible for the apoptosis signal. Activated TRADD mediates apoptosis through binding with Fas associated death domain (FADD). FADD contains in addition a death effector domain (DED) that binds to pro-caspase-8 leading to its oligomerization and thus activation to caspase-8 by self-cleavage. Caspase-8 then activates its downstream effector caspase-3 which initiates apoptosis. The release of cytochrome C from the mitochondria into the cytosol however is also believed to be the initial step in the initiation of apoptosis.

Upon release from the mitochondria, cytochrome c forms a complex with pro-caspase-9, apoptosis protease activation factor-1 (Apaf-1) and deoxyadenosine triphosphate (dATP) to form what is called the apoptosome. Once the apoptosome has been formed, pro-caspase-9 cleaves and activates itself which then converts pro-caspase-3 to the active enzyme caspase-3, which is the effector protease that proceeds to degrade most of the cellular targets (Saini *et al*, 2006; Dirks *et al*, 2006; Dupont-Versteegden, 2005). The activation of caspases subsequently leads to the reorganization of the cytoskeleton, DNA fragmentation, the disruption of the nuclear structure and finally the disintegration of the cell into apoptotic bodies.

Since most of the effects of TNF-α are mediated through its receptors, the present study will be conducted to assess the putative involvement of TNF-α on the activity of PI3-K and its downstream target the Akt serine/threonine kinase, which plays a role in the activation of the NF-κB pathway as well as the effect of PTEN on TNF-α-induced muscle wasting. Using a standardized cell culture model, we would test the **hypothesis** that increasing levels of TNF-α induces muscle proteolysis via the suppression (inhibition) of the PI3-K/Akt signalling pathway and may possibly stimulation ROS production. In order to achieve this, the hypothesis was approached by three **aims**:

1. To assess the proteolytic effects of increasing TNF-α levels *in vitro*
2. To assess the effect of TNF-α on signalling proteins in relation to muscle protein loss
3. To determine the role of ROS in our model

CHAPTER 2

2.1. Materials and Methods

2.1.1. *Experimental model (cultured myogenic cell line)*

Myoblasts derived from rat skeletal muscle (L6 cells; ATCC, Manassas, Virginia, USA) were maintained in 6-well plates containing Dulbecco's modified Eagle's medium (DMEM) supplemented with 10% heat-inactivated fetal calf serum (FCS), 1% Penstrep, 4% L-Glutamine and 0.4% Gentamicin at 37 ºC under a humidified 5% CO_2/95% O_2 atmosphere. When myoblasts were approximately 60-65% confluent (Figure 2.1.1), myotube differentiation was initiated by replacing the growth medium with differentiation medium: DMEM supplemented with 1% heat-inactivated horse serum (HS).

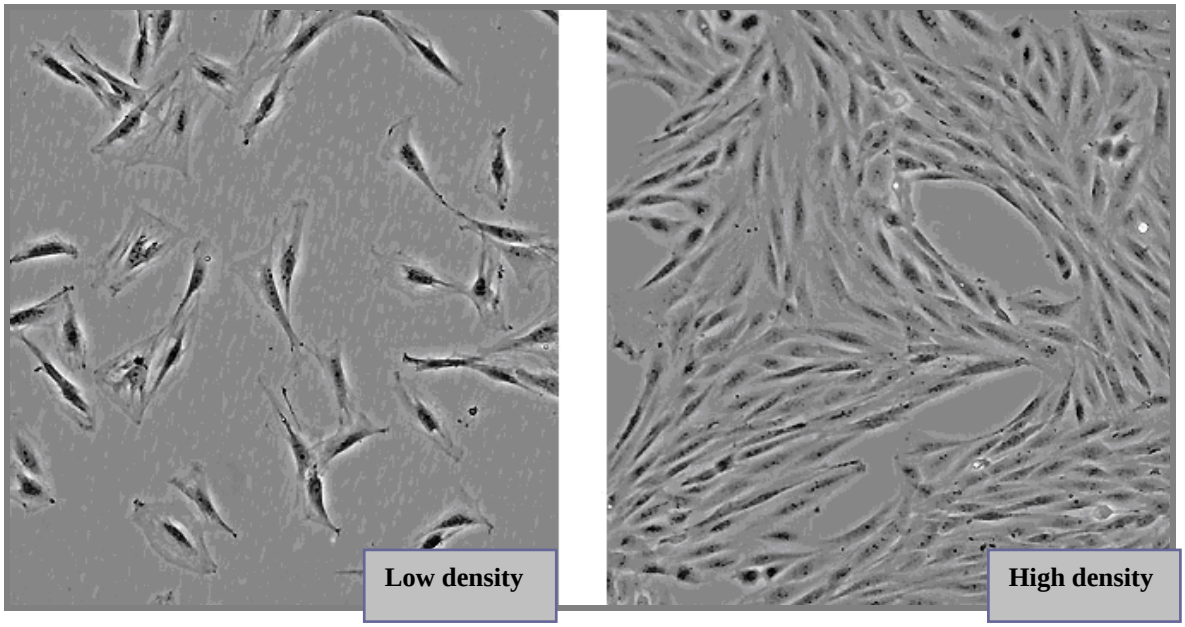

Figure 2.1.1: The L6 myogenic line shown at low (25% confluence) and high densities (80% confluence). L6 cells fuse in culture to form multinucleated myotubes as well as striated fibers.

Differentiation was allowed to continue for a period of eight days before experimentation, with changing to fresh medium every 48 hours. The muscle cells were examined for evidence of myotube formation and growth by using a light microscope (Figure 2.1.2). Cell numbers were determined following trypsinization.

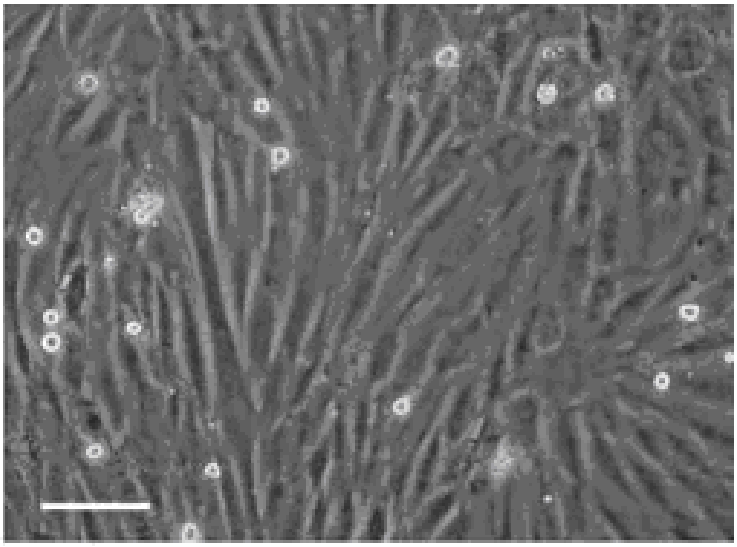

Scale bar: 45 µm

Magnification: 40X

Figure 2.1.2: Fully differentiated (8 days) L6 myotubes. The myoblastic component of the L6 cell line depletes rapidly if the cells are allowed to become confluent. Therefore, differentiation should commence at 60-65% confluency. The cells should be subcultured before they become too confluent in order to delay the loss of differentiating ability.

Myotubes were then treated with recombinant rat TNF-α (PreproTech, New Jersey, USA) by adding different concentrations of recombinant rat TNF-α to 2 ml differentiation medium for 45 minutes, 24 and 48 hours. For the 3-[4, 5-dimethylthiazol-2-yl]-2, 5-diphenyl tetrazolium bromide (MTT) assay and Trypan Blue exclusion technique, L6 myotubes were seeded onto 6-well plates (80 000). For the Western Blotting, L6 myotubes were seeded onto T25 flasks (150 000). For the Propidium Iodide and Hoechst 33342 stain however, L6 myotubes were seeded onto 18 mm diameter glass coverslips at a seeding density of 50 000 cells. All cells were studied between the ninth and twelfth passage. To avoid variability related to differences between cultures, replicate experiments were carried out using cells from separate cultures.

All experiments were conducted in triplicate and three independent experiments for were done for each parameter measured.

2.1.2. *Treatment of cells with Recombinant TNF-α*

Stock solutions of TNF-α were prepared in sterile PBS (phosphate buffered saline) and stored at -4 ºC until required for use. Fully differentiated L6 myotubes were treated and incubated for 45 minutes, 24 and 48 hours with 0, 1, 3 6 and 10 ng/ml recombinant rat TNF-α. Following treatment of cells, the differentiation medium was removed and the cells were washed gently with PBS and prepared for Western blot analysis. For control experiments, the cells were incubated with PBS only.

2.1.3. *PI3-Kinase ELISA Assay*

The production of PI(3, 4, 5)P_3 from PI(4, 5)P_2 by PI3-K is important in multiple signalling pathways. Usually, experiments to measure PI3-K activity have entailed phosphorylation of a phosphoinositide substrate using ^{32}P, followed by withdrawal of radioactive products and lastly, partitioning using thin-layer chromatography. The assay plate technique developed by Echelon Biosciences, Inc. allows the user to determine PI3-K activity by utilising either recombinant or immunoprecipitated enzymes by means of a regular ELISA (Enzyme-Linked ImmunoSorbent Assay) format thus abolishing the requirement for radioactivity, organic solvents and thin-layer chromatography.

The assay is a competitive ELISA in which the signal is inversely proportional to the amount of PI(3, 4, 5)P_3 produced. After the PI3-K reactions are complete, reaction products are first mixed and incubated with a PI(3, 4, 5)P_3 detector protein. This is then added to the PI(3, 4, 5)P_3–coated microplate for competitive binding to the plate. A peroxidase-linked secondary detector and colorimetric detection is used to detect PI(3, 4, 5)P_3 detector binding to the plate. The colorimetric signal is inversely proportional to the amount of PI(3, 4, 5)P_3 produced by PI3-K. A detailed explanation is provided in the appendix section.

2.1.4. *Assessment of cell viability (MTT Assay)*

L6 myotube viability was analysed at 24 and 48 hours post treatment via the MTT assay described by Gomez and collegues (1997). This assay is based upon the principal of reducing MTT into blue formazan pigments by viable mitochondria in healthy cells. At the end of the

experimental procedure, medium was removed from the cells, 1.5 ml PBS and 500 µl MTT (0.01 g/ml) solution was carefully added to each 6-well plate and incubated at 37 ºC for 2 hours at an atmosphere of 5% CO_2. This time period was found to be optimal for the development of colour that is associated with formazan product formation. If there were cells that have loosened, the contents were transferred to centrifuge tubes and centrifuged gently for 2 minutes at 1000 rpm. The supernant was decanted; 2 ml HCL (hydrogen chloride)-isopropanol/Triton (1% HCL in isopropanol; 0.1% Triton X-100; 50:1) solution was added to each pellet and resuspended. The resuspended cells were added back to the plates were some cells remained attached. If no cells loosened, 2 ml HCL-isopropanol/Triton solution was added to each well, covered with foil and placed on belly shaker for 5 minutes. This mechanism caused lysis of cell membranes and release of the formazan pigments. The cell suspension was transferred to 2 ml eppindorf tubes and centrifuged for 2 minutes at 1400 rpm. The optical density (OD) was determined spectrophotometrically at a wavelength of 540 nm and HCL-isopropanol/Triton solution was used as the blank. The values obtained are expressed as percentages of the control values. This viability assay was further confirmed with the Trypan Blue exclusion technique (discussed below) in which the Trypan Blue dye penetrates cells with damaged cell membranes, dyeing them blue whereas the undamaged cells retain their natural colour.

2.1.5. *Trypan Blue stain for cell viability*

After a 24 and 48 hour incubation period with the different TNF-α concentrations, myotubes were washed with warm PBS, detached from the wells using trypsin where after trypsin was neutralized using growth medium. Cell solutions from each well were centrifuged, the supernant decanted and the pellet resuspended in 500 µl PBS and 500 µl 0.4% trypan blue solution and incubated for 2 minutes at room temperature. This technique analyses the incorporation of Trypan blue entering cells with a damaged membrane, dyeing them blue (Kitakaze *et al*, 1997). The percentage of blue cells/total cells was counted using a haemocytometer. To avoid false positives, the count was performed within 5 minutes after exposure of cells with Trypan blue. Results are expressed as the percentage (%) of viable cells.

2.1.6. *Morphological Analysis of Cell Death*

For fluorescence staining, L6 myotubes were incubated with a fluorescent probe, Propidium Iodide (PI) (Roche), which was added to the cells at a concentration of 5 mg/ml in a 1:200 dilution for 20 minutes at room temperature. This probe is a red fluorescent, cell impermeable dye that is widely used to detect dead or dying cells and only penetrates the cell when the cell membrane is injured thus binding to the DNA. This would serve as an indication for necrosis. The Hoechst 33342 dye was additionally added (10 mg/ml) in a 1:200 dilution and further incubated for 10 minutes at room temperature. This dye would serve to indicate nuclear condensation and the formation of apoptotic bodies (apoptosis). The rationale for distinguishing between these two types of cell death was to test for whether the concentrations used were not toxic to the cells and if indeed cell death was taking place by which form of cell death. A third form of cell death (autophagy) which is known to take place in cells was not tested for. Images were acquired with a Nikon Eclipse E 400 microscope, equipped with ACT-1 acquisition software, using a 20X Nikon Plan Fluor objective, after the cells were fixed and mounted onto microscope slides. Once the PI dye has bound to nucleic acids, fluorescence images were visualised using a rhodamine filter (excitation at 530-560 nm and emission at 580 nm). The Hoechst dye however stains the nuclei blue and a DAPI (4',6-Diamidino-2-phenylindole) filter (excitation at 340-380 nm and emission at 430 nm) was used. A specific evaluation system was used to detect both apoptotic and necrotic cells; three randomly chosen fields per experimental condition were analysed of which all the cells (apoptotic and normal) in those fields were counted. The data was expressed as arbitrary values, transferred onto Microsoft excel and analysed statistically. The data is represented as the number of apoptotic cells/total number of cells counted X 100 (Imoto *et al*, 2006; Lacerda *et al*, 2006; Engelbrecht *et al*, 2007).

2.1.7. *Detection of Apoptosis-DNA Isolation and Fragmentation Assay*

Apoptosis was evaluated by both detection of DNA fragmentation and measurement of DNA content by incorporation of propidium iodide as previously described. For detection of DNA fragmentation, DNA from fully differentiated L6 myoblasts was first isolated as follows: cells were removed from the surface of the plate by trypsinization as previously described. The cells were pelleted and washed 3 times with cold PBS. 500 µl lysis buffer and 2 µl RNase (10

μg/ml) was then added after which the samples were incubated on a heating block at 37ºC for 1 hour. 10 μl Proteinase K (100 μg/ml) was added and placed on the heating block at 55ºC overnight. After transferring the contents into eppindorf tubes, 250 μl of Phenol and 250 μl Chloroform Isoamyl alcohol (1:1 PCI) was added, mixed gently for 5 minutes and centrifuged for 10 minutes at 10 000 rpms at 22ºC. The top layer (DNA) was removed, placed into new eppindorf tubes, 500 μl Chloroform Isoamyl alcohol was added, mixed gently for 2 minutes and centrigufed for 1 minute. DNA was once again transferred into new eppindorfs tubes and 40 μl NaCl (Sodium chloride) (5 M) and 1000 μl 100% ethanol was added. Incubation proceeded for 1 hour at -20ºC. Contents of the tubes were centrifuged at 1400 rpms for 20 minutes at room temperature. The supernatant was discarded, the pellet washed in 1000 μl 70% ethanol, mixed gently for a few seconds and centrifuged at 1400 rpms for 20 minutes at room temperature. The supernatant was discarded, the pellet air dried for 5 minutes, 40 μl TE buffer was added and let to incubated at 4ºC overnight. DNA fragmentation was subsequently analysed by 1.6% agarose gel electrophoresis in the presence of ethidium bromide.

2.1.8. *Hematoxylin and Eosin staining method*

The HE stain or hematoxylin and eosin stain, is a popular staining method in histology. The staining method involves application of the basic dye hematoxylin, which colors basophilic structures with blue-purple hue, and alcohol-based acidic eosin Y, which colors eosinophilic structures bright pink. The basophilic structures are usually the ones containing nucleic acids, such as the ribosomes and the chromatin-rich cell nucleus, and the cytoplasmatic regions rich in RNA. The eosinophilic structures are generally composed of intracellular or extracellular protein. In an effort to determine muscle fiber diameter, the cells were grown on coverslips and differentiated as previously described.

The fully differentiated cells were then treated as described where after the staining procedure was conducted as follows: After the removal of medium from the cells, the cells were washed once with sterile PBS. Xylene was added for 10 minutes after which 100%, 95% and 70% alcohol was added for 10-15 seconds respectively. The coverslips (containing cells) were hydrated in distilled water. Harris haematoxylin was added for 3 minutes, washed in distilled water and acid alcohol, blued in Scott's tap water and then eosin was added for a further 2 minutes. The coverslips were once again hydrated in distilled water and 70%, 95% and 100%

alcohol was added for 10-15 seconds respectively. Xylene was added for an additional 10-15 seconds where after coverslips were mounted on microscope slides. Cells were visualized using a Nikon Eclipse E 400 fluorescent microscope fitted with a Nikon DMX 1200 digital camera at 20X magnification. Four representative, random areas of interest for each sample were chosen to determine muscle fibre diameter. 25 muscle fibres from each area containing two or more nuclei were measured in micro molar (μm) and an average was then calculated. Approximately 250 fibres per treatment were counted.

2.1.9. *Measurement and detection of mitochondrial ROS*

To determine the source of ROS production after treatment of cells with TNF-α, the mitochondria specific fluorescent dye, MitoTracker Red CM-H_2 X ROS (Molecular Probes) was used. The reduced probe does not fluoresce until it enters an actively respiring cell, where it is oxidised to a fluorescent mitochondrion-selective probe that becomes selectively sequestered in the mitochondria (Lacerda *et al*, 2006; Imoto *et al*, 2006). ROS are not only produced in the mitochondria but also in various other cellular organelles such as the lysosome. We selected mitochondrial ROS production as this is the main source of ROS production within the cell and experimental investigations imply that increasing levels of TNF-α may stimulated increased ROS production. The L6 myotubes were grown in 35 mm Petri dishes and differentiated as previously described. The fully differentiated myotubes were treated and then stained with MitoTracker Red CM-H_2 X ROS at a concentration of 100 nM for 1 minute at 37ºC. The Petri dish was placed onto a microscope and the cells visualised using a Nikon Eclipse E 400 fluorescent microscope fitted with a Nikon DMX 1200 digital camera at 20X magnification. An image was captured using Simple PCI software (Compix Inc, Imaging Systems, Pennsylvania, USA) after a suitable field was chosen. The signal from this fluorescent probe is excited at 488 nm and emitted at approximately 600 nm.

2.1.10. *Immunohistochemistry for the detection of Ubiquitin*

Immunohistochemistry is a method of analyzing proteins and identifying cell types based on the binding of antibodies to specific components of the cell. It is sometimes referred to as immunocytochemistry. Immunohistochemical staining is widely used in the diagnosis of abnormal cells such as those found in cancerous tumors. Specific molecular markers are

characteristic of particular cellular events such as proliferation or cell death. Visualizing an antibody-antigen interaction can be accomplished in a number of ways. In the most common instance, an antibody is conjugated to an enzyme, such as peroxidase, that can catalyze a colour-producing reaction. Alternatively, the antibody can also be tagged to a fluorophore, such as FITC or Texas Red. The latter method is of great use in confocal laser scanning microscopy, which is highly sensitive and can also be used to visualize interactions between multiple proteins.

For this technique medium was removed and the monolayer of cells was washed twice with sterile PBS (0.1 M). A 1:1 ratio of the fixative methanol/acetone (1ml/coverslip) was added, kept on ice and incubated at 4ºC for 10 minutes. The fixative was subsequently removed and cells were air dried for 20 minutes at room temperature. Cells were rinsed with PBS there after the coverslips were transferred onto temporary microscope slides. 100 µl 5% donkey serum was added for 20 minutes at room temperature. After draining the serum, 100 µl primary antibody solution (ubiquitin; 1:50) was added. This was incubated overnight at 4ºC. The primary antibody solution was removed and the cells were once again rinsed carefully with PBS. The L6 myotubes were incubated with a FITC (Fluorescein isothiocyanate) conjugated secondary antibody solution (1:100) for 30 minutes at room temperature. In addition, 100 µl Hoechst 33342 (1:200) dye was added for a further 10 minutes. The cells were finally washed 3 times with PBS and mounted on permanent microscope slides. The serum, primary and secondary antibodies and Hoechst dye were made up with sterile PBS. Flourescent images were acquired with a Nikon Eclipse E 400 microscope, equipped with ACT-1 acquisition software, using a 20X Nikon Plan Fluor objective. Four random areas within each image (and concentration) were chosen and using the software provided, the mean green areas (representing ubiquitin expression) were measured. These values were then transferred to Excel and statistical analysis was conducted.

2.1.11. *Preparation of cell extracts*

Differentiated myoblasts were washed thoroughly in warm PBS after which 250 µl ice cold RIPA (Radio immunoprecipitation assay)/lysis buffer containing (in mM): tri-(hydroxylmethyl)-aminomethane (TRIS)-HCl 50, NP-40 1%, Na-Deoxycholate 0.25%, EDTA (Ethylenediaminetetraacetic acid) 1, sodium fluoride (NaF) 1, soybean trypsin inhibitor

(SBTI) 4 μg/ml, phenylmethyl sulphonyl fluoride (PMSF) 1, Benzamidine 1, leupeptin 1μg/ml and Triton X-100 1000 μl was added to each well for 5 minutes. The cells were scraped free from the wells and transferred into already chilled eppendorfs tubes. While working on ice, the cells were homogenized for a few seconds to break down the cell wall and release proteins. Centrifugation commenced (8000 rpm at 4ºC for 10 minutes) to remove nuclei and cell debri.

2.1.12. *Western Blotting Analysis*

The cell lysates were diluted in Laemmli sample buffer, boiled for 5 minutes and centrifuged for 15 seconds. Equal amounts of protein from the supernants were fractioned by 10% or 12% Sodium dodecyl sulphate polyacrylamide gel electrophoresis (SDS-PAGE). The lysate protein content was determined using the Bradford technique (Bradford *et al*, 1976). The separated proteins were transferred to a PVDF membrane (Immobilon^{TM} P, Millipore). These membranes were routinely stained with Ponceau Red for visualisation of proteins. Non-specific binding sites on the membranes were blocked with 5% fat-free milk in TRIS-buffered saline-Tween (TBS-T) and then incubated with the primary antibodies that recognise phospho-specific p38 MAPK (Thr^{180}/Tyr^{182}), NF-κB, PI-3K (p85 subunit), Akt (PKB; ser473), FKHR (FoxO), MuRF-1, MAFbx, caspase-3, JNK, PTEN, TNF-R1, MyoD, Myogenin , β-Actin as well as their related total-specific antibodies. Membranes were subsequently washed with large volumes of TBS-T (5 x 5 min) and the immobilized antibody was conjugated with a diluted horseradish peroxidase-labelled secondary antibody (Amersham LIFE SCIENCE). After thorough washing with TBS-T, membranes were covered with ECL^{TM} detection reagents and quickly exposed to an autoradiography film (Hyperfilm ECL, RPN 2103) to detect light emission through a non-radioactive method (ECL^{TM} Western blotting). Films were densitometrically analysed (UN-SCAN-IT, Silkscience version 5.1) and phosphorylated protein values were corrected for minor differences in protein loading if required.

2.1.13. *Statistical Analysis*

All data are presented as the means ± SEM. Comparisons between the different groups of were performed by one-way analysis of variance (ANOVA) followed by Bonferroni's post

hoc test conducted with the statistical program GraphPad Prism, version 4.03 (GraphPad Inc.). A value of $p < 0.05$ was considered statistically significant.

CHAPTER 3

Results I

In this chapter of the results section, results are demonstrated from the experiments in which four different concentrations of TNF-α were tested on the L6 myogenic cell line. Our preliminary work was to establish the susceptibility of L6 myotubes to increasing doses of TNF-α in a time dependent manner. The effect of various concentrations on proliferation and cell viability was assessed by MTT assays and the Trypan Blue exclusion technique. Three independent experiments were conducted for accuracy.

3.1. *The effect of different TNF-α concentrations on proliferation and cell viability*

L6 myoblasts were cultured until 60-65% confluency after which myotube differentiation was initiated by replacing the growth medium with differentiation medium. Differentiation continued for a period of 8 days where after cells were supplemented with 0 (control), 1, 3, 6 and 10 ng/ml TNF-α for 24 and 48 hours. MTT assays were employed to evaluate the effects of treatment with TNF-α on cellular function and/or proliferation (Figure 3.1). As stated before, this assay is based upon the principal of reducing MTT into blue formazan pigments by viable mitochondria in healthy cells. Therefore, this assay demonstrates the percentage of metabolically active cells following treatment, where the final absorption measurements show a direct relationship with an increased ability of essential reduction enzymes in the mitochondria to reduce to MTT. Cell activity was shown to be slightly reduced to 90.33 ± 6.009% and 63.00 ± 13.89% for 24 and 48 hours respectively compared to their controls. Unexpectedly, the medium dose at 48 hours appeared to have improved cell activity, thus less MTT reducing capacity, to 113.7 ± 9.528% compared to the control. However, significance was noticed only at 48 hours when comparing the medium and very high dose (*$p < 0.01$) as well as the high and very high dose (**$p < 0.05$). No significance was observed at 24 or 48 hours when compared to their respective controls.

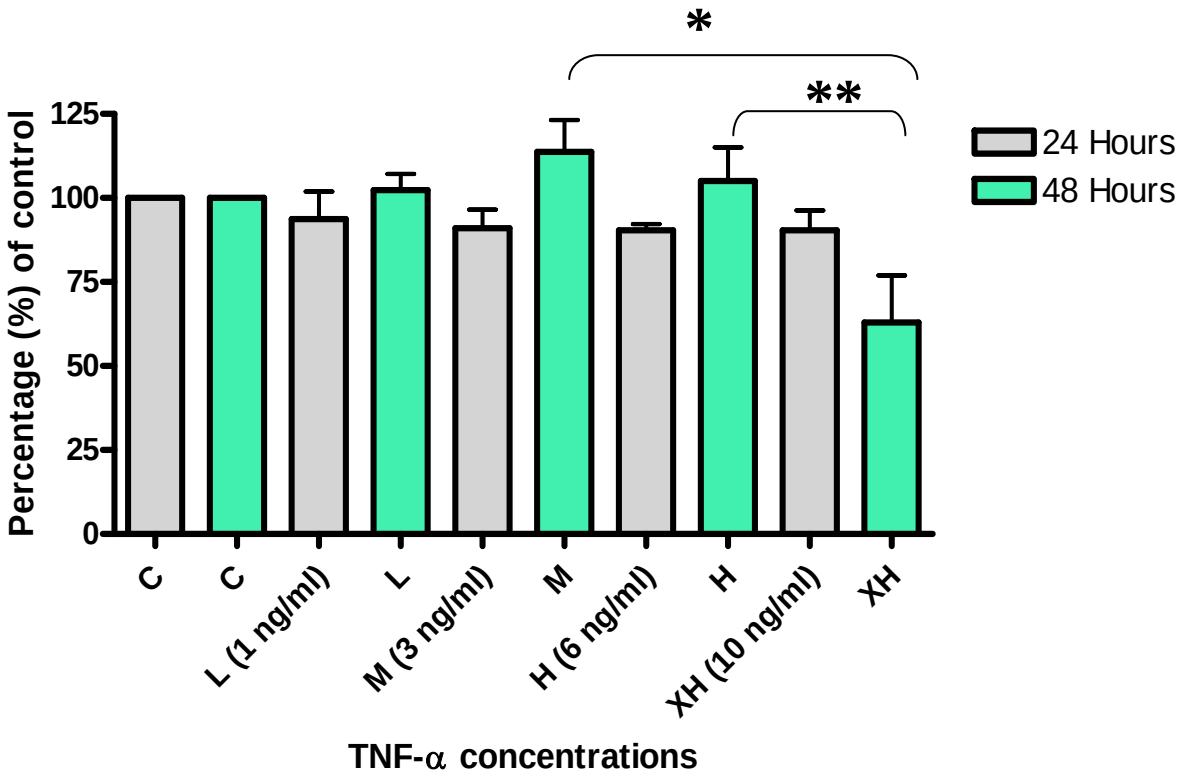

Figure 3.1: Effect of different TNF-α doses on proliferation and cell viability of fully differentiated L6 myotubes (8 days). L6 myotubes were incubated with 0, 1, 3, 6 and 10 ng/ml TNF-α for 24 and 48 hours and their cell activities were assessed at these time points. Cell activities were quantified by the MTT assay as described in the methods section. Values are conveyed as percentages of controls (100%) and presented as means ± S.E.M (n ≥ 3). * P < 0.05, ** P < 0.01

3.2. *The effect of different TNF-α concentrations on cell viability*

In addition to the MTT assay, a second assay to measure cell viability, the Trypan Blue exclusion technique was used. Trypan Blue dye enters cells with a damaged cell membrane, dyeing them blue. L6 myotubes that were maintained in their normal environment for the full experimental protocol without TNF-α (control group) had a viability of 100% (Figure 3.2). Myotubes incubated for 24 and 48 hours with various TNF-α concentrations showed very little reduction in viability to 93.33 ± 0.333% and 94.00 ± 1.155% respectively compared to the control groups. Results obtained from this technique did not convey the same idea as the previous technique (MTT Assay) in that a very high TNF-α dose (10 ng/ml) decreased myotube viability.

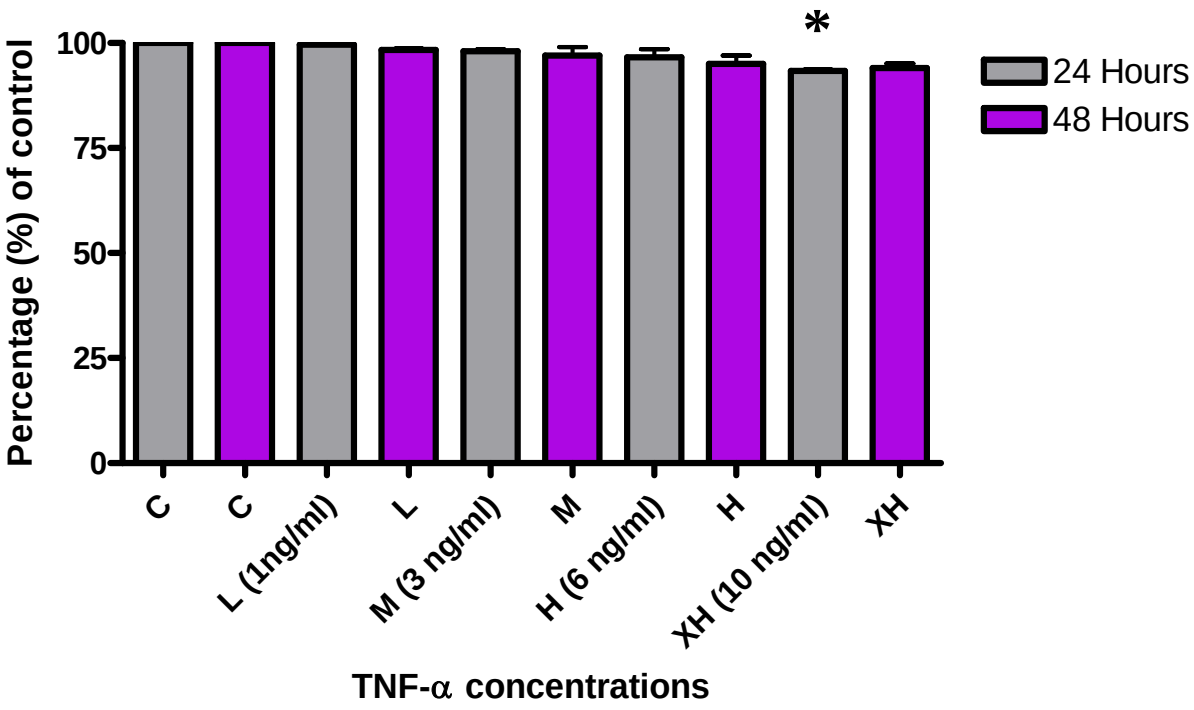

Figure 3.2: Effect of different TNF-α doses on cell viability of fully differentiated L6 myotubes (8 days) using the Trypan Blue exclusion technique. L6 myotubes were incubated with 0, 1, 3, 6 and 10 ng/ml TNF-α for 24 and 48 hours and their cell activities were assessed at these two time points. Myotube viability only very slightly decreased when compared to the controls, even at very high concentrations Values are conveyed as percentages of controls (100%) and presented as means ± S.E.M (n ≥ 3). * P < 0.05

CHAPTER 4

Results II

After the preliminary work was accomplished, we desired to determine what effect these different doses of TNF-α would have on cell morphology. Two staining techniques were employed, namely: Hoechst 33342 and PI. Three independent experiments were conducted for accuracy.

4.1. *Effect of different TNF-α doses on L6 myotube morphology*

The Hoechst and PI staining techniques have been exploited by many laboratories for discriminating between apoptotic and necrotic cell death respectively (Lizard *et al*, 1998 and Hseih *et al*, 2000). In this experiment, the nuclei of untreated cells (control) displayed loose chromatin formation, stained blue with Hoechst 33342 dye and did not stain red with the PI dye (Figure 4.1***a, b*** and ***c*** and Figure 4.2 ***a, b*** and ***c***). Treatment of cells with increasing doses of TNF-α produced no significance at the low, medium or high doses, but exhibited significance at the very high dose ($p < 0.001$) when stained with Hoechst 33342 at both 24 and 48 hours (Figure 4.1***b*** and 4.2***b***). Apoptotic cells showed signs of nuclear chromatin condensation as well as apoptotic bodies. When the cells were stained with PI, only the very high dose ($p < 0.001$) produced significant PI-positive stained cells (Figure 4.1***c*** and 4.2***c***). This is an indication that the cell membrane is damaged thus incorporating the PI dye in the cytoplasm and ultimately into the DNA. Long term treatment with increasing doses of TNF-α appeared to have a strong apoptotic (Figure 4.3***a***) and necrotic (Figure 4.3***b***) effect on L6 myotube morphology which continued up to 48 hours. The results will be displayed beginning with the 24 hour data, followed by the 48 hour data. A combination of the two (24 and 48 hour) data will then be displayed at the end.

Hoechst 33342 **Propidium Iodide**

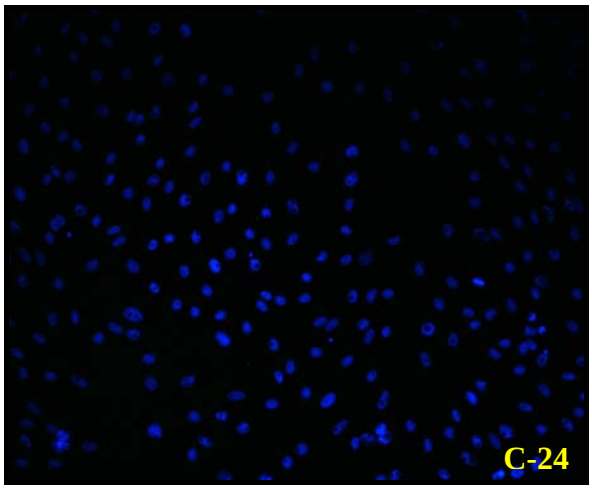

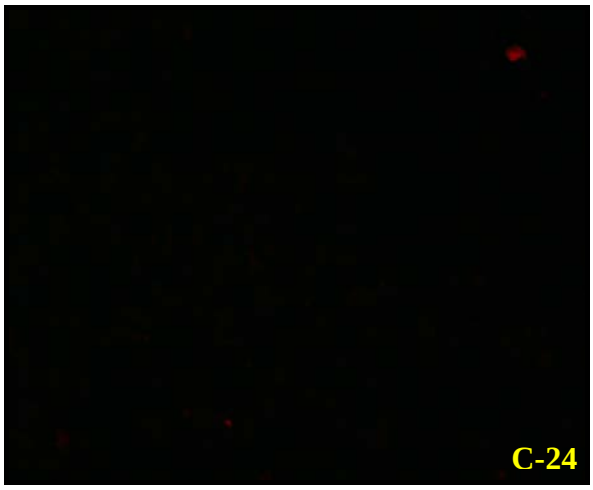

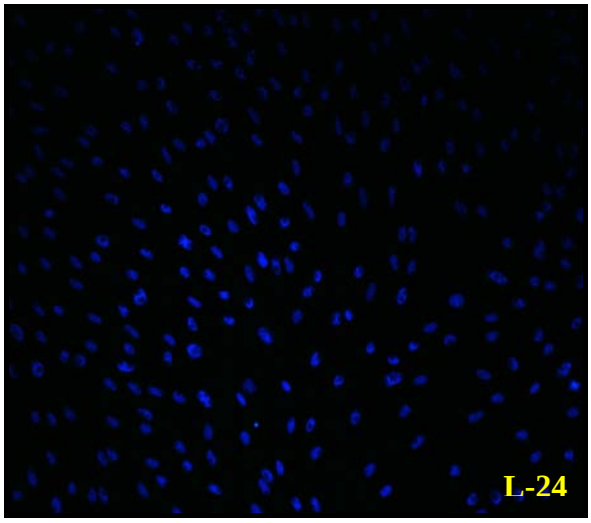

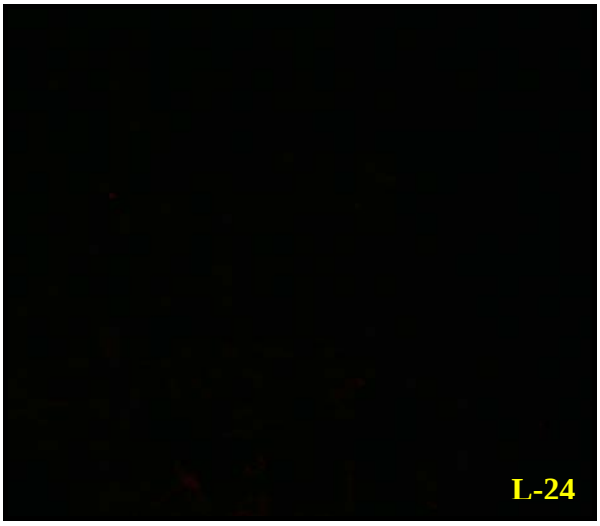

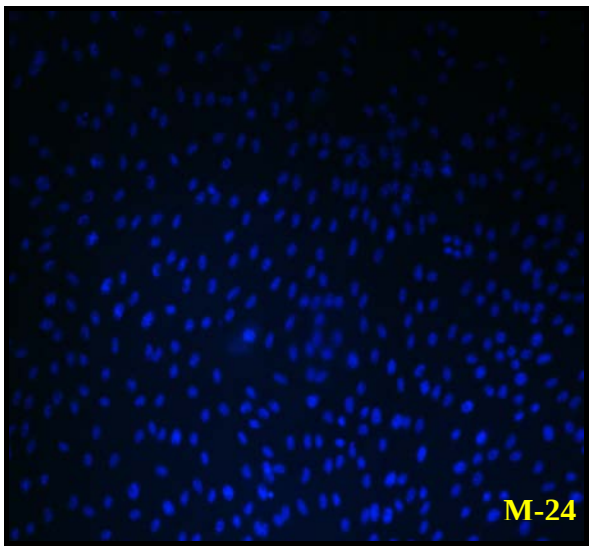

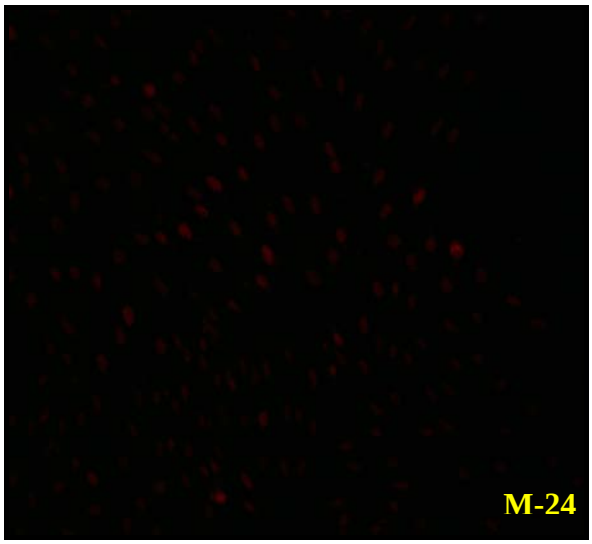

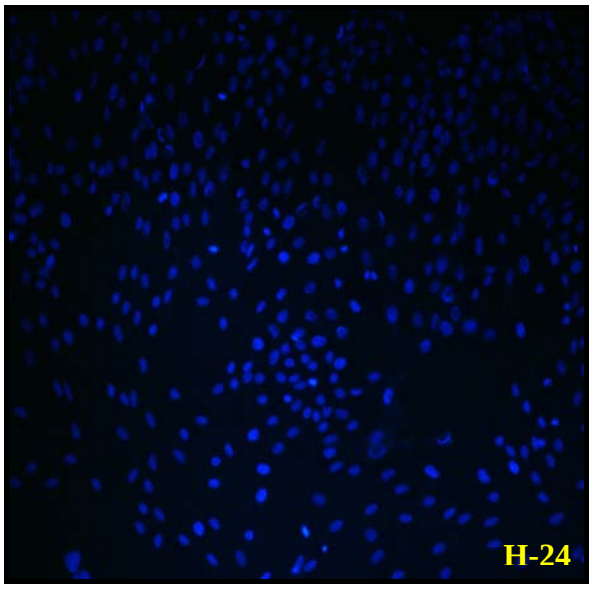
H-24

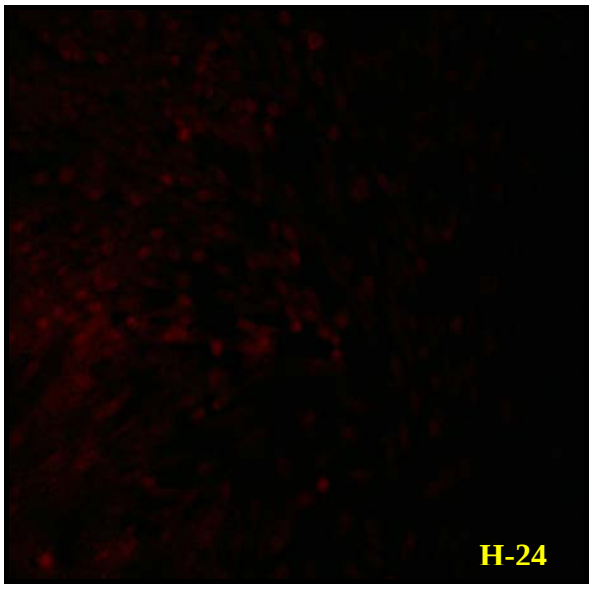
H-24

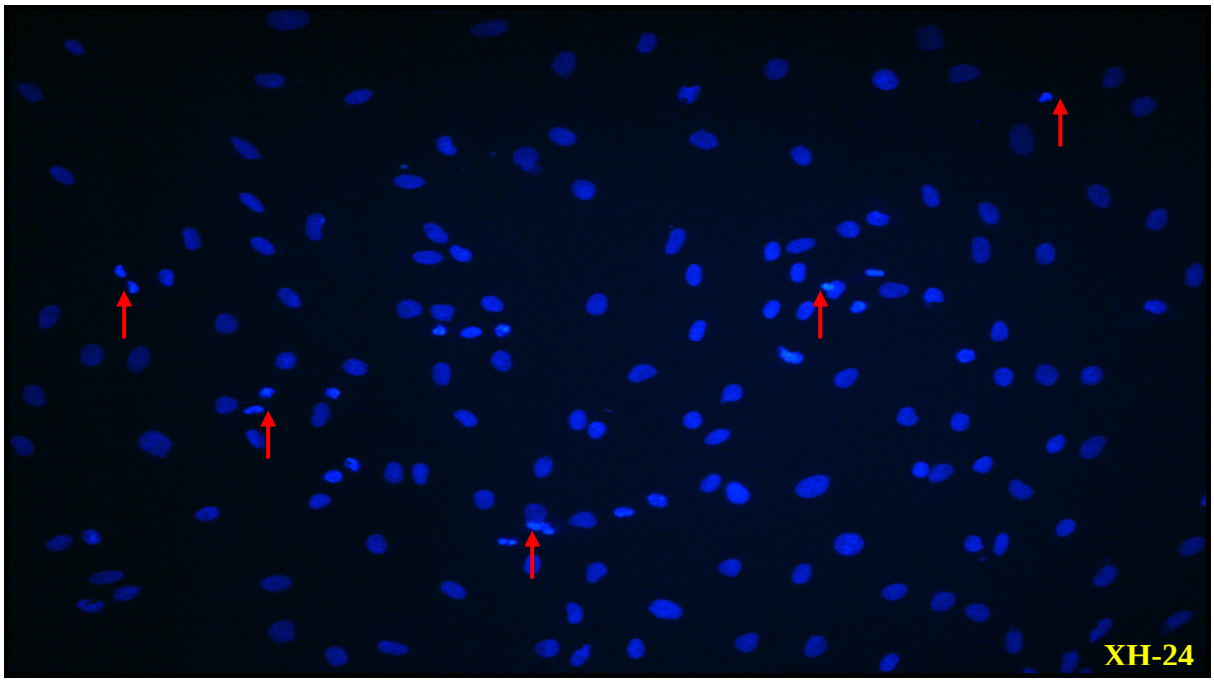
XH-24

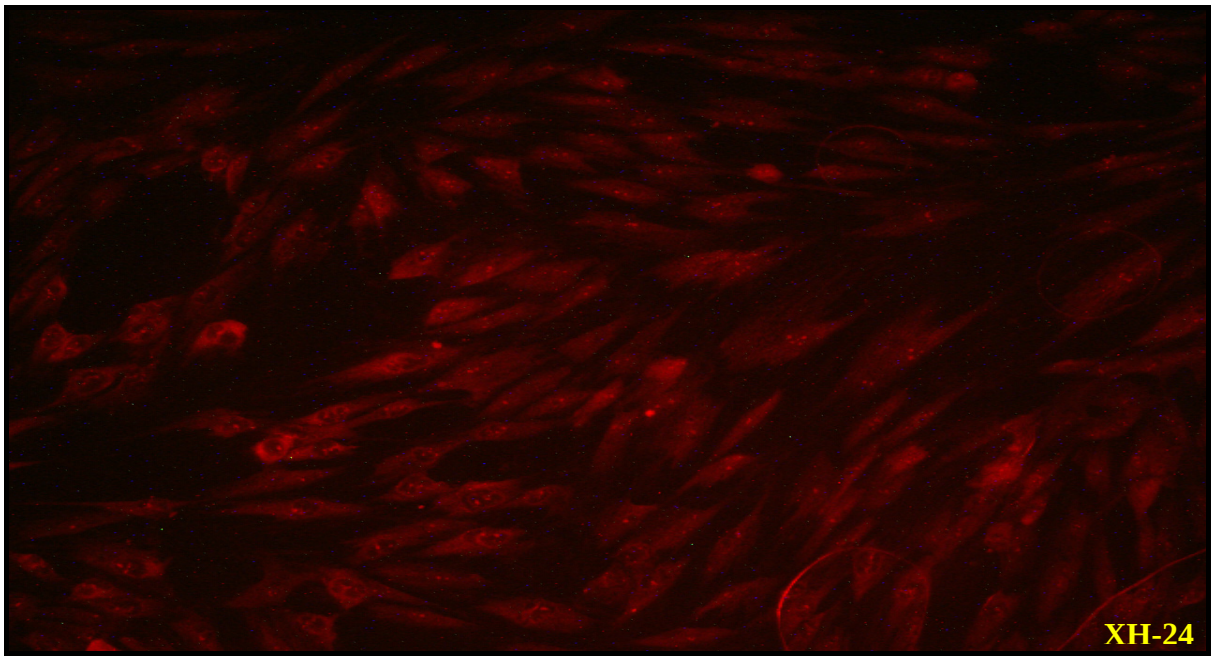

Figure 4.1 (a): The effect of increasing doses of TNF-α on apoptosis and necrosis in L6 myotubes (24 hours). Myotubes were stained with both Hoechst 33342 (blue) and PI (red) and scrutinized for apoptosis and necrosis using fluorescence microscopy. The red arrows indicate apoptotic cells or apoptotic bodies (n ≥ 3). C-24, control for 24 hours; L-24, low dose for 24 hours; M-24, medium dose for 24 hours; H-24, high dose for 24 hours; XH-24, very high dose for 24 hours

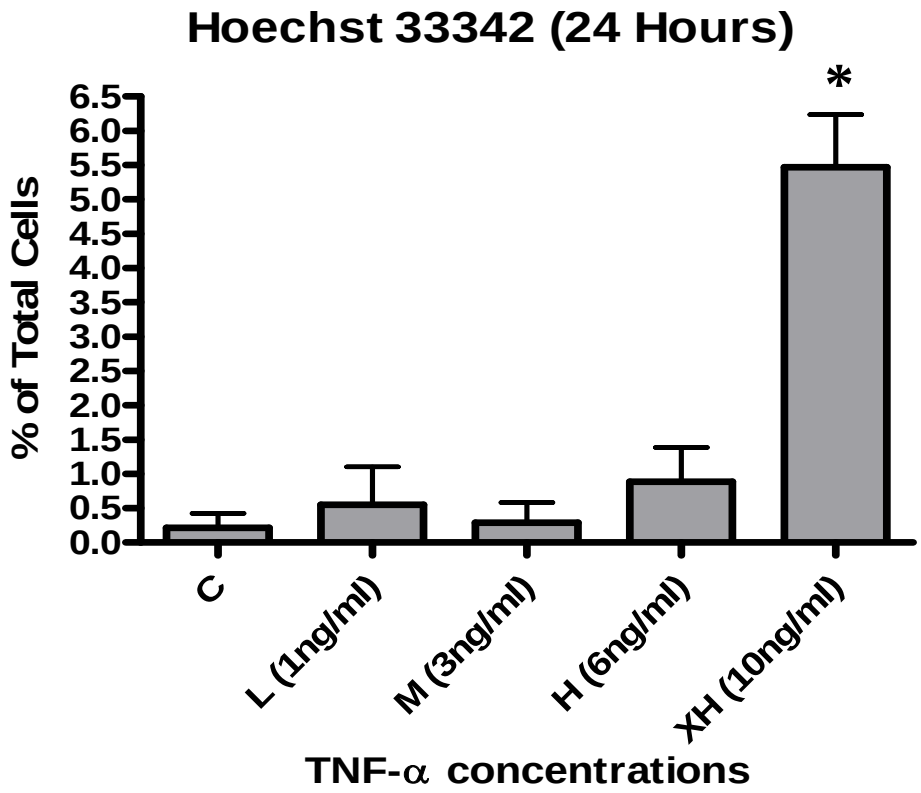

Figure 4.1 (b): The effect of increasing doses of TNF-α on apoptosis in L6 myotubes (24 hours). Myotubes were stained with Hoechst 33342 (blue) and scrutinized for apoptosis using fluorescence microscopy. Atleast 200 cells per experiment were selected, tallied and assessed for signs of apoptosis. Results are presented as their mean ± SEM. *P < 0.001 versus control (n ≥ 3)

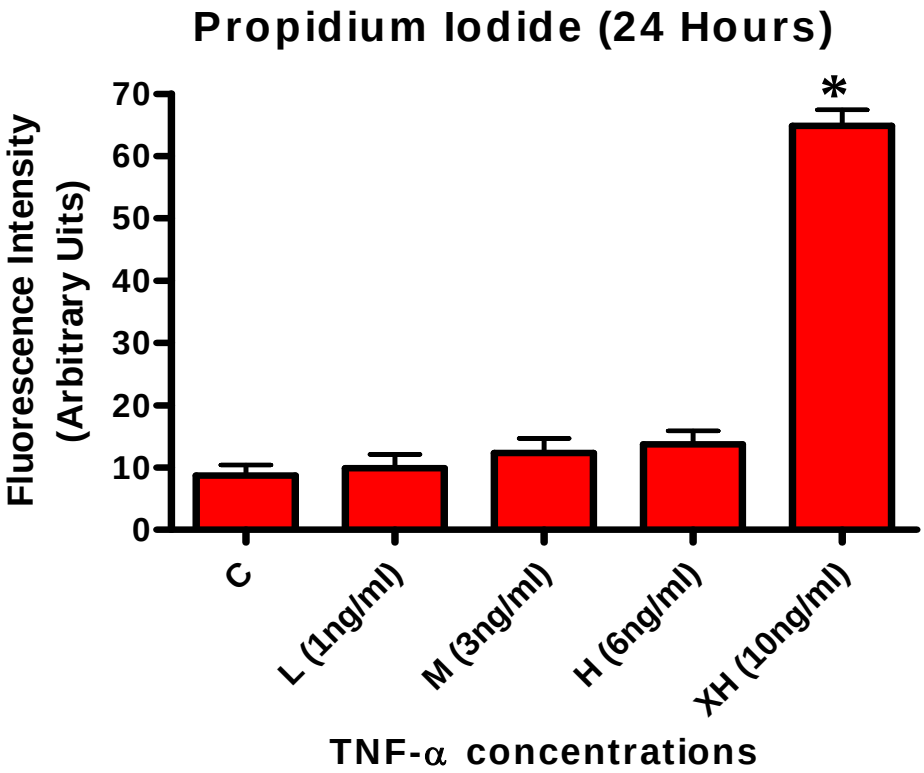

Figure 4.1 (c): Quantification of PI (fluorescence) intensity in L6 myotubes with increasing doses of TNF-α (24 hours). Myotubes were stained with PI (red) and scrutinized for necrosis using fluorescence microscopy. Atleast 200 cells per experiment were selected, tallied and assessed for signs of necrosis. Results are presented as their mean ± SEM. *P < 0.001 versus control (n ≥ 3)

Hoechst 33342 **Propidium Iodide**

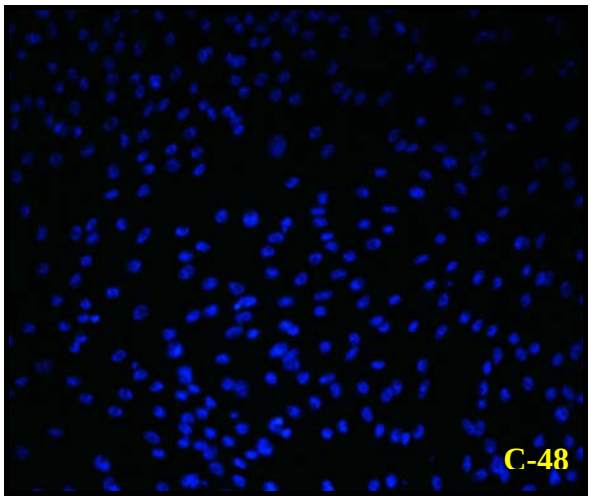

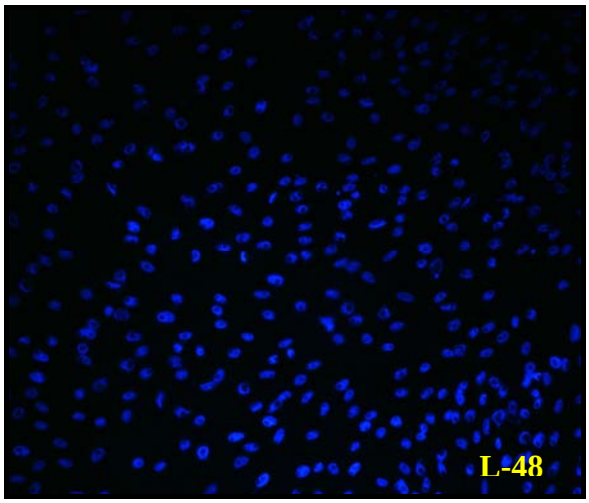

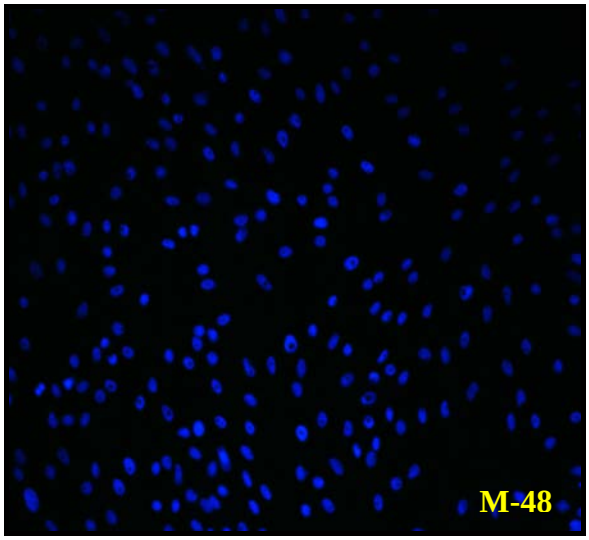

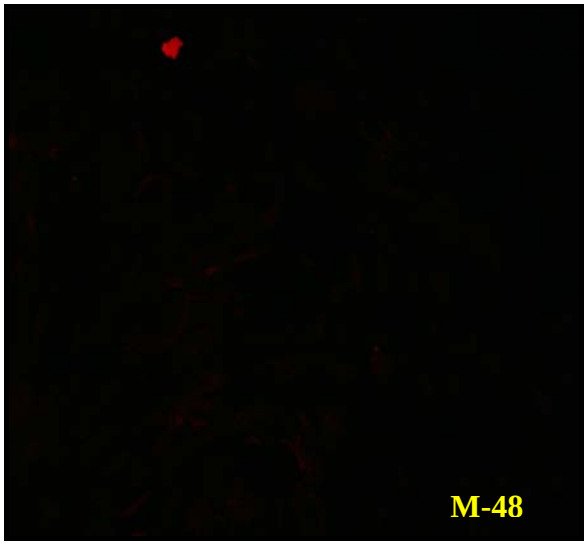

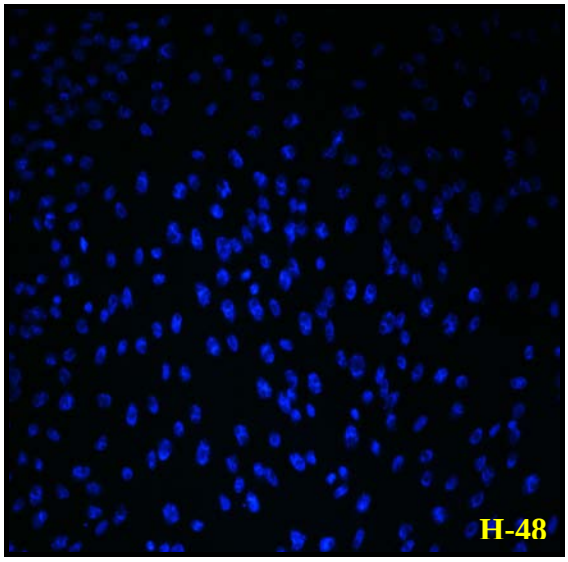
H-48

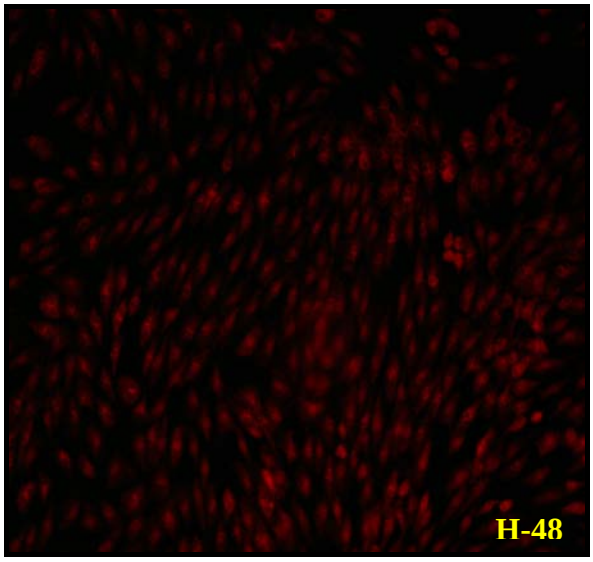
H-48

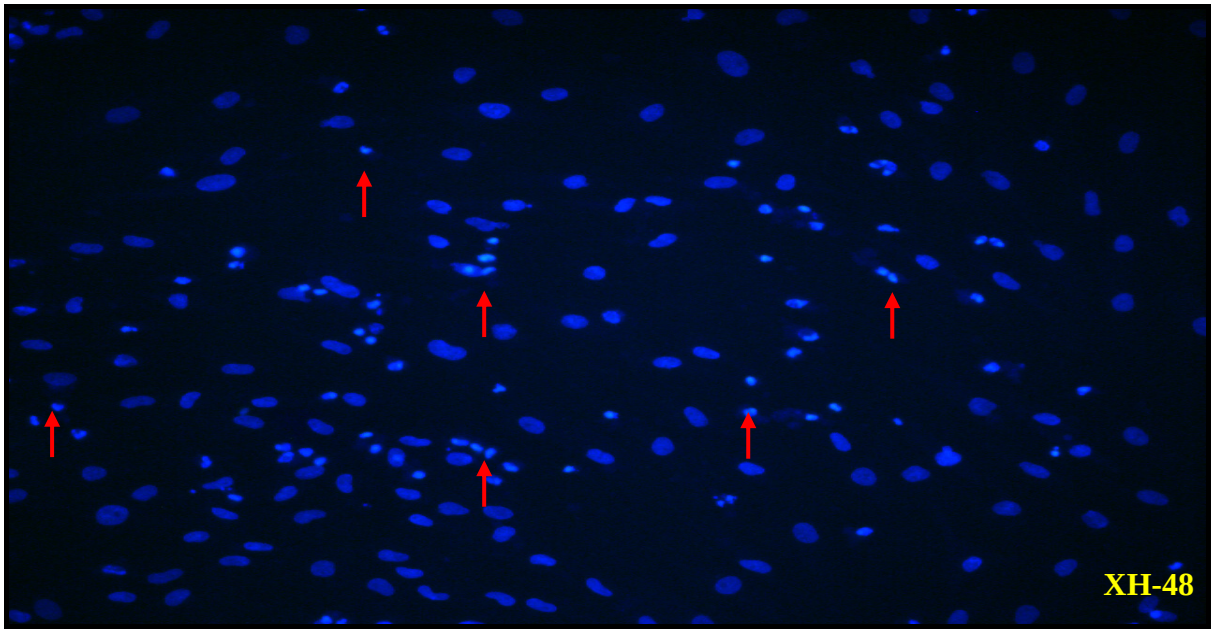
XH-48

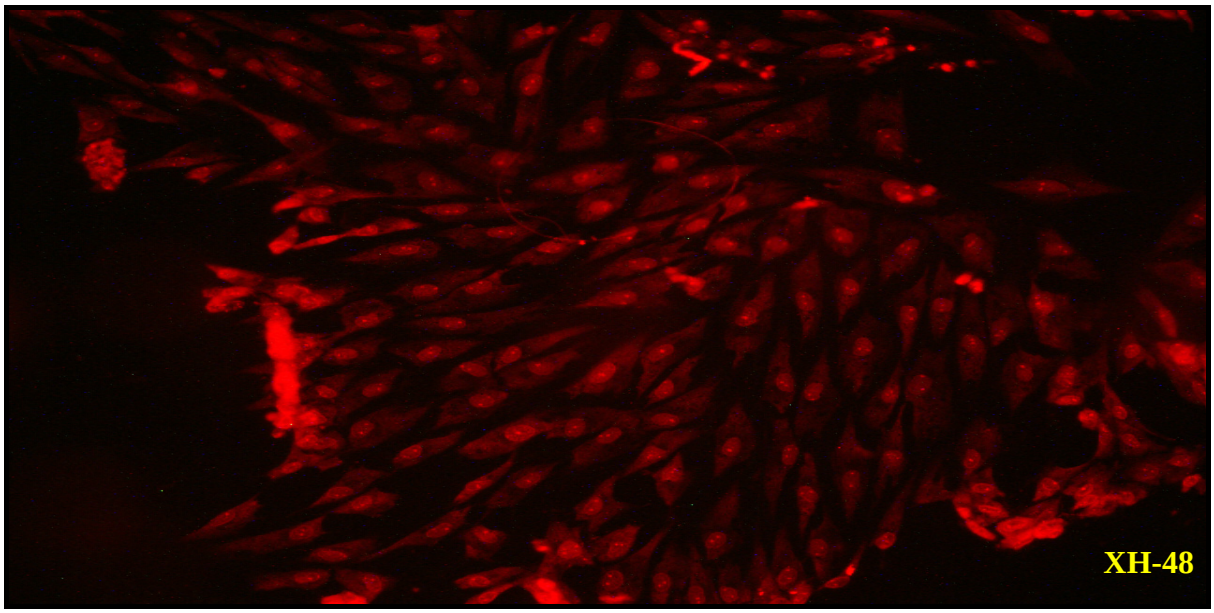

Figure 4.2 (a): The effect of increasing doses of TNF-α on apoptosis and necrosis in L6 myotubes (48 hours). Myotubes were stained with both Hoechst 33342 (blue) and PI (red) and scrutinized for apoptosis and necrosis using fluorescence microscopy. The red arrows indicate apoptotic cells or apoptotic bodies (n ≥ 3). C-48, control for 48 hours; L-48, low dose for 48 hours; M-48, medium dose for 48 hours; H-48, high dose for 48 hours; XH-48, very high dose for 48 hours

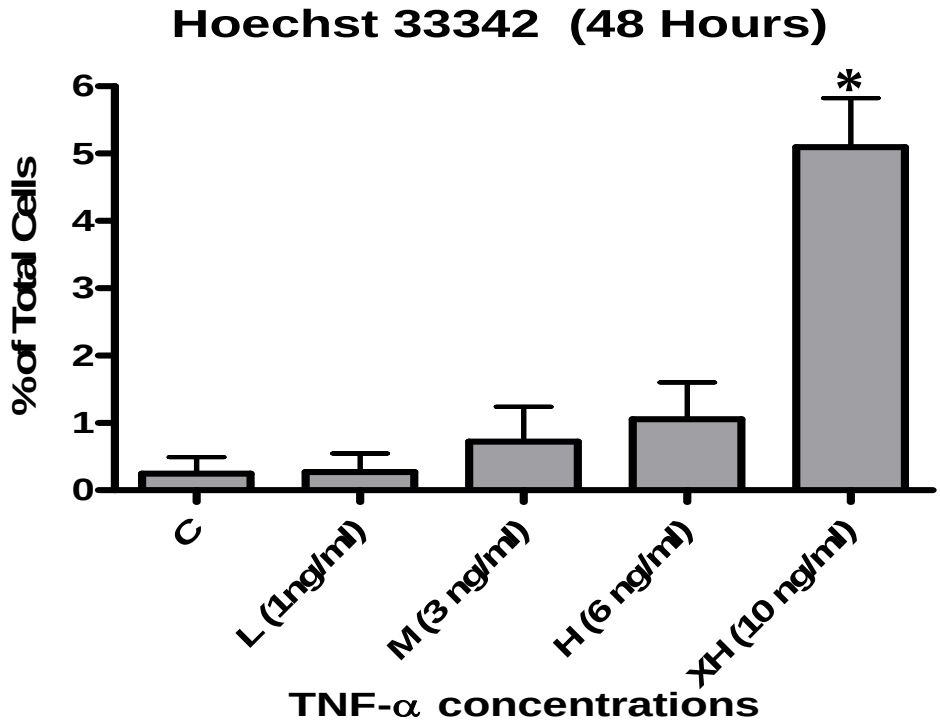

Figure 4.2 (b): The effect of increasing doses of TNF-α on apoptosis in L6 myotubes (48 hours). Myotubes were stained with Hoechst 33342 (blue) and scrutinized for apoptosis using fluorescence microscopy. Atleast 200 cells per experiment were selected, tallied and assessed for signs of apoptosis. Results are presented as their mean ± SEM. *P < 0.001 versus control (n ≥ 3)

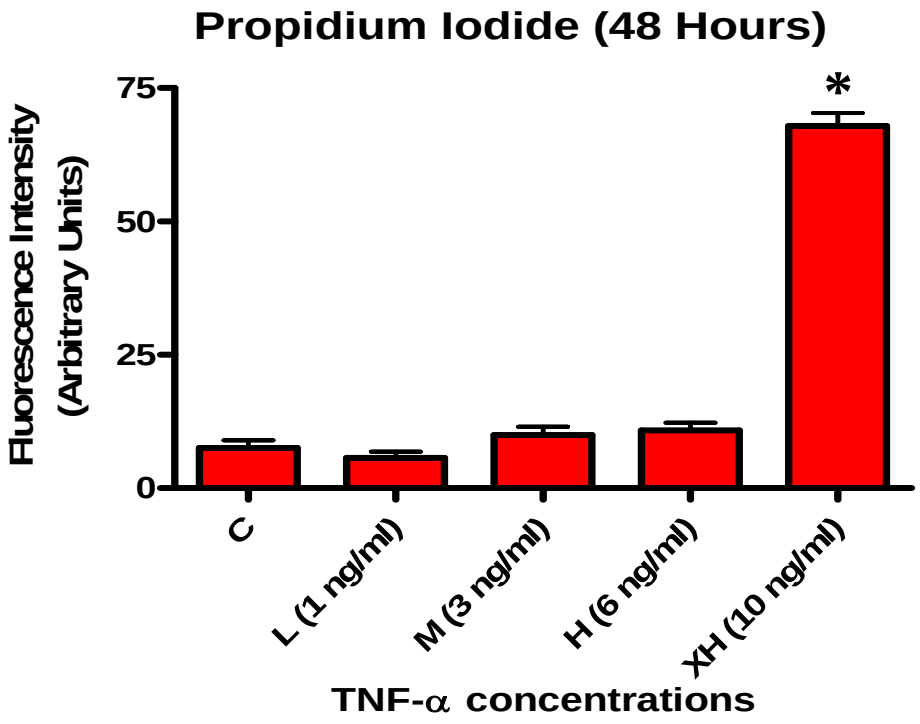

Figure 4.2 (c): Quantification of PI (fluorescence) intensity in L6 myotubes with increasing doses of TNF-α (48 hours). Myotubes were stained with PI (red) and scrutinized for necrosis using fluorescence microscopy. Atleast 200 cells per experiment were selected, tallied and assessed for signs of necrosis. Results are presented as their mean ± SEM. *P < 0.001 versus control (n ≥ 3)

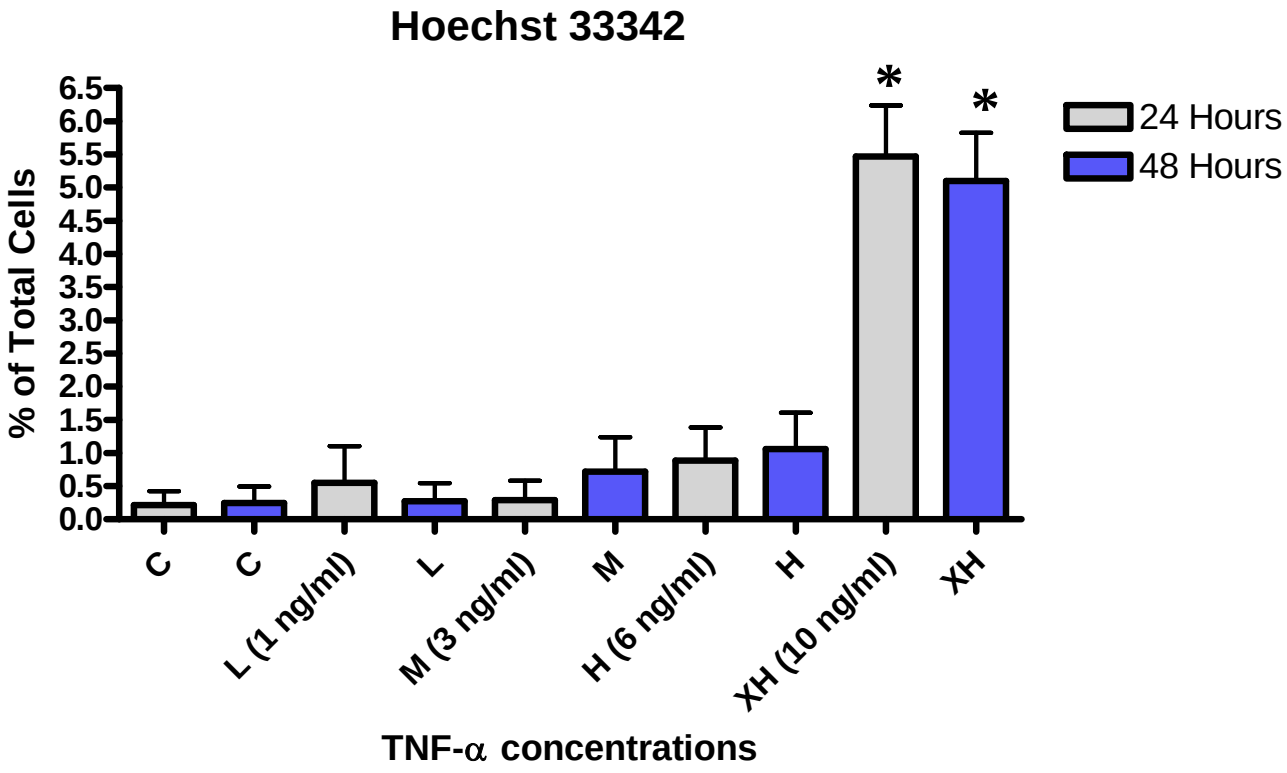

Figure 4.3 (a): The effect of increasing doses of TNF-α on apoptosis in L6 myotubes (24 and 48 hours). Myotubes were stained with Hoechst 33342 (blue) and scrutinized for apoptosis using fluorescence microscopy. Atleast 200 cells per experiment were selected, tallied and assessed for signs of apoptosis. Results are presented as their mean ± SEM. *P < 0.001 versus control (n ≥ 3)

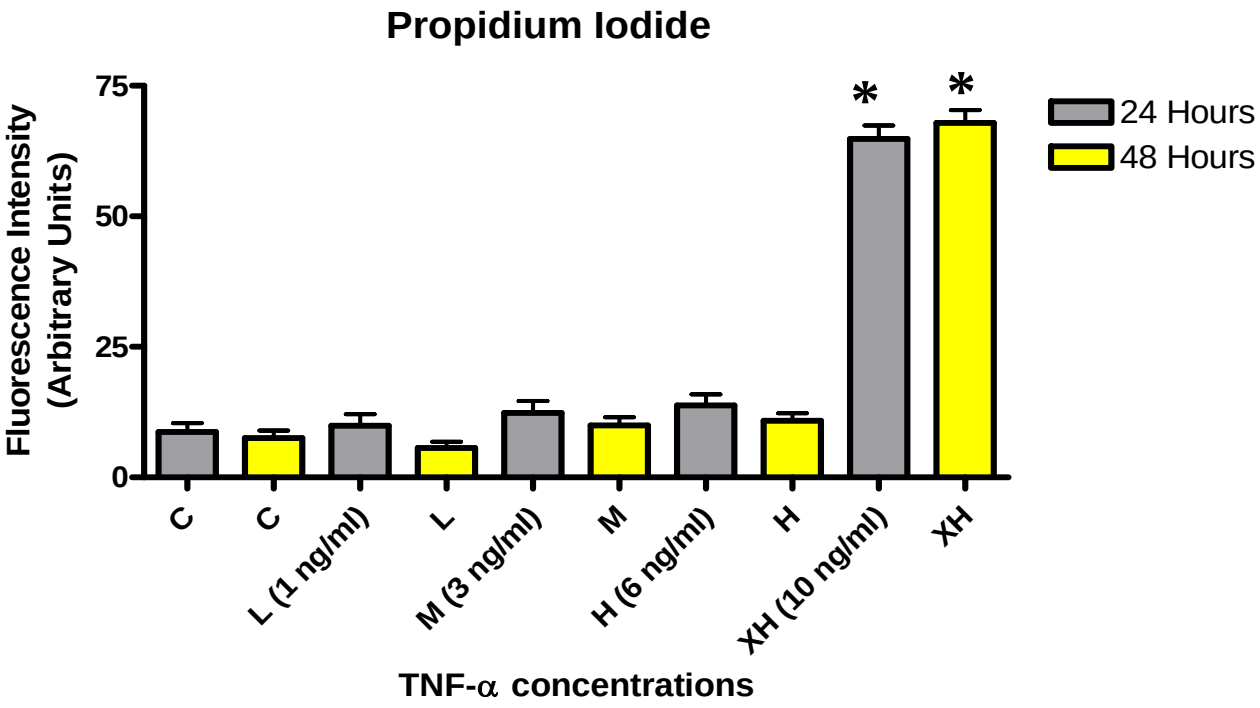

Figure 4.3 (b): Cell viability in L6 myotubes using the propidium iodide technique for 24 and 48 hours. Atleast 200 cells per experiment were selected, tallied and assessed for signs of necrosis. Results are presented as their mean ± SEM. *P < 0.001 versus control (n ≥ 3)

4.2. *Short- and/or long-term treatment with TNF-α influences phosphorylation or dephosphorylation of various signalling molecules*

The short-term and long-term effects of TNF-α on L6 myotubes were assessed by Western blotting. L6 myotubes were cultured until 60-65% confluency after which myotube differentiation was initiated by replacing the growth medium with differentiation medium. Differentiation continued for a period of 8 days and then the cells were supplemented with 0 (control), 1, 3, 6 and 10 ng/ml TNF-α for varying time periods raging from 45 minutes (short-term treatment), 24 and 48 hours (long-term treatment). The phosphorylation of numerous signalling molecules was measured using phospho-specific antibodies. Changes in total protein levels were also measured with antibodies that identify the proteins of interest regardless of their phosphorylation status. Protein expression intensities are conveyed relative to baseline values (always control). The controls on each Western blot were normalised and all protein levels are expressed as a percentage of these.

4.2.1. *TNF-R1 (Western blots)*

The behaviour of TNF-α is mediated by its high affinity binding to cell specific receptors that occupy totally different intracellular domains. In response to TNF-α and via a series of intracellular processes, TNF-R1 and TNF-R2 are then expressed on the cell surface of most cell types. In this experiment, Western blotting with TNF-R1 and TNF-R2 specific antibodies showed that TNF-R1 to be the only receptor that was upregulated. This glycoprotein containing a single transmembrane is devoid of any enzymatic activity, associating with a number of different intracellular proteins (Song *et al*, 1994; Hsu *et al*, 1995; Stanger *et al*, 1995; Rothe, *et al*, 1994; Mosialos *et al*, 1995). At 24 hours, there appears to be an increasing amount of receptors present on the cell surface with increasing doses of TNF-α. However at the very high (XH) dose, receptor downregulation seems to occur although not significant. At 48 hours, the same pattern appears to occur in that there is a significant increase in receptor upregulation ($P < 0.001$) which significantly decreases at the very high dose (Figure 4.4***b***). The expression intensity of the receptors using the western blot procedure gives the impression that with increasing TNF-α treatment, there seems to be a gradual increase in receptor

upregulation which ultimately declines over time (Figure 4.4***a***). This may suggest that the receptors may have become saturated thus not expressing the proteins as well as the 24 hour data. Another possible explanation for this observation could be a result of the increased necrosis where the cell membranes are damaged and the membrane-bound receptors could therefore be lost. These results also show that TNF-R1 bind to TNF-α with a lower affinity and with a lower dissociation rate than TNF-R2. Significant differences were also observed when comparing each concentration of TNF-α at 24 hours with the same concentration at 48 hours.

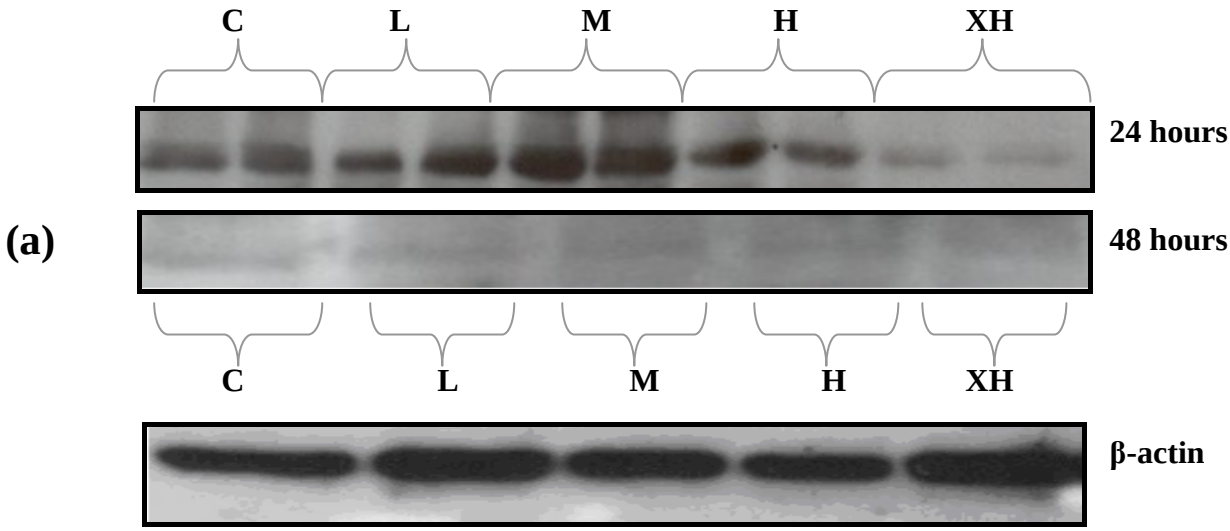

(a)

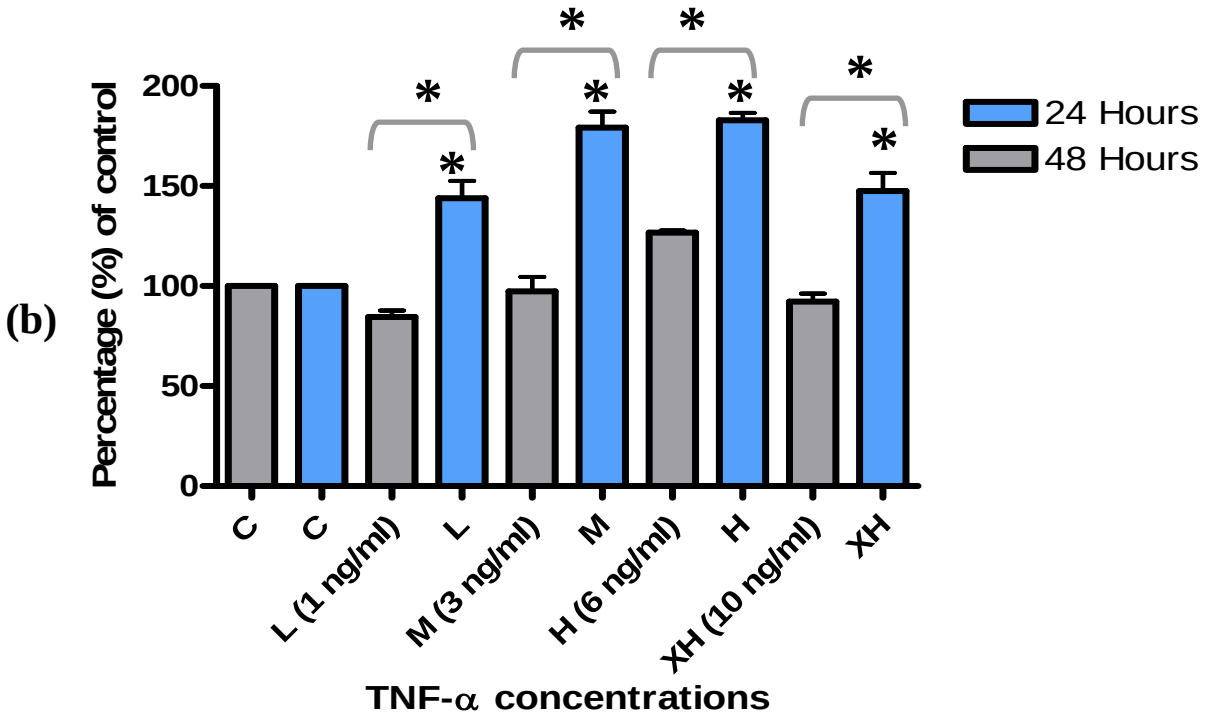

Figure 4.4 (a), (b): Representative western blots demonstrating the effect of different TNF-α concentrations have on TNF- α receptor 1 upregulation in L6 myotubes over a period of 24 and 48 hours. Results are presented as their mean ± SEM. *P < 0.001 versus control (n ≥ 3)

4.2.2. *Phosphorylation of p38 and JNK MAPKs (Western blots)*

Both p38 and JNK are members of the MAPK family. These stress-responsive MAPKs are closely related Serine/Threonine (Ser/Thr) kinases activated by a cascade downstream of both tyrosine receptor kinases such as insulin as well as G-protein coupled receptors such as angiotensin II, resulting in the initiation of various adaptive events ranging from gene expression to apoptosis. We systematically examined TNFα's effects on MAPK activity in differentiated L6 myotubes.

With long-term (24 hours) TNF-α treatment, a distinct trend was observed towards increased phosphorylation of the p38-MAPK. The low dose appeared to have the most phosphorylation of p38 compared to the other doses used in this experiment (Figure 4.5***a*** and ***b***). This phosphorylation however slightly declined at the medium dose which ultimately reached a plateau at the higher doses. At 48 hours, phosphorylation of the p38-MAPK increased significantly ($p < 0.001$) a great deal more than at 24 hours. Phosphorylation increased with increasing TNF-α

treatment except at the very high dose which tended to decline. The total protein levels of p38 at 24 and 48 hours produced no significant results.

Phosphorylation of JNK on the other hand produced significant ($p < 0.001$) increases at 24 hours with increasing TNF-α treatment except for the high dose which produced a significantly lower decrease in phosphorylation (Figure 4.6). This trend was well established in three successive experiments. At 48 hours however, there appeared to be no significant differences between groups when compared to the control.

Data obtained from these experimental procedures indicate that TNF-α activates both MAPKs and may pose as potential second messengers for TNF-α. This observation has also been seen by several researchers and their associates (Garg, *et al*, 2002; Li *et al*, 2003; Liu *et al*, 2005; Li *et al*, 2007). p38-MAPK has been previously recognised as a prospective regulator of muscle catabolism (Tracey *et al*, 2002). In addition, current studies reveal that p38 activity in skeletal muscle is elevated by procatabolic states (Childs *et al*, 2003; Di Giovanni *et al*, 2004). JNK phosphorylation has also been shown to significantly increase and this inspection correlated with the development of atrophy induced by TNF-α (Childs *et al*, 2003; Hilder *et al*, 2003; Morris *et al*, 2004). Therefore within a physiological context, p38- and JNK-MAPK act concurrently and frequently in combination with one another to yield a biological response.

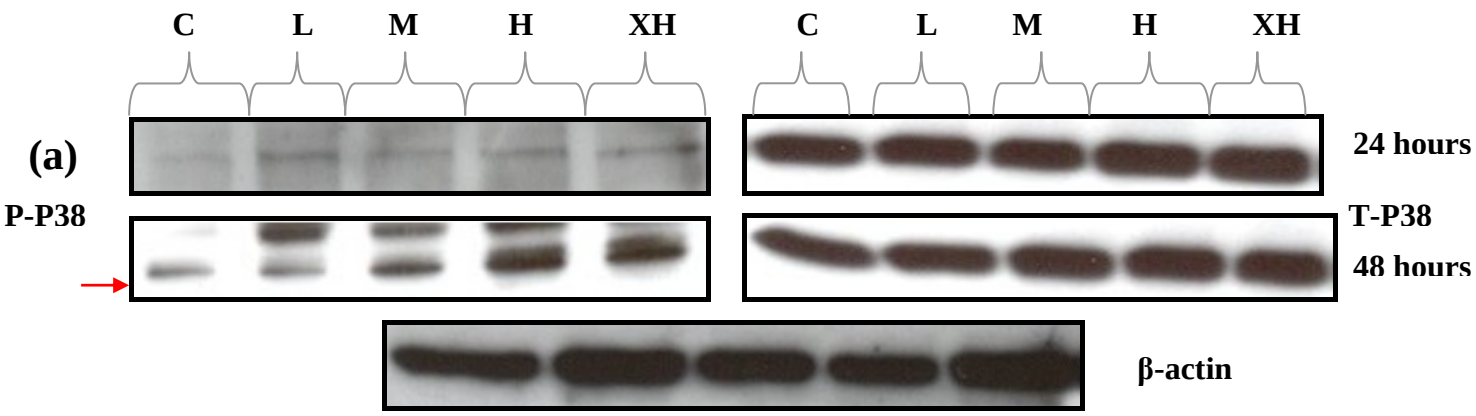

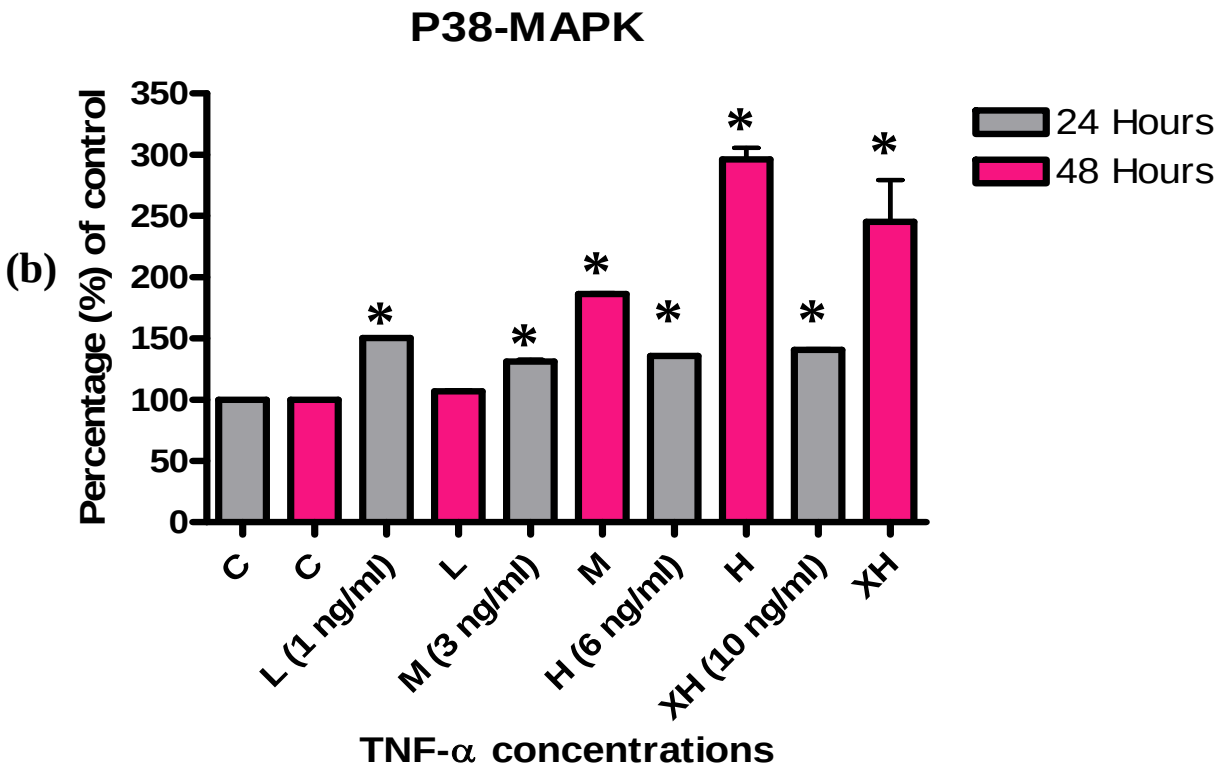

Figure 4.5 (a), (b): Representative Western blots demonstrating the effect of different TNF-α concentrations have in the phosphorylation of the p38-MAPK in L6 myotubes over a period of 24 and 48 hours. Results are presented as their mean ± SEM. *P < 0.001 versus control (n ≥ 3). P-p38, phosphorylated p38; T-p38, total p38

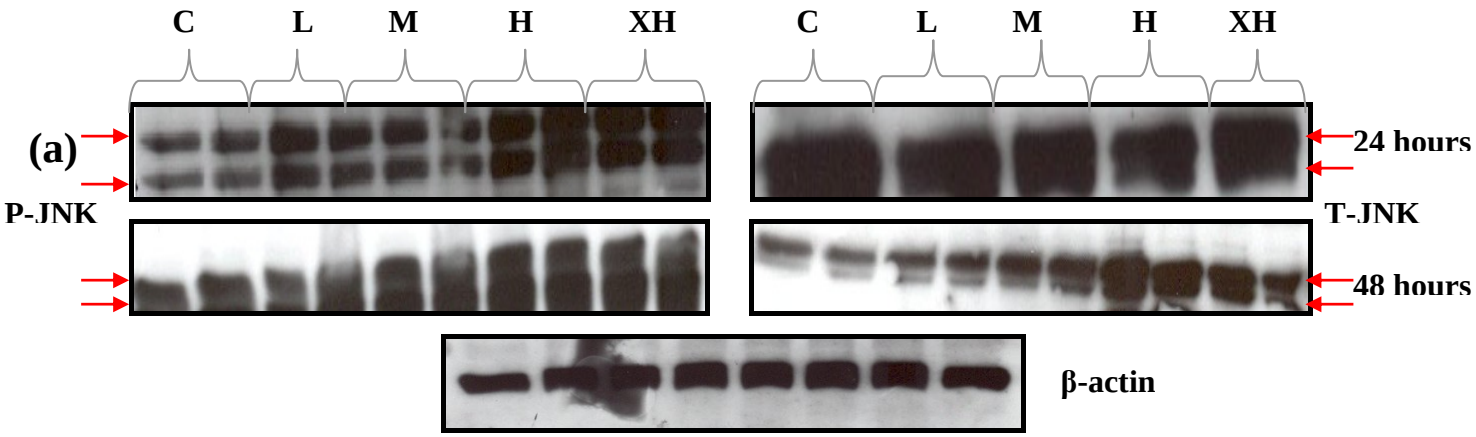

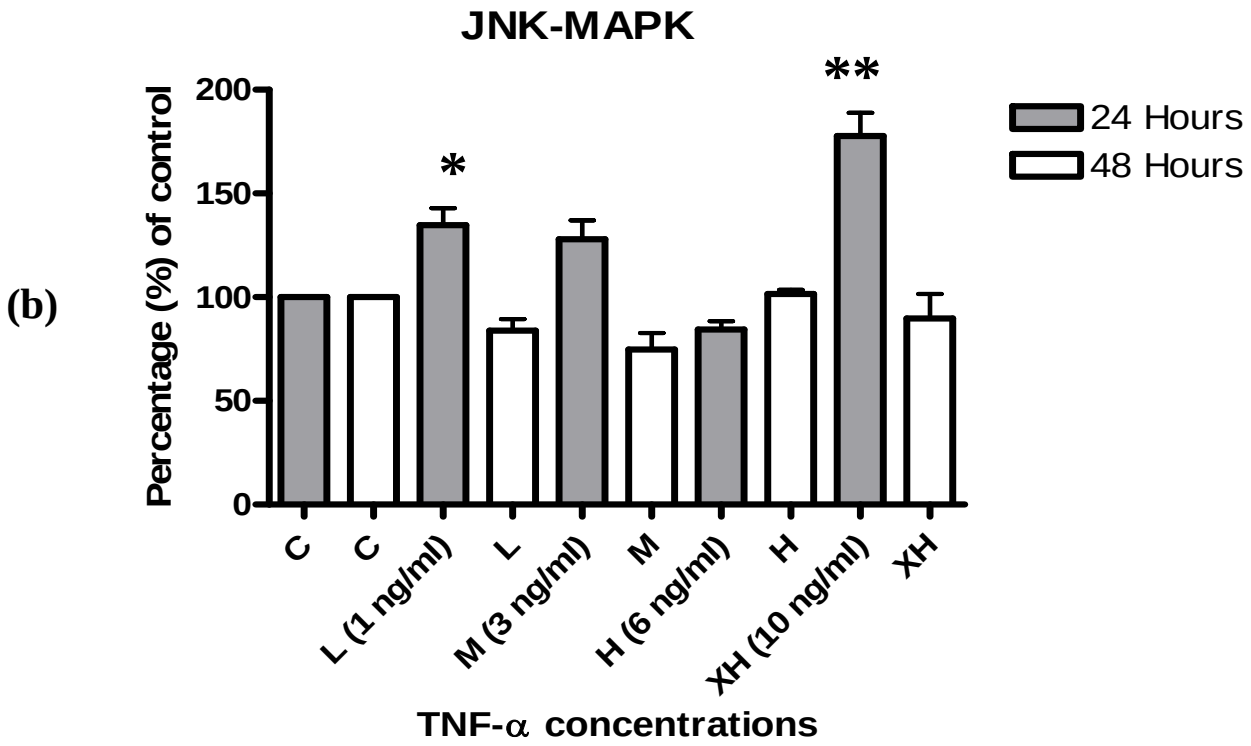

Figure 4.6 (a), (b): Representative Western blots demonstrating the effect of different TNF-α concentrations have in the phosphorylation of the JNK-MAPK in L6 myotubes over a period of 24 and 48 hours. Results are presented as their mean ± SEM. *P < 0.05; **P < 0.001 versus control (n ≥ 3). P-JNK, phosphorylated-JNK; T-JNK, total-JNK

4.2.3. Phosphorylation of the transcription factors FKHR and NFκB (Western blots)

FKHR proteins function for the most part as transcription factors in the nucleus and bind as monomers to their associated DNA targeting sequences (Clark *et al*, 1993). These transcription factors have transpired to be a critical family of proteins that modulate the expression of genes involved in the cell cycle, DNA damage repair, apoptosis and cell differentiation. FKHR proteins are regulated by a manifold of mechanisms and often, if not always, endure inhibitory phosphorylation and subsequent inactivation by protein kinases such as Akt in response to internal and external stimuli to promote cell survival. Only one of these mammalian transcription factors is assessed here, namely FKHR (FOXO-01) which is phosphorylated at three sites (Thr 24, Ser 256 and Ser 319).

Short-term (40 mins) TNF-α supplementation of L6 myotubes yielded significant decreases in the phosphorylation of FKHR in a dose dependent manner. Compared to the control samples (100%), there appeared to be almost 70% reduction in phosphorylation at those specific threonine and serine sites (Figure 4.7***a*** and ***b***). This suggests that FKHR transcription factors are inactivated rapidly in response to TNF-α. This level of reduction in phosphorylation was maintained at 24 hours reaching a value of 20.07 ± 0.80% (Figure 4.8***a*** and ***b***) and at 48 hours reaching a value of 33.13 ± 1.39%. This dramatic decline in the phosphorylation of FKHR proteins could pose a threat to the cell for the reason that they (FKHR proteins) are now able to translocate to the nucleus, where they promote the transcription of various genes that may potentially harm the cell.

The NF-κB family of transcription factors play a significant role in the activation of immune and inflammatory responses. All family members are present in skeletal muscle, existing in unstimulated cells as homo- or heterodimers bound to the inhibitory IκB proteins. TNF-α is potent stimulator of the NF-κB pathway and can induce catabolic actions in different ways (Kandarian *et al*, 2006). Possible mechanisms include the direct action of TNF-α on skeletal muscle to induce catabolism or indirectly by modifying the hormones that regulate protein turn-over such as IGF-1 or simply just by inducing anorexia (Granado *et al*, 2006).

Short-term TNF-α treatment produced signification activation of the NF-κB pathway via its phosphorylation (Figure 4.9***a*** and ***b***). This phosphorylation increased 40 fold compared to the control. As with FKHR proteins, phosphorylation of this pathway is rather rapid. At 24 hours however, phosphorylation and subsequent activation of the NF-κB pathway decreased but remain significantly higher ($p < 0.001$) than the control samples (Figure 4.10***a*** and ***b***). The same pattern of phosphorylation was maintained right throughout the 48 hour treatment resulting in significant increases ($p < 0.001$) when compared to the control. The total protein levels yielded non significant results when compared to their respective controls. This data suggests that activation of the NF-κB pathway is a swift and specific process that reaches its peak within 40 minutes which eventually declines even though significance is maintained.

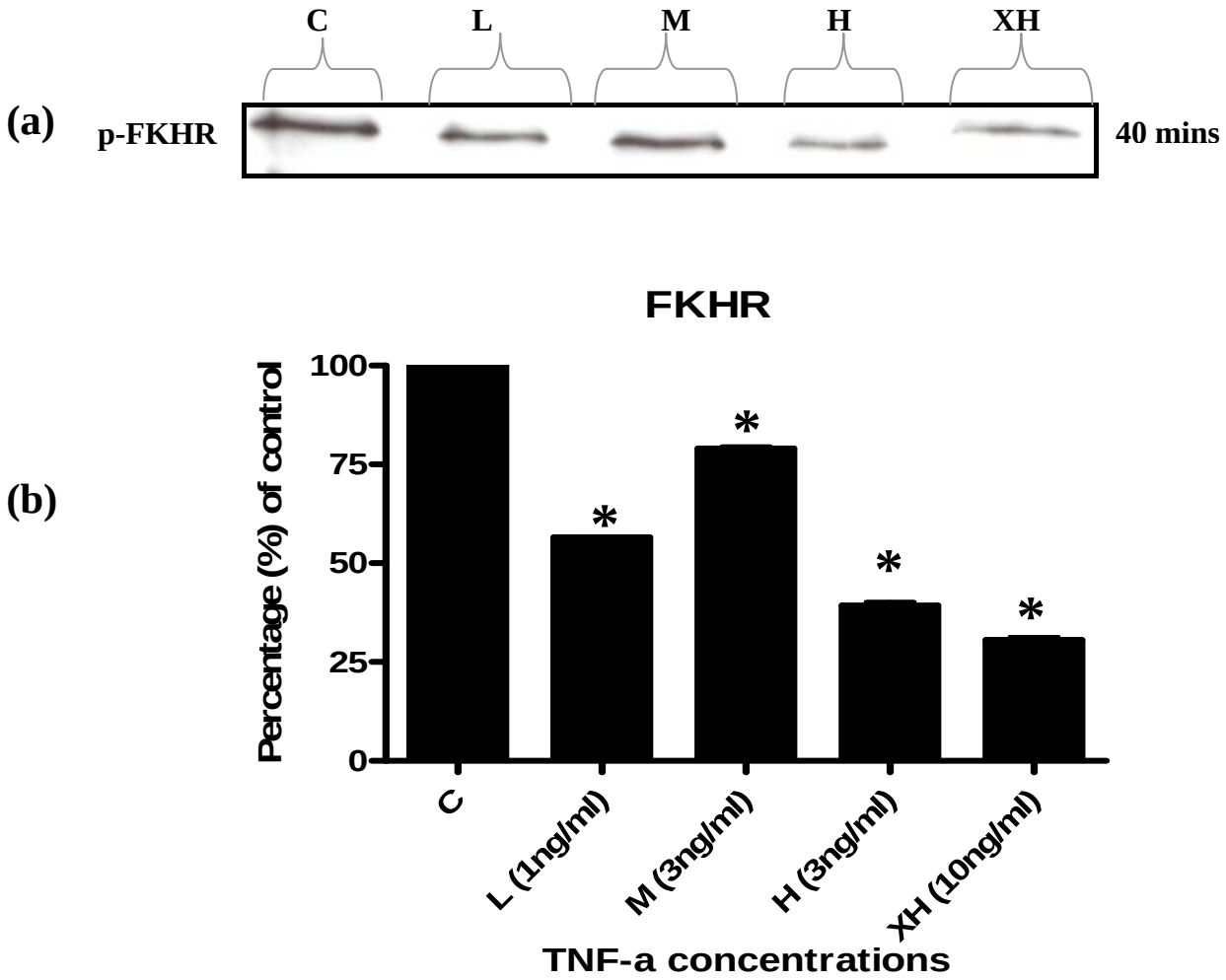

Figure 4.7 (a), (b): Representative Western blots demonstrating the effect of different TNF-α concentrations have in the phosphorylation of FKHR in L6 myotubes over a period of 40

minutes. Results are presented as their mean ± SEM. *P < 0.001 versus control (n ≥ 3). P-FKHR, phosphorylated-FKHR

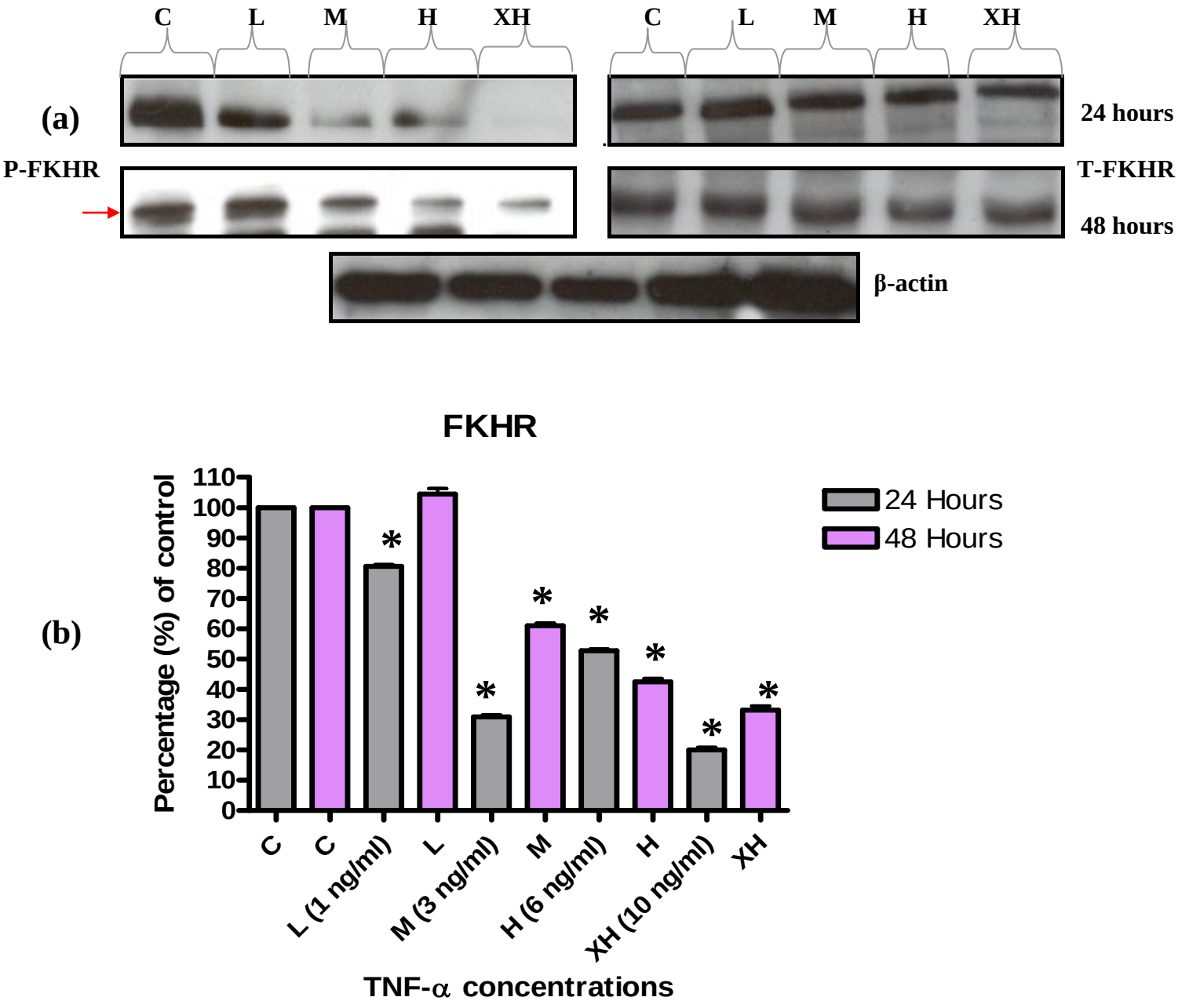

Figure 4.8 (a), (b): Representative Western blots demonstrating the effect of different TNF-α concentrations have in the phosphorylation of the FKHR in L6 myotubes over a period of 24 and 48 hours. Results are presented as their mean ± SEM. *P < 0.001 versus control (n ≥ 3). P-FKHR, phosphorylated-FKHR; T-FKHR, total-FKHR

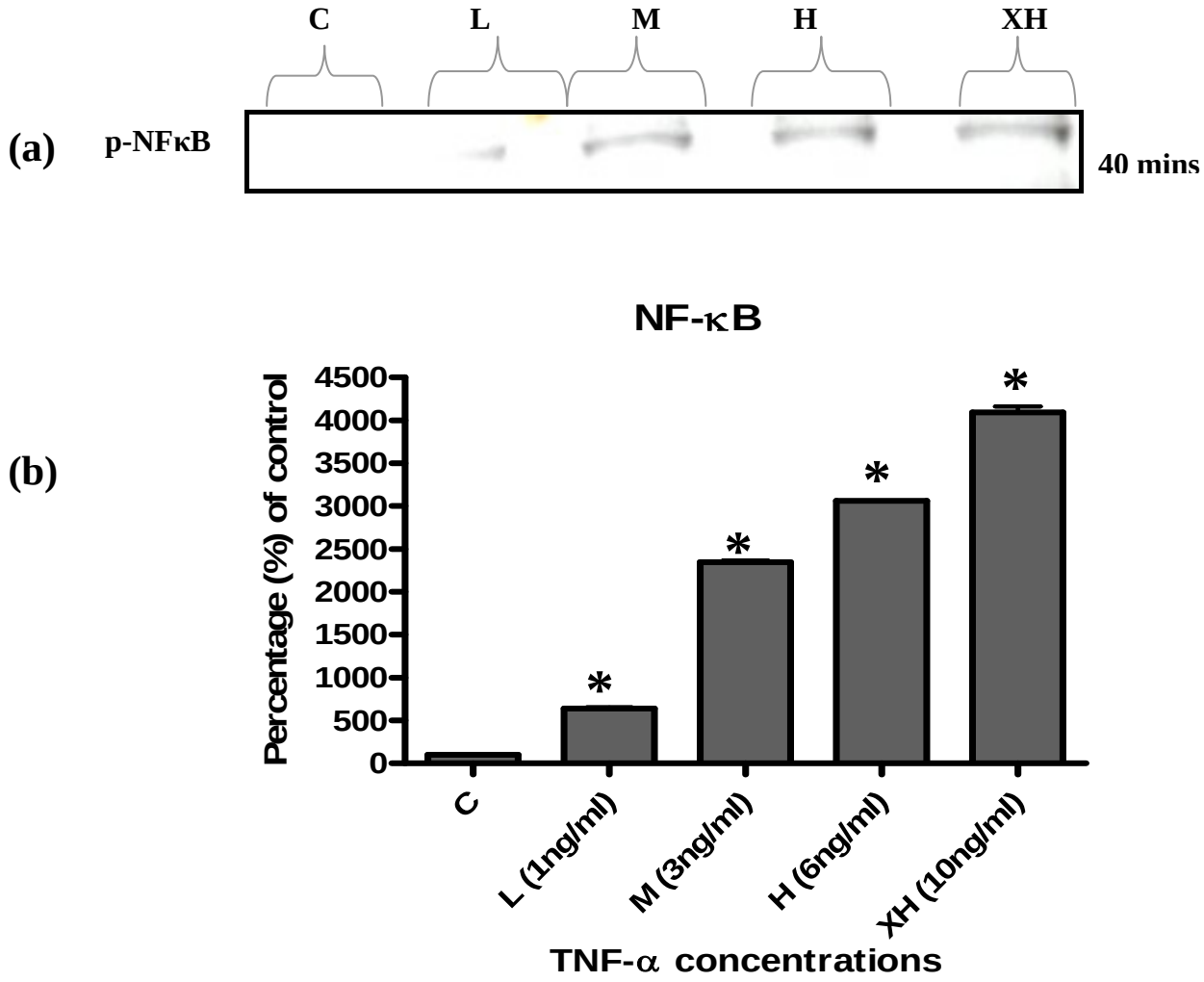

Figure 4.9 (a), (b): Representative Western blots demonstrating the effect of different TNF-α concentrations have in the phosphorylation of the NF-κB in L6 myotubes over a period of 40 minutes. Results are presented as their mean ± SEM. *P < 0.001 versus control (n ≥ 3). P-NFκB, phosphorylated NFκB

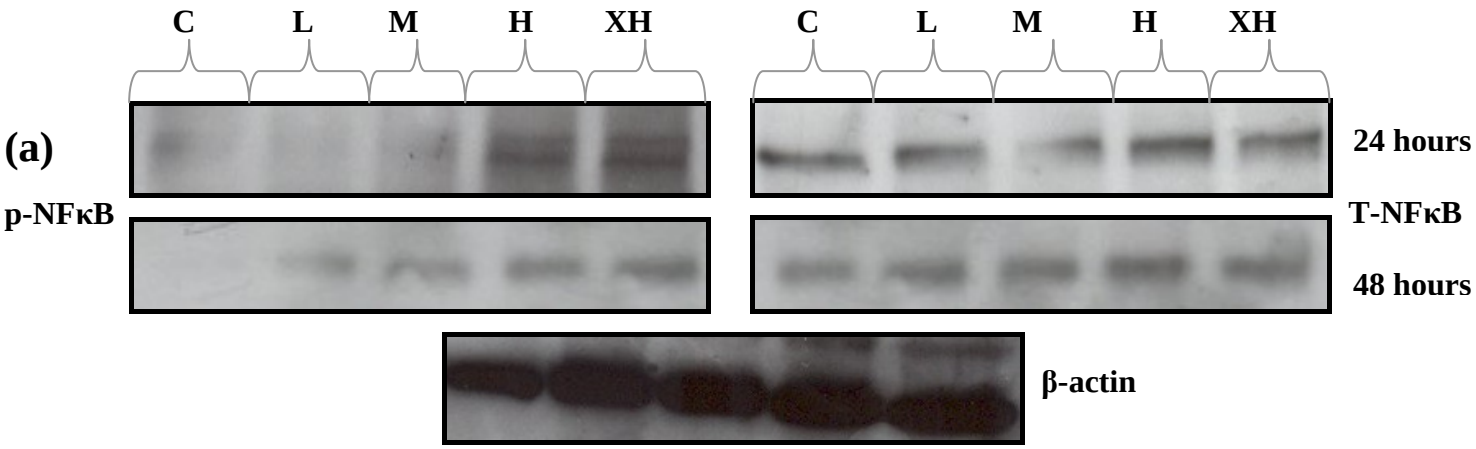

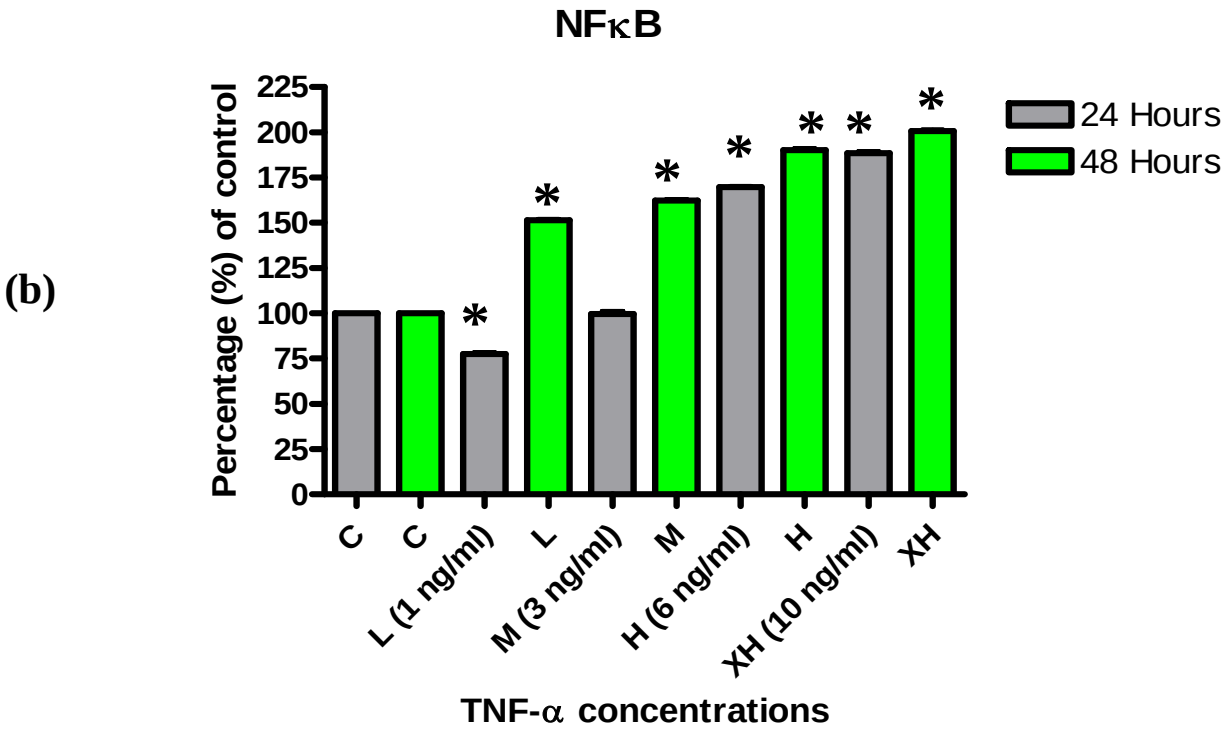

Figure 4.10 (a), (b): Representative Western blots demonstrating the effect of different TNF-α concentrations have in the phosphorylation of the NFκB in L6 myotubes over a period of 24 and 48 hours. Results are presented as their mean ± SEM. *P < 0.001 versus control (n ≥ 3). P-NFκB, phosphorylated-NFκB; T-NFκB, total-NFκB

4.2.4. The effect of TNF-α on caspase-3 (Western blots)

Cell survival requires the active inhibition of apoptosis, which is accomplished by inhibiting the expression of pro-apoptotic factors as well as promoting the expression of anti-apoptotic factors. One of the most widely recognised biochemical features of apoptosis is the activation of a class of cysteine proteases known as caspases. These proteases are present in the cell as inactive procaspases that are cleaved and activated in response to apoptotic stimuli. TNF-α can induce apoptosis by activating caspase-8 and -10, the former resulting in activating caspase-3, a key effector protein of the apoptotic machinery. Aside from apoptosis, caspase-3 is actively involved in muscle atrophy by cleaving actin from actinomyosin into smaller fragments that are degraded by the ubiquitin proteosome pathway (Chacon Heszele *et al*, 2004).

The 33 kD fragment of caspase-3 was analysed here using Western blotting. A monoclonal antibody which detects this subunit was used. Detection of this fragment of caspase-3 decreased significantly at the low and medium doses when compared to the control. The high and very high doses of TNF-α treatment however produced significant increases in the short-term (Figure 4.11***a*** and ***b***). With long-term (24 hours) TNF-α treatment, caspase-3 activation significantly decreased below the basal value to 77.83 ± 0.39 %. At 48 hours, this trend was not maintained but rather resulting in significant expression of caspase-3 protein levels (Figure 4.12***a*** and ***b***). It appears that at 24 hours caspase-3 cleavage had already occurred thus indicating apoptosis whereas at 48 hours caspase-3 protein expression return to normal thus no cleavage and consequently less apoptosis. Long-term TNF-α treatment yielded conflicting results in three successive experiments with regard to caspase-3 activation, and no meaningful conclusions could be made although statistical significance was observed.

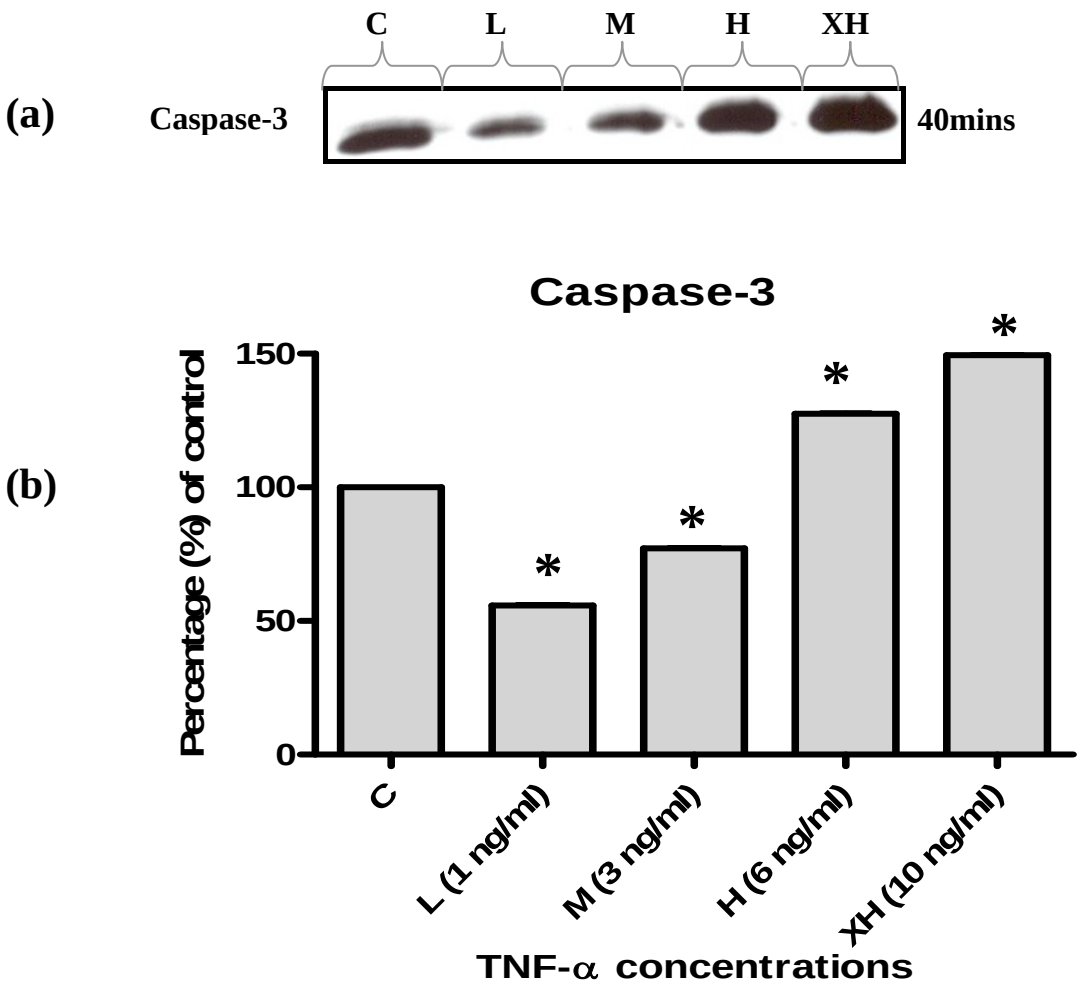

Figure 4.11 (a), (b): Representative Western blots demonstrating the effect of different TNF-α concentrations have on caspase-3 activation in L6 myotubes over a period of 40 minutes. Results are presented as their mean ± SEM. *P < 0.001 versus control (n ≥ 3)

(a)

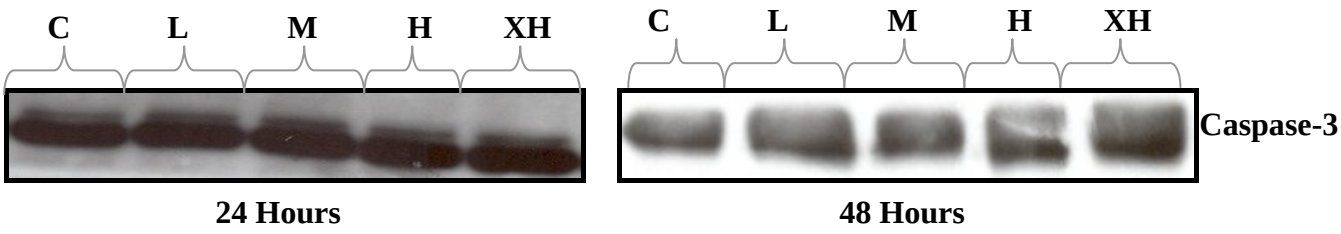

(b)

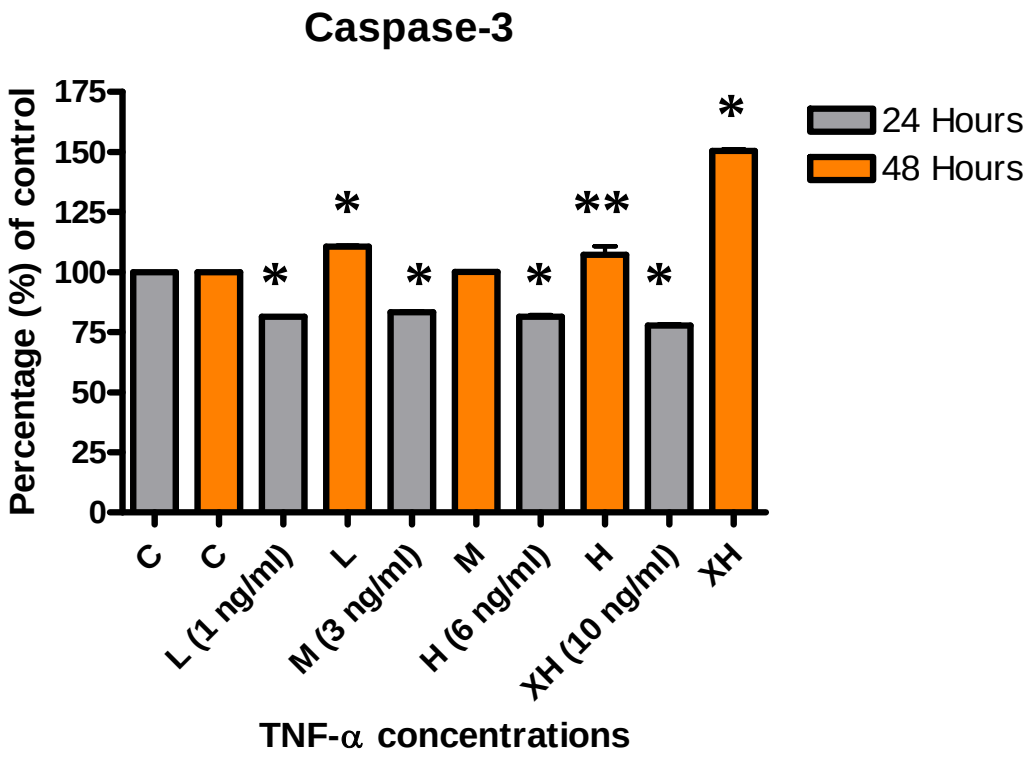

Figure 4.12 (a), (b): Representative Western blots demonstrating the effects of different TNF-α concentrations have in the activation of caspase-3 in L6 myotubes over a period of 24 and 48 hours. Results are presented as their mean ± SEM. *P < 0.001, **P < 0.05 versus control (n ≥ 3)

4.2.5. The effect of TNF-α on the expression of Ubiquitin involved in the ubiquitin-proteosome pathway

Ubiquitin is an important peptide that is involved in the targeting of proteins undergoing cytosolic proteolysis. In order to achieve our goal of detecting the expression levels of ubiquitin in response to increasing concentrations of TNF-α, we utilised the process of immunohistochemistry to accomplish this (Figure 4.13)

With long-term TNF-α supplementation at 24 hours, there appears to be an increase in the expression levels of ubiquitin, particularly at the very high dose although no significance was observed. At 48 hours however, ubiquitin expression levels significantly increased with increasing TNF-α supplementation when compared to the control (Figure 4.14).

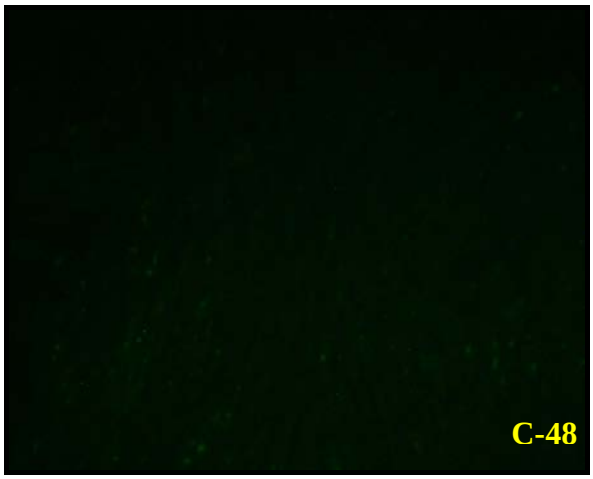

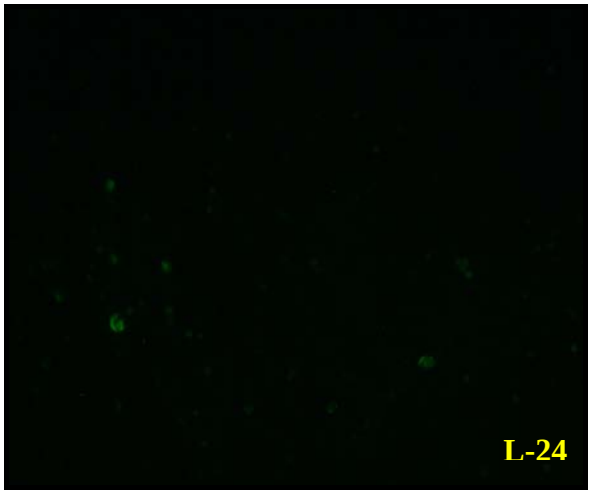

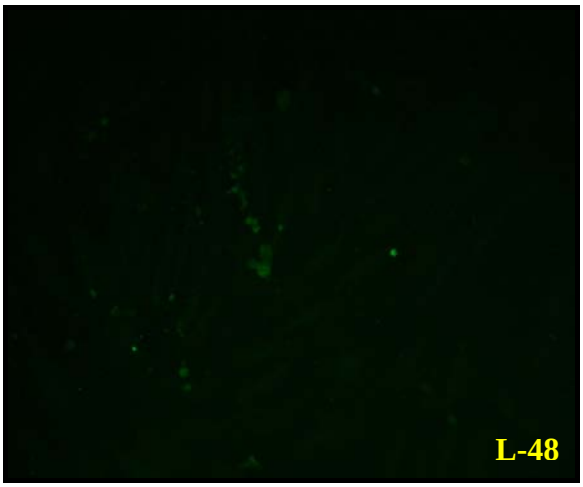

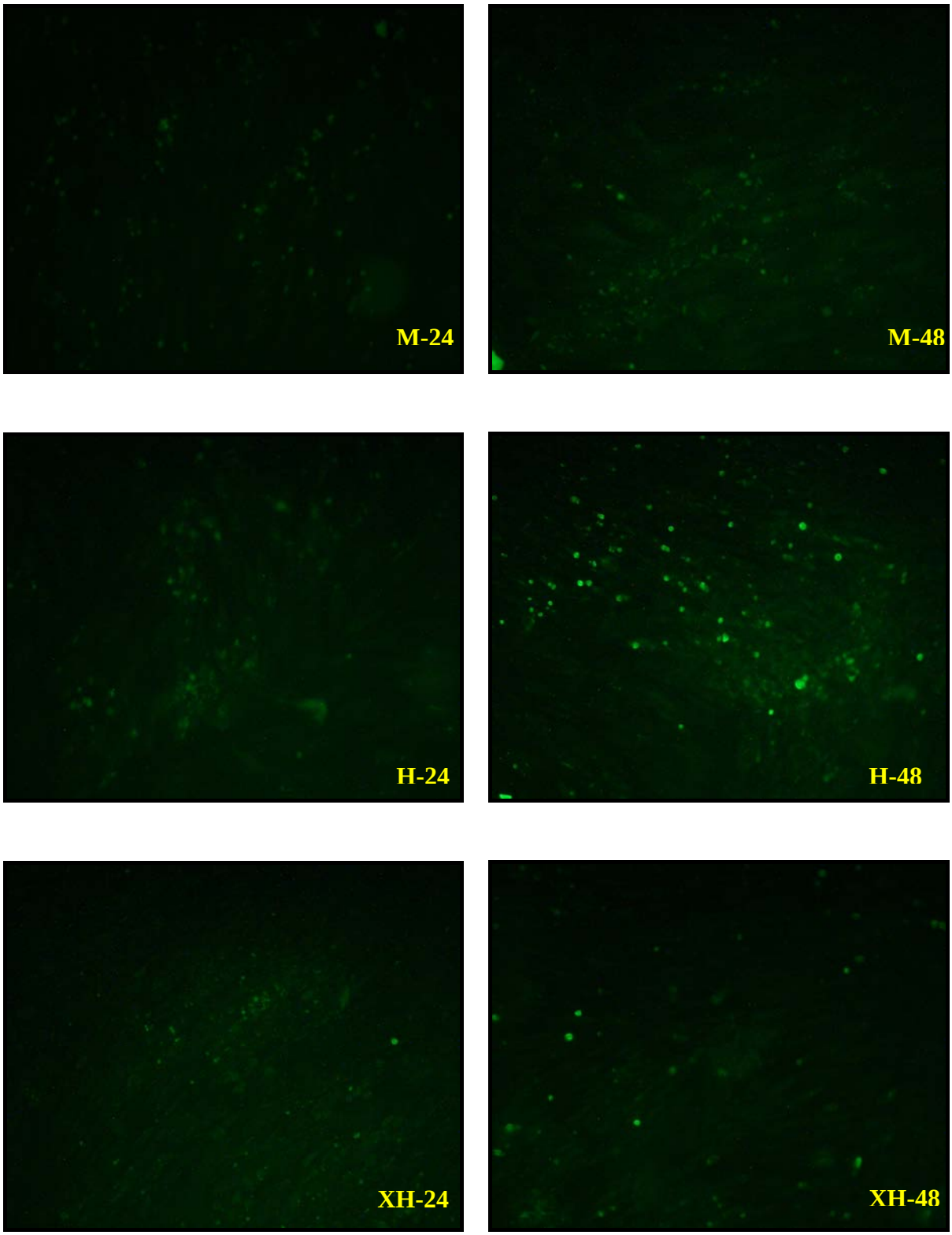

Figure 4.13: The effect of increasing doses of TNF-α on the expression levels of ubiquitin in L6 myotubes. Myotubes were stained with a FITC conjugated antibody (green) and scrutinized for the presence of ubiquitin using fluorescence microscopy. (n ≥ 3). C-24/48, control

for 24/48 hours; L-24/48, low dose for 24/48 hours; M-24/48, medium dose for 24/48 hours; H-24/48, high dose for 24/48 hours; XH-24/48, very high dose for 24/48 hours

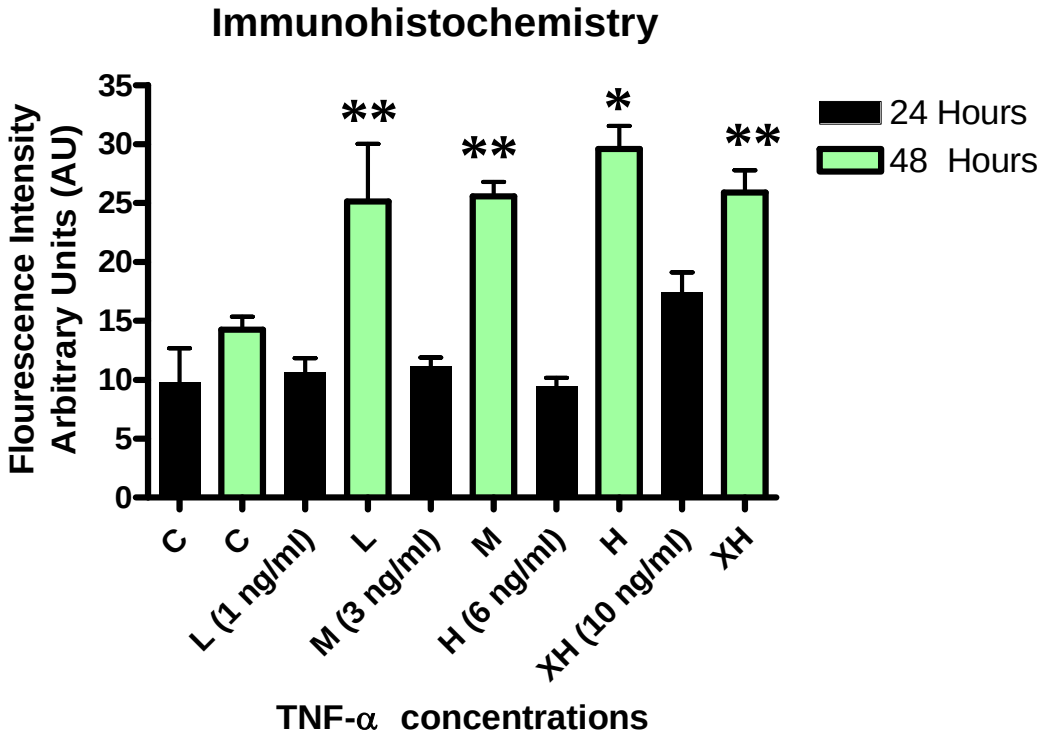

Figure 4.14: The effect of increasing doses of TNF-α on the expression of ubiquitin in L6 myotubes. Myotubes were stained with a FITC conjugated antibody (green) and scrutinized for the presence of ubiquitin using fluorescence microscopy. Results are presented as their mean ± SEM. *P < 0.05, **P < 0.001 versus control (n ≥ 3)

4.2.6. The effect of TNF-α on the expression of the E_3 ubiquitin ligases MuRF-1 and MAFbx involved in the ubiquitin-proteosome pathway (Western blots)

The ubiquitin-proteosome pathway is one of three known proteolytic systems involved in muscle protein breakdown. This pathway has been previously shown to arbitrate a large part of the degradation of either short-lived proteins or long-lived myofibrillar proteins in skeletal muscle. Notably, two E_3 protein ligases, MuRF-1 and MAFbx, are expressed uniquely and increase more significantly than any other component of this proteolytic pathway. This outcome has suggests that these muscle-specific proteins play a pivotal role in the atrophy process.

Long-term TNF-α supplementation yielded significant increases ($p < 0.001$) in the expression of MuRF-1. Although the expression levels decreased at 48 hours, results still remained statistically significant producing a 2 fold increase when compared to the control (Figure 4.15***a*** and ***b***). Long-term TNF-α supplementation for MAFbx on the other hand, produced a similar significant pattern of expression at 24 hours after which decreases at 48 hours still being able to maintain its significance ($p < 0.001$) (Figure 4.16***a*** and ***b***). This may imply that both MuRF-1 and MAFX reach their peak at 24 hours and decreases with additional supplementation of TNF-α at 48 hours. These data correlate with the previous experimental data of the p38-MAPK and FKHR since they regulate the transcription of these ubiquitin ligases.

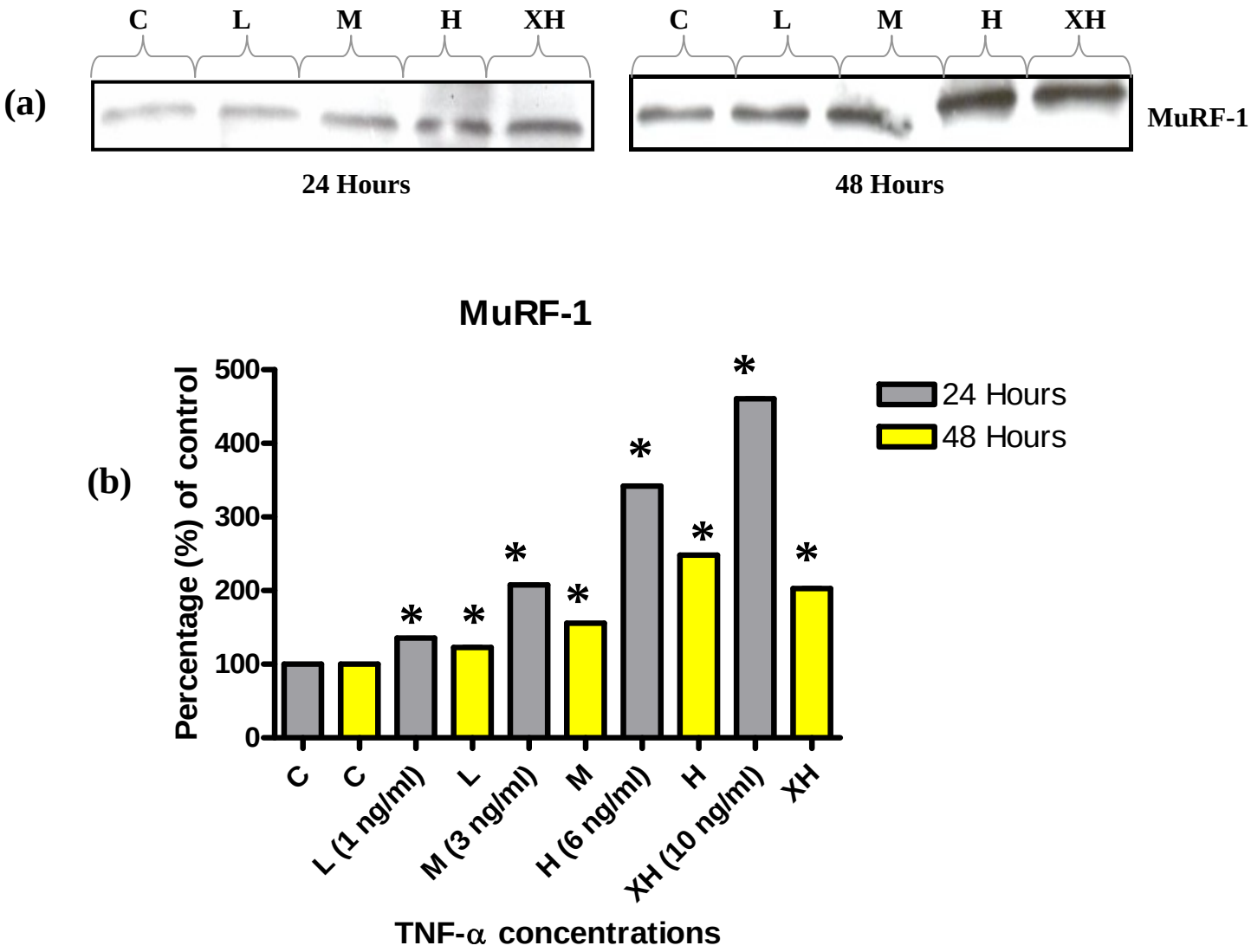

Figure 4.15 (a), (b): Representative Western blots demonstrating the effect of different TNF-α concentrations have on the upregulation of the E_3 ubiquitin ligase MuRF-1 in L6 myotubes over a period of 24 and 48 hours. Results are presented as their mean ± SEM. *P < 0.001 versus control (n ≥ 3)

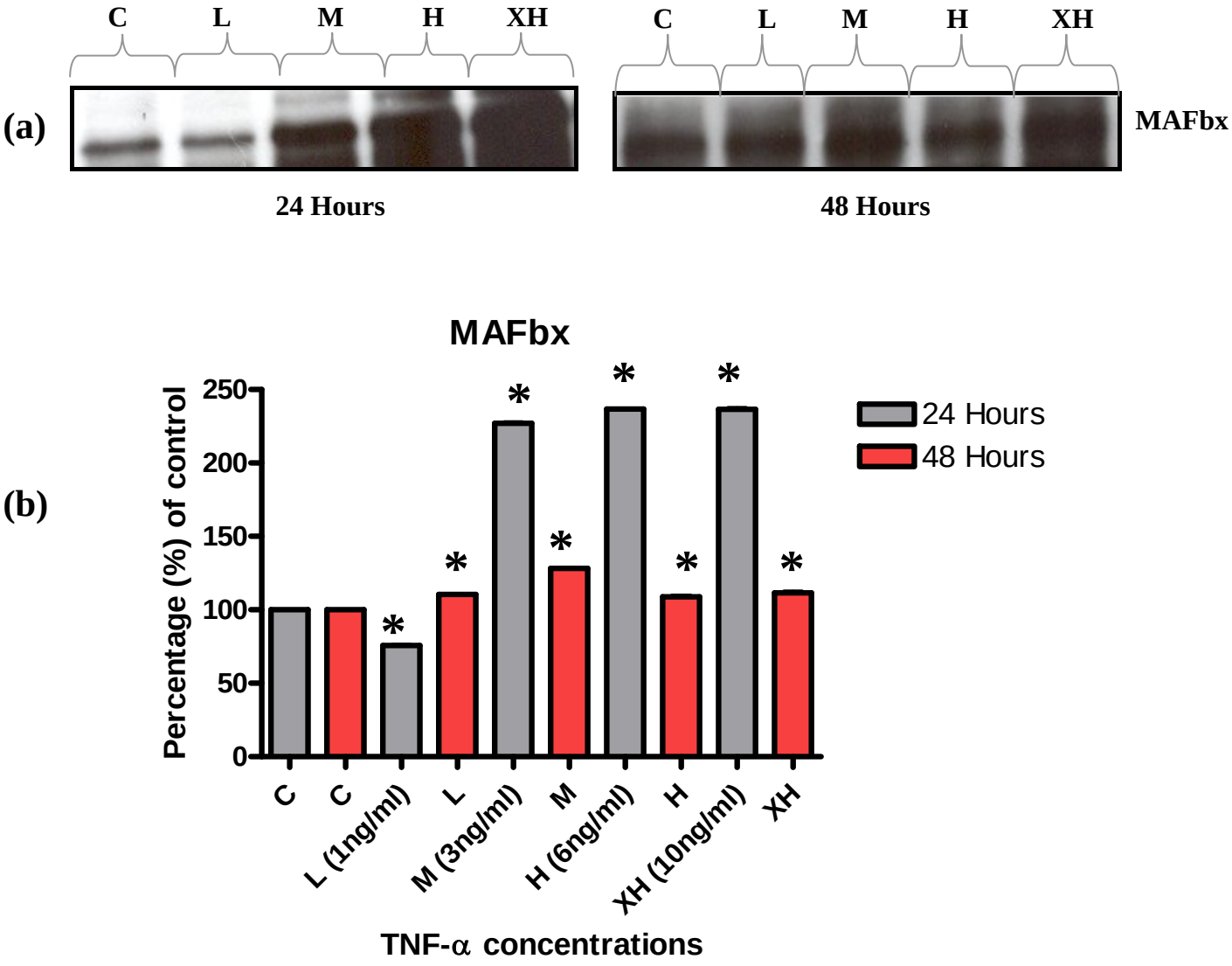

Figure 4.16 (a), (b): Representative Western blots demonstrating the effects of different TNF-α concentrations have on the upregulation of the E_3 ubiquitin ligase MAFbx in L6 myotubes over a period of 24 and 48 hours. Results are presented as their mean ± SEM. *P < 0.001 versus control (n ≥ 3)

4.2.7. The effect of TNF-α on the PI3-kinase pathway (Western blots)

Conditions accelerating muscle proteolysis are often allied with defective PI3-K/Akt signalling and reduced PI3-K-generated PIP_3. PI3-kinase and Akt constitute an integral signalling intersection that plays a role in a multitude of cellular processes which include the regulation of cell death, hypertrophy and in this case, atrophy. In addition, inositol phospholipids such as PIP_3, produced by the action of PI3-K, are important substrates of PTEN, a lipid phosphatase that acts to inhibit Akt. In this section of the results we evaluated the expression and activity of PI3-K, Akt and PTEN and studied the effects of TNF-α on these signalling components of the PI3-K pathway.

The p85 regulatory subunit of PI3-K was found to be constitutively expressed in L6 myotubes differentiated for eight days. Compared to the control samples, PI3-K activity significantly decreased ($p < 0.001$) with increasing TNF- α supplementation at 24 hours (Figure 4.17***a*** and ***b***). At 48 hours, TNF- α induced an even stronger inactivation of endogenous levels of PI3-K by reducing the expression levels by approximately 80%.

In addition to the Western Blotting technique, we utilised the p85 subunit of PI3-K that was immunoprecipitated from cell extract. A PI3-K ELISA was then conducted in order to substantiate the data obtained from the Western Blot analysis. Analysis of our data showed a similar trend to that of the Western Blot results. Data obtained from the ELISA technique concludes that PI3-Kα is a constitutively expressed protein in L6 myotubes. PI3-K activity appeared to decrease with increasing TNF-α supplementation at both 24 and 48 hours. Significance was observed at all concentrations used when compared to the control.

Following a decrease in PI3-K activity, phosphorylation Akt (ser473) is subsequently affected. Akt phosphorylation levels drastically decreased in response to increasing TNF-α treatment and significance was observed at all concentrations used (Figure 4.19). Data also shows that there was a 25% decrease in the phosphorylation of Akt between 24 and 48 hours when comparing only the very high TNF- α doses (10 ng/ml). Taken together, these data suggest that both PI3-K activity and Akt phosphorylation are influenced in a dose-dependent manner.

PTEN results consistently echoed the data obtained above. At 24 hours phosphorylation of PTEN was significantly reduced to 38.07 ± 0.34% when compared to the control (Figure 4.20***a*** and ***b***). At 48 hours however, phosphorylation of PTEN behaved differently. Whereas phosphorylation was expected to decrease, phosphorylation significantly increased especially at the medium dose. At the high and very high doses of TNF- α however, the level of phosphorylation was significantly reduced ($p < 0.001$) and almost completely abolished.

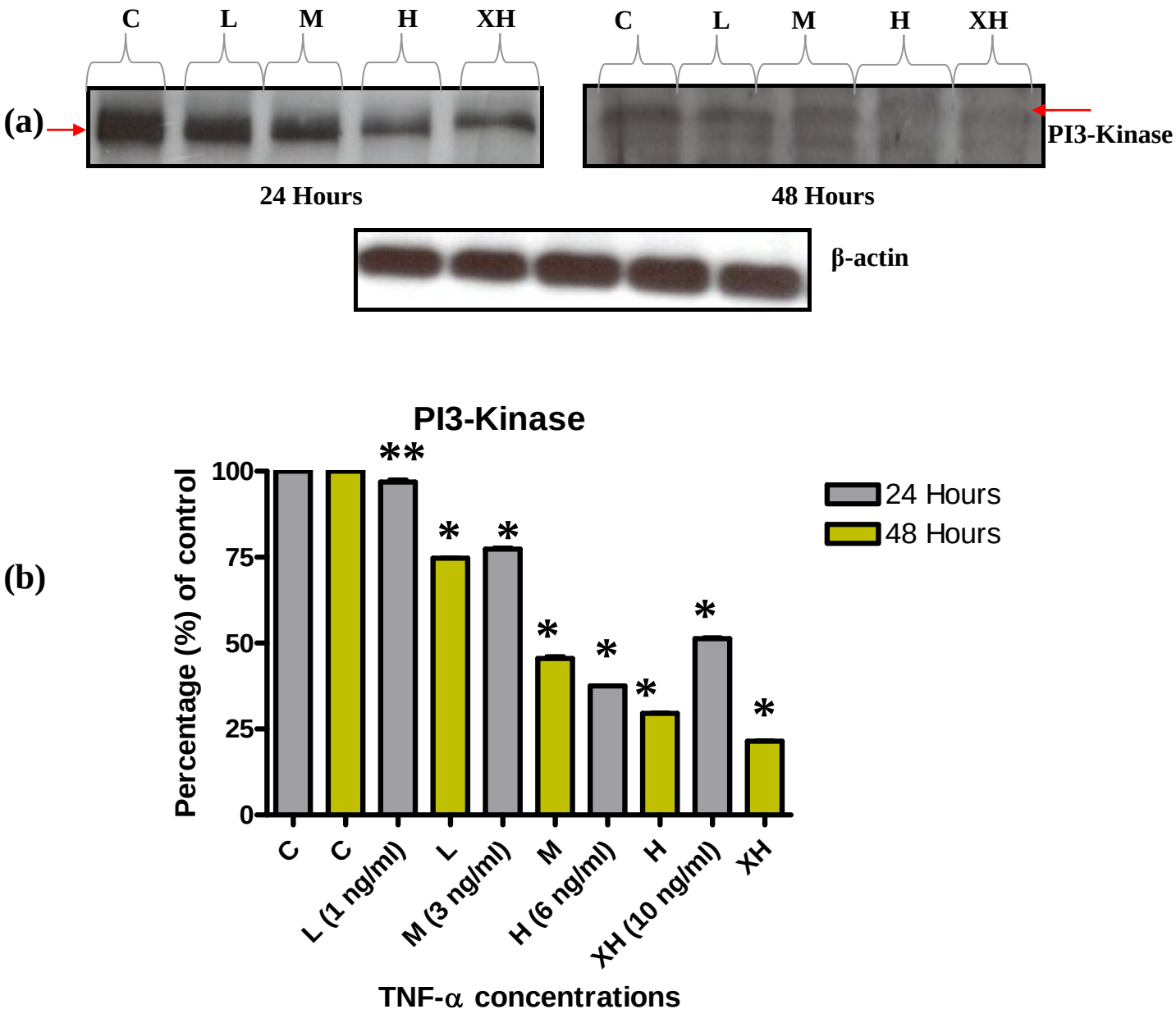

Figure 4.17 (a), (b): Representative Western blots demonstrating the effect of different TNF-α concentrations have on the PI3-kinase p85 regulatory subunit in L6 myotubes over a period of 24 and 48 hours. Results are presented as their mean ± SEM. *$P < 0.01$, **$P < 0.001$ versus control ($n \geq 3$)

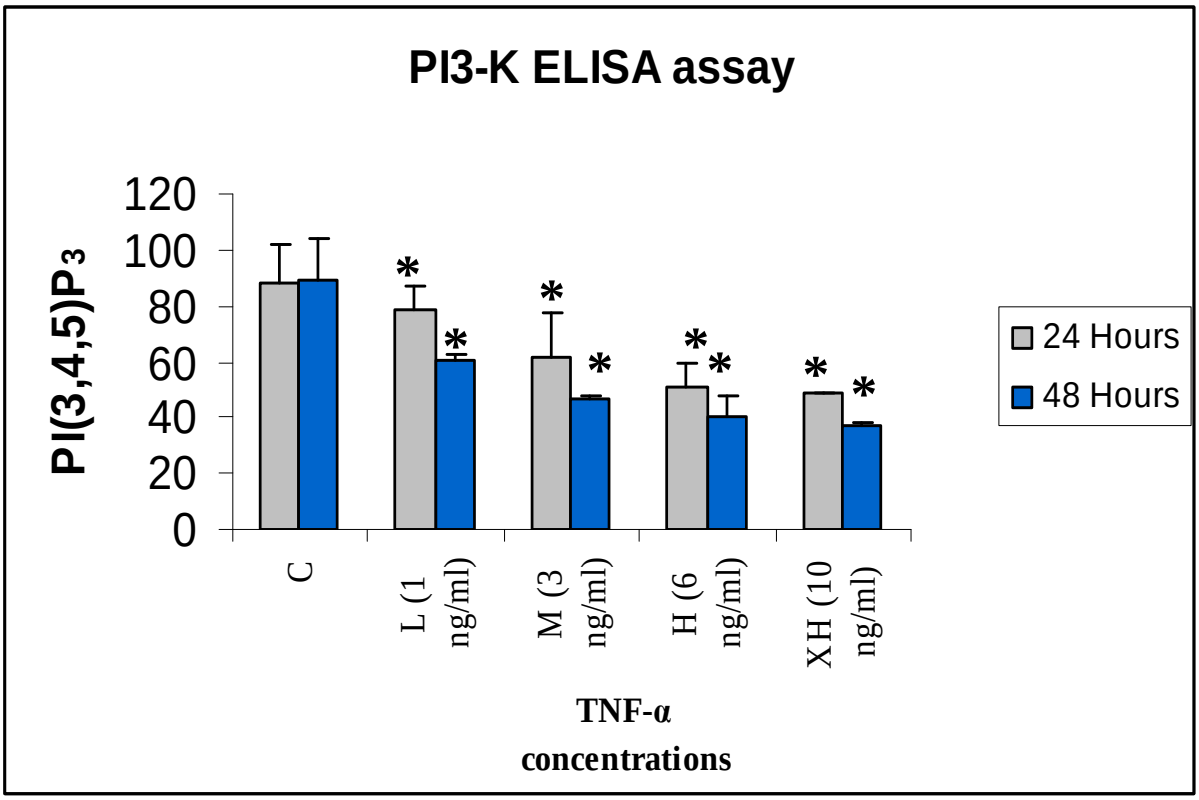

Figure 4.18: The effect of increasing TNF-α supplementation on the PI3-Kα catalysed production of PI(3, 4, 5)P_3 in L6 myotubes (24 hours). The p85 subunit of the PI3-K was immunoprecipitated from cell lysates using an anti-PI3-K antibody before a competitive ELISA assay was used to detect the amount of PI(3, 4, 5)P_3 produced from a substrate. Results are presented as their mean ± S.E.M, *P < 0.001 vs. control (n≥ 3).

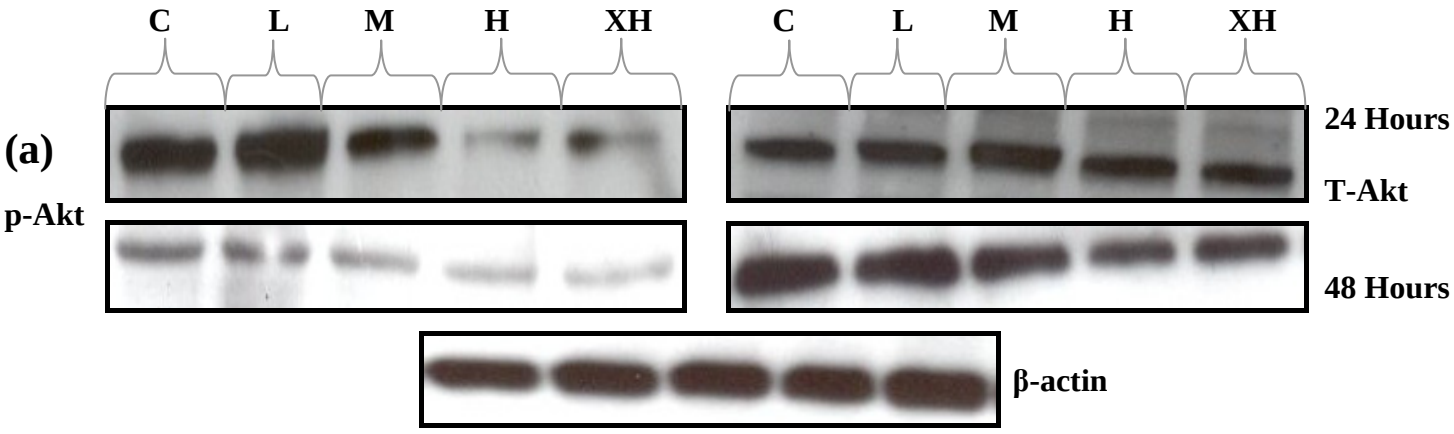

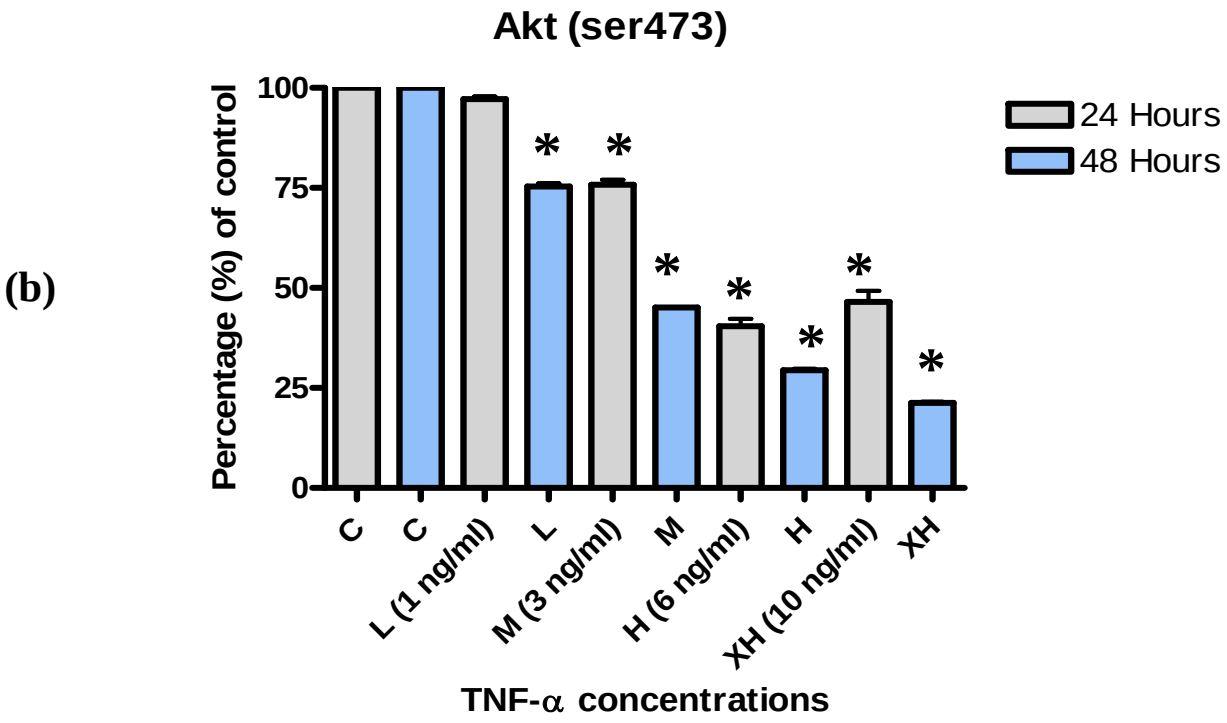

Figure 4.19 (a), (b): Representative Western blots demonstrating the effect of different TNF-α concentrations have on the phosphorylation of Akt in L6 myotubes over a period of 24 and 48 hours. Results are presented as their mean ± SEM. *P < 0.001 versus control (n ≥ 3). P-Akt, phosphorylated-Akt; T-Akt, total-Akt

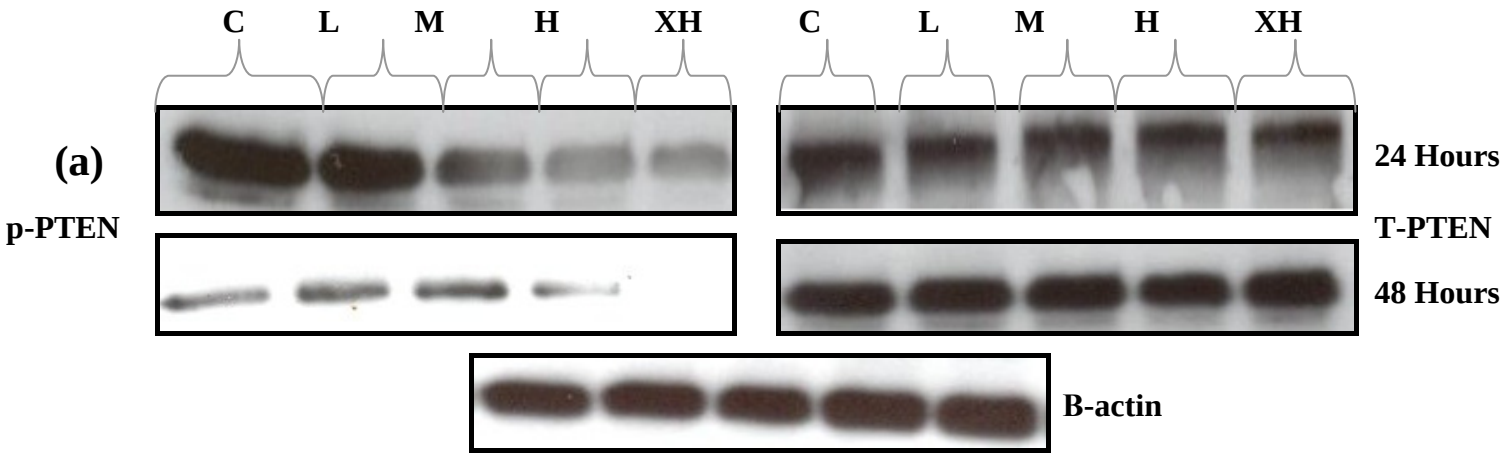

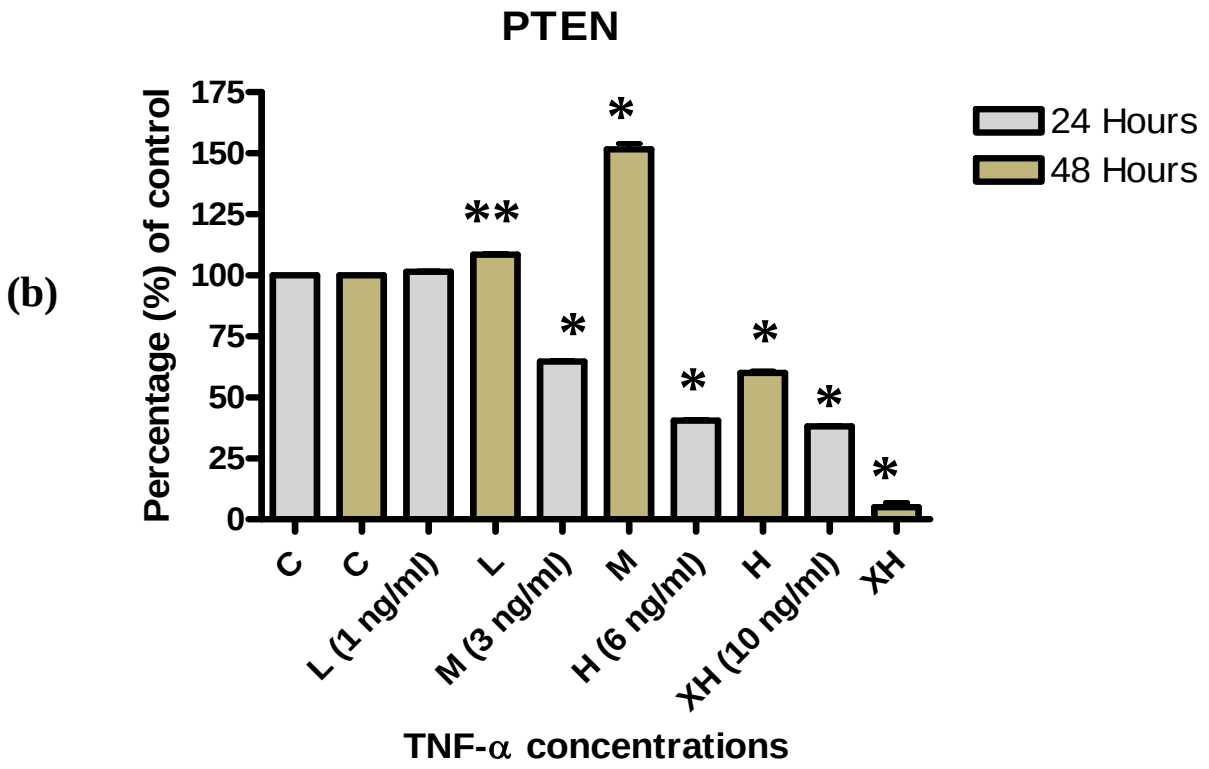

Figure 4.20 (a), (b): Representative Western blots demonstrating the effect of different TNF-α concentrations have on the phosphorylation of PTEN in L6 myotubes over a period of 24 and 48 hours. Results are presented as their mean ± SEM. *P < 0.001, **P < 0.01 versus control (n ≥ 3). P-PTEN, phosphorylated-PTEN; T-PTEN, total-PTEN

4.2.8. The effect of TNF-α on protein content and fiber diameter

Now that we have established which pathways were affected by TNF- α treatment, we then set out to learn how much protein is actually present in the L6 myotubes and if this had any effect on muscle fiber size. Protein content was assessed using the Bradford technique and fiber size was determined by staining the cells with hematoxylin and eosin after which the fiber diameter was measured. For this experiment a fiber is defined as a cell containing two or more nuclei.

The protein content results obtained were not what we expected. At 24 hours protein content appeared to be significantly elevated ($p < 0.01$) especially at the high dose. The high dose at 48 hours produced a similar trend although remaining insignificant (Figure 4.21). The very high doses at both time points appeared to have lower protein content although the results were insignificant. No meaningful conclusions could be drawn from these results.

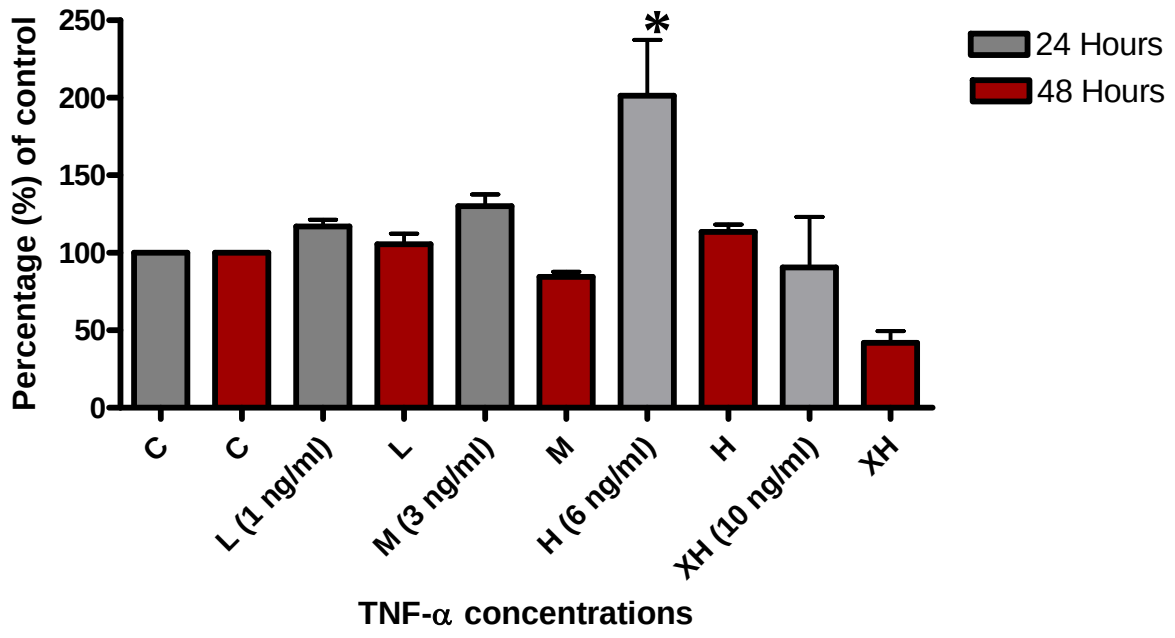

Figure 4.21: The effect of different TNF-α concentrations have on protein content in L6 myotubes over a period of 24 and 48 hours. Results are presented as their mean ± SEM. *P < 0.01 versus control (n ≥ 4)

Data obtained from the H & E staining method produced positive results (Figure 4.22). At 24 hours there appears to be a gradual decrease in muscle fiber diameter size with increasing TNF-α concentrations. Significance was only observed at the very high dose ($p < 0.05$). At 48 hours on the other hand, the low dose produced a slightly higher difference in fiber diameter size when compared to the control group. This difference was however not maintained with the other doses. Compared to the control samples, the very high dose produced an almost 50% decrease in fiber diameter size which resulted in its significance ($p < 0.05$) (Figure 4.23).

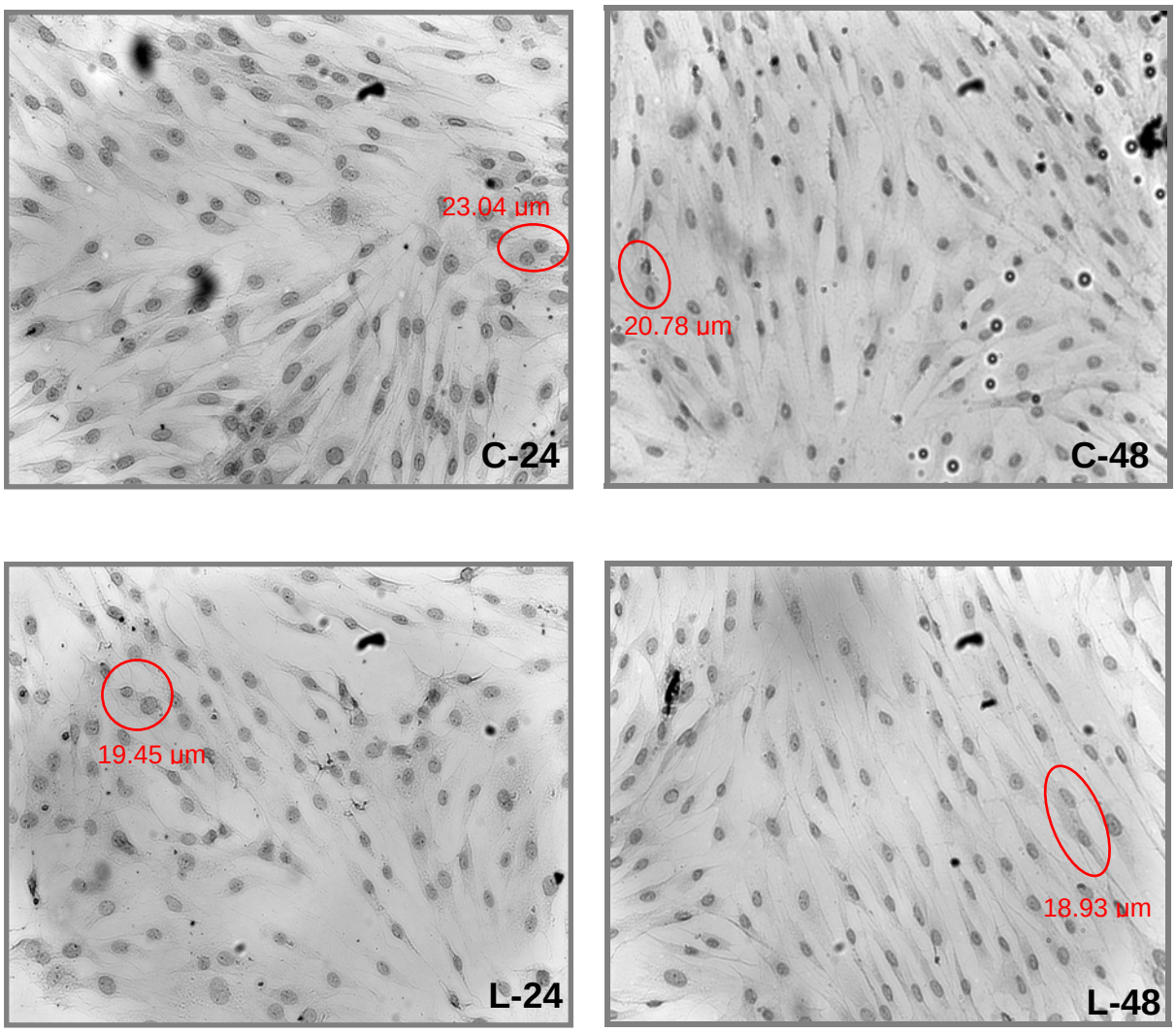

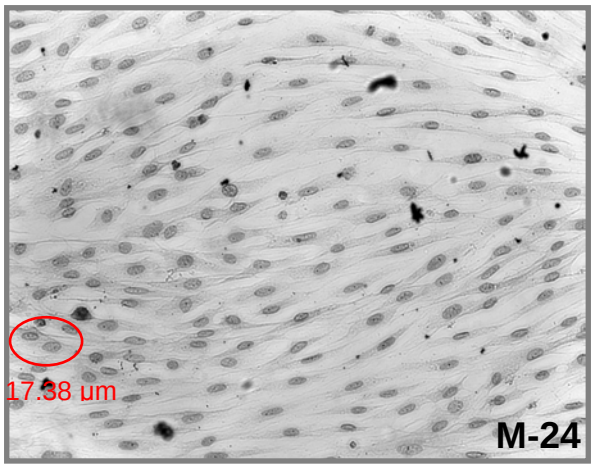
17.38 µm
M-24

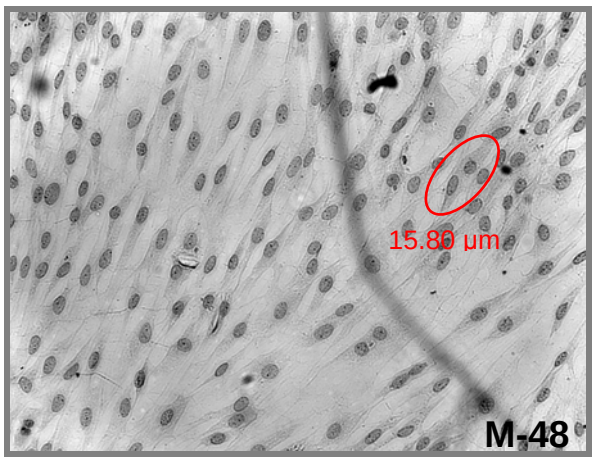
15.80 µm
M-48

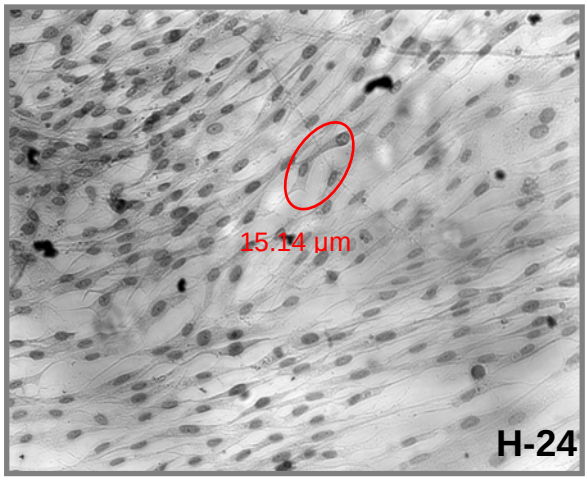
15.14 µm
H-24

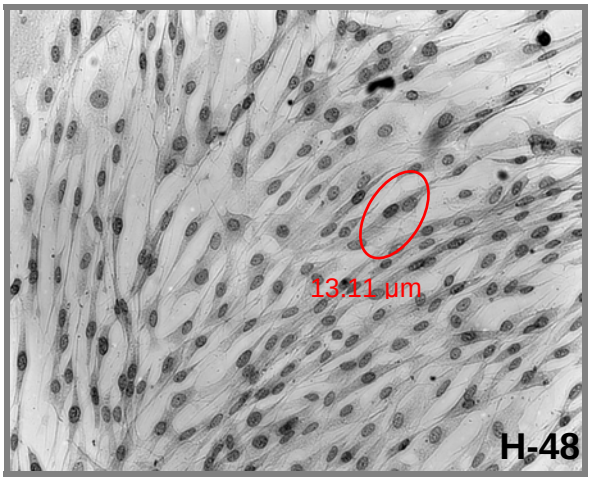
13.11 µm
H-48

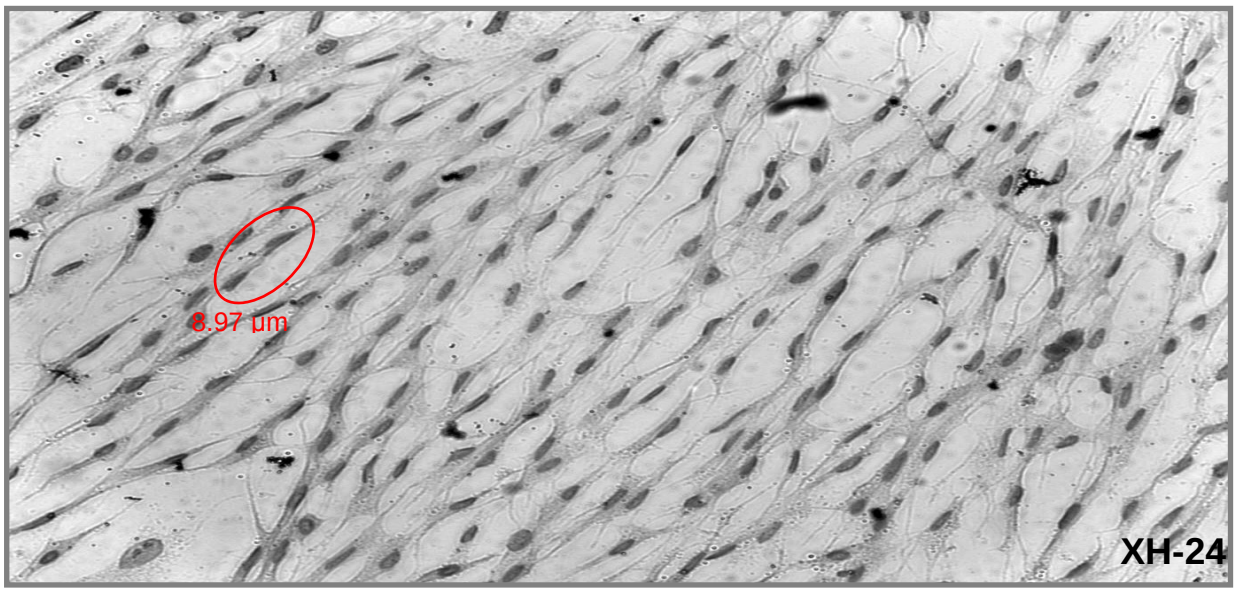
8.97 µm
XH-24

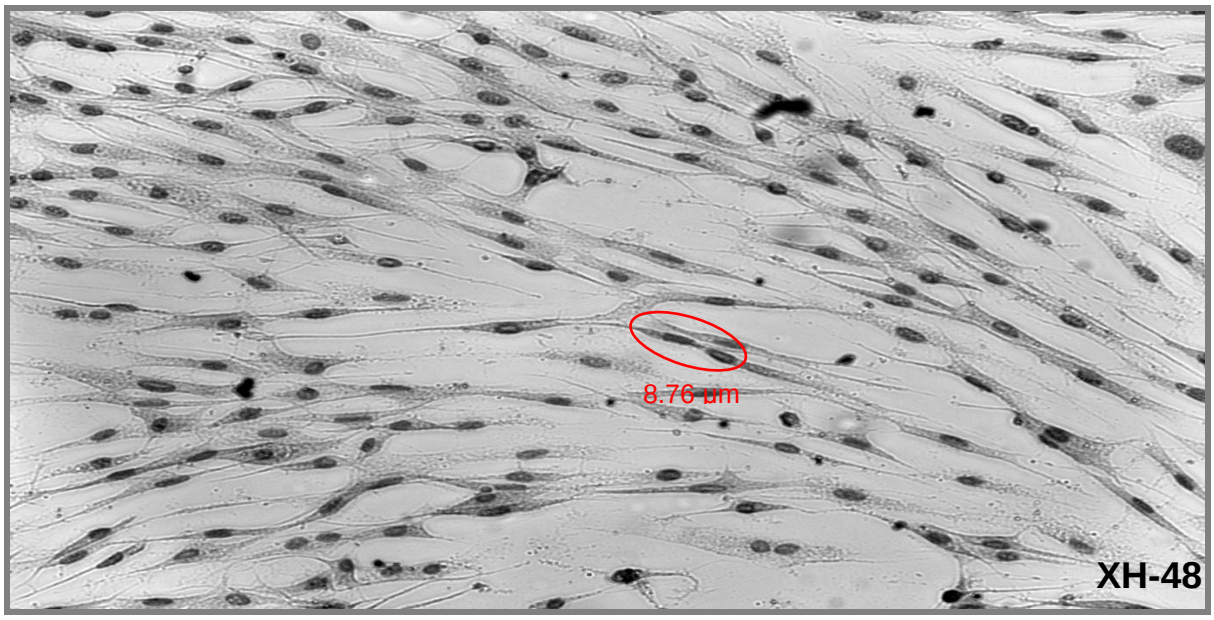

Figure 4.22: The effect of different TNF-α concentrations on fiber diameter in L6 myotubes over a period of 24 and 48 hours. L6 myotubes were grown on coverslips, differentiated for 8 days and ultimately stained using the H and E technique. Red circles indicate differences in fiber diameter when compared to the control. Magnification: 20X

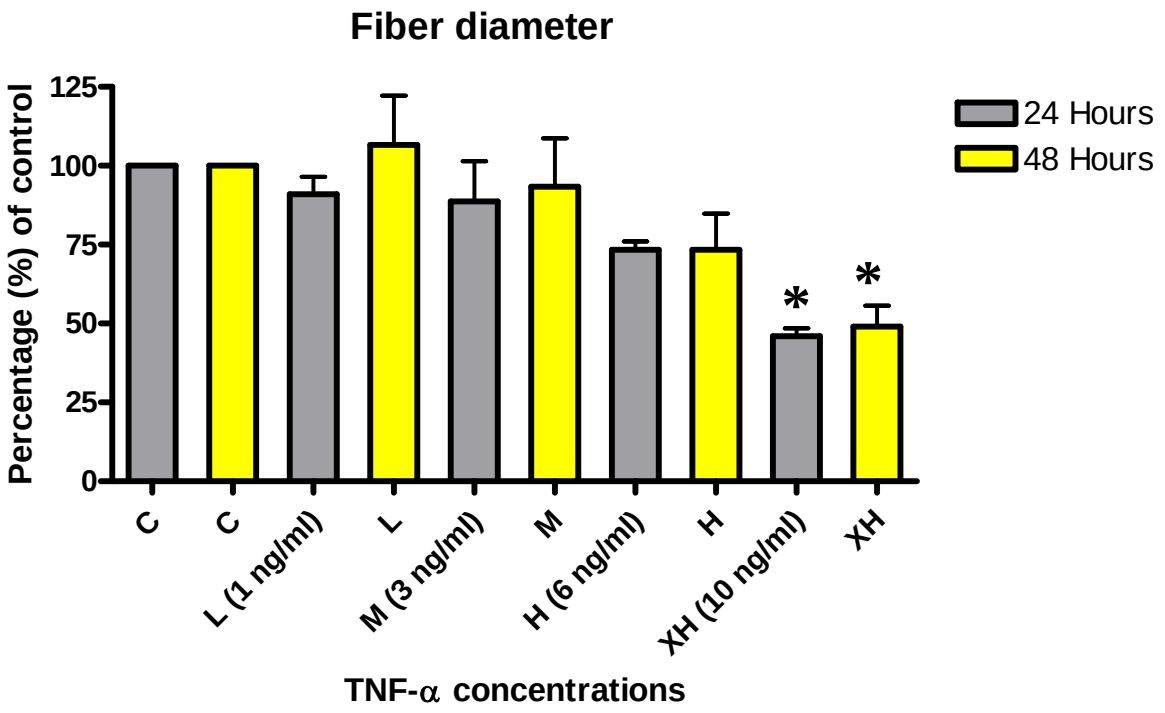

Figure 4.23: The effect of different TNF-α doses have on fiber diameter in L6 myotubes over a period of 24 and 48 hours. Results are presented as their mean ± SEM. *P < 0.05 versus control (n ≥ 3)

4.2.9. The effect of TNF-α on the markers of differentiation (Western blots)

MyoD and myogenin proteins belong to the group of muscle regulatory factors (MRFs) that play an important role in differentiation. MyoD is the principal regulatory molecule of myogenic differentiation and plays a vital role in the cell cycle exit of differentiating myoblasts, muscle-specific gene expression, and myotube formation and is crucial for skeletal muscle lineage determination. Myogenin on the hand is necessary for natural biochemical and morphological differentiation of skeletal muscle but is not requisite for the obligation of cells to the myogenic lineage. These two muscle proteins are considered here.

MyoD expression at 24 hours produced significant decreases ($p < 0.001$) when compared to the control samples. At 48 hours on the other hand the low dose appeared to significantly increase MyoD expression. This increase was however not maintained for long. The medium, high and very high TNF-α doses produced significant decreases in MyoD expression with the very high dose experiencing a 90% decrease compared to the control (Figure 4.24***a*** and ***b***).

Myogenin protein expression at 24 hours produced conflicting results. The low and medium doses seemed to significantly increase myogenin expression whereas the high and very high doses produces significantly lower myogenin expression when compared to the control. At 48 hours however, myogenin protein expression decreases with increasing TNF-α concentrations (Figure 4.25***a*** and ***b***).

Between the two muscle-specific proteins, MyoD protein expression appears to be the most affected by the adverse effects of increasing TNF-α levels.

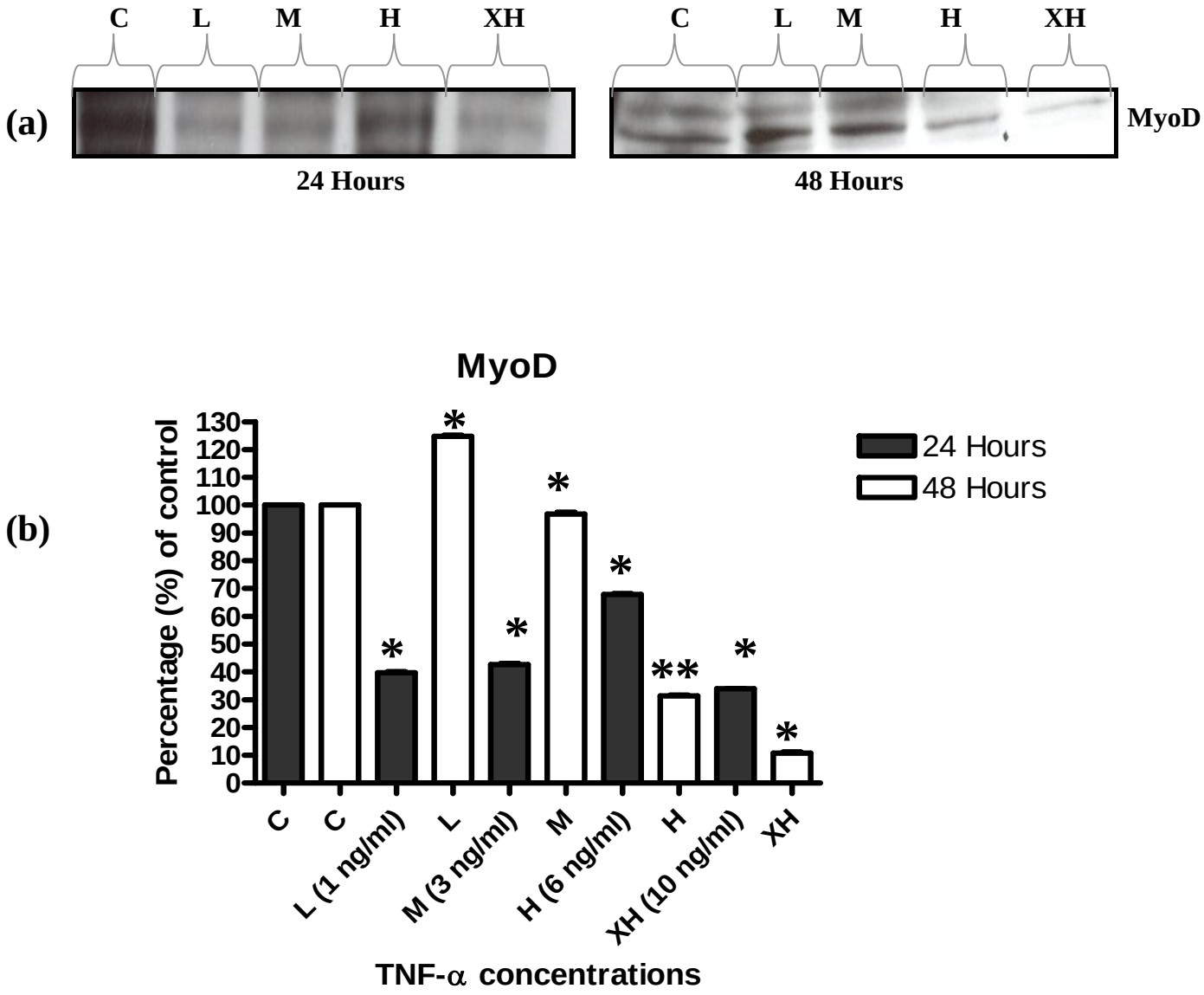

Figure 4.24 (a), (b): Representative Western blots demonstrating the effect of different TNF-α concentrations have on MyoD protein expression in L6 myotubes over a period of 24 and 48 hours. Results are presented as their mean ± SEM. *P < 0.001, **P < 0.05 versus control (n ≥ 3)

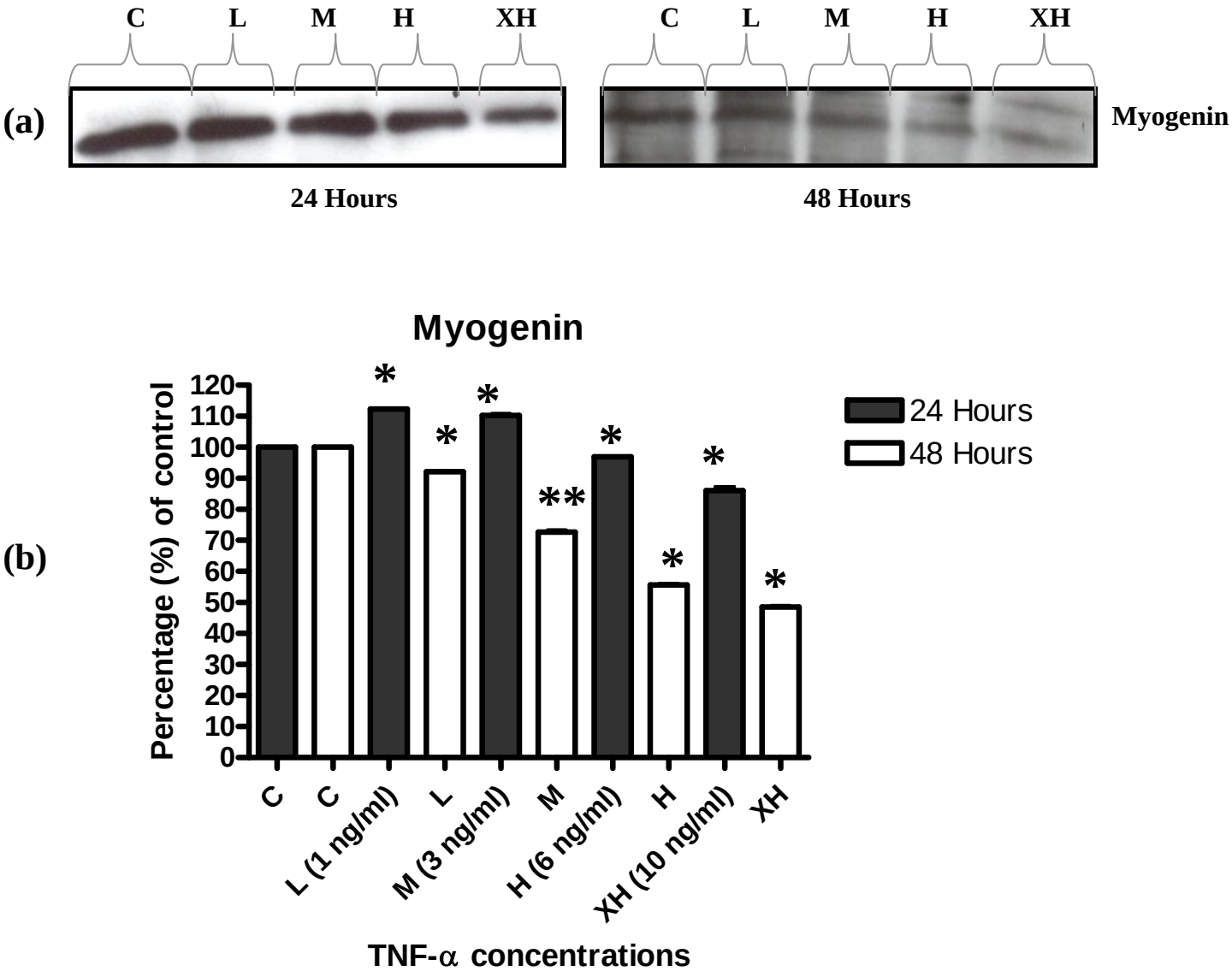

Figure 4.25 (a), (b): Representative Western blots demonstrating the effect of different TNF-α concentrations have on Myogenin protein expression in L6 myotubes over a period of 24 and 48 hours. Results are presented as their mean ± SEM. *P < 0.001, **P < 0.05 versus control (n ≥ 3)

4.2.10. Analysis of apoptosis

In order to assess the apoptotic effect of increasing TNF-α concentrations in L6 myotubes, we isolated DNA (chromatin) from treated myotubes and performed a DNA fragmentation assay which was analysed by 1.6% agarose gel electrophoresis in the presence of ethidium bromide (Figure 4.28). Only the 24 hour samples were analysed.

Although we observed a significant number of apoptotic cells in the very high dose (Figure 4.1***a***), we did not observe TNF-α induced changes in the amount of apoptosis at this time point and at this TNF-α concentration. In fact very little DNA fragmentation was seen in all the TNF-α concentrations tested at 24 hours.

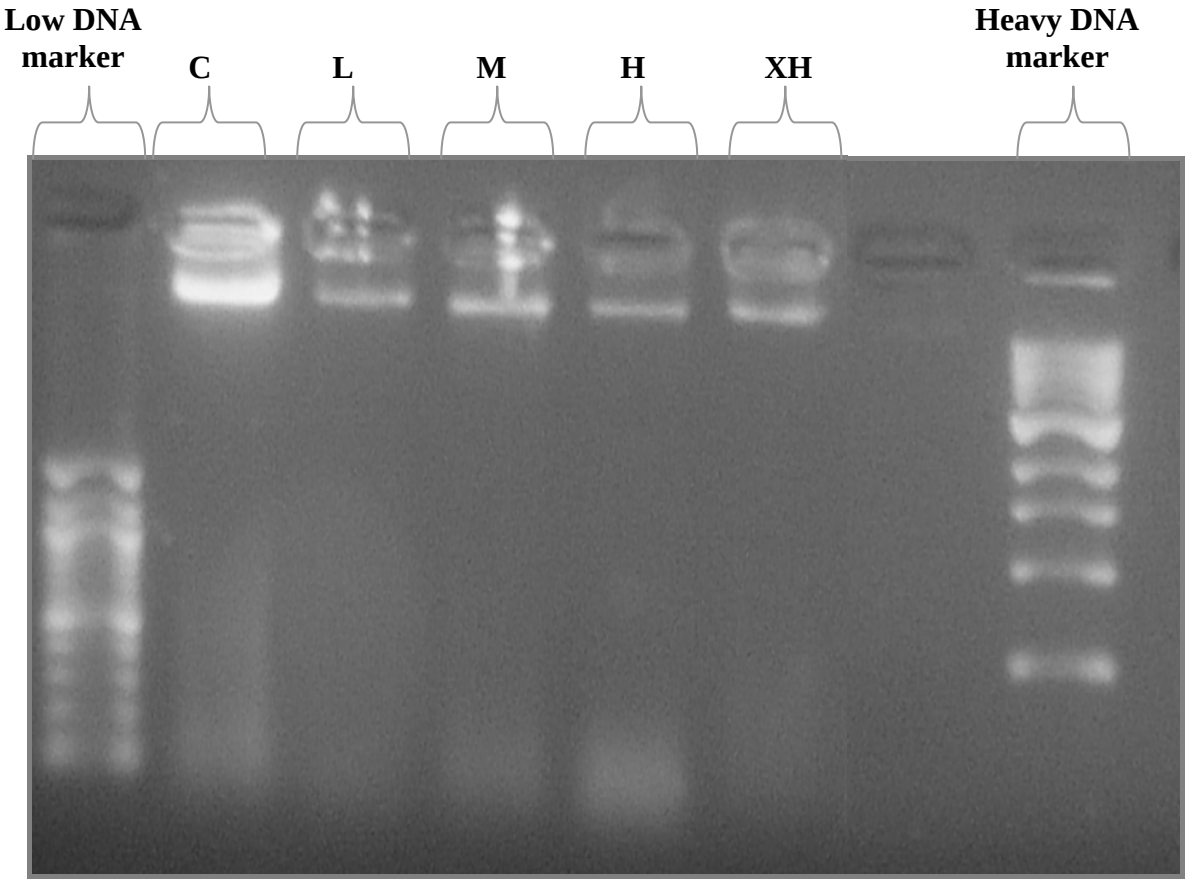

Figure 4.26: DNA fragmentation assay on L6 myotubes supplemented with increasing TNF-α concentrations as indicated. DNA ladders were observed with all TNF-α concentrations used for a period 24 hours. One representative image is shown from two experiments that yielded similar results.

4.2.11. The effect of TNF-α on oxidative stress (ROS)

Profuse research displays that oxidative stress contributes to muscle atrophy. Oxidative stress has been implicated to play a key role in regulating signalling pathways, leading to increased muscle protein degradation and muscle proteolysis. Mitochondria are able to generate ROS species via autooxidation of molecular oxygen at complex I or complex III of the electron chain transport. To determine whether the ROS yielded by the addition of TNF-α to L6 myotubes were produced by mitochondria, the mitochondria-specific fluorescent dye, Mito-Tracker Red CM-H_2 X ROS was used. A fluorescent imaging technique was then employed to establish the likely source of ROS production subsequent to TNF-α supplementation (Figure 4.26).

Long-term TNF-α supplementation at both 24 and 48 hours induced modest increases of ROS production although no significance was observed (Figure 4.27). This observation is supported by several other studies implicating TNF-α induced ROS production, evidently released from mitochondria (Li *et al*, 1998; 1999 and 2000). This experiment and others may propose a potential function of ROS as a possible cause to cytokine-induced muscle wasting.

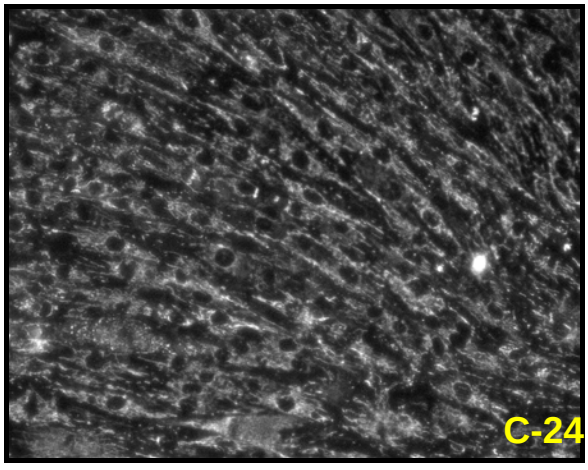

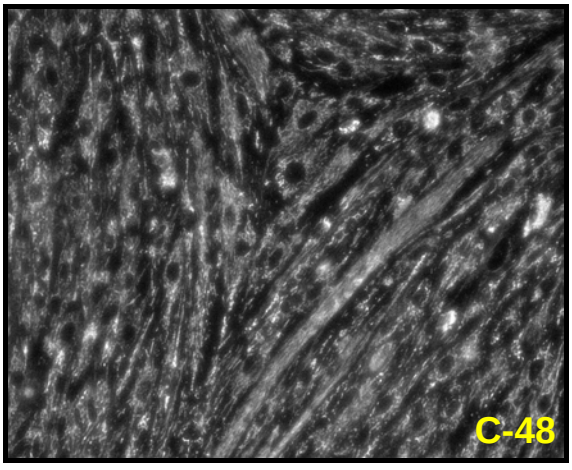

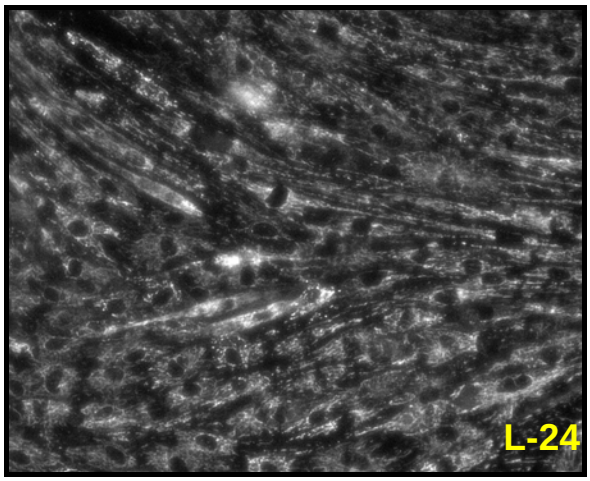
L-24

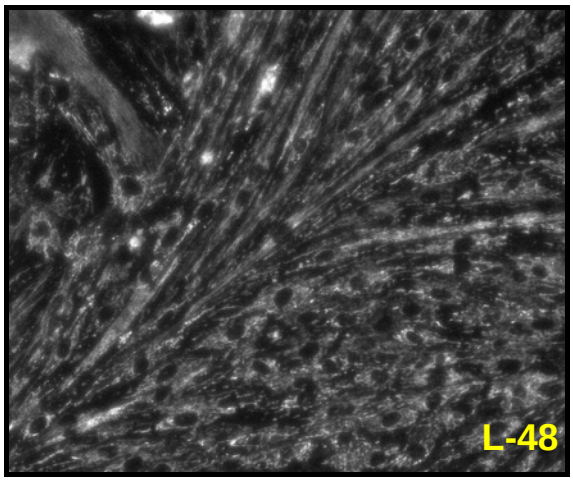
L-48

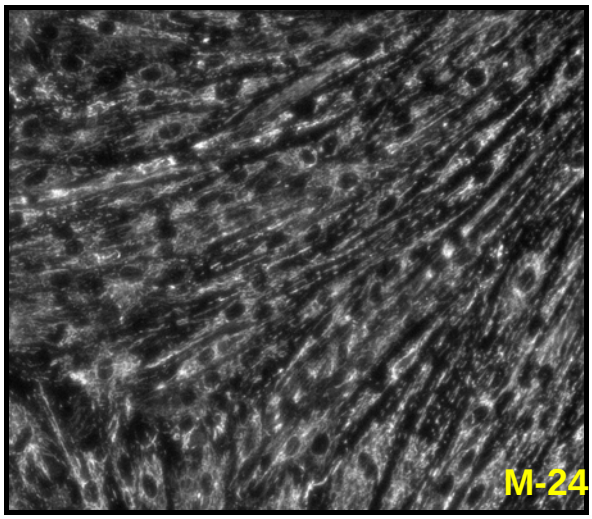
M-24

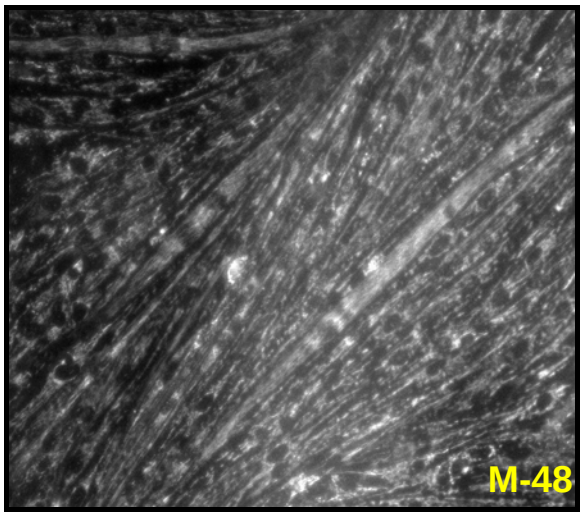
M-48

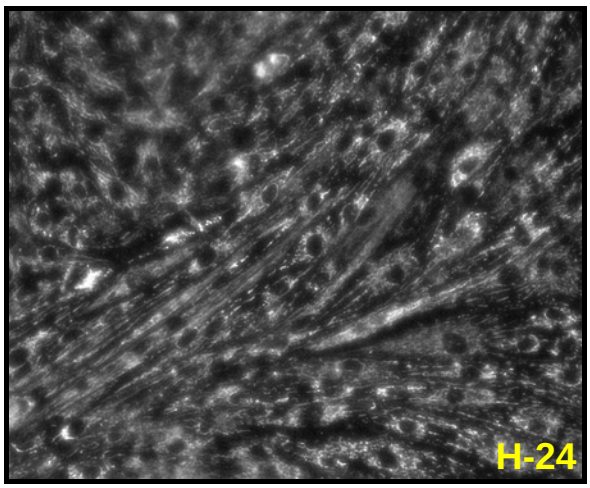
H-24

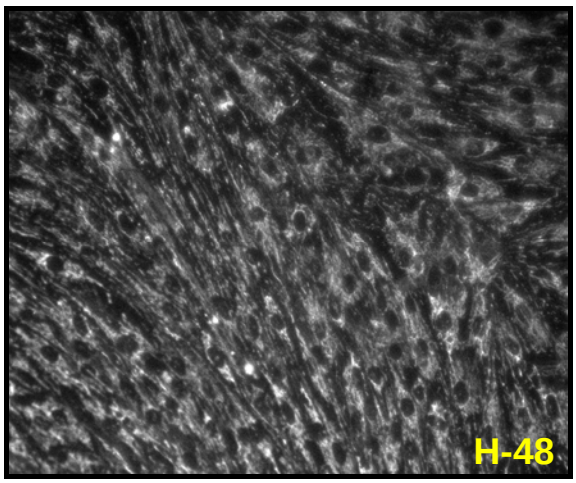
H-48

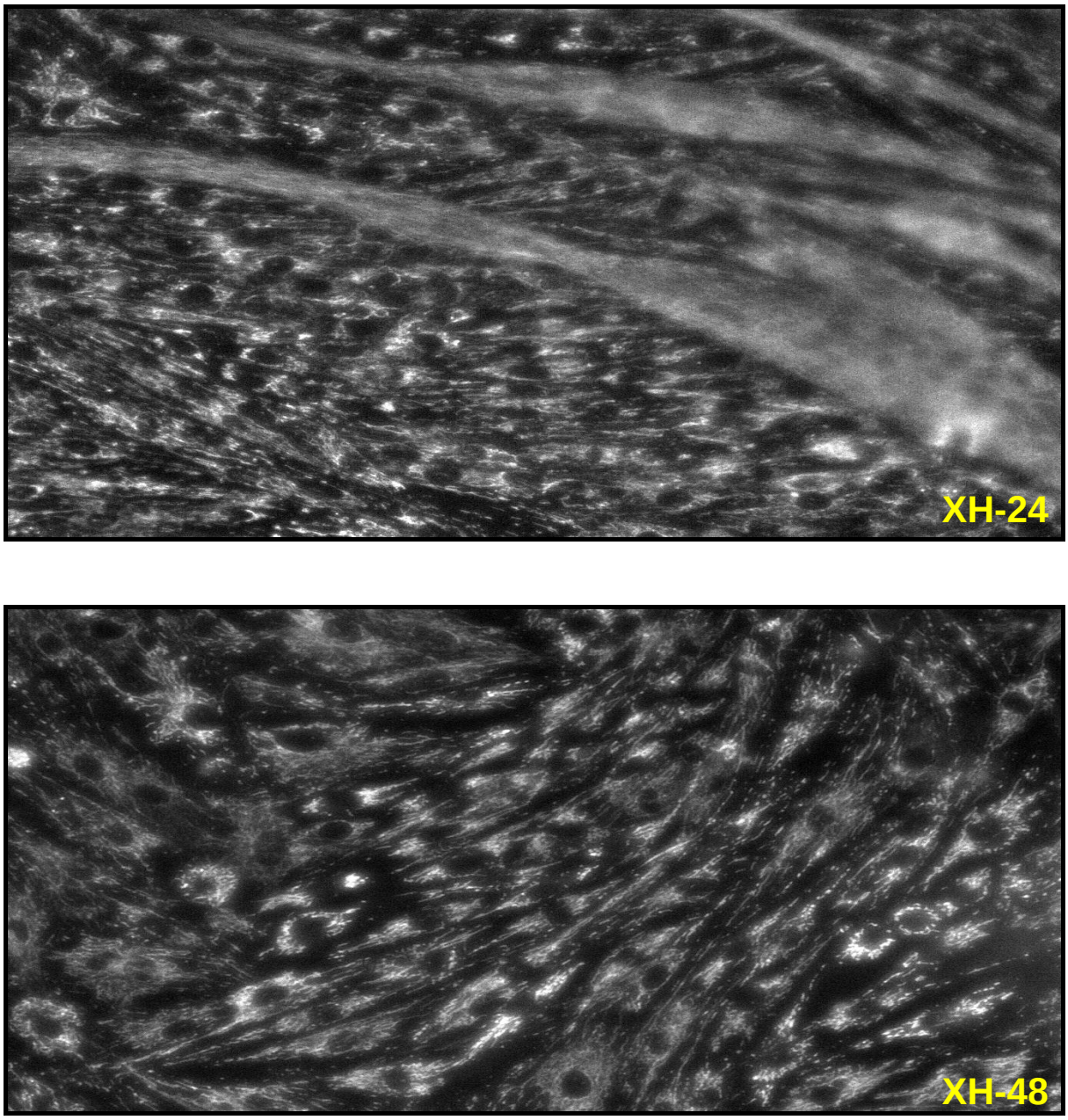

Figure 4.27: The effect of increasing TNF-α concentrations have on ROS production in L6 myotubes over a period of 24 and 48 hours. The mitochondria-specific fluorescent dye, Mito-Tracker Red CM-H_2 X ROS was used. A fluorescent imaging technique was used to determine possible ROS production where the mean grey area was measured (n = 3)

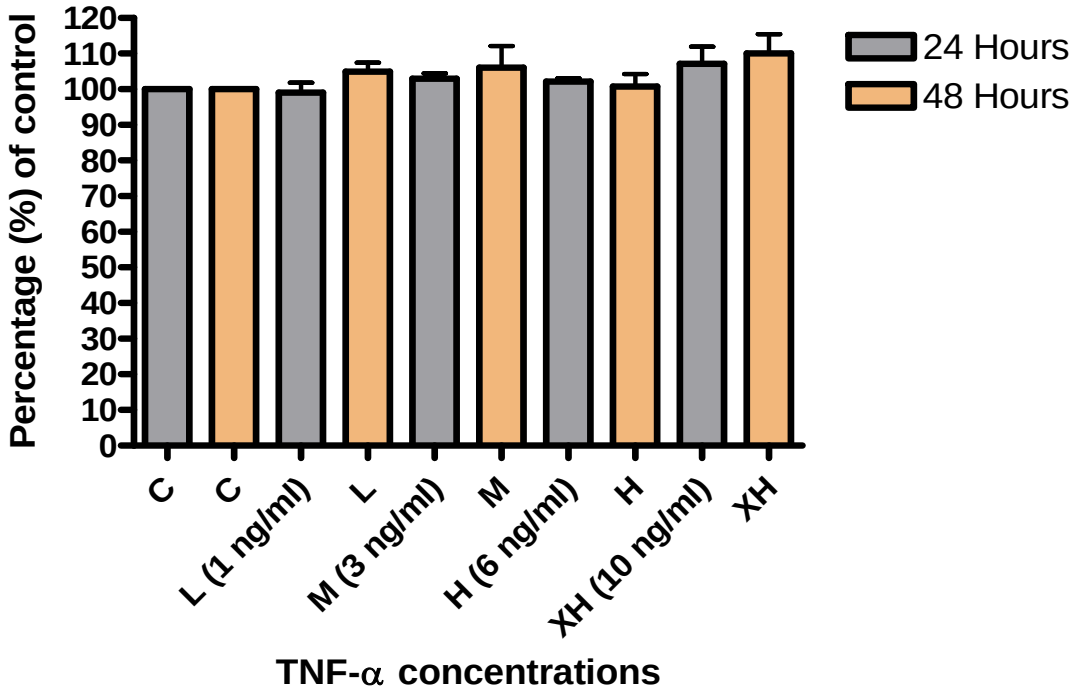

Figure 4.28: The effect of different TNF-α concentrations have on ROS production in L6 myotubes over a period of 24 and 48 hours. Although there appears to be increases in ROS accumulation post treatment, no significance was observed. Results are presented as their mean ± SEM. *P < 0.05 versus control (n ≥ 3)

CHAPTER 5

Results III

Although only slight but insignificant increases in ROS production were observed with supplementation of 10 ng/ml TNF-α, we decided to test the effect of a commercially available antioxidant (pictured below) on various parameters.

5.1. *Long-term treatment with TNF-α and Oxiprovin on cell viability and ROS accumulation*

Oxiprovin is a pure grape seed extract with tremendous antioxidant properties. Antioxidants are involved in the prevention of cellular damage which is the universal pathway for a wide variety of chronic inflammatory diseases. This antioxidant contains compounds known as OPCs (Oligometric proanthocyanidins) that are naturally occurring polyphenolic bioflavonoids and it is this compound that eradicates free radicals. The use of this product in our study was to determine its effect in combination with TNF-α, on cell viability (MTT Assay) and ROS production.

5.1.1. The effect of TNF-α and Oxiprovin on proliferation cell viability

TNF-α (10 ng/ml) alone produced no significant changes on cell viability at 24 hours when compared to the control. The antioxidant alone (50 and 100 μM) on the other hand significantly reduced cell viability ($P < 0.001$) by approximately 30%. The combination of TNF-α and Oxiprovin also produced significantly lower results than the control (Figure 5.1). The results presented here imply that concentrations of 50 μM or higher of the antioxidant are detrimental to the cell and may possibly increase apoptosis which is a strong contributor to muscle atrophy. The ROS present in the cells may in fact benefit the cell in one way or another. The addition of TNF-α proved not to aggravate the situation.

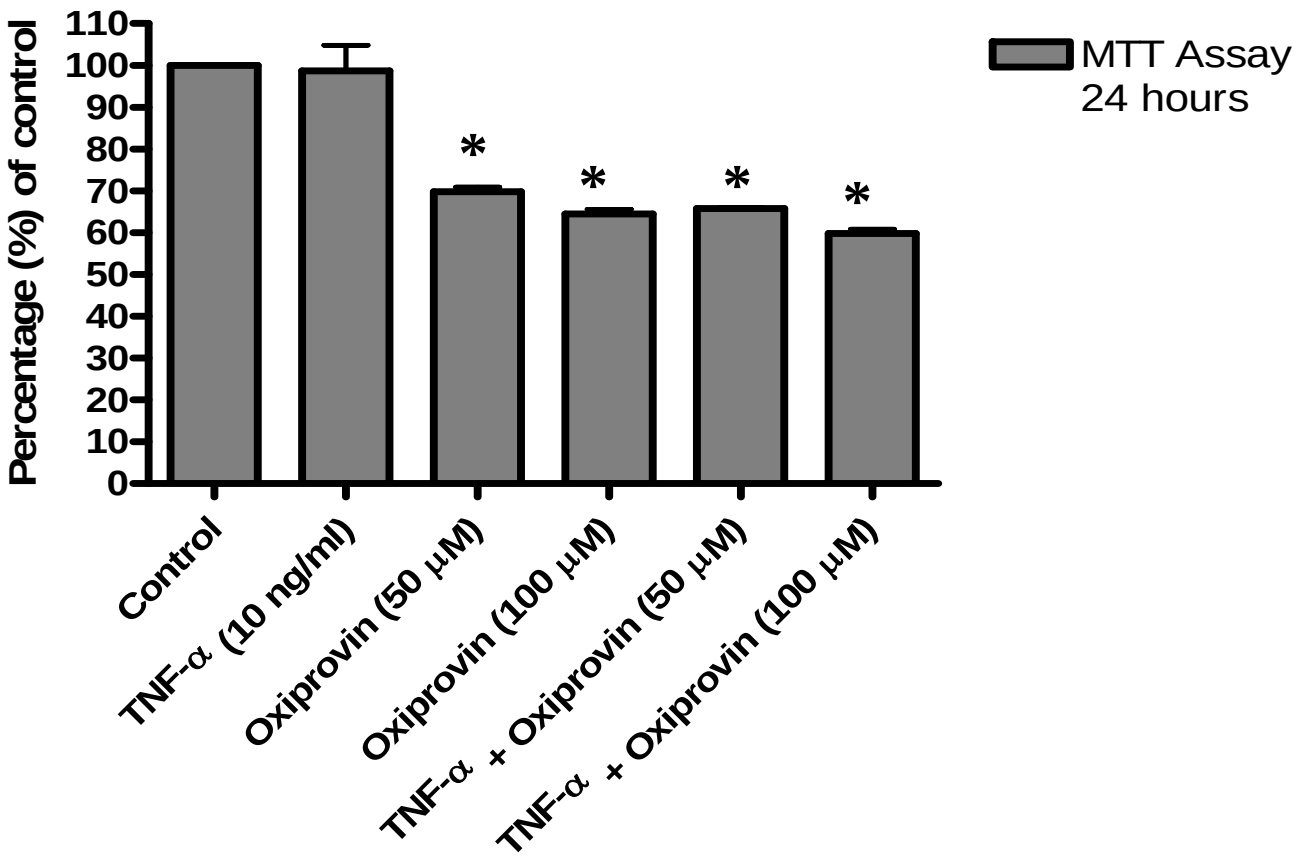

Figure 5.1.: Effect of TNF-α and Oxiprovin on cell viability of fully differentiated L6 myotubes (8 days). L6 myotubes were incubated with 10 ng/ml TNF-α and 50 μM or 100 μM for 24 hours and their cell activities were assessed at this time point. Cell activities were quantified

by the MTT assay as described in the methods section. Values are conveyed as percentages of controls (100%). Results are presented as their mean ± SEM. *P < 0.001 vs control (n ≥ 3)

5.1.2. The effect of TNF-α and Oxiprovin on mitochondrial ROS production

TNF-α (10 ng/ml) alone produced no significant changes on ROS accumulation in the cells at 24 hours when compared to the control. The antioxidant alone (50 and 100 μM) on the other hand significantly reduced ROS accumulation (P < 0.001) by approximately 15% and 35% respectively. The combination of TNF-α and Oxiprovin (50 μM) produced no significant results (Figures 5.2 and 5.3). But the combination of TNF-α and Oxiprovin (100 μM) produced significantly lower ROS production than the control. The results presented here imply that Oxiprovin is indeed a powerful antioxidant that is able to reduce cell viability and the levels of ROS in our cell culture model. Another interesting observation is the significance observed between the lower dose of the antioxidant alone and the combination of TNF-α and the lowest dose of the antioxidant (p < 0.01). This may suggest a possible mechanism whereby TNF-α is able to counteract the effects of the antioxidant. The combination with TNF-α had no apparent effect on the functionality of this antioxidant. This may suggest that in our culture model, the ROS that is present in our cells is actually beneficial since the antioxidant decreased cell viability.

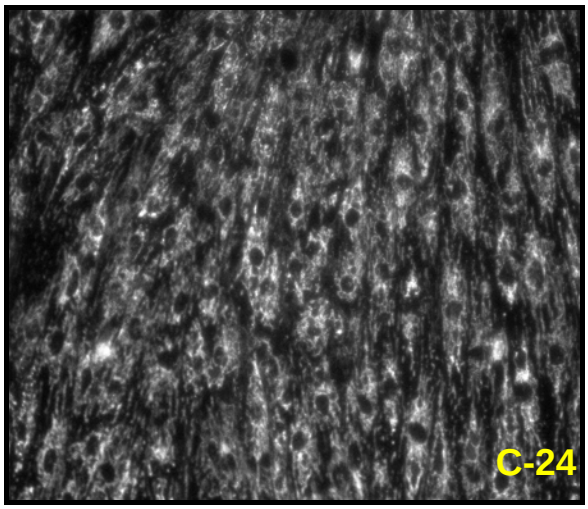

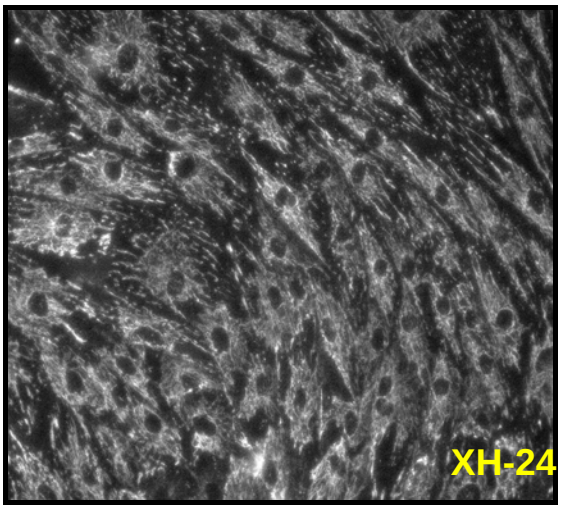

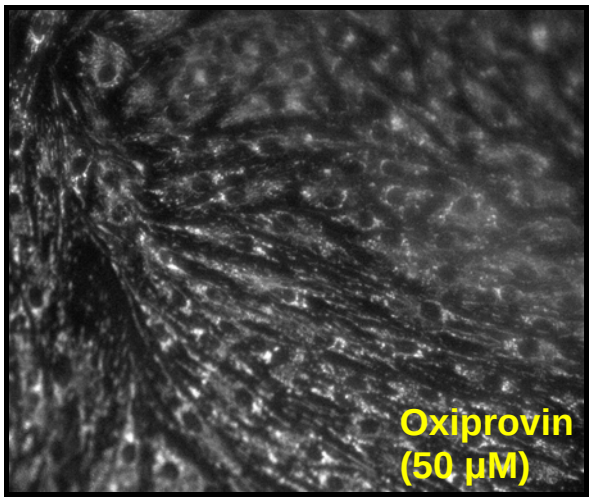
Oxiprovin
(50 µM)

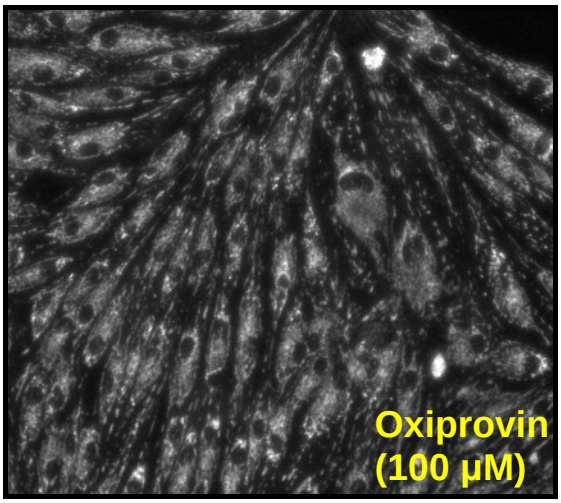
Oxiprovin
(100 µM)

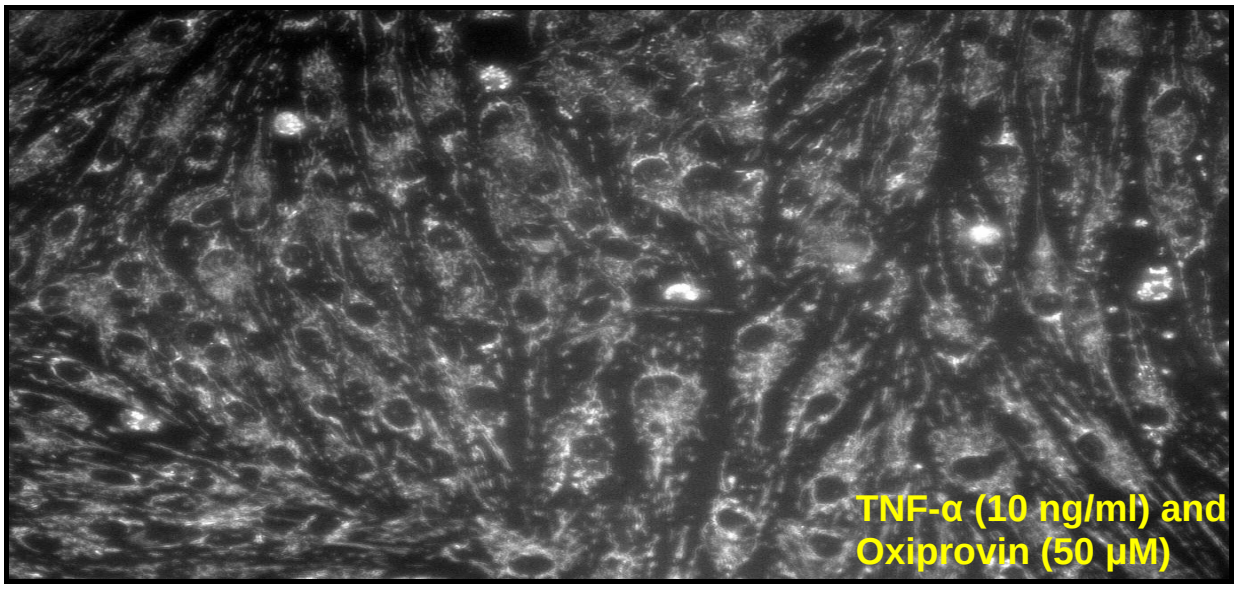
TNF-α (10 ng/ml) and
Oxiprovin (50 µM)

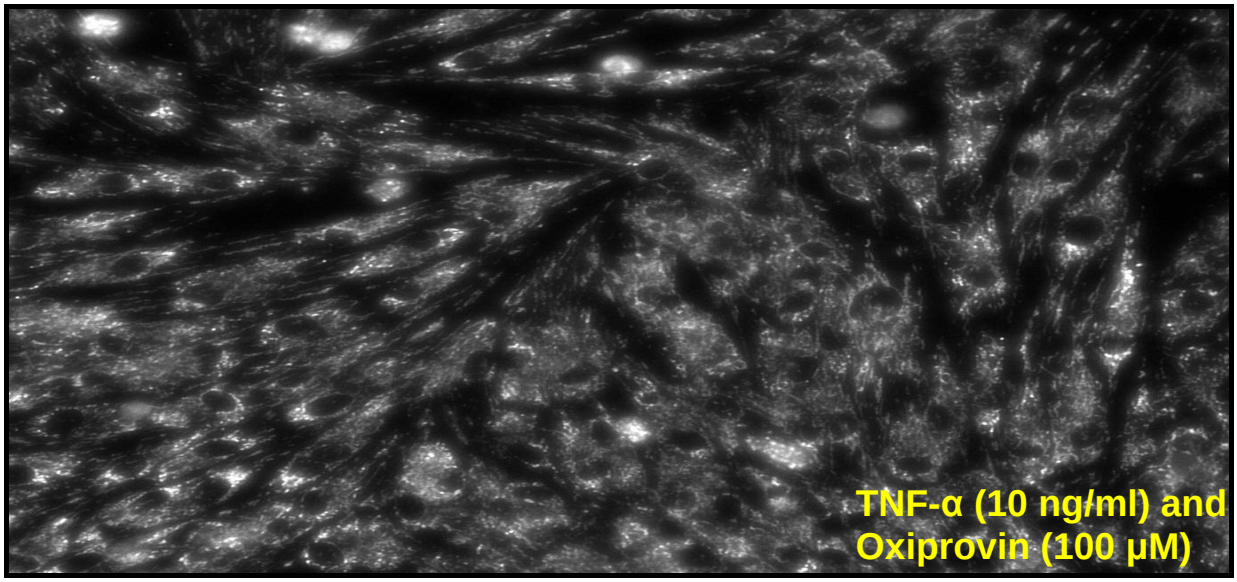

Figure 5.2: The effect of TNF-α (10 ng/ml) in combination with the antioxidant Oxiprovin on ROS production. Two concentrations of Oxiprovin were tested over 24 hours and a fluorescent image was captured for each where the mean grey area was measured (n ≥ 3)

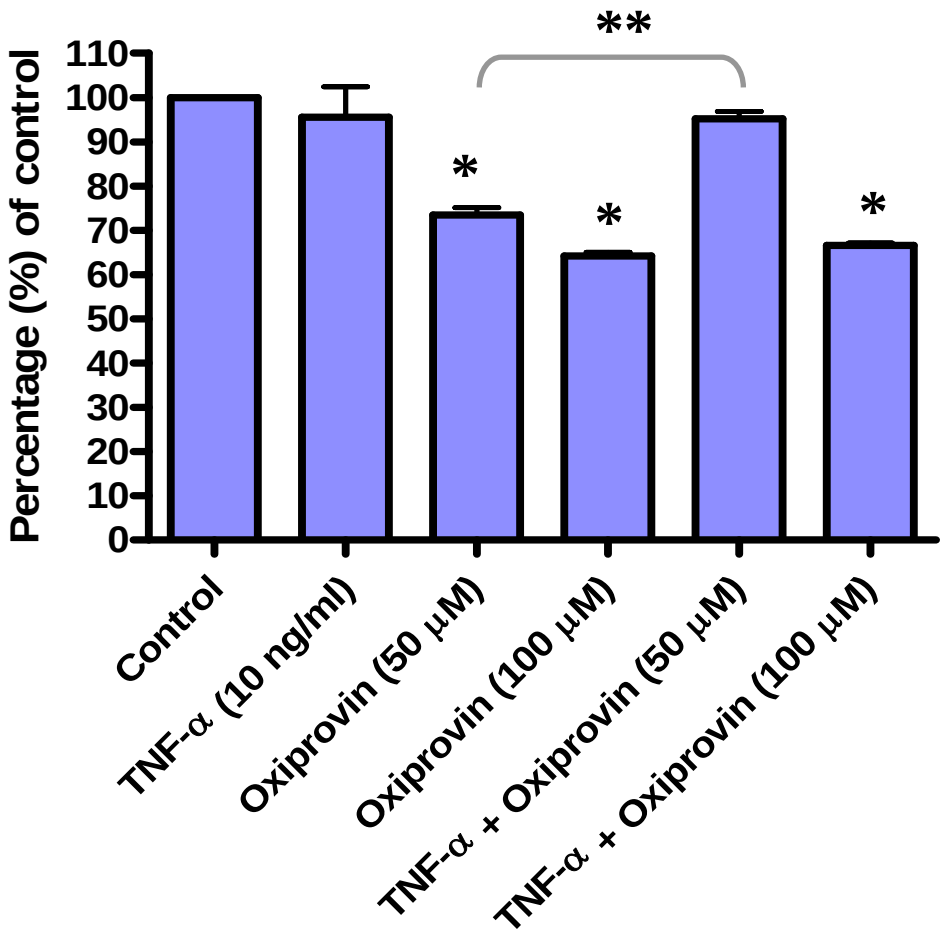

Figure 5.3: Effect of TNF-α and Oxiprovin on ROS production of fully differentiated L6 myotubes (8 days). L6 myotubes were incubated with 10 ng/ml TNF-α and 50 μM or 100 μM for 24 hours. A fluorescent image was captured for each type of experiment performed. Values are conveyed as percentages of controls (100%). Results are presented as their mean ± SEM. *P < 0.001, **P < 0.01 vs control (n ≥ 3)

CHAPTER 6

Discussion

Tumor necrosis factor-α, involved in muscle atrophy and weakness is associated with an assortment of chronic inflammatory diseases. It has long been correlated with muscle pathology and was initially assigned the name of 'cachectin' in acknowledgement of its catabolic actions. Despite its plausible significance in muscle pathology, the immediate consequences of TNF-α on skeletal muscle have remained unknown until recently. We have studied the direct proteolytic effects of TNF-α on signalling proteins in relation to muscle protein loss *in vivo*. This was the first complete study, to our knowledge, to investigate the vast range of catabolic actions of increasing TNF-α levels on specific signalling proteins involved in different cellular processes such as cell proliferation, cell viability, cell death, differentiation, protein content and expression, oxidative stress and signal transduction in the context of muscle protein degradation. This comprehensive study has clearly shown that the various TNF-α concentrations used, have multiple degradative effects on the three major pathways believed to be of critical importance in muscle atrophy although having no apparent effect on cell viability. Our impressions are recapitulated in an experimental model illustrated in Figure 7.1. We propose that TNF-α can act directly on L6 myotubes to:

(i) stimulate protein loss, an action arbitrated by NF-κB, a prime mediator of transcriptional organisation and a key mediator of catabolic signalling (Chen *et al*, 2002),

(ii) activate both p38- and JNK-MAPKs, designated triggers for the transcriptional upregulation of ubiquitin ligases and FKHR respectively and

(iii) negatively affect the PI3-K/Akt signalling pathway, which is strongly implicated as the potential mediator of skeletal muscle hypertrophy (Murgia *et al*, 2000).

Intermediary actions in the TNF-α/NF-κB signalling comprise the augmentation of TNF-R1 and the likely production of ROS via the mitochondrial electron transport chain. NF-κB performance in response to TNF-α emerges to elevate the activity of the ubiquitin-proteosome pathway, which hastens the regulated breakdown of skeletal muscle proteins and thus the endorsement of muscle weakness.

6.1 TNF-α induces its effects via direct or indirect mechanisms

The mechanism by which TNF-α generates its effects in *vivo* continues to remain ambiguous even though it has been long understood that TNF-α may induce catabolic actions by means of indirect systems. TNF-α changes the levels of circulating hormones and growth factors that modulate growth and influence tissue sensitivity. TNF-α may in addition encourage the synthesis of various proteolytic cytokines thus inducing anorexia. Anyone one of these resulting effects may obliquely promote muscle wasting. The direct mechanism by which TNF-α incites muscle proteolysis however, appears to be much clearer although some facts remain largely unknown. The inhibition of myoblast differentiation appears to be one potential mechanism (Guttridge *et al*, 2000; Layne *et al*, 1999), consequently restraining the regenerative ability of satellite cells to muscle injury (Thaloor *et al*, 1999). Apoptosis seems to be another mechanism by which TNF-α directly contributes to muscle catabolism but some researchers have regarded this pathway less significant (Li *et al*, 1999 and 2000). The third and final way by which TNF-α can induce its proteolytic effects includes the direct action on fully differentiated myotubes (mature fibers) by means of activating several signal transduction pathways and this was the focus of our research.

6.2 TNF-R1

The catabolic effects of TNF-α on skeletal muscle are apparent but varied depending on the cell line and species. Studies conducted by Carbo *et al* (2002) and Li *et al* (1998 and 2000) have revealed that animals instilled with exogenous TNF-α show considerable muscle wasting. Genetically manipulated TNF-R1 knockout mice inserted with cachexia-inducing tumors, ultimately producing elevated TNF-α levels, profoundly demonstrate less muscle wasting compared to their respective controls. These data undeniably imply that TNF-α induces muscle wasting *in vivo* and that signalling mediated by TNF-R1 appears to be responsible for constructing these effects (Dirks *et al*, 2006). This also appears to be the case *in vitro*, as demonstrated by our study. We have shown significant increases in TNF-R1 with increasing TNF-α concentrations at 24 hours. Compared to the other doses used at this time point, the highest concentration (10 ng/ml) of TNF-α produced slightly lower receptor expression although remaining significantly higher than the control. Furthermore, at 48 hours no significant differ-

ences were observed between the groups when weighed against the control. This may suggest that when the stimulus resulting from TNF-α remains elevated, there is possible saturation of receptors thus resulting in their downregulation. While this phenomenon has not yet been demonstrated by other studies, we can only speculate that in this particular cell line chronic TNF-α stimulation causes TNF-R1 saturation and their eventual downregulation even though the effects are still evident long after downregulation. We also attempted obtaining TNF-R2 protein expression but to no avail, further confirming TNF-R1 as the receptor subtype that functions in muscle cells.

6.3 TNF-α/NF-κB signalling

NF-κB stimulation has been previously demonstrated to be required for muscle protein loss in muscle wasting and is closely linked to chronic inflammation (Ladner *et al*, 2003; Guttridge *et al*, 2000). What was thought to trigger the loss of skeletal muscle mass is the rise of inflammatory cytokine production in these conditions (Guttridge *et al*, 2000; Kawamura et al, 1999). We and others (Li *et al*, 1998, 1999, 2000 and 2001, Langen et al, 2001, Guttridge *et al*, 2000; Sen et al, 1997) have shown that TNF-α stimulates the activation and translocation of NF-κB in skeletal muscle cells. NF-κB activity in our model was detected within 40 minutes of TNF-α exposure resulting in a ± 40-fold increase at the highest concentration of TNF-α used (Figure 4.9). Although increases in NF-κB activation continued at 24 and 48 hours, the fold increase decreased dramatically to ± 2-fold compared to the control. NF-κB activation thus appears to be a rapid, time-dependent and dose-dependent response that seems to reach its peak according to some studies as early as 15 minutes (Li *et al*, 1998) or 30 minutes (Reid *et al*, 2001) and then rapidly decays. This seemingly transient stimulus amends gene expression and brings about long-lasting changes in muscle protein levels including adult fast-type myosin heavy chain (MHCf) (Li *et al*, 1998 and 2000). The decrements in MHCf are apparently not escorted by modification in the synthesis rate but rather a rise in the degradation (myofibrillar protein degradation).

NF-κB activation is tightly controlled by the IKK complex. This complex consists of three subunits namely IKK-α, IKK-β and IKK-γ. Cells lacking the IKK-β subunit are defective in NF-κB activation in response to TNF-α and interleukins. In other words, IKK-β plays a pivotal role in IKK activation and the subsequent activation of NF-κB (Li *et al*, 1999). In a study

by Li and collegues (1999), the average IKK-β expression was instantaneously amplified by 34% succeeding two weeks of immobilization. In a another similar study, Cai *et al* (2004) illustrated NF-κB activation as well as NF-κB selective inhibition in skeletal muscle via muscle-specific expression of either a constitutively active IKK-β (MIKK) or a dominant inhibitor form of IKβ-α (MISR) *in vivo*. Two conclusions were drawn from this study:

(i) NF-κB activation by IKK-β is adequate to induce muscle atrophy as the muscle mass in MIKK mice was considerably decreased when compared to its wild-type control, with the fast twitch muscle experiencing the most modifications. MISR mice showed typical body weight and appearance.

(ii) The loss of muscle mass is not only stimulated by NF-κB activation but can be inhibited by genetic suppression of NF-κB at the IKβ-α level. Long-term treatment (6 months) with high doses of salicylates has been shown to suppress IKK-β and NF-κB.

As a result, although activation of NF-κB is enough to induce muscle atrophy *in vivo*, obstruction of the NF-κB pathway may well profoundly but moderately diminish protein loss during muscle atrophy.

6.4 The requirement of specific MAPKs for TNF-α signalling

We have shown that p38- and JNK-MAPK activation was significantly increased with increasing TNF-α supplementation at 24 and 48 hours. This increased phosphorylation of certain MAPKs observed with TNF-α supplementation (Figures 4.5 and 4.6) has also been shown repeatedly by other studies (Li *et al*, 2000, 2003 and 2005; Liu *et al*, 2005; Childs *et al*, 2003; Hilder *et al*, 2003; Morris *et al*, 2004; Hirosumi *et al*, 2000). TNF-α exposure also transcriptionally upregulated MuRF-1 and MAFbx, ubiquitin ligases that play pivotal roles in the ubiquitin-proteosome pathway leading to the degradation of muscle proteins (Glass, 2003 and 2005). Interestingly, inhibition of p38-MAPK using either curcumin or SB203580 (specific inhibitor of p38), significantly blunted increases in MAFbx protein expression whereas the use of SP600125, a JNK-MAPK inhibitor, had no effect on MAFbx expression. These data propose that the MAFbx gene is a downstream target of p38-MAPK signalling. Therefore, p38 could be the upstream trigger involved in the upregulation of MAFbx in muscle atrophy (Childs *et al*, 2003). NF-κB appears to be the other trigger responsible for the transcriptional upregulation of MuRF-1 (Glass, 2003 and 2005). This is in accordance to proteosome

inhibitory studies where the complete translocation of NF-κB to the nucleus was prevented, thus denoting that ubiquitin/proteosome communications are essential for TNF-α/NF-κB signalling in muscle proteolytic conditions (Li *et al*, 1998).

The progression of muscle atrophy is often complimented by a rise in insulin resistance especially in the slow twitch muscles (Hirose *et al*, 2000). Furthermore, this observation was shown to correlate with JNK activity in skeletal muscle undergoing atrophy (Li *et al*, 2007). A possible mechanism by which JNK is linked to insulin resistance is its negative regulation of insulin resistance. This occurs through serine phosphorylation of residue 307 contained by the insulin-receptor substrate (IRS)-1. The subsequent rise in serine phosphorylation of IRS-1 averts its attachment with the β-subunits of the insulin receptor and the activation of PI3-K which is insulin dependent. In addition, Hilder *et al* (2003) noted a depression in the activities of Akt and GSK-3β (enzymes typically activated in response to insulin) in atrophic muscle, further implicating increasing JNK activity to insulin resistance in muscle atrophy.

6.5 The role of the ubiquitin-proteosome pathway in muscle atrophy

Virtually all of the conditions causing muscle protein losses are associated with activation of the ubiquitin-proteosome pathway to degrade proteins (Mitch *et al*, 1996; Lecker *et al*, 2006). This was indeed the case in our cell culture model. Ubiquitin expression modestly increased at 24 hours. At 48 hours however, ubiquitin expression significantly increased in a robust fashion. Our data suggests that ubiquitin protein expression is rather a time dependent than a dose dependent response as there was no significant change in ubiquitin expression as TNF-α supplementation increased. Because ubiquitin cannot degrade complex polymers of actin and/or myosin fibers, another mechanism has been identified to deal with this complication. Activation of caspase-3 appears to be the solution this problem. Active caspase-3 in its cleaved form breaks down intricate actin fibers to produce 14 kD actin fragments. These smaller actin fragments then serve as substrates for the ubiquitin-proteosome pathway with which it can degrade. The presence of the 14 kD actin fragments in the muscle of animal models of diabetes as well as in patients suffering from renal (kidney) failure, disuse atrophy or burn injury is enough evidence to implicate the initial cleavage of actin and/or myosin as the initiating occurrence in muscle proteolysis (Wang *et al*, 2006; Du *et al*, 2006; Lee *et al*,

2004; Workneh *et al*, 2006). Although we did not investigate for the presence of actin monomers in our study, the manifestation of this phenomenon was observed in our study in the form of cleaved caspase-3. Caspase-3 was detected as early as 40 minutes after supplementation, increasing with increasing TNF-α concentrations (Figures 4.11 and 4.12). In spite of this observation, 24 hour data showed a significant reduction and maintenance of the observed plateau in caspse-3 induction. We contemplate that caspse-3 at this time-point had already been cleaved. Interestingly after 48 hours of TNF-α supplementation, there was a significant increase in cleaved caspase-3 expression which was not pronounced with the very high dose (10 ng/ml). This supports the phenomenon previously described where cleaved caspase-3 can break down actin fibers in order to produce the 14 kD fragments (Wang *et al*, 2006; Du *et al*, 2006; Lee *et al*, 2004; Workneh *et al*, 2006).

The control of caspase-3 activity appears to be a complex process involving a number of interconnected signalling pathways. Caspase-12 (via a calcium release pathway) and caspase-9 (via a mitochondrial pathway) seem to possibly activate caspase-3 in diabetes-induced muscle atrophy. A common feature in these pathways is that they are both stimulated by ROS suggesting a potential interaction between these caspase-3 activation pathways (Primeau *et al*, 2002). Furthermore, added to the complexity of this phenomenon, was the identification of calpastatin as a substrate for both caspase-3 and calpain. Several researchers have demonstrated that increases in caspase-3 or calpain activity leads to reduced levels of calpastatin in cells and the promotion of calpain activity. Additionally, increases in calpain activity can also lead to caspase-3 activation (Du *et al*, 2004; Doll *et al*, 2003; Wang *et al*, 1998; Chen *et al*, 2002). Taken together, these data imply a promising cross-talk between the calpain and caspase-3 proteolytic systems. These systems may in fact play a critical role in the regulation of myofilament release in skeletal muscle during muscle atrophy (Powers *et al*, 2007).

6.6 The requirement of FKHR and PI3-K/Akt in muscle proteolysis

It has long been understood that a delicate balance exists between protein synthesis and protein degradation in skeletal muscle: clinical conditions which include hypertrophy have been associated with increases in protein synthesis, and an increase in protein loss has been shown to occur during atrophy (Goldspink *et al*, 1993). Many reports have linked catabolic condi-

tions to a decrease in activity of the PI3-K/Akt signalling pathway (Wang *et al*, 2006; Du *et al*, 2004; Lee *et al*, 2004; Bailey *et al*, 2006). Activation of Akt on the other hand prevents denervation-induced atrophy (Huang *et al*, 2007). A direct relation between these two proceedings has only just recently been discovered. TNF-α-induced muscle atrophy significantly reduced the activity of the PI3-K/Akt pathway (Figures 4.17 and 4.18). This in turn leads to the activation of FKHR (FoxO) (Figure 4.7 and 4.8) and induction of the ubiquitin ligases MuRF-1 and MAFbx (Figure 4.15 and 4.16). Sandri *et al* (2004) further confirmed our data (Huang *et al*, 2007). Stitt *et al* (2004) previously illustrated that the IGF/PI3-K/Akt pathway inhibits the induction of both ubiquitin ligases. Therefore, the observed inhibition may well be associated to Akt-mediated inactivation of FKHR transcription factors. Transgenic mice overexpressing FKHR have been generated in order to obtain more insight into the plausible role of FKHR in skeletal muscle (Kamei *et al*, 2004). These mice showed decreased muscle masses which were pale in colour compared to their control counterparts. Gene expression results revealed that MuRF-1, MAFbx and cathepsin L production increased, type I (red muscle) fiber-related genes decreased and the sizes of both type I and type II muscle fibers also decreased. From the data, we are able to deduce that the observed rise in muscle protein degradation is an important factor to the loss of muscle mass in these mice. Interestingly, exercising muscles (which are energy rich) showing increased expression of PGC (peroxisome-proliferator-activated receptor γ coactivator)-1α, a seemingly critical coregulator for many transcription factors opposed to muscle atrophy. Contrariwise, expression of PGC-1α mRNA is shown to be significantly decreased in muscle undergoing atrophy as well as in rodent models of cancer cachexia, diabetes and renal failure (Sandri *et al*, 2006). More importantly PGC-1α is said to favour type I gene expression and contributes to the activation of various nuclear receptors. This proposes a mechanism by which exercise may counteract muscle atrophy and thus designating FKHR as a negative regulator in skeletal muscle as well as the expression of type I fiber-related genes. A recent discovery by Hishiya *et al* (2006) involves the identification of a zinc finger protein, ZNF216. Increased expression of ZNF216 appears to bind directly to polyubiquitin chains and attaches itself to the 26S proteosome in fasting- and denervation-induced muscle atrophy. FKHR transcription factors thus mediate atrophy and/or hypertrophy through several pathways.

6.7 Regulation of muscle protein degradation by PI3-K

In the previous paragraph we have highlighted the importance of the activity of the PI3-K/Akt signalling pathway in muscle pathology. This pathway is considered to be a crucial intracellular regulator (mediator) of muscle hypertrophy as well as being a key signalling molecule in distinct processes ranging from the activation of transcription factors (Pfeffer *et al*, 1997) and glucose transport (Hara *et al*, 1994) to cell survival (Yao *et al*, 1995; Kennedy *et al*, 1997; Dudek *et al*, 1997; Kaufmann-Zeh *et al*, 1997; Kulik *et al*, 1997). Even though skeletal muscle atrophy is not merely contrary to hypertrophy, many studies have proved that there are certain vital associations between proteolytic activity and the expression of proteolytic genes and the suppression or inactivation of the PI3-K/Akt signalling pathway (Cheng *et al*, 1996). In order to induce protein synthesis via activation of PI3-K/Akt, Sacheck *et al* (2004) utilised both IGF-1 and insulin. In response to these agents, there appeared to be a reduction in the expression of ubiquitin ligases. As seen in our study, TNF-α-induced muscle atrophy resulted in significant depression of PI3-K/Akt activity and specific increases in ubiquitin ligases. This is in agreement with other researchers who used dexamethasone instead of TNF-α to induce atrophy but also observed the same phenomenon (Cao *et al*, 1996; Lee *et al*, 1997). Moreover, the expression of a dominant negative Akt (Wang *et al*, 1998), decreased the fiber size of myotubes in cell culture. Therefore, in an attempt to manage muscle mass, not only does the PI3-K/Akt pathway elevate protein synthesis on the whole, it down regulates muscle protein degradation as well as the expression of atrophy-related ubiquitin ligases (Lee *et al*, 2004).

At the present moment, the mechanism of activation of Akt is nevertheless controversial even though it is an extensively researched topic. There are three distinct genes that code for Akt mRNAs which are subsequently translated into three independent Akt proteins titled Akt1, Akt2 and Akt3. Akt-1 and -2 are extensively expressed in insulin-sensitive tissues whilst Akt-3 is minimal in skeletal muscle (Masure *et al*, 1999). It is clear that Akt is activated by phospholipid attachment to the plextrin-homology domain, thus encouraging conformational alteration that allows phosphorylation of the Thr 308 residue by PDK-1. Akt is capable of being autophosphorylated at Thr 72 and Ser 246 and any mutation at these sites causes radical obstruction of the capability of IGF-1 to induce kinase activity (Frost *et al*, 2007). Another site of phosphorylation of Akt by mTOR is at Ser 473, and it is predominantly thought that phosphorylation occurs at Thr 308 before phosphorylation at Ser 473 takes place (Hresko *et al*,

2005; Li *et al*, 2006). Akt plays an important role in the integration of anabolic and catabolic responses by growth factors, nutrients, muscle contraction and cytokine signals by means of transformation in the phosphorylation of its various substrates (Frost *et al*, 2007). In addition, it emerges that Akt is positioned at the intersection of a multitude of signalling pathways and operates as a pivotal downstream effector of many receptors that stimulate PI3-K activity (Reddy *et al*, 2000).

Malfunctioning of PI3-K/Akt signalling decreases the quantity of the PI3-K-generated product, PIP_3, ultimately leading to decreased activation (phosphorylation) of Akt. Another mechanism that can potentially reduce PIP_3 levels and has entertained inadequate attention is a "reciprocal change" in PTEN activity for the reason that it can dephosphorylate PIP_3 to an inactive PIP_2 (Maehama *et al*, 1998; Dupont *et al*, 2002). PTEN is only active in its dephosphorylated state and data from our research shows that at both 24 and 48 hours there was a significant decrease in PTEN phosphorylation, thus promoting the conversion from PIP_3 to PIP_2, rendering the PI3-K pathway inactive. It is postulated that the mechanism that suppresses PTEN in cultured myotubes is linked to acute inhibition of PI3-K activity. In other words, PTEN activity increases with increased TNF-α supplementation. Gericke *et al* (2006) indicated that post-translational modification is a mechanism by which PTEN in muscle can be downregulated. Torres *et al* (2003) took this suggestion further and found that caspase-3 activity can cleave the COOH-terminus of PTEN which may perhaps clarify decreases in PTEN phosphorylation. This is appropriate since acute insulin deficiency activates caspase-3 (Lee *et al*, 2004). In another study involving insulin, PTEN stability is alleviated by PIP_3–induced PKC (protein kinase C) phosphorylation, thus recommending a different mechanism to decrease PTEN stability via insulin deficiency (Birle *et al*, 2002). Total PTEN levels however remained at base-line. Our study and others suggest that an increase in PTEN activity acts in unison with a reduction in IRS-1-associated PI3-K activity in order to decrease PIP_3. This reaction presents a positive-feed forward mechanism to activate muscle proteolysis.

6.8 TNF-α inhibits myogenic differentiation

Over the past several years, an increasing body of researchers have incriminated TNF-α/NF-κB in skeletal muscle differentiation. This process is regulated by various transcription factors including MyoD, Myf5, Myogenin, MRF4/Myf6/Hercyclin and MEF-2A-D (Naya and Olson,

1999; Sabourin and Rudnicki, 2000; Ponwall *et al*, 2002) which together act to control myoblasts to endure growth arrest and fuse to develop multinucleated myotubes (Hyatt *et al*, 2003). It has been previously shown that TNF-α-orchestrated inhibition of myogenesis involves multiple pathways that eventually lead to MyoD and Myogenin downregulation (Guttridge *et al*, 2000; Mitchell *et al*, 2001; Mitchell *et al*, 2004; Szalay *et al*, 1997), reduced MyoD protein stability (Langen *et al*, 2004) as well as the stimulation of proliferation via cyclin-D1 (Guttridge *et al*, 1999; Moresi *et al*, 2008; Bakkar *et al*, 2008). In contrast, TNF-α can regulate myogenesis and muscle regeneration by activating p38-MAPK (Chen *et al*, 2007; Mourkiot and Rosenthal, 2007). Our study demonstrates that MyoD protein expression decreased by ± 70% and ± 90% at 24 and 48 hours respectively with 10 ng/ml (XH) TNF-α treatment (Figure 4.24). Interestingly, the low (1 ng/ml) and medium (3 ng/ml) TNF-α doses produced significant increases in MyoD expression at 48 hours. Myogenin data also produced similar results. Low and medium TNF-α doses showed elevated myogenin protein expression whereas the higher doses of TNF-α resulted in significant decreases. At 48 hours on the other hand, myogenin expression gradually decreased with increasing TNF-α supplementation. In our cell line, we have also shown that 10 ng/ml TNF-α dose increased protein content at 24 hours but the same concentration at a different time point (48 hours) resulted in decreased protein content. Li *et al* (1998) however reported that 10 ng/ml TNF-α decreased protein content in C2C12 myotubes whereas Langen *et al* (2001) reported a stimulatory effect of TNF-α on protein content in the same cell line. We and Li *et al* (1998) used 2% horse serum whereas Langen *et al* (2001) used Matrigel coated dishes. These observations together suggest that TNF-α might have beneficial effects in skeletal muscle in certain circumstances. This beneficial effect however is limited by several aspects which include the concentration of TNF-α, cell type, time of exposure, culture conditions, the state of the cell (disturbed or normal) and the cells stage of differentiation. In addition, our data may imply that at certain time points and at certain TNF-α concentrations, TNF-α may have a beneficial effect on differentiation and/or differentiated myotubes. Guttridge *et al* (2000) proposed that MyoD downregulation by TNF-α-induced NF-κB activation occurs at a posttranslational level which in turn leads to a decline in myofibrillar (protein) synthesis. It appears that the p65 (RelA) NF-κB family member alone causes this downregulation and the introduction of a dominant negative IκB protein in cultured cells, salvages excessive MyoD expression. From this study we can deduce that MyoD is a potential "indirect" target gene of NF-κB. Although the mechanisms mediating TNF-α effects on skeletal muscle remain largely undefined, a novel pathway by which TNF-α prevents differentiation has been hypothesised. Coletti and colleagues (2002) have

demonstrated that TNF-α inhibits muscle differentiation via caspase activation but without apoptosis. The mechanism by which this occurs is solely dependent on PW1 (also termed and is identical to paternally expressed gene 3 or Peg3 (Mourkioti and Rosenthal, 2007) expression and is independent of NF-κB stimulation. This hypothesis is supported by other researchers who have observed that in cultured myogenic cells, PW1 engages p53-dependent apoptotic pathways which include Bax-translocation to mitochondria and downstream caspase activation and together contribute to the management of myogenesis. Moreover, caspase activation emerges as an important role player in the arbitration of cell differentiation in particular lineages (Moresi *et al*, 2008).

6.9 TNF-α induces ROS production by mitochondria

ROS have been identified as mediators of intracellular signal transduction. Even though TNF-α/NF-κB signalling is believed to be susceptible to ROS (Langen *et al*, 2002), the magnitude of ROS production in NF-κB stimulation seems to be "cell type specific" (Li *et al*, 1999). This is established upon years of research illustrating that metal scavengers or antioxidants inhibit cytokine-induced activation of NF-κB. The addition of antioxidants to particular cell types however, is enough to stimulate NF-κB activation (Li *et al*, 1998; Sen *et al*, 1998). The present study has revealed that increasing TNF-α supplementation at 24 and 48 hours produced no significant changes in ROS production (Figures 4.27 and 4.28). We speculate that in this particular cell line (L6), TNF-α had no effect on ROS production and that the minute increases we observed are actually beneficial to the cells. This is in conflict with other studies where the opposite effect in myotubes treated with TNF-α was observed (Li *et al*, 1998, 1999 and 2000). It appears that the source of TNF-α-induced ROS production is the mitochondrial electron transport chain (Li *et al*, 1999; Jackman *et al*, 2004; Reid *et al*, 2001; Corda *et al*, 2001; Li *et al*, 2000; Kiritoshi *et al*, 2003). Myotube studies have highlighted that TNF-α-induced NF-κB activation is inhibited by catalase (which enzymatically dehydrates hydrogen peroxide) treatment, resulting in limited protein loss. The addition of exogenous hydrogen peroxide however, independently activates NF-κB (Reid *et al*, 2001; Jackman *et al*, 2004). This proposes a mechanism by which ROS acts as a second messenger for TNF-α signalling in skeletal muscle by directly or indirectly activating NF-κB. Additionally, this may be a novel mechanism by which ROS is able to induce muscle wasting – for example ROS via alterations of sarcoplasmic reticulum function, modifications in mitochondrial respiration or

oxidation of vital sulfhydryl groups on contractile proteins, which result in increased myofibrillar protein degradation, contributes to reduced force production and fatigue. The use of the antioxidant, Oxiprovin in our study, profoundly reduced cell viability (Figure 5.1) as well as ROS production (Figures 5.2 and 5.3) in the presence of TNF-α. Once again, this observation suggests that ROS in moderate concentrations is not detrimental to the cells and that use of the antioxidants (to reduce ROS production) in high concentrations is. We however cannot explain the observed rise in ROS production in the presence of both TNF-α (10 ng/ml) and Oxiprovin (50 μM).

CHAPTER 7

Conclusion

Skeletal muscle atrophy is a condition which occurs in muscle as a result of disuse (denervation, muscle unloading and immobilisation), starvation, ageing and a multitude of disease states (diabetes, cancer, AIDS). Regardless of this inciting event, skeletal muscle atrophy is a mitigating complication that is characterised by a reduction in muscle fiber cross-sectional area, decreased force, elevated fatigability and insulin resistance. The different types of conditions producing muscle atrophy imply differences in the type of molecular triggers and signalling pathways for muscle wasting. TNF-α is implicated in most if not all muscle catabolic conditions that lead up to the massive effect of muscle protein loss. Given the significance of TNF-α signalling in muscle, this study was conducted to assess post-receptor mechanisms which are mediated by TNF-α. Our study has focused on four main pathways that are believed to be either activated or suppressed in response to increasing TNF-α supplementation. These include: (i) the NF-κB pathway, (ii) the ubiquitin-proteosome pathway, (iii) the MAPK pathway and (iv) PI3-K/Akt signalling pathway.

We have demonstrated that TNF-α directly induces muscle protein degradation signalling pathways in differentiated L6 skeletal muscle myotubes, where it rapidly activates NF-κB. This induction of protein loss also appears to be NF-κB dependent. Activation of this pathway leads to NF-κB's translocation to the nucleus where it induced the transcriptional upregulation of MuRF-1, a ubiquitin ligase. Another ubiquitin ligase, MAFbx, was also seen to be significantly upregulated. Both these ubiquitin ligases are actively involved in the ubiquitin-proteosome pathway to degrade proteins and are seen to be extensively upregulated more than other proteins that participate in this pathway.

The activation of several MAPKs in response to TNF-α was also observed in our research. Increased phosphorylation of p38-MAPK might be responsible for the significant increase in expression of MAFbx. Increased phosphorylation of JNK on the other hand, might induce the transcription and subsequent activation of FKHR. FKHR is in its active state when it is

dephosphorylated; however when it is phosphorylated by PKB/Akt, it translocates to the cytoplasm where it binds to 14-3-3 proteins, rendering it inactive. Therefore the observed decrease in phosphorylation we observed confirmed its activity.

A decrease in the activity of the PI3-K/Akt signalling pathway correlated with increased muscle atrophy. The observed decline in PI3-K activity also negatively affected Akt phosphorylation which was decreased. This, in turn, might have lead to caspase-3 and FKHR activation. The former causes actomyosin cleavage which is proposed to be the initiating event during muscle atrophy conditions and the latter stimulates increased ubiquitin ligase expression. The activity of another important molecule that lies upstream of Akt which is actively involved in this pathway was analysed. PTEN is also active in its dephosphorylated state. We observed a significant decrease in the phosphorylation levels of this protein. This results in increased PTEN activity which causes dephosphorylation of the PI3-K-generated product PIP_3 to inactive PIP_2, rendering the PI3-K pathway inactive, a common phenomenon observed during muscle proteolysis.

Our research further focused on two differentiation markers, MyoD and Myogenin, and how they are affected in response to long-term treatment with increasing TNF-α supplementation. Data showed that both differentiation markers were downregulated, thus implying that TNF-α, via various pathways inhibited or suppressed differentiation of myoblasts.

Finally, we determined the effect of TNF-α on ROS production. In our study, minute insignificant changes in ROS production were observed. This may suggest that in this particular model of muscle atrophy, ROS plays no significant role in relation to muscle protein break down. This is in contrast to what was observed in other studies where the observed rise in ROS production in response to TNF-α, suggested a possible function for ROS in other models of atrophy such as immobilisation. Interestingly, although TNF-α did not induce significant changes in ROS production, Oxiprovin (an antioxidant) however, significantly reduced cell viability and ROS production.

The effects of TNF-α on skeletal muscle are varied, depending on cell lines and species. Differences in cell culture conditions might also cause different responses even in the same cell line. Fundamentally, our findings imply that at certain concentrations and certain time points of TNF-α, has both positive and negative effects on muscle proteolysis in L6 myotubes. This

action is mediated by various signal transduction pathways that are thought to cooperate with each other. More understanding of these pathways as well as their subsequent upstream and downstream constituents is obligatory to clarify the central mechanism/s that control physiological and pathophysiological effects of TNF-α in skeletal muscle.

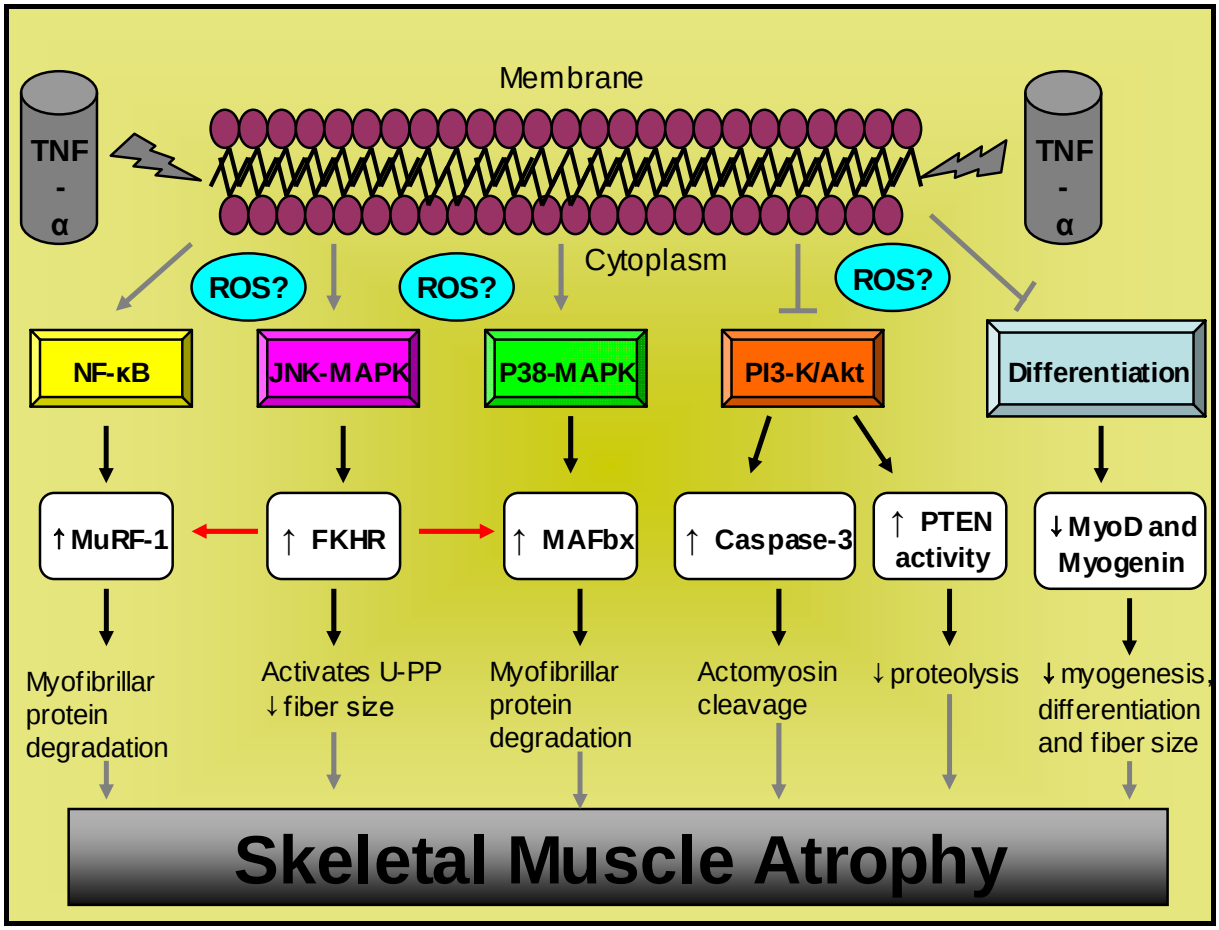

Figure 7.1: Proposed signalling mechanisms of TNF-α in L6 myotubes. *Abbreviations*: TNF-α, tumor necrosis factor-α; ROS, reactive oxygen species; NF-κB, nuclear factor-kappa B; JNK, c-Jun-N-terminal-kinase; MAPK, mitogen activated protein kinase; PI3-K, phosphotidylinositol 3- kinase; MuRF-1, muscle RING finger-1; MAFbx, muscle atrophy F-box; PTEN, phosphatase and tensin homologue; U-PP, ubiquitin proteosome pathway

REFERENCES

1. Adreyev, A.Y., Kushnareva, Y.E., Starkov, A.A. 2005. Mitochondrial metabolism of reactive oxygen species. *Biochemistry (Moscow)*. 70: 246-264
2. Appell, H.J., Duarte, J.A., Soares, J.M. 1997. Supplementation of Vitamin E may attenuate skeletal muscle immobilization atrophy. *International Journal of Sports Medicine*. 18: 157-160
3. Archaryya, S., Ladner, K., Nelson, L.L., Damrauer, J., Reiser, P.J., Swoap, S., Guttridge, D.C. 2004. Cancer cachexia is regulated by selective targeting of skeletal muscle gene products. *Journal of Clinical Investigation*. 114: 370-378
4. Atish, T.P., Vikrantish, M.G., Kamlesh, K.B. 2006. Modulating TNF-α signalling with natural products. *Drug Discovery Today*. 11: 725-732
5. Azzawi, M., Hasleton, P. 1999. Tumour necrosis factor alpha and the cardiovascular system: its role in cardiac allograft rejection and heart disease. *Cardiovascular Research*. 43: 850-859
6. Bailey, J.L., Price, S.R., Zheng, B., Hu, Z., Mitch, W.E. 2006. Chronic kidney disease causes defects in signaling through the insulin receptor substrate/phosphotidylinositol 3-kinase/Atk pathway: implications for muscle atrophy. *Journal of the American Society of Nephrology*. 17: 1388-1394
7. Bakkar, N., Wang, J., Ladner, K.J., Wang, H., Dahlman, J.M., Carathers, M., Acharyya, S., Rudnicki, M.A., Hallenbach, A.D., Guttridge, D.C. 2008. IKK/NF-κB regulates skeletal myogenesis via a signaling switch to inhibit differentiation and promote mitochondrial biogenesis. *The Journal of Cell Biology*. 180: 787-802
8. Baldwin Jr, A.S. 1996. The NF-κB and IκB proteins: new discoveries and insights. *Annual Reviews of Immunology*. 14: 649-681
9. Beguinot, F. 2007. PTEN targeting: the search for novel insulin sensitisers provides new insight into obesity research. *Diabetologia*. 50: 247-249
10. Birle, D., Bottini, N., Williams, S., Huynh, H., deBelle, I., Adamson, E., Mustelin, T. 2002. Negative feedback regulation of the tumour suppressor PTEN by phosphoinositide-induced serine phosphorylation. J*ournal of Immunology*. 169: 286-291
11. Bodine, S.C., Latres, E., Baumhueter, S., Lai, V.K.-M., Nunez, L., Clarke, B.A., Poueymirou, W.T., Panaro, F.J., Na, E., Dharmarajan, K., Pan, Z.-Q., Valenzuela,

D.M., DeChiara, T.M., Stitt, T.N., Yancopoulos, G.D., Glass, D.J. 2001. Identification of ubiquitin ligases required for skeletal muscle atrophy. *Science*. 294: 1704-1708

12. Bradford, M.M. 1976. A rapid and sensitive method for the quantification of microgram quantities of protein utilizing the principal of protein-dye binding. *Analytical Biochemistry*. 72:248-254
13. Cai, D., Frantz, J.D., Tawa Jr, N.E., Melendez, P.A., Oh, B.C., Lidov, H.G., Hesselgren, P.O., Frontera, W.R., Lee, J., Glass, D.J., Shoelson, S.E. 2004. IKKbeta/NF-kappaB activation causes severe muscle wasting in mice. *Cell*. 119: 285-298
14. Cao, Z., Henzel, Z.W., Gao, X. 1996. IRAK: a kinase associated with the interleukin-1 receptor. *Science*. 271: 1128-1131
15. Carbo, N., Busquets, S., van Royen, M., Alvarez, B., Lopez-Soriano, F.J., Argiles, J.M. 2002. TNF-alpha is involved in activating DNA fragmentation in skeletal muscle. *British Journal of Cancer*. 86: 1012-1016
16. Carswell, E., Old, L., Kassel, R., Green, N., Fiore, N., Williamson, B. 1975. An endotoxin-inducedserum factor that causes necrosis of tumors. *Proceedings of the National Academy of Science*. 72: 3666-3670
17. Celec, P. 2004. Nuclear factor kappa B-molecular biomedicine: the next generation. *Biomedicine and Pharmacotherapy*. 58: 365-371
18. Chacon Heszele, M.F., Price, S.R. 2004. Insulin-like growth factor 1: The yin and yang of muscle atrophy. *Endocrinology*. 145: 4803-4805
19. Chen, G., Goeddel, D.V. 2002. TNFR1 signaling: a beautiful pathway. *Science*. 296: 1634-1635
20. Chen, M., Won, D.J., Krajewski, S., Gottlieb, R.A. 2005. Calpain and mitochondria in ischemia/reperfusion injury. *Journal of Biochemical Chemistry*. 277: 29181-29186
21. Chen, S.-E., Jin, B., Li, Y.P. 2007. TNF-alpha regulates myogenesis and muscle regeneration by activating p38 MAPK. *American Journal of Physiology-Cell Physiology*. 292: C1660-C1671
22. Cheng, G., Baltimore, D. 1996. TANK, a co-inducer with TRAF2 of TNF- and CD40L-mediated NF-κB. *Genes and Development*. 10: 963-973
23. Childs, T.E., Spangenburg, E.E., Vyas, D.R., Booth, F.W. 2003. Temporal alterations in protein signalling cascades during recovery from muscle atrophy. *American Journal of Physiology*. 285: C931-C938
24. Clark, K.L., Halay, E.D., Lai, E., Burley, S.K. 1993. Co-crystal structure of the HNF-3/fork head DNA-recognition motif resembles histone 5. *Nature*. 364: 412-420

25. Coletti, D., Yang, E., Marazzi, G., Sassoon, D. 2002. TNF-α inhibits skeletal myogenesis through a PW1-dependent pathway by recruitment of caspase pathways. *The EMBO Journal*. 21: 631-642
26. Collins, R.A., Grounds, M.D. 2001. The role of tumor necrosis factor-alpha (TNF-α) in skeletal muscle regeneration: studies in TNF-α (-/-) and TNF-α (-/-)/LT-α (-/-) mice. The Journal of Histochemistry and Cytochemistry. 49: 989-1001
27. Corda, S., Laplace, C., Vicaut, E., Duranteau, J. 2001. Rapid reactive oxygen species production by mitochondria in endothelial cells exposed to tumor necrosis factor-α is mediated by ceramide. *American Journal of Cellular and Molecular Biology*. 24: 762-768
28. Corda, S., Laplace, C., Vicaut, E., Duranteau, J. 2001. Rapid reactive oxygen species production by mitochondria in endothelial cells exposed to tumor necrosis factor-α is mediated by ceramide. *The American Journal of Respiratory Cell Mol Biol*. 24: 762-768
29. Cuschieri, J., Maier, R.V. 2005. Mitogen-activated protein kinase (MAPK). *Critical Care Medicine*. 33: S417-S419
30. Davidson College. 2000. TNF-Alpha. Available from:
31. Dehoux, M., Gobier, C., Lause, P., Bertrand, L., Ketelsleger, J.-M., Thissen, J.-P. 2007. IGF-1 does not prevent myotube atrophy by proinflammatory cytokines despite activation of Akt/Foxo and GSK-3β pathways and inhibition of atrogin-1 mRNA. American Journal of Physiology-Endocrinology and Metabolism. 292: E145-E150
32. Di Giovanni, S., Molon, A., Broccolini, A., Melcon, C., Mirabella, M., Hoffman, E.P., Servidei, S. 2004. Constitutive activation of MAPK cascade in acute quadriplegic myopathy. *Annals of Neurology*. 55: 195-206
33. Di Marco, S., Mazroui, R., Dallaire, P., Chittur, S., Tenenbaum, S.A., Radzioch, D., Marette, A., Gallouzi, I. 2005. NF-κB-mediated MyoD decay during muscle wasting requires nitric oxide synthase mRNA stabilization, HuR protein, and nitric oxide release. *Molecular and Cellular Biology*. 25: 6533-6545
34. Dirks, A.J., Leeuwenburgh, C. 2006. Tumor necrosis factor α signalling in skeletal muscle: effects of age and caloric restriction. *Journal of Nutritional Biochemistry*. 17:501-508
35. Du, J., Mitch, W.E., Wang, X., Price, S.R. 2000. Glucocorticoids induce proteosome C3 subunit expression in L6 muscle cells by opposing the suppression of its transcription by NF-κB. *The Journal of Biological Chemistry*. 275: 19661-19666

36. Du, J., Wang, X., Miereles, C., Bailey, J.L., Debigare, R., Zheng, B., Price, S.R., Mitch, W.E. 2004. Activation of caspase-3 is an initial step triggering accelerated muscle proteolysis in catabolic conditions. *Journal of Clinical Investigation.* 113: 115-123
37. Dudek, H., Datta, S.R., Franke, T.F., Birnbaum, M.J., Yao, R., Cooper, G.M., Segal, R.A., Kaplan, D.R., Greenberg, M.E. 1997. Regulation of neuronal survival by the serine-threonine protein kinase Akt. *Science*. 275: 661-665
38. Dunpont, J., Renou, J.P., Shani, M., Hennighausen, L., LeRoth, D. 2002. PTEN overexpression suppresses proliferation and differentiation and enhances apoptosis of the mouse mammary epithelium. *Journal of Clinical Investigation*. 110: 815-825
39. Dunpont-Versteegden, E.E. 2005. Apoptosis in muscle atrophy: Relevance to sarcopenia. *Experimental Gerontology*. 40: 473-481
40. Engelbrecht, A.-M., Mattheyse, M., Ellis, B., Loos, B., Thomas, M., Smith, R.M., Peters, S., Smith, C., Myburgh, K. 2007. Proanthocyanidin from grape seeds inactivates the PI3-kinase/PKB pathway and induces apoptosis in a colon cancer cell line. *Cancer Letters*. 258: 144-153
41. Ferreira, L.F., Reid, M.B. 2008. Muscle derived ROS and thiol regulation in muscle fatigue. *Journal of Applied Physiology*. 104: 853-860
42. Frost, R.A., Lang, C.H. 2007. Protein kinase B/Akt: a nexus of growth factor and cytokine signaling in determining muscle mass. *Journal of Applied Physiology*. 103: 378-387
43. Garg. A.K., Aggarwal, B.B. 2002. Reactive oxygen intermediates in TNF signalling. *Molecular Immonology*. 39: 509-517
44. Gericke, A., Munson, M., Ross, A.H. 2006. Regulation of the PTEN phosphatase. *Gene*. 374: 1-9
45. Glass, D.J. 2003. Signalling pathways that mediate skeletal muscle hypertrophy and atrophy. *Nature Cell Biology*. 5: 87-90
46. Glass, D.J. 2005. Skeletal muscle hypertrophy and atrophy signalling pathways. *The International Journal of Biochemistry and Cell Biology*. 37:1974-1984
47. Glass, D.J. 2007. Two tales concerning skeletal muscle. *The Journal of Clinical Investigation*. 117: 2388-2391
48. Glickman, M.H., Ciechanover, A. 2002. The ubiquitin-proteolytic pathway: destruction for the sake of construction. *Physiological Reviews*. 82: 373-428

49. Goldspink, D.E., Garlick, P.J., McNurlan, M.A. 1983. Protein turnover measured *in vivo* and *in vitro* in muscles undergoing compensatory growth and subsequent denervation atrophy. *Biochemical Journal*. 210: 89-98
50. Goll, D.E., Thompson, V.F., Li, H., Wei, W., Cong, J. 2003. The calpain system. *Physiology Reviews*. 83: 731-801
51. Gomes-Marcondes, M.C., Tisdale, M.J. 2002. Induction of protein catabolism and the ubiquitin-proteosome pathway by mild oxidative stress. *Cancer Letters*. 180: 69-74
52. Gomez, L.A, Alekseev, A.E., Aleksandrova, L.A., Brady, P.A., Terzic, A. 1997. Use of MTT assay in adult ventricular cardiomyocytes to assess viability. Effects of adenosine and potassium on cellular survival. *Journal of Molecular and Cellular Cardiology*. 29: 1255-1266
53. Granado, M., Martín, A.I., Priego, T., López-Calderón, A., Villanúa, M.A. 2006. Tumor necrosis factor blockade did not prevent the increase of muscular muscle RING finger-1 and muscle atrophy F-box in arthritic rats. *Journal of Endocrinology*. 191:319-326
54. Guttridge, D.C., Albanese, C., Reuther, J.Y. et al. 1999 NF-kappaB controls cell growth and differentiation through transcriptional regulation of cyclin D1. *Molecular and Cell Biology*. 19: 5785-5799
55. Guttridge, D.C., Mayo, M.W., Madrid, L.V., Wang, C.Y., Baldwin, A.S. 2000. NF-κB-induced loss of MyoD messenger RNA: possible role in muscle decay and cachexia. *Science*. 289: 2363-2366
56. Hara, K., Yonezawa, K., Sakaue, H., Ando, A., Kotani, K., Kitamura, T., Kitamura, Y., Ueda, H., Stevens, L., Jackson, T.R. et al. 1994. 1-Phosphatidylinositol 3-kinase activity is required for insulin-stimulated glucose transport but not for RAS activation in CHO cells. *Proceeding of the National Academy of Science USA*. 91: 7415-7419
57. Hesselgren, P.O., Fischer, J.E. 1997. The ubiquitin-proteosome pathway: a review of a novel intracellular mechanism of muscle protein breakdown during sepsis and other catabolic conditions. *Annals of Surgery*. 225: 307-316
58. Hilder, T.L., Tou, J.C., Grindeland, R.E., Wade, C.E., Graves, L.M. 2003. Phosphorylation of insulin receptor substrate-1 serine 308 correlates with JNK activity in atrophic skeletal muscle. *FEBS Letters*. 553: 63-67
59. Hirose, M., Kaneki, M., Sugita, H., Yasuhara, S., Martyn, J.A. 2000. Immobilization depresses insulin signalling in skeletal muscle. *American journal of Physiology-Endocrinology and Metabolism*. 279: E2135-E2141

60. Hirosumi, J., Tuncman, G., Chang, L., Gorgun, C.Z., Uysal, K.T., Maeda, K., Karin, M., Hotamisligil, G.S. 2000. A central role for JNK in obesity and insulin resistance. *Nature*. 420:-333-336
61. Hishiya, A., Iemura, S., Natsume, T., Takayama, S., Ikeda, K., Watanabe, K. 2006. A novel ubiquitin-binding protein ZNF216 functioning in muscle atrophy. *EMBO Journal*. 25: 554-564
62. Hresko, R.C., Mueckler, M. 2005. mTOR RICTOR is the Ser473 kinase for Akt/protein kinase B in 3T3-L1 adipocytes. *Journal of Biological Chemistry*. 280: 40406-40416
63. Hsieh, C.C., Ten, M.H., Liu, H.W., Lau, Y.T. 2000. Lysophosphatidylcholine induces apoptosis and non-apoptotic death in vascular smooth muscle cells: In comparison with oxidised LDL. *Atherosclerosis*. 151: 481-491
64. Hsu, H., Xiong, J., Goeddel, D. 1995. The TNF receptor 1-associated protein TRADD signals cell death and NF-kappa B activation. *Cell*. 81: 495-504 http://www.bio.davidson.edu/COURSES/Immunology/Students/spring2000/wolf/tnfalpha.html [Cited on 12 May 2008]
65. Hu, Z., Lee, I.H., Wang, X., Sheng, Zhang, L., Du, J., Mitch, W.E. 2007. PTEN expression contributes to the regulation of muscle protein degradation in diabetes. *Diabetes*. 56: 2449-2456
66. Huang, H., Tindall, D.J. 2007. Dynamic FoxO transcription factors. *Journal of Cell Science*. 120: 2479-2487
67. Hunter, R.B., Stevenson, E.J., Koncarevic, A., Mitchell-Felton, H., Essig, D.A., Kandarian, S.C. 2002. Activation of an alternative NF-κB pathway in skeletal muscle during disuse atrophy. *The FASEB Journal*. 16: 529-538
68. Hyatt, J.-P.K., Roy, R.R., Baldwin, K.M., Edgerton, V.R. 2003. Nerve activity-independent regulation of skeletal muscle atrophy: role of MyoD and myogenin in satellite cells and myonuclei. *American Journal of Physiology-Cell Physiology*. 285: C1161-C1173
69. Imoto, K., Kukidome, D., Nishikawa, T., Matsuhisa, T., Sonoda, K., Fujisawa, K., Yano, M., Motoshima, H., Taguchi, T., Tsuruzoe, K., Matsumura, T., Ichijo, H., Araki, E. 2006. Impact of mitochondrial reactive oxygen species and apoptosis signal-regulating kinase-1 on insulin signaling. *Diabetes*. 55: 1197-1204
70. Jackman, R.W., Kandarian, S.C. 2004. The molecular basis of skeletal; muscle atrophy. *American Journal of Cell Physiology*. 287: 834-843

71. Kabe, Y., Ando, K., Hirao, S., Yoshida, M., Handa, H. 2005. Redox regulation of NF-κB activation: distinct redox regulation between the cytoplasm and the nucleus. *Anti-oxidants and Redox Signaling*. 7: 395-403
72. Kamei, Y., Miura, S., Suzuki, M., Kai, Y., Mizukami, J., Taniguchi, T., Mochida, K., Hata, T., Matsuda, J., Aburatani, H., Nishino, I., Ezaki, O. 2004. Skeletal muscle FOXO01 (FKHR) transgenic mice have less skeletal muscle mass, down-regulated Type 1 (slow twitch/red muscle) fiber genes, and impaired glycemic control. *The Journal of Biological Chemistry*. 279: 41114-41123
73. Kamei, Y., Mizukami, J., Miura, S., Suzuki, M., Takahashi, N., Kawana, T. Taniguchi, T., Ezaki, O. 2003. A forkhead transcription factor FKHR upregulates lipoprotein lipase expression in skeletal muscle. *FEBS Letters*. 536: 232-236
74. Kandarian, S.C., Jackman, R.W. 2006. Intracellular signalling during skeletal muscle atrophy. *Muscle and Nerve*. 33:155-165
75. Kaufmann-Zeh, A., Rodriguez-Viciana, P., Ulrich, E., Gilbert, C., Coffer, P., Downward, J., Evan, G. 1997. Suppression of *c-myc*-induced apoptosis by Ras signaling through PI(3)K and PKB. Nature. *385*: 544-548
76. Kawamura, I., Morishita, R., Tomita, N., Lacey, E., Aketa, M., Tsujimoto, S. et al. 1999. Intratumoral injection of olinucleotides to the NF kappa B binding site inhibits cachexia in a mouse tumor model. *Gene Therapy*. 6: 91-97
77. Kennedy, S.G., Wagner, A.J., Conzen, S.D., Jordan, J., Bellacosa, A., Tsichlis, P.N., Hay, N. 1997. The PI-3K/Akt signaling pathway delivers an anti-apoptotic signal. *Genes and Development*. 11: 701-713
78. Kiritoshi, S., Nishikawa, T., Sonoda, K., Kukidome, D., Senokuchi, T., Matsuo, T., Matsumura, T., Tokunaga, H., Brownlee, M., Araki, E. 2003. Reactive oxygen species from mitochondria induce cyclooxygenase-2 gene expression in human mesangial cells: potential role in diabetic nephropathy. *Diabetes*. 52: 2570-2577
79. Kitakaze, M., Fong, M., Yoshitake, M., Minamino, T., Node, K., Okuyama, Y., Terade, N., Kambayashi, T., Hori, M. 1997. Vesnarinone inhibits adenosine uptake in endothelial cells, smooth muscle cells and monocytes, and mediates cytoprotection. Journal of Molecular and Cellular Cardiology. 29: 3413-3417
80. Kondo, H., Miura, M., Itokawa, Y. 1991. Oxidative stress in skeletal muscle atrophied by immobilization. *Acta Physiologica Scandinavica*. 142: 527-528

81. Kondo, H., Miura, M., Nakagaki, I., Sasaki, S., Itokawa, Y. 1992. Trace element movement and oxidative stress in skeletal muscle atrophied by immobilization. *American Journal of Physiology-Endocrinology and Metabolism*. 262: E583-E590
82. Kulik, G., Klippel, A., Weber, M.J. 1997. Antiapoptotic signaling by the insulin-like growth factor 1 receptor, phosphatidylinositol 3-kinase and Akt. *Molecular and Cell Biology*. 17: 1595-1606
83. Lacerda, L., Smith, R.M., Opie, L., Lecour, S. 2006. TNF-α-induced cytoprotection requires the production of free radicals within mitochondria in C_2C_{12} myotubes. *Life Sciences*. 79: 2194-2201
84. Ladner, K.J., Caligiuri, M.A., Gittridge, D.C. 2003. Tumor necrosis factor-regulated biphasic activation of NF-κB is required for cytokine –induced loss of skeletal muscle gene products. *Journal of Biological Chemistry*. 278: 2294-2303
85. Langen, R.C., Van Der Velden, J.L., Schols, A.M., Kelders, M.C.J.M., Wouters, E.F.M., Janssen-Heininger, Y.M.W. 2004. Tumor necrosis factor-alpha inhibits myogenic differentiation through MyoD protein destabilization. *FASEB Journal*. 18:227-237
86. Langen, R.C.J., Schols, A.M.W.J., Kelders, M.C.J.M., Van Der Velden, J.L.J., Wouters, E.F.M., Janssen-Heininger, Y.M.W. 2002. Tumor necrosis factor-α inhibits myogenesis through redox-dependent and –independent pathways. *American Journal of Physiolohy-Cell Physiology*. 283: C714-C721
87. Langen, R.C.J., Schols, A.M.W.J., Kelders, M.C.J.M., Wouters, E.F.M. 2001. Inflammatory cytokines inhibit myogenic differentiation through activation of nuclear factor-κB. FASEB Journal. 15: 97-104
88. Latres, E., Amini, A.R., Amini, A.A., Griffiths, J., Martin, F.J., Wei, Y., Lin, H.C., Yancopoulos, G.D., Glass, D.J. 2004. IGF-1 inversely regulates atrophy-induced genes via the PI3K/Akt/mTOR pathway. *The Journal of Biological Chemistry*. 280: 2737-2744
89. Layne, M.D., Farmer, S.R. 1999. Tumor necrosis factor-alpha and basic fibroblast growth differentially inhibit the insulin-like growth factor-1 induced expression of myogenin in C2C12 myoblasts. *Experimental Cell Research*. 249: 177-187
90. Lecker, S.H., Goldberg, A.L., Mitch, W.E. 2006. Protein degradation by the ubiquitin-proteosome pathway in normal and diseased states. *Journal of the American Society of Nephrology*. 17: 1807-1819

91. Lecker, S.H., Jagoe, R.T., Gilbert, A., Gomez, M., Baracos, V., Bailey, J., Price, S.R., Mitch, W.E., Goldberg, A.L. 2004. Multiple types of skeletal muscle atrophy involve a common program of changes in gene expression. *FASEB Journal*. 18: 30-51
92. Lecker, S.H., Solomon, V., Mitch, W.E., Goldberg, A.L. 1999. Muscle protein breakdown and the critical role of the ubiquitin-proteosome pathway in normal and disease states. *Journal of Nutrition*. 129: 227S-237S
93. Lecker, S.H., Solomon, V., Price, S.R., Kwon, Y.T., Mitch, W.E., Goldberg, A.L. 1999. Ubiquitin conjugation by the N-end rule pathway and mRNAs for its components increase in muscles of diabetic rats. *The Journal of Clinical Investigation*. 104: 1411-1420
94. Lee, F.S., Hagler, J., Chen, Z.J., Maniatis, T. 1997. Activation of the IκB kinase complex by MEKK1, a kinase of the JNK pathway. *Cell*. 88: 213-222
95. Lee, S.W., Dai, G., Hu, Z., Wang, X., Du, J., Mitch, W.E. 2004. Regulation of muscle protein degradation: coordinated control of apoptotic and ubiquitin-protein systems by phosphatidylinositol 3 kinase. *The Journal of American Society of Nephrology*.15: 1537-1545
96. Li, G., Barrett, E.J., Barrett, M.O., Cao, W., Liu, Z. 2007. Tumor necrosis factor-α induces insulin resistance in endothelial cells via a p38 mitogen-activated protein kinase-dependant pathway. *Endocrinology*. 148: 3356-3363
97. Li, X., Lu, Y., Jin, W., Liang, K., Mills, G.B., Fan, Z. 2006. Autophosphorylation of Akt at threonine 72 and serine 246. A potential mechanism of regulation of Akt kinase activity. *Journal of Biological Chemistry*. 281: 13837-13843
98. Li, Y., Chen, Y., John, J., Moylan, J., Jin, B., Mann, D.L., Reid, M.B. 2005. TNF-α acts via p38 MAPK to stimulate expression of the ubiquitin ligase atrogin1/MAFbx in skeletal muscle. *The FASEB Journal*. 19: 362-370
99. Li, Y., Reid, M.B. 2000. NF-κB mediates the protein loss induced by TNF-α in differentiated skeletal muscle myotubes. *American Journal of Physiology-Regulator integrative and Comparative Physiology*. 279: R1165-R1170
100. Li, Y.P. 2003. TNF-α is a mitogen in skeletal muscle. *American Journal of Physiology-Cell Physiology*. 285: C370-C376
101. Li, Y.P., Atkins, C.M., Sweatt, J.D., Reid, M.B. 1999. Mitochondria mediate tumor necrosis factor-α/NF-κB signalling in skeletal muscle myotubes. *Antioxidants and Redox Signaling*. 1: 97-104

102. Li, Y.P., Chen, Y., Li, A.S., Reid, M.B. 2003. Hydrogen peroxide stimulates ubiquitin-conjugating activity and expression of genes for specific E2 and E3 proteins in skeletal muscle myotubes. *American Journal of Physiology-Cell Physiology*. 285: C806-C812

103. Li, Y.P., Jiang, B., Ensign, W.Y., Vogt, P.K., Han, J., 2000. Myogenic differentiation requires signalling through both phosphotidylinositol 3-kinase and p38 MAP kinase. *Cell Signalling*. 12: 751-757

104. Li, Y.P., Schwarts, R.J. 2001. TNF-α regulates early differentiation of C2C12 myoblasts in an autocrine fashion [Abstract]. *FASEB Journal*. 15: A1080

105. Li, Y.-P., Schwartz, R.J., Waddell, I.D., Holloway, B.R., Reid, M.B. 1998. Skeletal muscle myocytes undergo protein loss and reaction oxygen-mediated NF-κB activation in response to tumor necrosis factor α. *The FASEB Journal*. 12: 871-880

106. Li, Z.W., Chu, W., Hu, Y., Delhase, M., Deerinck, T., Ellisman, M., Johnson, R., Karin, M. 1999. The IKKbeta subunit of IkappaB kinase (IKK) is essential for nuclear factor kappaB activation and prevention of apoptosis. *The Journal of Experimental Medicine*. 189: 1839-1845

107. Liu, Y., Shen, T., Randall, W.R., Schneider, M.F. 2005. Signaling pathways in activity-dependent fiber type plasticity in adult skeletal muscle. *Journal of Muscle Research and Cell Motility*. 26: 13-21

108. Lizard, G., Gueldry, S., Sordet, O., Monier, S., Athias, A., Miguet, C., Bessede, G., Lamaire, S., Solary, E., Gambert, P. 1998. Glutathione is implied in the control of 7-ketocholesterol induced apoptosis, which is associated with radical oxygen species production. *FASEB Journal*. 12: 1651-1663

109. Llovera, M., Garcia-Martinez, C., Lopez-Soriano, J., Agell, M., Lopez-Soriano, F.J., Garcia, I., Argiles, J.M. 1998. Protein turnover in skeletal muscle of tumor-bearing mice overexpressing the soluble TNFreceptor-1. *Cancer Letters*. 130: 19-27

110. Llovera, M., Garcia-Martinez, C., Lopez-Soriano, J., Carbo, N., Agell, M., Lopez-Soriano, F.J., Argiles, J.M. 1998. Role of TNF receptor 1 in protein turnover during cancer cachexia using gene knockout mice. Molecular and Cell Endocrinology. 142: 183-189

111. Maehama, T., Dixon, J.E. 1998. The tumor suppressor, PTEN/MMAC1, dephosphorylates the lipid second messenger, phosphatidylinositol 3, 4,5-triphosphate. *Journal of Biological Chemistry*. 273: 13375-13378

112. Mahoney, D.J., Kaczor, J.J., Bourgeois, J., Yasuda, N., Tarnopolsky, M.A. 2006. Oxidative stress and antioxidant enzyme upregulation in SOD1-G93A mouse skeletal muscle. *Muscle Nerve*. 809-816

113. Martindale, J.L., Holbrook, N.J. 2002. Cellular response to oxidative stress: Signalling for suicide and survival. *Journal of Cellular Physiology*. 192: 1-15

114. Masure, S., Haefner, B., Wesselink, J.J., Hoefnagel, E., Mortier, E., Verhasselt, P., Tuytelaars, A., Gordon, R., Kambadur, R., Richardson, A. 1999. Molecular cloning, expression and characterization of the human serine/threonine kinase Akt-3. *European Journal of Biochemistry*. 265: 353-360

115. Mayo, M.W., Madrid, L.V., Westerheide, S.D., Jones, D.R., Yuan, X.-J., Baldwin Jr, A.S., Whang, Y.E. 2002. PTEN blocks tumor necrosis factor-induced NF-κB-dependent transcription by inhibiting the transactivation potential of the p65 subunit. *The Journal of Biological Chemistry*. 277: 11116-11125

116. Mitch, W.E., Goldberg, A.L. 1996. Mechanisms of muscle wasting: the role of the ubiquitin-proteosome system. *New England Journal of Medicine*. 335: 1897-1905

117. Mitchell, P.O., Pavlath, G.K. 2001. A muscle precursor cell-dependent pathway contributes to muscle growth after atrophy. *American Journal of Physiology-Cell Physiology*. 281: C1706-C1715.

118. Mitchell, P.O., Pavlath, G.K. 2004. Skeletal muscle atrophy leads to loss and dysfunction of muscle precursor cells. *American Journal of Physiology-Cell Physiology*. 287: C1753-C1762

119. Moresi, V., Pristerià, A., Schicchitano, B.M., Molinaro, M., Teodori, L., Sassoon, D., Adamo, S., Coletti, D. 2008. Tumor necrosis factor-α inhibition of skeletal muscle regeneration is mediated by a caspase-dependent stem cell response. *Stem Cells*. 26: 997-1008

120. Morris, R.T., Spangenburg, E.E., Booth, F.W. 2004. Responsiveness of cell signalling pathways during failed 15-day regrowth of aged skeletal muscle. *Journal of Applied Physiology*. 96: 398-404

121. Mosialos, G., Birkenbach, M., Yalamanchilli, R., VanArsdale, T., Ware, C., Kieff, E. 1995. The Epstein-Barr virus transforming protein LMP1 engages signaling proteins for the tumor necrosis factor receptor family. *Cell*. 80: 389-399

122. Mourkioti, F., Rosenthal, N. 2007. NF-κB signaling in skeletal muscle: prospects for intervention in muscle diseases. *Journal of Molecular Medicine*. 747-759

123. Muller, F.L., Song, W., Jang, Y.C., Liu, Y., Sabia, M., Richardson, A., Van Remmen, H. 2007. Denervation-induced skeletal muscle atrophy is associated with increased mitochondrial ROS production. *American Journal of Physiology-Regulatory Integr Comp Physiol*. 293: R1159-R1168

124. Munoz, M.A., Satarug, S., Tischler, M.E. 1993. Time course of the response of myofibrillar and sarcoplasmic protein metabolism to unweighting of the soleus muscle. *Metabolism*. 42: 1006-1012

125. Murgia, M., Serrano, A.L., Calabria, E., Pallafacchina, G., Lomo, T., Schiaffino, S. 2000. Ras is involved in nerve-activity-dependent regulation of muscle genes. *Nature Cell Biology*. 2: 142-147

126. Murray, J., Barbara, J., Dunkley, S., Lopez, A., Van Ostade, X., Condliffe, I., Haslett, C., Chilvers, E. 1997. Regulation of neutrophil apoptosis by tumor necrosis factor-alpha: Requirements for TNF-R55 and TNF-R75 for induction of apoptosis in vitro. *Blood*. 90: 2772-2783

127. Naya, F.J., Olsen, E. 1999. MEF2: a transcription target for signaling pathways controlling skeletal muscle growth and differentiation. *Current Opinion in Cell Biology*. 11: 683-688

128. Ozes, O.N., Akza, H., Mayo, L.D., Gustin, J.A., Maehama, T., Dixon, J.E., Donner, D.B. 2001. A phosphatidylinositol 3-kinase/Akt/mTOR pathway mediates and PTEN antagonizes tumor necrosis factor inhibition of insulin signalling through insulin receptor substrate-1. *PNAS*. 98:4640-4645

129. Pantano, C., Reynaert, N.L., Vliet, A.V., Janssen-Heininger, Y.M. 2006. Redox-sensitive kinases of the nuclear factor- kappaB signalling pathway. *Antioxidants and Redox Signaling*. 8: 1791-1806

130. Pearson, G., Robinson, F., Beers Gibson, T., Xu, B.E., Karandikar, M., Berman, K., Cobb, M.H. 2001. Mitogen-activated protein (MAP) kinase pathways: regulation and physiological functions. *Endocrine Reviews*. 22: 153-183

131. Peterson, J.M., Feeback, K.D., Baas, J.H., Pizza, F.X. 2006. Tumor necrosis factor-α promotes the accumulation of neutrophils and macrophages in skeletal muscle. *Journal of Applied Physiology*. 101: 1394-1399

132. Pfeffer, L.M., Mullersman, J.E., Pfeffer, S.R., Murti, A., Shi, W., Yang, C.H. 1997. Stat3 an adaptor to couple phosphotidylinositol 3-kinase to the IFNARI chain of the type 1 interferon receptor. *Science*. 276: 1418-1420

133. Phillips, T., Leeuwenburgh, C. 2005. Muscle fiber-specific apoptosis and TNF-α signaling in sarcopenia are attenuated by life-long calorie restriction. *The FASEB Journal*. 668-670

134. Powers, S.K., Kavazis, A.N., DeRuisseau, K.C. 2005. Mechanisms of disuse muscle atrophy: role of oxidative stress. *American Journal of Physiology-Regulatory Integrative and Comparative Physiology*. 288: R337-R344

135. Powers, S.K., Kavazis, A.N., McClung, J.M. 2007. Oxidative stress and disuse muscle atrophy. *Journal of Applied Physiology*. 102: 2389-2397

136. Pownall, M.E., Gustafsson, M.K., Emerson Jr, C.P. 2002. Myogenic regulatory factors and the specification of muscle progenitors in vertebrate embryos. *Annual Review of Cell and Development Biology*. 18; 747-783

137. Primeau, A.J., Adhihetty, P.J., Hood, D.A. 2002. Apoptosis in heart and skeletal muscle. *Canadian Journal of Applied Physiology*. 27: 349-395

138. Qi, C., Pekala, P.H. 2000. Tumor necrosis factor-α-induced insulin resistance in adipocytes. *P.S.E.M.B.* 223: 128-135

139. Qi, M., Elion, E.A. 2005. MAP kinase pathways. *Journal of Cell Science*. 118: 3569-3572

140. Reddy, S.A.G., Huang, J.H., Liao, W.S.-L. 2000. Phosphatidylinositol 3-kinase as a mediator of TNF-induced NF-κB activation. *The Journal of Immunology*. 164: 1355-1363

141. Reid, M.B., Li, Y.-P. 2001. Tumor necrosis factor-α and muscle wasting: a cellular perspective. *Respiratory Research*. 2: 269-272

142. Rink, L., Kirchner, H. 1996. Recent progress in the tumor necrosis factor-alpha field. *International Archives of Allergy and Immunology*. 111: 199-209

143. Rothe, M., Wong, S., Henzel, W., Goeddel, D. 1994. A novel family of putative signal transducers associated with the cytoplasmic domain of the 75 kDa tumor necrosis factor receptor. Cell. 78: 681-692

144. Sabourin, L.A., Rudnicki, M.A. 2000. The clinical regulation of myogenesis. *Clinical Genetics*. 57: 16-25

145. Sacheck, J.M., Ohtsuka, A., McLary, S.C., Goldberg, A.L. 2004. IGF-1 stimulates muscle growth by suppressing protein breakdown and expression of atrophy-related ubiquitin ligases, atrogin-1 and MuRF1. *American journal of Physiology-Endocrinology and Metabolism*. 287: E591-E601

146. Saini, A., Nasser, A., Stewart, C.E.H. 2006. Waste management-Cytokines, growth factors and cachexia. *Cytokine & Growth Factor Reviews*. 17:475-486

147. Sandri, M., Lin, J., Handschin, C., Yang, W., Arany, Z.P., Lecker, S.H., Goldberg, A.L., Spiegelman, B.M. 2006. PGC-1alpha protects skeletal muscle from atrophy by suppressing FoxO3 action and atrophy-specific gene transcription. *Proceedings of the National Academy of Sciences USA*. 103: 16260-16265

148. Sandri, M., Sandri, C., Gilbert, A., Skuck, C., Calabria, E., Picerd, A., Walsh, K., Schiaffino, S., Lecker, S.H., Goldberg, A.L. 2004. FOXo transcription factors induce the atrophy-related ubiquitin ligase atrogin-1 and cause skeletal muscle atrophy. *Cell*. 117: 399-412

149. Sen, C.K., Khanna, S., Resznick, A.Z., Roy, S., Packer, L. 1997. Glutathione regulation of tumor necrosis factor-α-induced NF-κB activation in skeletal muscle-derived L6 cells. *Biochemical and Biophysical Research Communications*. 237: 645-649

150. Solomon, V., Goldberg, A.L. 1996. Importance of the ATP-ubiquitin-proteosome pathway in the degradation of soluble and myofibrillar proteins in rabbit muscle extracts. *Journal of Biological Chemistry*. 271: 26690-26697

151. Song, H., Dunbar, J., Zhang, Y., Guo, D., Donner, D. 1994. Identification of a protein with homology to hsp90 that binds the type 1 tumor necrosis factor receptor. *Journal of Biological Chemistry*. 270: 3574-3581

152. Stanger, B., Leder, P., Lee, T., Kim, E., Seed, B. 1995. RIP: a novel protein containing a death domain that interacts with Fas/APO-1 (CD95) in yeast and causes cell death. *Cell*. 81: 513-523

153. Stitt, T.N., Drijan, D., Clarke, B.A., Panaro, F., Timofeyva, Y., Kline, W.O., Gonzalez, M., Yancopoulos, G.D., Glass, D.J. 2004. The IGF-1/PI3K/Akt pathway prevents expression of muscle atrophy-induced ubiquitin ligases by inhibiting FOXO transcription factors. *Molecular Cell*. 14: 395-403

154. Strieter, R., Kunkel, S., Bone, R. 1993. Role of tumor necrosis factor-alpha in disease and inflammation. *Critical Care Medicine*. 21: S447-S463

155. Szalay, K., Razga, Z., Duda, E. 1997. TNF inhibits myogenesis and downregulates the expression of myogenic regulatory factors myoD and myogenin. *European Journal of Cell Biology*. 74: 391-398

156. Thaloor, D., Miller, K.J., Gephart, J., Mitchell, P.O., Pavlath, G.K. 1999. Systemic administration of the NF-κB inhibitor Curcumin stimulates muscle regenerations after traumatic injury. *American Journal of Physiology*. 277: C320-C329

157. Thannickal, V.J., Fanburg, B.L. 2000. Reactive oxygen species in cell signalling. *American Journal of Physiology-Lung Cellular and Molecular Physiology*. 279: L1005-L1028

158. Tisdale, M.J. 2005. The Ubiquitin-proteosome pathway as a therapeutic target for muscle wasting. *The Journal of Supportive Oncology*. 3: 209-217

159. Torres, J., Rodriguez, J., Myers, M.P., Valiente, M., Graves, J.D., Tonks, N.K., Pulido, R. 2003. Phosphorylation-regulated cleavage of the tumor suppressor PTEN by caspase-3: implications for the control of protein stability and PTEN-protein interactions. *The Journal of Biological Chemistry*. 278: 30652-30660

160. Tracey, K., Cerami, A. 1990. Metabolic response to Cachetin/TNF. Annals of the New York Academy Sciences: Vol. 587. Eds. Boland, B., Cullinan, J., Kimball, C. New York: New York Academy Sciences. 325-330

161. Tracey, K.J. 2002. Lethal weight loss: the focus shifts to signal transduction. *Science's Signal Transduction Knowledge Environment*. 130: 21

162. Vander, A., Sherman, J., Luciano, D. (1998). Human Physiology: the mechanisms of body function. 7th Edition. New York, McGraw Hill. 288-291

163. Vescovo, G., Libera, L.D. 2006. Skeletal muscle apoptosis in experimental heart failure: the only link between inflammation and skeletal muscle wastage. *Current Opinion in Clinical Nutrition and Metabolic Care*. 9:416-422

164. Wang, K.K., Posmantur, R., Nadimpalli, R., Nath, R., Mohan, P., Nixon, R.A., Talanian, R.V., Keegan, M., Herzog, L., Allen, H. 1998. Caspase-mediated fragmentation of calpain inhibitor protein calpastatin during apoptosis. *Archives of Biochemistry and Biophysics*. 356: 187-196

165. Wang, X.H., Hu, Z., Hu, J.P., Du, J., Mitch, W.E. 2006. Insulin resistance accelerates muscle protein degradation: activation of the ubiquitin-proteosome pathway by defects in muscle cell signaling. *Endocrinology*. 147: 4160-4168

166. Wijesekara, N., Konrad, D., Eweida, M., Jefferies, C., Liadis, N., Giacca, A., Crackower, M., Sukuki, A., Mak, T.W., Kahn, C.R., Klip, A., Woo, M. 2005. Muscle specific Pten deletion protects against insulin resistance and diabetes. *Molecular and Cellular Biology*. 25: 1135-1145

167. Windsor, J.A., Hill, G.L. 1988. Risk factors for postoperative pneumonia: the importance of protein depletion. *Annals of Surgery*. 208: 209-214

168. Workeneh, B., Rondon-Berrios, H., Zhang, L., Hu, Z., Ayehu, G., Ferrando, A., Kopple, J.D., Wand, H., Storer, T.W., Fournier, M., Lee, S.W., Du, J., Mitch, W.E. 2006. Development of a diagnostic method for detecting increased muscle protein degradation in patients with catabolic conditions. *Journal of the American Society of Nephrology*. 17: 3233-3239

169. Yao, R., Cooper, G.R. 1995. Requirement for phosphatidylinositol 3-kinase in the prevention of apoptosis by nerve growth factor. *Science*. 267: 2003-2006

170. Yoo, L.I., Liu, D.W., Vu, S.L., Bronson, R.T., Wu, H., Yuan, J. 2006. Pten deficiency activates distinct downstream signalling pathways in a tissue-specific manner. *Cancer Research*. 66: 1929-1939

171. Zhang, P., Chen, X., Fan, M. 2007. Signaling mechanisms involved in disuse muscle atrophy. *Medical Hypothesis*. 69: 310-321

Appendices

Appendix A

Protocol 1: Cell culture

- Before work was started on the hood, hands were washed up to the elbows and gloves were worn. Hands were sprayed with 70% alcohol each time before putting them in-side the laminar flow to keep sterile
- T75 flasks containing L6 myoblasts that were approximately 60-65% confluent were split into smaller 6-well plates or T25 culture flasks containing ± 80 000 or ± 150 000 cells respectively for experimental purposes
- Cells were first washed with warm PBS (see Appendix B) to remove all traces of growth medium (GM) (see Appendix B) and were then loosened from the T75 flask surface using trypsin (4ml) which is a protease enzyme
- The flask was placed in a "shaking" incubator for 2-3 minutes at 37ºC (Trypsin is only active at this temperature). Cells were checked to see if they have detached under a microscope. If the cells had not loosened, the bottom of the flask was gently tapped to help the process
- Once the cells have eventually loosened, warm GM (double the volume of trypsin, thus 8ml) was added to the cells to neutralise the trypsin
- The cells/trypsin and medium were transferred to a 10ml falcon tube and centrifuged at 15000 rpm for 3 minutes
- The supernatant (medium containing trypsin) was decanted and the pellet (cells) at the bottom of the tube was resuspended with 3 ml fresh GM using a pipette
- To determine the average number of cells, 20µl from the cell suspension was pipetted onto a haemocytometer (see protocol 2)
- The number of cells per millilitre was determined using a simple calculation

Protocol 2: Cell counting using a haemocytometer

- The haemocytometer was first cleaned by wiping with 70% alcohol and then breathed on it to moisten the surface before placing a coverslip on top
- The coverslip was placed over the counting area on the haemocytometer and viewed under a microscope until Newton's rings appeared
- A sample (20µl) of the resuspended cell solution was then aspirated onto the coverslip using a micropipette
- The cell suspension was allowed to fill the chamber by capillary action and both counting grids covered (see example below)

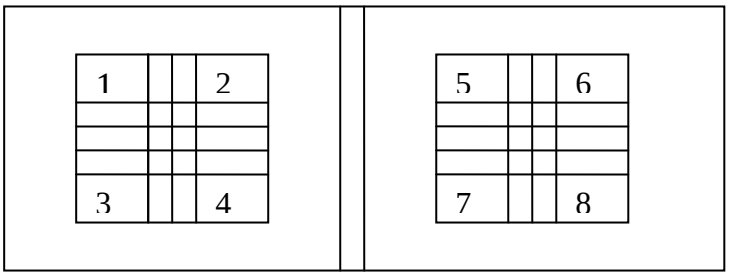

- The total number of cells was counted by counting areas 1 to 8 in both counting grids. The average number of cells was then calculated. This average was then multiplied by 10 000 to get the number of cells per millilitre of the original cell suspension

Protocol 3: Cell Harvesting

- This process removes the cells from the plastic substrate and breaks cell-to-cell bonds as gently as possible
- The old medium was discarded either by careful decanting or with a sterile pipette and the monolayer of cells was washed quickly with ice cold PBS. This wash step was re-peated three times to remove all traces of FBS
- The wash medium was decanted and then 250µl (6-well plates) or 1000µl (T25 flask) of RIPA buffer (see appendix B) was added to each well of the 6-well plate and flasks and placed on ice for 3-5 minutes
- The plates and flasks were swirled to make sure that the surface area was covered with the buffer

- After the time period had lapsed, the cells were scraped from the surface of each well and flask using a sterile cell scraper
- The buffer containing the cells was then pipetted into already chilled eppindorf tubes and stored at -80°C until further experiments were carried out.

Protocol 4: Extraction of proteins from cell samples

- Work on ice at all times to avoid the denaturing of proteins
- Thawed cell samples (from protocol 3) were placed in chilled test tubes and sonnicated. This process ruptures the cell walls in order to release proteins
- The metal piece of the sonnicator was rinsed before and after use with distilled water
- After sonnicating the cells, the cell solution was transferred in an eppendorf tube and centrifuged at 4ºC and 8000rpm for 10 minutes.

Protocol 5: Protein determination with Bradford reagent

- Work on ice at all times to avoid the denaturing of proteins
- For protein determination, make a 1:5 dilution of the Bradford reagent (see Appendix B) using distilled water. This solution needs to be filtered twice using 2 pieces of filter paper. The Bradford reagent is light sensitive therefore remember to use foil or work in the dark room when filtering
- Once the Bradford reagent has been made, a standard curve needs to be made in 7 different eppendorf tubes as follows:

	Distilled Water	**BSA** (see Appendix B)	**Bradford Reagent**
1	0µl	100µl	900µl
2	20µl	80µl	900µl
3	40µl	60µl	900µl
4	60µl	40µl	900µl
5	80µl	20µl	900µl
6	90µl	10µl	900µl
7	100µl	0µl	900µl (**BLANK**)

- Vortex the solutions thoroughly and let them stand in ice for ±5 minutes
- Zero the spectrophotometer using the blank and then read the absorbance values at 595nm using the Simple Reads program
- Once the absorbance readings were recorded, the reading were transferred onto an Excel spreadsheet and a standard curve was created (see graph below)

Samples:

- Pipette 5µl from each sample that was centrifuged into a new eppendorf tube and then add 95µl distilled water and 900µl Bradford reagent. Vortex solution and then read the absorbance values at 595nm using the Simple Reads program
- Using excel, plot the standard curve with protein concentration on the x-axis and the mean OD on the y-axis (see example below). Add in the absorbance values for the samples and determine final calculation for protein concentration in µl/ µg

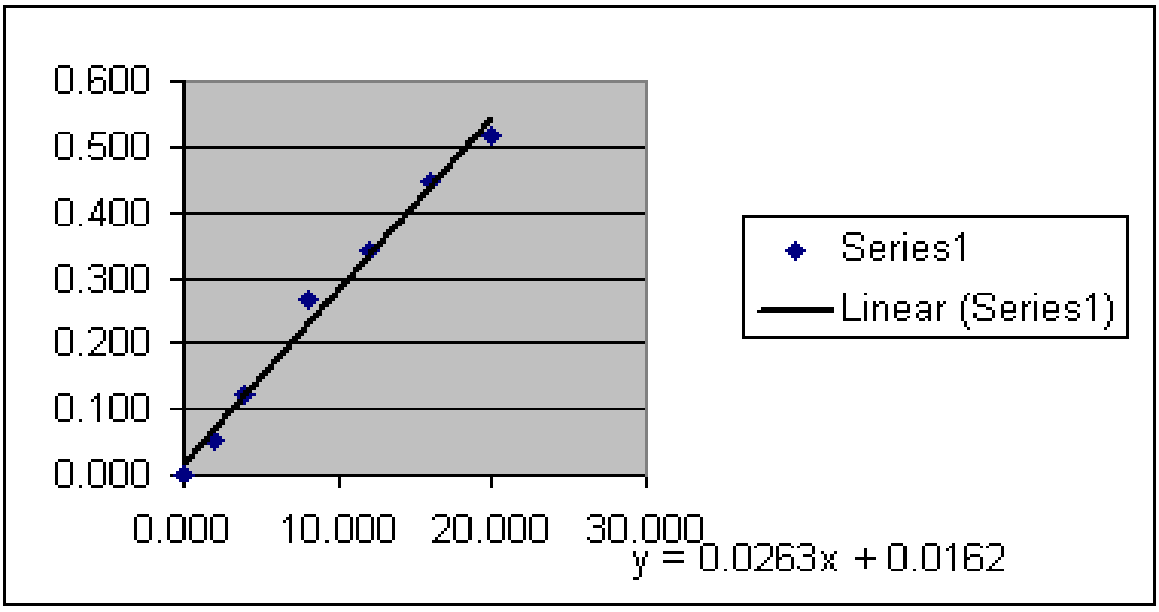

- Once the concentration of each sample has been worked out, pipette the desired amount into a new eppendorf tube and add the appropriate amount of sample buffer (see Appendix B)

Protocol 6: Western Blot Procedure

Preparation of assembly and gels

- Clean glass plates with 70% alcohol and place into assembly
- Place assembly onto plastic apparatus with rubber and firmly clip into place. Check for leaks with distilled water
- Mark on glass plate where separating gel comes to (1/2cm below top of glass plate)
- Make up the separating gel (10% or 12%) (see Appendix B)
- Using a squeeze pipette, add separating gel to assembly into the side. Avoid making bubbles
- Add a few drops of iso-butanol to prevent oxidation of gel and to ensure a straight line with no meniscus
- Allow to set for 30 minutes
- Wash of iso-butanol with distilled water
- Make up the stacking gel (4%) (see Appendix B)
- Using a squeeze pipette, add stacking gel on top of separating gel. Immediately add the 10 well comb at an angle to prevent bubbles until the wells come to the end of glass. Don't push in too deep and then take out
- Allow to set for 30 minutes. During this time prepare Running buffer and thaw your samples
- Denature samples by boiling at 50-70ºC for 5 minutes. Punch hole in each sample to release pressure
- Centrifuge samples for ±1 minute at 5000 revs.
- Remove combs carefully and rinse with distilled water. Drain excess water with blotting paper, being careful not to wipe away the wells
- Take glass off assembly stand and place onto U-shaped Core-latch and then click to secure
- Place the apparatus into tank and add Running buffer (see Appendix B) in the middle compartment just overflowing into the wells

Loading samples

- Place yellow well guide on top of apparatus in the middle compartment
- Using a 20µl pipette, add 10µl peqGOLD pre-stained marker in first well on the left and then your samples from the second well. Use a clean tip for every sample and marker
- Once all samples have been loaded, remove the well guide and add running buffer on the outer compartment up to ½ way from the bottom
- Place green lid on apparatus and attach electrodes – red to read and black to black
- Turn on electrophoresis machine and allow samples to run for 10 minutes at 400mA and 100V (fixed)
- Run samples for a second time for 50 minutes at 400mA and 200V

Transfer/blotting to membrane

- Soak PVDF membrane in methanol then rinse in distilled water and then soak in anode buffer 2 (see Appendix B) until needed
- Soak 4 pieces of blotting paper in anode buffer 1 (see Appendix B)
- Soak 2 pieces of blotting paper in anode buffer 2
- Soak 6 pieces of blotting paper in cathode buffer (see Appendix B)
- On the anode plate of the semi-dry apparatus, place the 4 papers (anode 1) on top. Using a test tube, roll out the excess liquid
- Place the 2 papers (anode 2) on top of the 4 papers and roll out excess liquid
- Go back to gel apparatus and remove the U-shaped core-latch. Remove the glass plates and separate them very carefully to avoid tearing the gel. Cut off the wells (stacking gel) and place the remaining (separating) gel in anode buffer 2
- Place PVDF membrane on top of the papers already on the semi-dry apparatus and then add the gel on top of membrane
- Finally place the 6 papers (cathode buffer) on top of the gel. Roll out excess liquid thoroughly
- Close the apparatus and then supply power for electron transfer: 15V, 0.5A, 300W for 1hour

- Once the time has elapsed, open semi-dry apparatus and remove the blotting papers on top carefully. Place membrane in methanol for a few minutes and allow to air dry completely
- Place membrane in blocking solution (see Appendix B) for a minimum period of 2 hours on the belly dancer on lowest setting or leave in the fridge (4ºC) overnight

Specific binding of proteins

- Wash membrane 3X (5 minutes each) with TBS-tween (see Appendix B)
- Make primary antibody (see Appendix B) solution in a 50ml falcon tube. Roll the membrane with proteins facing the inside and marker at the bottom and place inside the falcon tube
- Mix on the rotating machine in the corridor fridge for a minimum period of 8 hours or leave overnight
- Wash membrane 3X (5 minutes each) with TBS-tween
- Make secondary antibody (see Appendix B) solution in a 50ml falcon tube and add to membrane. Mix on the belly dancer on lowest setting for 1 hour

Exposure

- Wash membrane 3X (5 minutes each)
- Cut 2 pieces of transparent paper and tape them together on one side in a cassette (exposure tray)
- Mix ECL cocktails (500µl solution 1 + 500µl solution 2) in falcon tube
- Drain excess liquid from membrane using tissue paper and add the ECL on the membrane and leave on for 1minute
- Drain excess ECL from membrane and place membrane in between the transparencies. Remove the air bubbles
- In the dark room with the lights off, cut x-ray film and place on the exposure tray on top of the transparency. Place once and do not remove. Close exposure tray and leave for ±5 minutes
- After the time elapsed, take out the x-ray film and place in developer for ±5 minutes
- Rinse x-ray thoroughly in water and then place in fixative for ± 5minutes

- Rinse well and air dry

Stripping membranes

- Submerge membrane in stripping buffer (see Appendix B)
- Incubate in a water bath at 50-70ºC for 30 minutes with occasional agitation
- Wash membrane 3X (10 minutes each) in TBS-tween at room temperature
- Place membrane in blocking solution and carry on as usual for western blotting (This procedure completely removes all antibodies).

Protocol 7: MTT assay

Preparation of solutions

- 1% Isopropanol = 1ml Concentrated HCL added to 99ml Isopropanol
- 0.1 % Triton = 0.1ml Triton-X-100 made up to 100ml using distilled water
- Isopropanol/ Triton solution in 50/1 ratio = 50ml of 1% Isopropanol added to 1mL 0.1% Triton
- 1% MTT (0.01g/1ml PBS) made fresh before use. This solution was covered in foil to protect against the light as it is light sensitive. It was then filtered to remove any excess granules that were not dissolved

Method

- The medium from the cells was gently discarded. These cells were not rinsed with PBS as the cells may loosen
- 1.5ml PBS and 500µl MTT solution was added to each well. This was done very slowly so that the cells did not loosen.
- The plate was then covered in foil and place in the incubator for 2 hours

If some cells have loosened:

- The contents of wells were transferred to 2ml centrifuge tubes and spun down gently for 2 minutes at 1000rpm

- The supernatant was discarded and 2ml 'Isopropanol/Triton' solution was added to each pellet and the cells were resuspended. This resuspended solution was added back into wells were some cells may still be sticking to wells.

If no cells loosened:

- The contents of the wells were discarded and 2ml 'Isopropanol/Triton' solution was added to each well
- The plates were put on belly dancer shaker to mix for 5 minutes while still covered in foil. This loosens the cells from the bottom of the surface
- The content of each well was transferred to 2ml eppendorf tubes and centrifuged for 2 minutes at 1400rpm
- The absorbance values of the supernatant was read at 540nm on the spectrophotometer, using Isopropanol/Triton solution as the blank
- If any of the absorbance values of the supernatants were greater than one, the supernatant was diluted with the Isopropanol/Triton solution

Protocol 8: Trypan Blue exclusion technique

Trypan blue stock solution (0.4%) was prepared with PBS and stored in the dark at 4ºC (see appendix B)

Method

- Medium was removed from cells, washed with warm PBS and trypsonized as previously described (Protocol 1)
- Cell solution containing trypsin was neutralized using warm growth medium and centrifuged at 1300-1500 rpm for 3 minutes
- The cells (each well analysed separately) were then resuspended in 500µl warmed PBS and 500µl 0.4 % trypan blue solution and allowed to stand for 2-5 minutes prior to counting
- 50µl of the resuspended solution was placed into the haemocytometer and counting was conducted as previously described (Protocol 2)

Viable cells did not take up dye and non viable cells took up dye and stained blue

Protocol 9: Hoechst 33342 and Propidium Iodide (PI) staining techniques

For these techniques, cells were grown on 18 X 18mm coverslips which were first wrapped in foil before being autoclaved. Using tweezers, previously sterilized or sprayed with 70% ethanol, each coverslip was placed at the bottom of a 35mm Petri dish or well and cells were grown as previously described (Protocol 1). The experiments were performed in the staining lab where there is minimal light.

Method

- Medium was removed from cells and washed 3X with sterile PBS (0.1M)
- 100µl of PI solution (see Appendix B) was added to each coverslip and incubated for 20 minutes at 4ºC
- PI solution was then removed and the cells were rinsed twice with sterile PBS
- A cold fixative (1:1 methanol/acetone), enough to cover the monolayer of cells, was then added to each coverslip and incubated for 10 minutes at 4ºC
- The fixative was removed and the coverslips were left to air dry completely for a further 10 minutes
- After the time had elapsed, 150µl of Hoechst solution (see Appendix B) was added to each coverslip and incubated for 10 minutes at 4ºC
- Hoechst solution was removed and the coverslips containing cells were rinsed 5 times with sterile PBS to avoid or minimise background noise
- The coverslips were allowed to dry before being mounted on a microscope slide using a small drop of fluorescent mounting medium
- The slides now were placed face down on tissue paper and covered with foil to protect from the light
- The slides can now be stored at -20ºC for up to 2 weeks

Protocol 10: Hematoxylin and Eosin staining technique

For this technique, cells were grown on 18 X 18mm coverslips which were first wrapped in foil before being autoclaved. Using tweezers, previously sterilized or sprayed with 70% ethanol, each coverslip was placed at the bottom of a 35mm Petri dish or well and cells were grown as previously described (Protocol 1). Only 500µl of reagents was added to each coverslip for this staining method and incubation was conducted at room temperature.

Method

- Medium was removed from cells and washed once with sterile PBS
- Xylene was added for 10 minutes
- Xylene was discarded and 100% ethanol was added for 15 seconds
- 100% ethanol was discarded and 95% ethanol (see Appendix B) was added for 15 seconds. This step is repeated twice
- 95% ethanol was discarded and 70% ethanol (see Appendix B) was added for 15 seconds. This step is repeated twice
- 70% ethanol was discarded and coverslips were rinsed in distilled water
- Hematoxylin dye (see Appendix B) was then added for 3 minutes
- The coverslips were rinsed in distilled water first and then in acid alcohol (see Appendix B)
- The coverslips were rinsed in distilled water again after which the coverslips were blued in Scott's tap water (see Appendix B)
- After this was done, the coverslips were rinsed in distilled water before adding the eosin dye (see Appendix B) for 2 minutes
- After the time had elapsed, the coverslips were rinsed for a final time in distilled water and then 70% ethanol was added for 15 seconds
- 70% ethanol was discarded and 95% ethanol was added for 15 seconds. This step is repeated twice
- 95% ethanol was discarded and 100% ethanol was added for 15 seconds. This step is repeated twice
- 95% ethanol was discarded and xylene was added for 15 seconds. This step was also repeated twice

- Finally the coverslips were mounted on permanent labelled microscope slides. Allow the mounting medium to dry before use

Protocol 11: Immunohistochemistry

For this technique, cells were also grown on 18 X 18mm coverslips which were first wrapped in foil before being autoclaved. Using tweezers, previously sterilized or sprayed with 70% ethanol, each coverslip was placed at the bottom of a 35mm Petri dish or well and cells were grown as previously described (Protocol 1).

Method

- Medium was removed from cells and washed once with sterile PBS
- 1ml fixative (1:1 methanol/acetone) per coverslip was added and incubated for 10 minutes at 4ºC. This process was conducted whilst the cells were kept on ice
- The fixative was then removed and the coverslips were allowed to air dry for 20 minutes at room temperature
- The cells were rinsed with 1.5ml sterile PBS after which each coverslip was then transferred to a temporary but labelled microscope slide
- 100µl of a 5% donkey serum made in PBS (see Appendix B) was added to each coverslip and incubated for 20 minutes at room temperature
- After the time had elapsed, the serum was drained (NOT washed) and 100µl primary antibody solution in a 1:50 dilution (see Appendix B) was added to each coverslip and incubated overnight at 4ºC. In this particular case, the primary antibody that was used was ubiqiutin
- The cells were rinsed once with PBS, only 100µl was used for each coverslip, and 100µl secondary antibody solution in a 1:200 dilution (see Appendix B) was added. Incubation continued for 30 minutes at room temperature. The secondary antibody that was used in this experiment is tagged to a fluorophore (FITC) and was not grown in the same animal that the primary antibody was grown in. Therefore, since the ubiquitin antibody was grown in a mouse model and donkey serum was used, the secondary antibody should be a ‘donkey anti-mouse’ antibody. Remember to vortex and centrifuge the secondary antibody solution to avoid the formation of crystals

- In addition, 100µl Hoechst 33342 solution was added on top of the secondary antibody solution and incubated for another 10 minutes at room temperature
- The coverslips were lastly rinsed 3 times for and then mounted on new microscope slides using a small drop of fluorescent mounting medium
- The slides can now be used or stored wrapped in foil to avoid light for up to 2 weeks at -20ºC

Protocol 12: Measurement of ROS accumulation

For this technique, cells were also grown in 35mm Petri dishes as previously described (Protocol 1). The mitochondria specific fluorescent dye MitoTracker Red CM-H_2 X ROS was used to measure mitochondrial ROS accumulation in cells after treatment with TNF-α.

Method

- Medium was removed from cells and 500µl Mito tracker Red fluorescent dye (see Appendix B) was added to each Petri dish for 1 minute at room temperature
- After the time had elapsed, the Petri dish was placed onto a microscope and the cells visualised using a Nikon Eclipse E 400 fluorescent microscope fitted with a Nikon DMX 1200 digital camera at 40X magnification. An image was captured using Simple PCI software after a suitable field was chosen

Protocol 13: DNA isolation

For this technique, cells were grown in T25 culture flasks as previously described (Protocol 1).

Method

- Medium was removed from the cells and rinsed once with sterile PBS
- This was followed by trypsinization to remove the cells attached at the bottom of the flask

- Cells were counted on the haemocytometer (Protocol 2) while the rest were kept on ice
- The cells were pelleted for 3 minutes at 15000 rpm and the pellet was washed with sterile PBS. This step was repeated 3 times to remove any traces of differentiation medium
- After this was completed, 500µl lysis buffer (see Appendix B) and 2µl RNase (20mg/ml) was added and heated on a heating block at 37ºC for 1 hour
- 10µl proteinase K (20mg/ml) (see Appendix B) was added and incubated on a heating block at 55ºC overnight
- The contents were transferred into labelled eppindorf tubes and 250µl phenol solution and 250µl chloroform: isoamyl alcohol was added. This was gently inverted for 5 minutes at room temperature and then centrifuged at 22ºC, 10000 rpm for 10 minutes
- The top layer (DNA) was transferred into a new eppindorf tube and the bottom layer was discarded. 250µl Phenol solution and 250µl chloroform: isoamyl alcohol was added. This was gently inverted for 5 minutes at room temperature and then centrifuged at 22ºC, 10000 rpm for 10 minutes. This step was repeated twice
- The top layer (DNA) was transferred into a new eppindorf tube and the bottom layer was discarded. 500µl chloroform: isoamyl alcohol was added. This was gently inverted for 2 minutes at room temperature and then centrifuged at 22ºC, 10000 rpm for 1 minute
- The top layer (DNA) was once again transferred into a new eppindorf tube and the bottom layer was discarded. 40µl NaCl (20mM) and 1000µl 100% ethanol was added to the solution. This was gently mixed and incubated at -20ºC for 1 hour
- After the time had elapsed, the solution was centrifuged using a desktop centrifuge (maximum rpm) at room temperature for 20 minutes
- The ethanol was then discarded and the pellet that formed was washed in 1000µl 70% ethanol. The solution was centrifuged again using a desktop centrifuge (maximum rpm) at room temperature for 20 minutes
- The ethanol was discarded after which the pellet was left to air dry for 5 minutes maximum
- 40µl TE buffer (see Appendix B) was added to the pellet and incubated overnight at 4ºC

Protocol 14: DNA fragmentation Assay

Method

- Mix the samples of DNA with loading buffer by adding 10x loading buffer to a final concentration of 1x. The addition of loading buffer to samples allows to load gel wells more easily and to monitor the run of samples
- Place samples in a heating block at 65 °C for 10 minutes and immediately load 10-20 µl of them to each well of a standard 1 % agarose gel containing ethidium bromide 0.5 mg/ml. Appropriate DNA molecular weight markers should be included. Ethidium bromide is a potential carcinogen: wear gloves and handle with care.
- Run the electrophoresis in standard TE buffer after setting the voltage to the desired level. During electrophoresis it is possible to monitor the migration of samples by following the migration of bromophenol blue dye contained in the loading buffer.
- Stop the electrophoresis when the dye reaches about 3 cm from the end of the gel.
- To visualize DNA, place the gel on a UV transilluminator and take photos of the gel. Wear eye and skin protection when UV is on.

Protocol 15: PI3-Kinase ELISA Assay

Reagent Preparation

- Prepare 100 µM PI (4,5) P_2 substrate stock solution by adding 230 µl H_2O to the vial of diC_8 PI (4,5)P_2 substrate (K-1008, capped red). Vortex the vial shortly to fully reconstitute the lipid. Spin down and place vial on ice. The vial of PI (4,5)P_2 substrate contains enough for 90 reactions at 240 pmol per reaction. The unused portion of PI (4,5)P_2 substrate stock solution can be stored at -20 ºC for up to 3 months
- Prepare TBS buffer by adding 100 ml dH_2O to the provided TBS tablet. This TBS tablet is stable at room temperature
- Prepare TBS-T buffer by diluting 20 ml of the provided 10X TBS-T buffer with 180 ml dH_2O. TBS-T is also stable at room temperature

- Prepare 10X PI3-K reaction buffer on ice and store at -20 ºC after use
    - 200 mM Tris pH 7.4
    - 100 mM NaCl
    - 400mM $MgCl_2$
    - 250 μM ATP

Kinase reaction and incubation

- Isolate or prepare PI3-K accordingly:
    - Remove medium and place cells on ice. Add 10 ml per dish of ice cold Buffer A (20 mM Tris-HCl, pH 7.4, 137 mM NaCl, 1 mM $CaCl_2$, 1 mM $MgCl_2$ and 0.1 mM sodium orthovanadate). Rinse 3 times with this solution
    - Remove Buffer A and add 1 ml of ice cold Lysis Buffer (Buffer A plus 1 % NP-40 and 1 mM PMSF) Keep plates on ice for 20 minutes
    - Scrape cells from the dish and then transfer to 1.5 ml centrifuge tubes (eppi's). Centrifuge for 10 minutes to sediment insoluble material
    - Transfer supernatant to new tubes and add 5 μl of anti-PI3-Kinase antibody (Upstate Biotechnology, catalog #06-195) to each tube. Incubate for 1 hour at 4 ºC
    - Add 60 μl of a 50 % slurry of Protein A-agarose beads in PBS to each tube. Incubate with mixing for 1 hour at 4 ºC
    - Collect immunoprecipated enzyme by centrifuging 5 seconds, and wash with freshly prepared buffer as follows:
        - 3 times with Buffer A plus 1 % NP-40
        - 3 times with 0.1 M Tris-HCl, pH 7.4; 5 mM LiCl and 0,1 mM sodium orthovanadate
        - Twice with TNE (10 mM Tris-HCL, pH 7.4, 150mM NaCl, 5 mM EDTA) containing 0.1 mM sodium orthovanadate
    - Aspirate the last wash as completely as possible and proceed with kinase reactions
- PI3-Kinase reaction set up as shown in the diagram provided. All reactions, controls, and standards to be run in duplicate or triplicate.

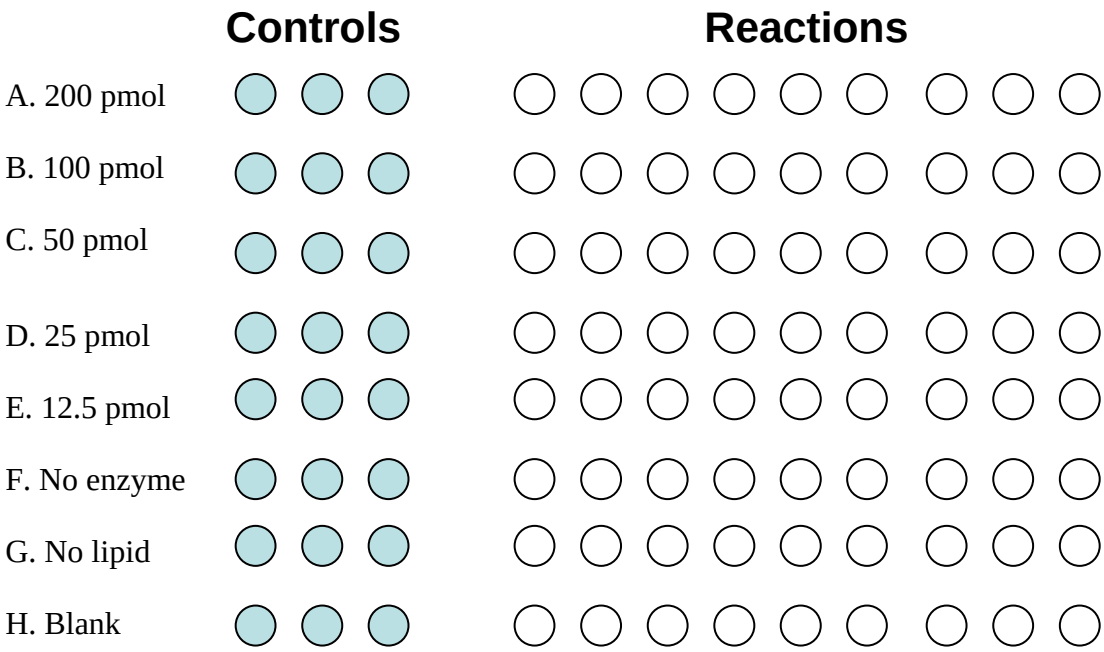

Incubation Plate

PIP3 Standards and Controls	PIP3, pmol per 50 µl solution
4 µM	200
2 µM	100
1 µM	50
0.5 µM	25
0.25 µM	12.5
No enzyme control	0
No lipid control	0

For each 60 µl PI3-K reaction, add 6 µl of 10X PI3-K reaction buffer, add 2.4 µl of 100mM PI (4,5) P_2 substrate (240 pmol), add required volume of dH_2O, then add desired volume of PI3-K enzyme to start reaction. Exclude PI3-K enzyme for the No enzyme controls in row F.

- Seal the plate and let the kinase reaction proceed without shaking for appropriate amount of time (usually 1-3 hours at room temperature)
- Prepare PI (3,4,5) P_3 standards and controls whilst waiting for the kinase reactions

- Prepare PI (3,4,5) P_3 standard stock solution by adding 1000 µl TBS-T buffer to the vial of diC_8 PI (3,4,5) P_3 standard (K-1009, capped blue). Vortex the vial shortly to fully reconstitute the lipid. Spin down and place vial on ice. Unused portion of PI (3,4,5) P_3 standard stock solution can be stored at -20 ºC for up to 3 months
- Make four 2-fold serial dilutions from the 4 µM stock with TBS, as explained previously
- Pipette 60 µl/well of each standard solution in triplicate or duplicate to rows A to E
- Pipette 60 µl/well of TBS to the No lipid control wells in row G
- Pipette 120 µl/well of TBS to the blank control wells in row H. No PI (3,4,5) P_3 detector

- Stop kinase reactions and incubate with PI (3,4,5) P_3 detector
  - Briefly centrifuge the vial of PI (3,4,5) P_3 detector (K-1006, capped green). Dilute the PI (3,4,5) P_3 detector 1:200 in TBS-T. Then add 63 µl of the 100mM EDTA (K-EDTA, capped violet) per ml of diluted PI (3,4,5) P_3 detector (final EDTA concentration is close 6 mM). Make only enough working solution of detector for the current assay and store the remainder of the PI (3,4,5) P_3 detector at -20 ºC for further use
  - Add 60 µl/well of above diluted PI (3,4,5) P_3 detector/EDTA to all reaction, standard and control wells except the blank controls in row H. Seal the incubation plate and incubate on a plate shaker with gentle shaking at room temperature for 1 hour

Detection

- Following the incubation, transfer the reacted mixtures to the detection plate (clear flat-bottom strip plate). Transfer 100 µl from each well to the corresponding well in the detection plate. Seal the plate and incubate for 60 minutes at room temperature with gentle agitation on a plate shaker. Discard the solution and wash the wells once with 200 µl/well TBS-T
- Briefly centrifuge the vial of secondary detector (K-SEC, capped yellow). Dilute secondary detector 1:40 with TBS-T. Dilute ONLY the amount you will use for the cur-

rent assay and store the remainder of the secondary detector at 4 ºC for future use. Discard the TBS-T wash from plate, and add 100 µl of diluted secondary detector to each well of the detection plate. Seal the plate and incubate for another 30 minutes on a plate shaker. Discard the solution and wash the wells briefly with TBS-T, twice with 200 µl/well and once with 300 µl/well

- Discard the last TBS-T wash from the plate completely, immediately add 100 µl of TBM solution (K-TBM1, amber bottle) to each well. Allow color to develop for 1-15 minutes in the dark (or cover the plate with aluminium foil). Watch for the blue color development and DO NOT overdevelop. Stop color development by adding 50 µl of 1 N H_2SO_4 stop solution (K-$STOP_t$, red capped bottle) to each well when the color is still clear to light blue in 200 pmol PI (3,4,5) P_3 standard wells and has turned ocean blue in No lipid control wells. Blue color will change to yellow color upon addition of stop solution. Eliminate any big air bubbles present in wells before reading the plate
- Read the absorbance at 450 mM on a plate reader

Results

PI3-Kinase activity can be estimated by comparing the absorbance values from the wells containing enzyme reaction products to the values in the standard curve. Plot the absorbance values obtained vs. log of PI (3,4,5) P_3 in pmol per standard to generate a standard curve using linear or non-linear one site completion correlation. Determine the PI (3,4,5) P_3 level in pmol by interpolation from absorbance values obtained from the enzyme reactions. PI3-K activity in your samples can be estimated by the percentage conservation from initial 200 pmol of PI (4,5) P_2 per assay point. There are 200 pmol of combined lipids – PI (3,4,5) P_3 products plus remaining PI (4,5) P_2 substrate, in each assay point. An example of what your graphs should look like is shown below

Bar Graph

Absorbance
450 nm

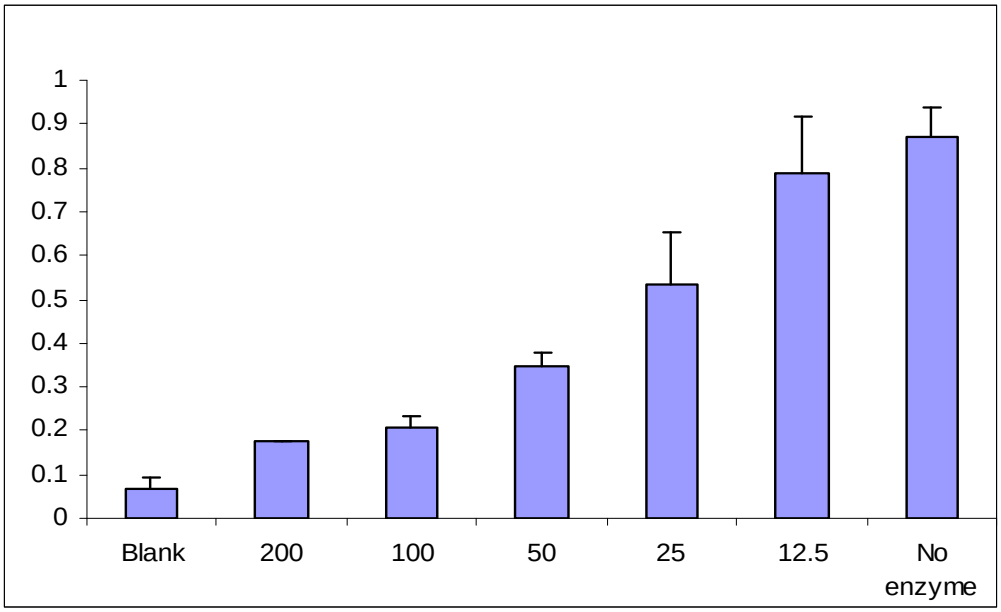

PI (3,4,5) P_3 pmol competion

PI (3,4,5)P3 Standard Curve

Absorbance
450 nm

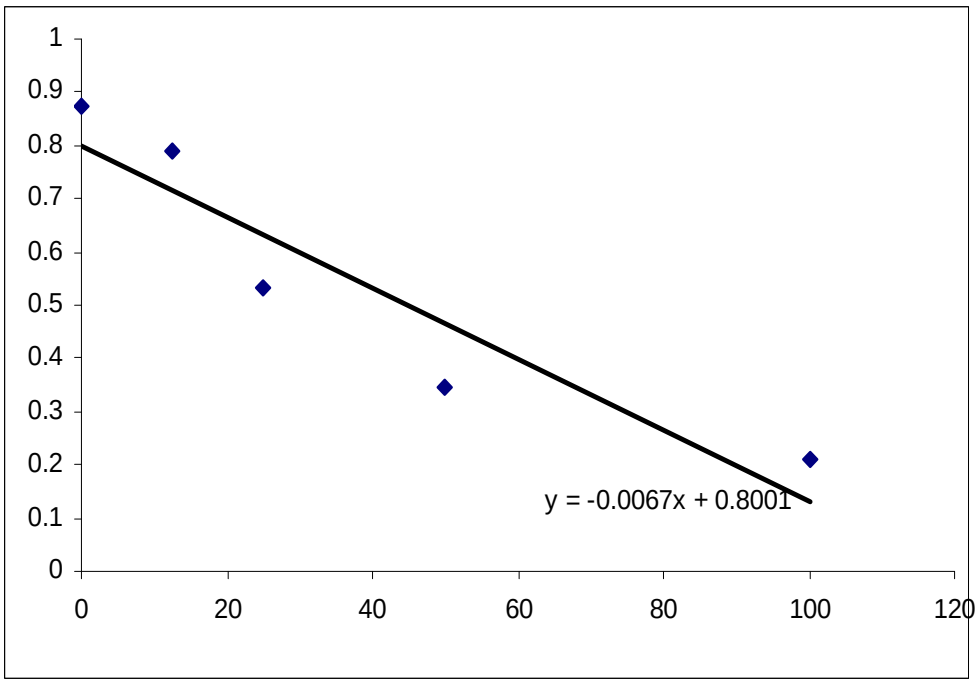

PI (3,4,5) P_3 pmol

Appendix B

Growth Medium

- 500ml Dulbecco's Modified Eagles Medium (DMEM)
- 56ml Fetal Bovine Serum (FBS) (filter first before use)
- 5.6ml Penstrep
- 20ml L-glutamine
- 2ml Streptomycin/Gentamicin

Differentiation Medium

- 500ml Dulbecco's Modified Eagles Medium (DMEM)
- 5.6ml Horse Serum (HS) (filter first before use)
- 5.6ml Penstrep
- 20ml L-glutamine
- 2ml Streptomycin/Gentamicin

X1 Phosphate Buffer Saline (PBS)-2L

Dissolve the following in 1L of water

- 16g NaCl
- 0.4g KCl
- 2.88g Na_2HPO_4 (di Sodium hydrogen phosphate)
- 0.48g KH_2PO_4 (potassium dihydrogen phosphate)

Adjust pH to 7.4, fill up to the 2L mark with distilled water and sterilize by autoclaving

Trypan Blue dye

- Weight out 40g trypan blue dye and dissolve this in 100ml PBS
- Store away at 4^{o}C

Propidium Iodide and Hoechst 33342 stain

- Dissolve 5µl Propium iodide in 1000µl sterile PBS
- Dissolve 5µl Hoechst 33342 in 1000µl sterile PBS
- These solutions are made fresh and must be kept on ice and away from light

10% Acid alcohol

- 10ml 1% HCl dissolved in 1L 70% alcohol

95% alcohol (1L)

- Dilute 950ml 100% ethanol with 50ml distilled water

70% alcohol (1L)

- Dilute 700ml 100% ethanol with 300ml distilled water

Harris Haematoxylin

- 5g Harris haematoxylin
- 100g Ammonium Alum
- 50ml 100% ethanol
- 1L distilled water
- 2.5g mercury oxide

To prepare: Dissolve haematoxylin in ethanol and add the ammonium alum to distilled water and heat to boiling point. Immediately add the mercuric oxide and shake until the solution has a purple-black colour. Cool rapidly in the fridge

For staining: Filter before use and add 4ml glacial acetic acid per 100ml of haematoxylin

Eosin

Stock solution: dissolve 10g eosin in 1L distilled water

Working solution: 10ml eosin stock solution dissolved in 90ml distilled water. This must be prepared fresh

For staining: Add 2-3 drops of glacial acetic acid per 100ml before use

Scott's Tap Water

- 3.5g $NaHCO_3$
- 20g $MgSO_4$
- 10ml 37% Formalin
- 1L tap water

To prepare: dissolve $NaHCO_3$ in the tap water first and then add $MgSO_4$ and formalin

5% donkey serum

- Dissolve 55µl donkey serum in 1100µl PBS. This solution is enough for 11 coverslips

Primary antibody solution

- Dissolve 20µl primary antibody with 1000µl PBS. This represents a 1:50 dilution

Secondary antibody solution

- Dissolve 5µl secondary antibody with 1000µl PBS. This represents a 1:200 dilution

Mitotracker Red Dye solution

- Dissolve 1µl dye to 1000µl growth or differentiation medium.

- Use 500µl solution for each Petri dish (35mm)

DNA lysis buffer

- 2mM EDTA 2ml of 1M
- 100mM Tris-HCl (pH = 8) 100ml of 1M
- 10mM NaCl 2ml of 5M
- 0.8% SDS (w/v) 8g

Make up to 1L with distilled water and store at room temperature

10mg/ml RNase A (Pancreatic RNase)

Ribonuclease A is an endoribonuclease that attacks single-stranded RNA and will precipitate out of concentrated solutions at neutral pH when heated to 100ºC

- Dissolve 100mg RNase A in 10ml of 0.01M sodium acetate solution (pH 5.2) (see below)
- Heat for 15 minutes at 100ºC to destroy DNase activity
- Allow to cool to room temperature
- Using 1M Tris-HCl (pH 7.4), adjust the pH to 5.2
- Prepare 1ml aliquots and store at -20ºC

0.01M Sodium acetate (pH 5.2)

- Prepare 200mM sodium acetate solution → 27.77g NaOAc
- Prepare 200mM acetic acid solution → 12.05ml glacial acetic acid diluted to 1L
- Mix 10.5ml acetic acid solution and 38.5ml sodium acetate solution and make up to 100ml
- Dilute 10ml of this solution with 90ml distilled water for a 0.01M sodium acetate solution with a pH of 5.2

20mg/ml Proteinase K

- Add 9.5ml distilled water to a 15ml falcon tube followed by 200mg proteinase K (always add proteins to aqueous solutions)
- Mix gently until everything has dissolved (do not vortex)
- Adjust the volume to 10ml with distilled water
- Aliquot and store at -20ºC

TE buffer (50x)

- 2M Trizma Base — 242g
- 1M acetate — 57.1ml of glacial acetic acid (17.4M)
- 100mM EDTA — 200ml of 0.5M EDTA (pH = 8)

RIPA buffer (100ml)

- Prepare 50mM Tris-HCl: add 790mg Tris to 75ml distilled water. Add 900mg NaCl and stir. Adjust pH to 7.4 using HCl. Pour the prepared Tris-HCL into a 100ml beaker. Add the following reagents in the beaker in the same order as they appear on the table

	Final concentration	**Volume**
NP-40	1%	10ml
Na-deoxycholate	0.25%	2.5ml
EDTA	1mM	1000 µl
Phenylmethylsulfonyl Flouoride (PMSF)	1mM	1000 µl
Leupeptin	1µg/ml	1 µl
SBTI-1	4 µg/ml	80 µl
Benzamidine	1mM	100 µl
Na_3VO_4	1mM	1000 µl
NaF	1mM	500 µl

- Add 1000µl Triton X-1000 to the solution and finally fill up to 100ml with distilled water and mix thoroughly
- Aliquot 1000 µl of RIPA buffer into eppendorf tubes and store at -20ºC

BSA (Bovine serum albumin 1mg/ml)

- For 1ml BSA, weight out 1mg BSA and add 1000 µl distilled water.
- For use during Western blotting, this BSA needs to be diluted. Pipette 100 µl from 1mg/ml BSA in new eppendorf tube and add 400 µl distilled water
- Mix well

Bradford Reagent (1L)

- Weight out 500mg Coomassie Brilliant Blue G and add it to 25oml 95% ethanol
- Add 500ml phosphoric acid and mix well
- Fill up to 1L with distilled water and store at 4ºC
- For use during Western blotting, this solution needs to be filtered twice and then a 1:5 dilution needs to be made

3X Sample buffer

- Measure 33.3ml stacking Tris (0.5M) and place in a beaker
- Weight out 8.8g SDS and 20g glycerol and place in the beaker
- Add a pinch of Bromo-phenol blue to the mixture
- Add and make up to 75.47ml with distilled water

Tris pH 8.8 (500ml)

- Weigh out 68.1g Tris (1.124M) and 1.5g SDS (0.3%) and place in a beaker.
- Add 400ml distilled water, stir and then adjust pH using HCL
- Add 100ml distilled water to make the final volume to 500ml

Tris pH 6.8 (500ml)

- Weigh out 30.3g Tris (0.5M) and 2g SDS (0.4%) and place in a beaker.
- Add 400ml distilled water, stir and then adjust pH using HCL
- Add 100ml distilled water to make the final volume to 500ml

Tris pH 6.8 (100ml) for Sample buffer

- Weigh out 6.06g Tris (0.5M) and 4ml 10%SDS and place in a beaker.
- Add 80ml distilled water, stir and then adjust pH using HCL
- Add 20ml distilled water to make the final volume to 100ml

Tris pH 6.7 (500ml)

- Weigh out 6.057g Tris (100mMM) and place in a beaker.
- Add 400ml distilled water, stir and then adjust pH using HCL
- Add 100ml distilled water to make the final volume to 500ml
-

10% Sodium dodecyl sulphate (SDS 500ml)

- Weight out 50g SDS and add 500ml distilled water

10% Ammonium persulphate (1000 µl)

- Weight out 0.1g APS into an eppendorf tube and add 1000 µl distilled water

10% acrylamide (separating) gel

➢ Distilled water	➢ 3.85ml
➢ 1.5M Tris-HCL (pH8.8)	➢ 2.5ml
➢ 10% SDS	➢ 100µl
➢ Acrylamide	➢ 2.5ml
➢ 10% APS	➢ 50 µl

➢ Temed	➢ 5 µl

12% acrylamide (separating) gel

➢ Distilled water	➢ 3.35ml
➢ 1.5M Tris-HCl (pH8.8)	➢ 2.5ml
➢ 10% SDS	➢ 100µl
➢ Acrylamide	➢ 3.0ml
➢ 10% APS	➢ 50 µl
➢ Temed	➢ 5 µl

4% acrylamide (stacking) gel

➢ Distilled water	➢ 6.1ml
➢ 0.5M Tris-HCl (pH6.8)	➢ 2.5ml
➢ 10% SDS	➢ 100µl
➢ Acrylamide	➢ 1ml
➢ 10% APS	➢ 100 µl
➢ Temed	➢ 20µl

Running buffer (1L)

- Weight out 3.03g Tris, 1.44g Glycine and 1g SDS into a 1L beaker. Add 500ml distilled water and stir until dissolved.
- Fill up to 1L with distilled water

Anode buffer 1 (500ml)

- Weigh out 18.2g Tris, add 380ml distilled water and stir. Adjust pH to 10.4 with HCL
- Add 100ml 100% methanol and fill up to 500ml with distilled water

Anode buffer 2 (500ml)

- Weigh out 1.51g Tris, add 380ml distilled water and stir. Adjust pH to 10.4 with HCL
- Add 100ml 100% methanol and fill up to 500ml with distilled water

Cathode buffer (500ml)

- Weigh out 1.51g Tris and 2.6g aminohexanoic acid, add 380ml distilled water and stir. Adjust pH to 10.4 with HCL
- Add 100ml 100% methanol and fill up to 500ml with distilled water

10X TBS (5L)

- Weight out 121g Tris and 80g NaCl into a 5L beaker. Add 2.5L distilled water and stir until dissolved.
- Adjust pH to 7.6 using HCl and then fill up to 5L with distilled water
- For use in Western blotting, take a 1L measuring cylinder and add 100ml 10X TBS and dilute with 900ml distilled water
- To make **TBST**, add 1ml tween to 1L diluted solution of TBS

Milk blocking solution (100ml)

- Weight out 5g non fat dry instant milk powder into a beaker. Add 100ml TBS and mix well
- Finally add 10µl Tween and mix well. This is sufficient for only one gel

Primary (1º) antibody

- Pipette 5µl 1º antibody and 5ml TBST in a 50ml falcon tube. This concentration is suitable for most 1º antibodies but others require a higher concentration

Secondary (2º) antibody

- Pipette 5µl 2º antibody and 20ml TBST in a 50ml falcon tube

Stripping buffer (100ml)

➢ 100mM Tris- HCl (pH6.7)	➢ 62.5ml
➢ 2-Mercaptoethanol	➢ 700µl
➢ 10% SDS	➢ 20ml

➢ Fill up to 100ml with distilled water. This solution is sufficient for 2 membranes (50ml each)

TNF-α dilution (20µg/ml) "STOCK"

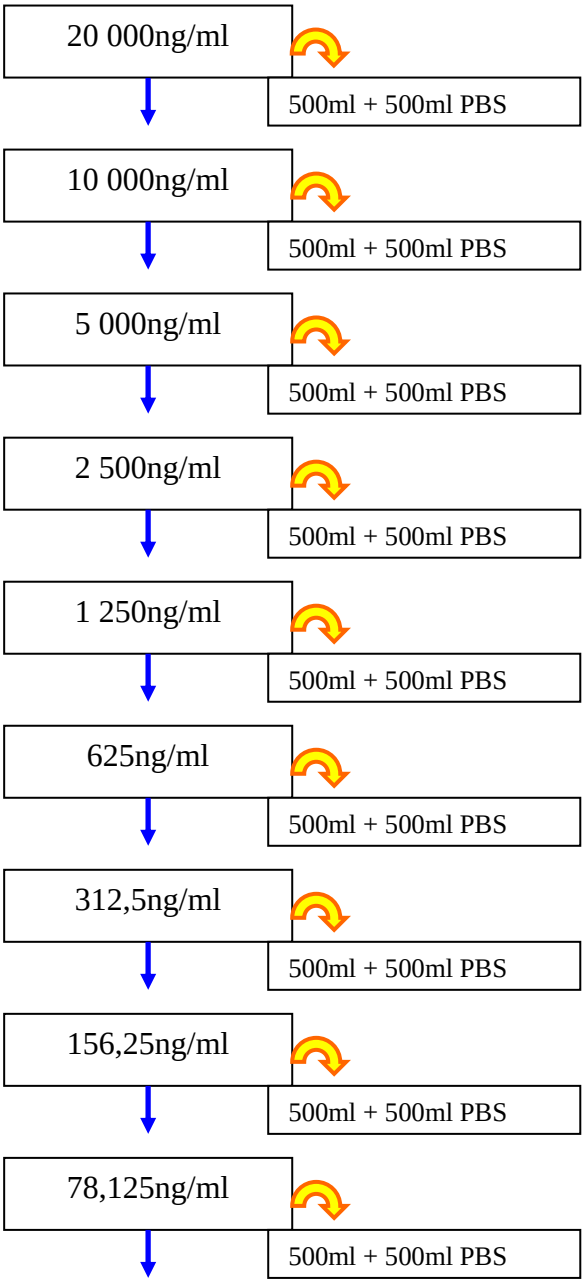

For 1ng/ml [TNF-α]

$C_1V_1 = C_2V_2$
$39{,}1\ V_1 = 1 \times 1$
$V_1 = 0.03ml\ (30µl)$

For 3ng/ml [TNF-α]

$C_1V_1 = C_2V_2$
$39{,}1\ V_1 = 3 \times 1$
$V_1 = 0.08ml\ (80µl)$

For 6ng/ml [TNF-α]

$C_1V_1 = C_2V_2$
$39{,}1\ V_1 = 6 \times 1$
$V_1 = 0.15ml\ (150µl)$

For 10ng/ml [TNF-α]

$C_1V_1 = C_2V_2$
$39{,}1\ V_1 = 10 \times 1$
$V_1 = 0.256ml\ (256µl)$

39,0625ng/ml = **WORKING STOCK**

Appendix C

Reagents	Catalogue Number	Company
Absolute alcohol	32221	Riedel deHaën
Agarose D-1 LE	39209080	Hispanagor
6-Aminohexanoic Acid	A7824	Sigma
Acrylamide	A3699	Sigma
Ammonium Alum	A2140	Sigma
Ammonium Persulphate (APS)	A3678	Sigma
Bovine Serum Albumin (BSA)	A4503	Sigma
Bradford Reagent	B6916	Sigma
Bromophenol Blue	32400A	UnivAR
Chloroform:Isoamyl alcohol	C059IQT	Sigma
Coomassie Brilliant Blue G	27815	Fluka
Coverslips (18 X 18mm)	S1815	Sigma
Dako Fluorescent Mounting media	S3023	DakoCytomation
Dulbecco's Modified Eagles medium (DMEM)	D5671	Sigma
Eosin	32617	Riedel deHaën
ECL™ Western Blotting analysis system	RPN2108	Amersham Biosciences
Ethidium Bromide	H5041	Promega
Fetal Bovine Serum	CN3255	Highveld Biological
Formalin	HTS0-1-128	Sigma
Gentamicin Sulphate 1%	CN3170	Highveld Biological
Glacial Acetic Acid	UN2789	Merck

Glycerol	G5516	UnivAR
Glycine	G8898	Sigma
Harris heamatoxylin	OB657122	Merck
Hoechst 33342	B2261	Sigma
Horse Serum	CN3280	Highveld Biological
Hydrochloric Acid (HCl)	UN1789	Merck
Iso-butanol	UN1212	Merk
Isopropanol	31,461-1	Sigma
L-glutamine	G7513	Sigma
Magnesium Sulphate ($MgSO_4$)	M2643	Sigma
Manual X-ray Developer	9X23018	Axim
Manual X-ray Fixative	9X23013	Axim
Mercuric Oxide	21,335-7	Sigma
Methanol	UN1250	Merck
Microscope slides (25 X 75mm)	S8400	Sigma
Mitotracker Red CM-H_2	53271	Sigma
MTT (Thiazolyl Blue Tetra-zolium Bromide)	M5655-16	Sigma
PecqGold prestained protein marker	27-2110	Peqlab
Penstrep	214	Highveld Biological
Phenol solution	P5447	Sigma
Phosphoric Acid	P5811	Merck
Ponceau S solution	P7170	Sigma
Precision plus protein dual color standards	161-0374	Bio-Rad
Propidium Iodide	P4170	Sigma
Rapid Mounting Media for Microscopy	UN1866	Merck
Sodium Dodecyl Sulphate (SDS)	L3771	Sigma

Sodium Hydrogen carbonate ($NaHCO_3$)	AC006329.500	Merck
Temed	T9281	Sigma
TNF-α (rat recombinant)	400-14	PeproTech Inc.
Triton X-100	X-100	Sigma
Trizma-base	93304	Fluka
Trypan Blue dye	T6146	Sigma
Trypsin		T4174
Tween 20	P5927	Sigma
Xylol	UN1307	Merck
Primary Antibodies		
Caspase-3	9665	Cell Signalling
MAFbx	Sc-33782	Santa Cruz Biotechnology
MuRF-1	ab-4125	Abcam
MyoD	Sc-304	Santa Cruz Biotechnology
Myogenin	Sc-12732	Santa Cruz Biotechnology
p-Akt	92755	Cell Signalling
p-FKHR	9461L	Cell Signalling
PI3-K	4292	Cell Signalling
p-JNK	9251L	Cell Signalling
p-NFκB	3031	Cell Signalling
p-P38 MAPK	9211	Cell Signalling
p-PTEN	95515	Cell Signalling
T-Akt	9272	Cell Signalling
T-FKHR	9462	Cell Signalling
T-JNK	9252	Cell Signalling
TNF-R1	sc-8436	Santa Cruz Biotechnology Inc.
T-NFκB	3034	Cell Signalling
T-P38 MAPK	9212	Cell Signalling
T-PTEN	9559	Cell Signalling
B-actin	4967	Cell Signalling

Secondary Antibodies		
ECL Anti-rabbit IgG, Horse-radish peroxidase linked whole antibody	NA934V	Amersham Life Science
Peroxidase labelled anti-mouse antibody	NIF825	Amersham Life Science
Paper and Film		
Hyperfilm	28-9068-36	Amersham Biosciences
Immobilon™ P transfer membrane (PVDF)	IPVH00010	Millipore
Paper (Blotting) Sheets	06-134	Lasec